Springer Mineralogy

Yuriy A. Litvin

Genesis of Diamonds and Associated Phases

Springer

Springer Mineralogy

More information about this series at http://www.springer.com/series/13488

Yuriy A. Litvin

Genesis of Diamonds and Associated Phases

Springer

Yuriy A. Litvin
Institute of Experimental Mineralogy
Russian Academy of Sciences
Chernogolovka, Moscow Region
Russia

ISSN 2366-1585 ISSN 2366-1593 (electronic)
Springer Mineralogy
ISBN 978-3-319-54542-4 ISBN 978-3-319-54543-1 (eBook)
DOI 10.1007/978-3-319-54543-1

Library of Congress Control Number: 2017933544

Printed on acid-free paper

This Springer imprint is published by Springer Nature
The registered company is Springer International Publishing AG
The registered company address is: Gewerbestrasse 11, 6330 Cham, Switzerland

Preface

Diamond-bearing upper mantle eclogite rock has been found in 1897 at South African kimberlitic pipe. It is now appreciated that this eclogite represents the first natural sample wherein diamonds have been combined with the genetically associated mineral phases. Later on, the diamond-associated phases were discovered as primary solid, hardened liquid and volatile inclusions of the great diversity. Several tens of years of a purposeful and intensive analytic investigation of the diamond-hosted mineral phases will allow the evidence of the multicomponent multiphase composition of natural parental media for diamonds and associated phases at 150–800 km depths of the Earth's mantle. And only in the last decade an understanding has arrived that a progress of the genetic mineralogy of diamonds and associated phases can be solely provided by a methodology of physicochemical experimental study of the relevant multicomponent heterogeneous diamond-producing mineral systems. The actual PT conditions at the upper mantle, transition zone and lower mantle depths are bound to be reproduced in the experimental research.

This book has the academic directionality and deals with the present state of genetic mineralogy of diamond and associated phases. Contents of the book may be referred to three main divisions. First, the analytic mineralogical data of evident genetic interest have been briefly characterized. Second part of the book is focused on high-pressure experimental studies of diamond-parental multicomponent mineral systems. Therewith their boundary compositions are specified having regard to the natural chemistry of diamond-hosted inclusions from the depths of the upper mantle, transition zone and lower mantle. Experimental physicochemical results allows to substantiate the completely miscible silicate-($\pm$oxide)-carbonatite melts with dissolved carbon as the parental media for diamonds and associated mineral phases over the all mantle depths. Experimental melting phase diagrams are lively presentative for the syngenesis relations of diamonds and minerals associated in their primary inclusions. The melting phase relations have made a direct determination of the physicochemical mechanism of diamond nucleation in carbon-oversaturated melts–solutions. Moreover, the melting diagrams offer a clearer view of how the joint crystallization of diamonds and paragenetic minerals may originate.

The combined physicochemical experimental and mineralogical data provide a means for substantiation of the mantle-carbonatite theory of genesis of diamonds and associated phases at the Earth mantle depths of 150–800 km. In the conclusive part, all the variety of mineral inclusions in diamonds of the upper mantle, transition zone and lower mantle is genetically classified. Along with this, partition coefficients of trace and scattered elements between minerals-in-inclusions and diamond-parental melts are first experimentally determined. The results of physicochemical experiments provide for investigation of mechanisms of fractional ultrabasic–basic evolution of diamond-parental melts which are responsible for paragenetic transitions in the course of the genetic processes for diamonds and associated phases under the upper and lower mantle conditions. Physicochemical experimental and analytical mineralogical data are compatible with the concept that the reservoirs–chambers of silicate-(±oxide)-carbonatite-carbon melts–solutions, parental for diamonds and associated phases, had been generated within the enclosing Earth's mantle rocks.

Chernogolovka, Moscow Region, Russia Yuriy A. Litvin

Acknowedgements

The author is grateful to Anna Spivak, Andrey Bobrov, Anastasia Kuzyura, Oleg Safonov, Anna Dymshits, Valentina Butvina, Natalia Solopova for effective collaboration in physicochemical experiments on the mantle-composed and diamond-producing multicomponent systems. I particularly thankful to my scientific advisers Prof. Dmitry Korzhinskii and Prof. Vilen Zharikov and hold them in remembrance. I would like to express my sincere thanks to Leonid Dubrovinsky and Natalia Dubrovinskaia (University of Bayreuth), Tibor Gasparik (Stony Brook University, New York), Luca Bindi (Univercity of Florence), Gero Kurat (Natural History Museum, Vienna), Masaki Akaogi (Gakushuin University, Tokyo) and Eiji Ohtani (Tohoku University, Sendai) for very fruitful collaboration at different times. For the useful scientific contacts Robert Liebermann (Stony Brook University, New York), Nikolay Sobolev (Institute of Geology and Mineralogy, Novosibirsk), Oded Navon (Hebru University, Jerusalem) and Felix Kaminsky (KM Diamond Exploration Ltd., Vancouver) are deeply acknowledged. I am utterly thankful to Svetlana Iantcen whose everyday help is invaluable.

Contents

Abbreviations

Alm	Almandine $Fe_3Al_2Si_3O_{12}$
Ap	Apatite $Ca_5(PO_4)_3(F,Cl)$
Arg	Aragonite $CaCO_3$
Bn	Bornite Cu_5FeS_4
Brd, FBrd	Bridgmanite $MgSiO_3$, $(Mg,Fe)SiO_3$
Cal	Calcite $CaCO_3$
CaPrv	Ca-perovskite $CaSiO_3$
Chal	Chalipite Fe_2C
Chr	Chromite $FeCr_2O_4$
Coe	Coesite SiO_2
Cog	Cogenite Fe_3C
Cpx	Clinopyroxene $(Ca,Na)(Mg,Fe)(Si,Al)_2O_6 \rightarrow (Di{\cdot}Hd{\cdot}Jd)_{ss}$
Cpy	Chalcopyrite $CuFeS_2$
Crn	Corundum Al_2O_3
D	Diamond C
Di	Diopside $CaMgSi_2O_6$
Dj	Djerfisherite $K_8(Cu,Fe,Ni)_{23}S_{26}Cl$
Dol	Dolomite $CaMg(CO_3)_2$
Egg	Al-phase $AlSiO_3OH$
En	Enstatite $MgSiO_3$
Fa	Fayalite Fe_2SiO_4
$FeNi^o$	Native Fe-Ni alloy
Fe^o	Native iron
Fo	Forsterite Mg_2SiO_4
Fs	Ferrosilite $FeSiO_3$
G	Graphite C
Gros	Grossularite $Ca_3Al_2Si_3O_{12}$
Grt	Garnet $(Mg,Fe,Ca)_3(Al,Cr)_2Si_3O_{12} \rightarrow (Prp{\cdot}Alm{\cdot}Gros)_{ss}$
Hax	Haxonite $(Fe,Ni,Co)_{23}$
Hd	Hedenbergite $CaFeSi_2O_6$

Hz	Heazlewoodite Ni_3S_2
Ilm, PIlm	Ilmenite $FeTiO_3$, picroilmenite $(Fe,Mg)TiO_3$
Jd	Jadeite $NaAlSi_2O_6$
Ky	Kyanite Al_2SiO_5
L	Liquid, melt
Mag	Magnetite $Fe^{2+}Fe_2^{3+}O_4$
Maj, MgMaj	Mg-majoritic garnet $Mg_3(Mg,Fe,Al,Si)_2Si_3O_{12}$
Mgs	Magnesite $MgCO_3$
Mois	Moissanite SiC
Mss	Monosulfide solid solution phases $(FeS{\cdot}NiS)_{ss}$
Nah	Nahkolite $NaHCO_3$
NaMaj	Na-majorite $Na_2MgSi_5O_{12}$
Nyer	Niererite $Na_2Ca(CO_3)_2$
Ol	Olivine $(Mg,Fe)_2SiO_4 \rightarrow (Fo{\cdot}Fa)_{ss}$
Omph	Omphacite, Jd-rich clinopyroxene
Opx	Orthopyroxene $(Mg,Fe)SiO_3 \rightarrow (En{\cdot}Fs)_{ss}$
Per, FPer	Periclase MgO, ferropericlase (Mg,Fe)O
Pn	Pentlandite $(Fe,Ni)_9S_8$
Po	Pyrrhotite FeS
Prp	Pyrope $Mg_3Al_2Si_3O_{12}$
Py	Pyrite FeS_2
Qtz	Quartz SiO_2
Rt	Rutile TiO_2
Rw	Ringwoodite Mg_2SiO_4
Sa	Sanidine $(K,Na)AlSi_3O_8$
Sd	Siderite $FeCO_3$
Spl, CrSpl	Spinel $MgAl_2O_4$, Cr-spinel $Mg(Al,Cr)_2O_4$
Sti	Stishovite SiO_2
TAPP	Tetragonal almandite-pyrope phase $(Mg,Fe^{2+})_2(Mg,Fe^{3+})(Al,Cr,Mn)_2Si_3O_{12}$
Ttn	Titanite $CaTiO_3$
Vio	Violarite Ni_3FeS_4
Wd	Wadsleite Mg_2SiO_4
Wus, MWus	Wustite FeO, magnesiowustite (Fe,Mg)O
Zrn	Zircon $ZrSiO_4$

Chapter 1
Introduction: Physico-Chemical Experiments as the Key to Diamond Genesis Problems

Crystal growth of diamonds at the Earth's mantle depths of 150–800 km had been accompanied by a fragmentary capturing minerals, melts and volatile compounds (as diamond-hosted inclusions) from the parental melts. This indicates convincingly that diamonds were originated jointly with the phases of primary hermetic inclusions in a common parental medium. This opens up possibilities for evaluating the general chemistry of natural diamond-producing systems from the compositions of significantly different phases associated with diamonds in primary inclusions. Of particular value is that it has been made possible to determine the boundary compositions for the experimental systems which duplicate the natural ones responsible for genesis of diamonds and associated phases. As a consequence, the principal problems of diamond genetic mineralogy may be formulated. It became apparent, that the methodology of physico-chemical experiments is of crucial importance in solution of the genetic problems for diamonds and associated phases.

1.1 Diamond-Hosted Inclusions as a "Window" into the Mantle Diamond-Parental Media

Mineralogy of diamond-hosted primary inclusions makes it possible to establish that diamonds have been transferred to the Earth's crust from depths of the upper mantle (150–400 km), transition zone (400–670 km) and upper horizons of the lower mantle (670–800 km). Comprehensive studies of physical relationships between diamonds and their inclusions prove with assurance that the growing diamonds have in essence sampled the heterogeneous fragments of diamond-parental media. In a certain sense natural diamonds and their primary inclusions may be considered as a peculiar kind of the in situ "window" into heterogeneous partial melts-solutions responsible for genesis of diamonds and associated phases. Minerals of the diamond-free upper-mantle rocks from xenoliths in kimberlites and

Y.A. Litvin, *Genesis of Diamonds and Associated Phases*,
Springer Mineralogy, DOI 10.1007/978-3-319-54543-1_1

diamond-hosted inclusions are similar by modality despite the different conditions of their genesis. At the same time the definite typomorphic properties point to a genetic relationship for the primary inclusions in diamonds and diamond-bearing peridotitic and eclogitic rocks of xenolths in kimberlites. Native transition-zone and lower-mantle rocks are yet unknown, but their experimental "copies" with upper-mantle pyrolitic compositions reveal the similar mineralogy with the primary inclusions in diamonds from relevant depths. At present it is beyond reason that minerals of the native diamond-free mantle rocks were formed at different chemical and phase compositions than minerals associated with diamonds in primary inclusions. There is little doubt that silicate-(±oxide) magmatism has played a dominant role in the origin of the mantle rocks. There are also varied reasons that diamond genesis along with primary inclusions had been performed in the mantle reservoirs-chambers of the parental silicate-(±oxide)-carbonatite-carbon melts. It is highly plausible that formation of diamonds with associated mineral phases and fractional ultrabasic-basic evolution of diamond-parental melts were carried out during the chambers cooling due to a heat transfer into the enclosing mantle rocks.

Determination of chemical and phase compositions of the growth medium responsible for the origin of most natural diamonds is the principal goal of genetic mineralogy of diamonds in kimberlitic and similar deposits. Solution of this problem makes it possible to ascertain a physico-chemical mode of diamond formation in the mantle and provide insights into formation conditions of minerals, melts, and volatiles initially incorporated into growing natural diamonds. The previous crystal morphological study of elementary layered growth faces of natural diamonds gave evidence for the liquid state of their parental medium. Growth melts are the most active agents of diamond formation and form the basis of parental media for diamonds and syngenetic inclusions contained therein. As follows from mineralogical studies, the parental media are chemically heterogeneous and consist of solid minerals, melts, and components of volatile compounds. The growing diamonds are capable to entrap both paragenetic and xenogenetic solid and liquid phases from parental media as hermetic inclusions irrespective of their origin. The important feature of primary entrapment of the parental medium fragments by growing diamonds is a residual pressure retained after cooling to room temperature in the hermetic inclusions with incorporated substance. The residual pressure permits to demonstrate over simple calculations that primary pressure at diamond genesis corresponds to the thermodynamic conditions of diamond stability. During release of the primary pressure to the residual value, the initial melt inclusions underwent certain phase transformations at hardening process. Thereby strongly compressed phases of excluded volatile compounds were inevitably formed from the components dissolved primary in diamond-producing melts.

1.2 General Composition of Diamond-Producing System from Syngenetic Inclusions

The data of analytic mineralogy open up possibilities for evaluating the general chemistry of natural diamond-producing system from the compositions of significantly different phases associated with diamonds in primary inclusions. The multicomponent multiphase composition of the system, parental for diamonds and associated phases, is established with use of analytic data for paragenetic and xenogenetic diamond-hosted ultrabasic and basic phases including Mg–Fe–Ca–Al–Na-silicates, Mg–Fe–Ca–Al–S–Ti–Cr–Zr-oxides, Mg–Fe–Ca–Na–K-carbonates, Ca-phosphate, Fe–Ni–Cu–K-sulfides, Fe–Ni–Cr-metals, C–O–H–N-volatile compounds, carbon C (diamond and metastable graphite). The general composition of the diamond parental multicomponent system may be defined as MgO–CaO–FeO (Fe, Fe_2O_3)–NiO (Ni)–MnO–Na_2O–K_2O–Al_2O_3–Cr_2O_3 (Cr)–TiO_2–ZrO_2–SiO_2–P_2O_5–CuS (Cu_2S)–FeS (FeS_2)–NiS–K_2S–KCl–NaCl–SiC–Fe_xC_y–CO_2 (CO, CH_4)–N_2–H_2O–C. Most likely the general chemical composition of diamond-producing system is basically reliable at the depths of upper mantle, transition zone and lower mantle.

In general terms, the analytic mineralogy data allow revealing extremely changeable multicomponent chemical compositions of heterogeneous partial parental melts of natural diamonds over all depths of the Earth's mantle. However a general composition of the parental medium, determined with the use of objective mineralogical data, does not provide the means of plausible and qualitative estimating a chemical composition of the growth melts which makes it solely possible the diamonds and associated phases genesis. Without knowledge of the growth melts compositions, there is no way of revealing physico-chemical mechanisms of nucleation and mass crystallization of natural diamonds. It is also impossible to estimate the physico-chemical conditions of joint genesis of diamonds and associated mineral phases for the upper mantle, transition zone and lower mantle.

High-pressure high-temperature experimental testing the capacity for diamond synthesis in melts of a variety of the mineral-inclusions has been carried out at many world-wide laboratories. As a result, an improved diamond-forming efficiency has made evident in several cases for the chemically dissimilar minerals. It was significantly turned out that their melts are not physico-chemically capable of producing jointly diamonds and a known multitude of the associated phases. As a consequence the key problems of diamond genetic mineralogy remain unsolved solely on the basis of analytic data for the phases associated with diamonds. The problems are also outstanding with the use of data of the analytic mineralogy of diamond-included phases in combination with the testing results on estimation of a diamond-forming efficiency for any relevant melts and volatiles.

Of particular value is that identification of mineral phases and determination of their chemical compositions in the frames of the general composition of the variable diamond-parental media have been made possible to determine the boundary

compositions for the experimental systems which are effective in solution of the genetic problems for diamonds and associated phases. As a consequence, the principal problems of diamond genetic mineralogy may be formulated.

1.3 Principal Problems in Genesis of Diamond and Associated Phases

Principal problems of diamond genetic mineralogy may be formulated as follows: (1) determination of chemical nature and compositions of the growth melts of diamonds and paragenetic phases over all the mantle depths; (2) elucidation of the physico-chemical mechanisms of diamonds and primary inclusions syngenesis; (3) substantiation of phase reactions that have formed the discrete ultrabasic and basic parageneses of mineral inclusions in natural diamonds, (4) elaboration of genetic classification of primarily diamond-associated paragenetic and xenogenetic phases. These problems may be reliably solved solely with the use of physico-chemical experiments which are capable to reveal the mechanisms of phase reactions in multicomponent heterogeneous diamond-producing systems. In this case, a substantiation of the experimental systems compositions using analytic data for the actual diamond-associated phases as well as for deep-seated mantle rocks must be the obligatory condition. Moreover, the truths of diamond-producing melts compositions deduced from physico-chemical experiments should be under control of the criterion of diamonds and primary inclusions syngenesis. By the criterion, the experimental growth melts are bound to realize the syngenesis of diamonds and associated phases similarly to the natural mode.

It has become apparent, that the methodology of physico-chemical experiments is of crucial importance in solution of the diamond genesis problems.

1.4 Physico-Chemical Experiments in Study of Diamond Origin

Physico-chemical experimental studies of the genetic mineralogy, petrology and geochemistry problems of the Earth's mantle magmatism is aimed at obtaining reliable information on the melting phase relations of multicomponent heterogeneous upper-mantle, transition-zone and lower-mantle mineral systems within a wide composition range. Its goal is the construction of equilibrium melting phase diagrams at the pressure-temperature-composition coordinates for the mantle systems, which are realistic in terms of composition and physical parameters. Melting phase diagrams of such a kind, which objectively reflect the physico-chemical properties of mantle materials, provide a fundamental basic for the analysis of its behavior in deep mantle magmatic processes including those responsible for genesis of diamonds and associated phases.

Samples of mantle rocks and minerals are the final products of the mantle physico-chemical processes, and they may be characterized by one or limited number of compositional points. Because of this, the samples bear little information on the initial boundary conditions and physico-chemical evolution of the processes of genetic-mineralogical, petrological and geochemical importance. Combination of theoretically-based physico-chemical means and modes, which have been developed in the physical chemistry of multicomponent multiphase systems (especially, phase complex, symplecial triangulation of phase diagrams, transformation of coordinates, two-dimensional poly-thermal sections, Rhines phase rule, and some others) together with high-pressure high-temperature experimental methods of investigation is extremely important as complementary and inseparable parts of the methodology of physico-chemical experiment dealing with the investigation of multicomponent heterogeneous mantle systems. Poly-thermal sections of the multicomponent mantle-magmatic and diamond-producing systems as convenient two-dimensional projections reveal the main physico-chemical peculiarities of a key genetic value. The correctness of the construction of phase diagrams and their topology are checked using the Rhines phase rule.

The kinetic effects of diamond formation in the experimental mantle-simulating conditions are also of particular importance for the genetic mineralogy of diamonds and associated phases. Among these there are physical mechanisms for generation of labile and metastable carbon-oversaturated in respect to diamond silicate-(±oxide)-carbonatite melts-solutions, PT-dependence of the nucleation density and growth rate of diamond phases (controlling formation from single-crystalline diamonds to poly-crystalline diamondites), inhibitory influence of silicate components on diamond growth rate, concentration barrier of diamond nucleation, the regime of fractional crystallization, etc.

Physico-chemical experiments will give the new insight into the mantle genesis of diamonds and associated phases due to the next principal results: (1) construction of generalized diagrams for the diamond-parental media, which reveal changeable compositions of the growth melts of diamonds and associated phases, their genetic relations to the mantle substance, and classification connections of the primary inclusions in natural diamonds; (2) experimental determination of equilibrium phase diagrams of syngenesis of diamonds and primary inclusions, which are of particular value as the basis for revealing the physico-chemical mechanism of diamond formation, including the kinetic conditions of nucleation and crystal growth of diamonds, and equilibrium conditions of a capture of paragenetic and xenogenetic minerals by the growing diamonds; (3) determination of the phase diagrams of diamonds and inclusions syngenesis under the regime of fractional crystallization, which are discovering the regularities of ultrabasic-basic evolution and paragenesis transitions in the diamond-forming systems of the upper and lower mantle; (4) the evidence of the physico-chemically united mode of diamond genesis at all the mantle depths with different mineralogy.

1.5 Early Assumptions for Diamond-Parental Medium

Early opinions on the chemical nature of diamond-parental medium were exclusively based on mineralogical, petrological and geochemical data for diamond-bearing rocks and mineral inclusions in the upper-mantle diamonds. Diamond-transporting kimberlitic magmas were among the first candidates. Modal likeness of minerals at the upper-mantle peridotite and eclogite rocks, on one hand, and diamond-hosted inclusions of peridotitic and eclogitic parageneses, on the other, has led to a widespread presumption of silicate parental chemistry. As the results of such "brain attack", there were also presumed sulfide, carbonate, C–O–H-fluid, metallic compositions for the natural diamond-parental systems. None of the proposals can satisfy to the criterion of syngenesis of diamonds and associated phases.

Diamond-forming efficiency of carbon solutions in melts of mineral phases, associated with natural diamonds, can make evident in experimental testing syntheses of diamonds. It was found that carbon-oversaturated melts of simple carbonates, some alkaline silicates, sulfides, chlorides, native metals as well as overcritical fluid phases of water, carbon dioxide (as alone as mixed with water) are effective. But all the positive tests are not in agreement with the syngenesis criterion.

At PT-conditions of thermodynamic stability of diamond, the completely miscible silicate-(±oxide)-carbonate melts are characterized by the capacity to effective dissolving rock-forming and accessory mantle minerals, solid carbon phases, and C–O–H–N-volatile compounds. Multicomponent multiphase melts-solutions of this kind are capable to providing formation of diamonds and associated paragenetic phases and, at the same time, are not threw obstacles to penetration inward of xenogenetic minerals and melts. The silicate-(±oxide)-carbonate-carbon melts-solutions, parental for diamonds and associated phases, are in excellent agreement with the syngenesis criterion for diamonds and associated phases.

Finally, the physico-chemical mechanisms of origin and evolution of the mantle magmas and diamond-producing melts-solutions have been made revealed in experimental physico-chemical investigating the multicomponent multiphase systems of the major geospheres of the Earth's mantle under high pressure and high temperature. The experimental results in common with mineralogical, petrological and geochemical data found the basis of the inwardly agreed mantle-carbonatite conception of genesis of diamond and associated phases. The physico-chemical experimental and theoretical studies are presented with a new possibility of clarifying the regularities for the ultrabasic-basic evolution of the mantle magmas and diamond-producing melts-solutions, for genesis of the Earth's mantle rocks and minerals of ultrabasic and basic parageneses which are associated with natural diamonds.

Chapter 2
Mantle Rocks and Diamond-Associated Phases: Role in Diamond Origin

The components of rock-forming and accessory minerals of the upper mantle, transition zone and lower mantle rocks have been involved into the processes of diamond genesis. Through their dissolving in primary carbonate melts, the mantle minerals have turned into components of the parental silicate-(±oxide)-carbonate-carbon melts-solutions for diamonds and co-crystallized paragenetic minerals. The minerals newly crystallized from the melts-solutions have been fragmentarily included into diamonds commonly growing with them. Xenogenetic accessory solid and liquid phases of the mantle rocks easily penetrating into the low-viscous diamond-parental melts can also be trapped by the growing diamonds. So, the mantle petrological processes are marked by the diamond-forming episodes that is of significant importance for solution of the diamond genesis problem. Therewith, the crucial information is directly related to the origin of primary mineral inclusions in natural diamonds of the deep Earth's interiors. Realization of new lines of attack to the problem of genesis of not numerous diamond-bearing peridotites and eclogites, which were discovered together with the upper-mantle diamond-free xenoliths in kimberlites, has been made possible in the context of the mantle-carbonatite conception of genesis of diamonds and associated phases. All the above will allow an understanding of the role of minerals and rocks associated with diamonds in resolution of the principal problems of the genetic mineralogy of diamond. In the current comprehension, genesis of diamonds and associated phases have been proceeded within the detached reservoirs-chambers of diamond-parental melts inside of the enclosing them upper mantle, transition zone and lower mantle rocks.

Y.A. Litvin, *Genesis of Diamonds and Associated Phases*,
Springer Mineralogy, DOI 10.1007/978-3-319-54543-1_2

2.1 Xenoliths of Native Upper-Mantle Rocks in Kimberlites

The mineralogical, petrological and geochemical features of differentiated rocks of the upper-mantle at the depths, where diamond is a thermodynamically stable phase, are of great concern in an investigation of genesis of diamonds and associated phases. The components of major and accessory minerals of the mantle rocks had been involved into diamond genesis through their dissolution in primary carbonate melts of metasomatic origin. The native upper-mantle rocks serve also as an enclosing matrix for the upper-mantle reservoirs-chambers of parental melts for diamonds and their syngenetic mineral inclusions. Garnet-bearing peridotites, pyroxenites, eclogites, and grospydites, which are presented as xenoliths in kimberlites, belong to the upper-mantle garnet-peridotite facies. The upper-mantle rocks have been withdrawn by the ascending kimberlitic magmas along with products of physico-chemical activity of the diamond-producing systems in the detached reservoirs-chambers (Litvin et al. 2014) and were carried out from the depths of 150–250 km (Ringwood 1975; Sobolev 1977; Dawson 1980). The peridotitic rocks at kimberlitic pipes of South Africa (Mathias et al. 1970) are represented as garnet dunites and garnet werhlites as well as most widespread garnet lherzolites (43%), garnet harzburgites (18%), harzburgites (16%) and lherzolites (14%). The modal mineral contents for garnet lherzolites are changeable and comprise for olivine 50–75%, orthopyroxene 12–34%, clinopyroxene 1–17%, garnet 1–15% at medium compositions $Ol_{64}Opx_{27}Cpx_3Grt_6$. About the same modal mineral relations are found for the xenoliths of garnet lherzolites from kimberlitic pipes of Yakutia ($Ol_{66}Opx_{25}Cpx_3Grt_6$) (Ringwood 1975) and Lesotho ($Ol_{65}Opx_{25}Cpx_4Grt_6$) (Dawson 1980). Pyroxenitic rocks of the garnet-peridotite facies are presented by garnet- and garnet-olivine orthopyroxenites, clinopyroxenites and websterites. Among eclogites there are predominantly bimineralic omphacite-garnet rocks and relatively few in number corundum-, kyanite-, coesite/quartz-, and orthopyroxene-eclogites.

Composition diagram for isoconcentric ternary section (Ol, Grt)–(Opx, Grt)–(Cpx, Grt) of the upper-mantle peridotite-pyroxenite system olivine Ol–orthopyroxene Opx–clinopyroxene Cpx–garnet Grt is shown in Fig. 2.1 as a basis for classification of ultrabasic rocks of the upper-mantle garnet-peridotite facies. The garnet-free ultrabasic peridotites and pyroxenites were classified using the ternary boundary join Ol–Opx–Cpx earlier (Streckeisen 1976).

Schematic composition diagram-complex for the upper-mantle peridotite-pyroxenite-eclogite system olivine Ol–(clinopyroxene Cpx/omphacite Omph)–corundum Crn–coesite Coe (Fig. 2.2) combines all the representative ultrabasic and basic rocks (Litvin 1991; Litvin et al. 2016). Ultrabasic and basic compositions are separated by the inner Opx–Cpx/Omph–Crn boundary plane between two ultrabasic (A, B) and three basic (C, D, E) diagrams-simplexes. The ultrabasic compositions consolidate the conjugate garnet-peridotite-pyroxenite Ol–Opx–Cpx–Grt (A) and olivine-eclogite Ol–Cpx–Grt–Crn (B) simplexes. The eclogitic simplexes

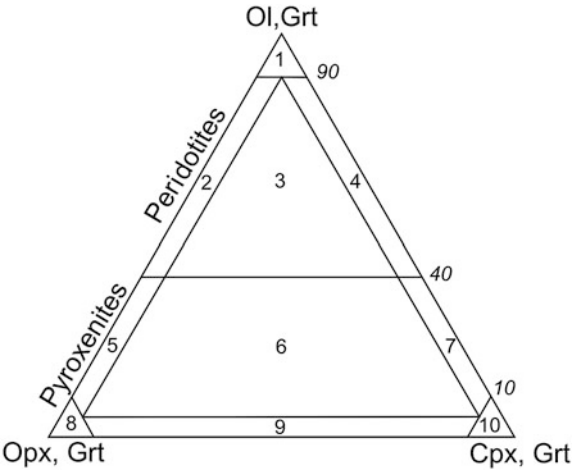

Fig. 2.1 Schematic classification for ultrabasic rocks of the garnet-peridotite facies, correspondingly, peridotites: *1* Grt-dunite, *2* Grt-harzburgite, *3* Grt-lherzolite, *4* wherlite; and pyroxenites: *5* Grt-Ol-orthopyroxenite, *6* Grt-Ol-websterite, *7* Grt-Ol-clinopyroxenite, *8* Grt-orthopyroxenite, *9* Grt-websterite, *10* Grt-clinopyroxenite. The composition boundaries are marked by ciphers in vol%

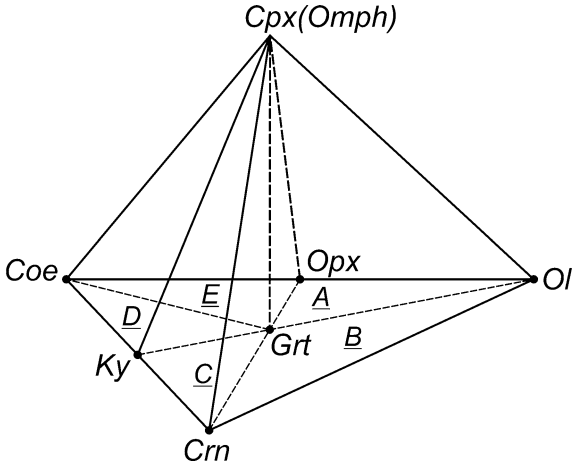

Fig. 2.2 The complex coordinate framework for ultrabasic and basic rocks of the garnet-peridotite facies, correspondingly, ultrabasic rocks: (*A*) peridotitic Ol–Opx–Cpx–Grt, (*B*) Ol–Crn–eclogitic Ol–Crn–Cpx–Grt; and basic rocks: (*C*) Crn–Ky–eclogitic Cr–Ky–Omph–Grt, (*D*) Ky–Coe–eclogitic Ky–Coe–Omph–Grt, (*E*) Coe–Opx–eclogitic Coe–Opx–Omph–Grt

Crn–Omph–Grt–Ky (C), Ky–Omph–Grt–Coe (D) and Coe–Omph–Grt–Opx (E) belong to the basic compositions. It should be remarked, that xenoliths of ultrabasic olivine eclogites are exceptionally rare (Dawson 1980) or missed in kimberlites (Mathias et al. 1970). At the same time, the olivine eclogites are reasonably representative for xenoliths of the less deep upper-mantle spinel-peridotite facies.

The upper-mantle peridotitic rocks have been to a variable degree differentiated and depleted with alkaline, ferriferous and other low-melting components. This was bound up with partial melting of hypothetic primary rock and redistribution of the low-melting components into the melts. As a consequence, relatively refractory restitic peridotitic rocks were occurred and carried out by kimberlitic magmas as xenoliths to the Earth's crust. This consideration was taken into account at elaboration of a pyrolite model of the undepleted chemical composition of the upper

mantle primary rock (Ringwood 1975). The xenoliths of least depleted garnet lherzolites have been also considered as the natural specimens of the upper-mantle primitive rock (Takahashi 1986).

All of the peridotite-pyroxenite conversions from garnet dunite via garnet harzburgites and lherzolites to garnet websterites, garnet oethopyroxenites and garnet clinopyroxenites are demonstrated by xenoliths of the upper-mantle rocks in kimberlites (Dawson 1980). Complete peridotite-pyroxenite modal transitions as the markers of fractional crystallization have been disclosed in the pipe Matsoku (Harte et al. 1975).

Bimineralic omphacite-garnet varieties comprise 78% and predominate among basic eclogitic rocks of the garnet-peridotite facies (Mathias et al. 1970; Dawson 1980). High aluminous corundum, kyanite and corundum-kyanite eclogites and grospydites are reasonably representative (18%), but opthopyroxene and coesite eclogites are less common (4%). The accessory minerals of the garnet-peridotite facies are Cr-spinel, coesite, sanidine, sillimanite, orthopyroxene, kyanite, corundum, rutile, ilmenite, pyrrhotite, pyrite, chalcopyrite, pentlandite, djerfisherite.

Relative proportions of xenoliths of the ultrabasic and basic upper-mantle-rocks in kimberlites of South Africa and Yakutia make it possible to establish that 95% of them are peridotitic-pyroxenitic and only 5% eclogitic (MacGregor and Carter 1970; Ringwood 1975). Xenoliths of pyroxenites dominate in the pipe Matsoku (Lethoto). The exceptions are represented by the kimberlitic pipes Roberts-Victor (South Africa) with 20% of ultrabasic and 80% of eclogitic xenoliths as well as Bobbeyan and Ritfonstein (South Africa), Orapa (Botswana), Garnet-Ridj and Mozes-Rock (USA), Zagadochnaya (Yakutia) with eclogite xenoliths predominantly or completely (Dawson 1980). The examples of a radical predominance of eclogite xenoliths over peridotite ones in the upper-mantle composition testify that both peridotites so eclogites may be served as the enclosing rocks for the reservoirs-chambers of parental melts for diamonds and associated phases.

At the complex diagram of peridotite-pyroxenite-eclogite system Ol–Cpx/Omph–Crn–Coe (Fig. 2.2), the ultrabasic peridotite-pyroxenite Ol–Opx–Cpx–Grt (A) and eclogite Ol–Cpx–Grt–Crn (B) simplexes are supplemented by the basic simplexes Crn–Omph–Grt–Ky (corundum-kyanite eclogites) (C), Ky–Omph–Grt–Coe (kyanite-coesite eclogites) (D) and Coe–Omph–Grt–Opx (coesite-orthopyroxene eclogites) (E). The high aluminous grospydites are crucially distinguished from kyanite eclogites for a higher content (more than 50%) of the grossularite component in garnet. Eclogites are comparable with basalts by contents of their major components. On the basis of high-pressure experimental data on subsolidus transformations of basalts into eclogite, it was assumed (Yoder and Tilley 1962) that each of the main basalts type has the chemically equivalent eclogite. However it was pointed out essential difference between basalts and eclogites of the garnet-peridotite facies, which are in a noticeable content of potassium component in basalts with a negligible quantity in eclogites (Forbes 1965). Evidence that the compositions of mantle eclogites and basalts are not equivalent was repeatedly considered (Dawson 1980; Snyder et al. 1997). These features have assumed an obvious significance in the context of the problem of

origin of basic eclogite rocks of the upper mantle during differentiation of primary ultrabasic magmas generated by the primitive garnet lherzolites (pyrolites). The potentialities of these processes in the regime of fractional evolution of ultrabasic-basic magmas are supported by the smooth trends for the change in contents of characteristic components at clinopyroxenes and garnets of peridotites, pyroxenites and eclogites of the garnet peridotite facies (Sobolev 1977; Marakushev 1984). Alternatively, the subduction version of origin for eclogites of the upper mantle and the deeper mantle basic rocks from the oceanic basalts material is substantiated. A certain supporting for the subduction version was arose by idea of "eclogitic thermal barrier" (O'Hara and Yoder 1967; O'Hara 1968) evolved from experimental studies of the upper mantle systems with simplified "model" compositions. The idea is a peculiar kind of physico-chemical blockade to a possibility for ultrabasic-basic evolution of the upper-mantle magmas.

Along with this, an experimental discovery of the effect of olivine garnetization owing to its reaction with jadeite component at pressures of higher 4.5 GPa (Gasparik and Litvin 1997) makes possible to come afresh to solution of the problem of ultrabasic-basic magmatic evolution of the native silicate substance and diamond-producing silicate-(±oxide)-carbonatite melts of the upper mantle (Litvin 2012; Litvin et al. 2016).

2.2 Transition-Zone and Lower-Mantle Petrology from High-Pressure Experiments

The plausible evidence for xenoliths of native lower-mantle rocks which are accessible for analytical investigations remains unknown (Stachel et al. 2005). Discrete mineralogical data for the transition-zone substance have received in studies of chromitites from the peridotite complex Luobusa (Tibet) which had been transferred to the Earth's surface along the boundary between Indian and Asian blocks. Inside the chromitites the primary inclusions of metamorpfic microdiamonds, siliceous rutile and coesite were identified; there was also crystallographic evidence of transition-zone wadsleite in the form of "retrograde olivine" (Satsukawa et al. 2015). Initially the data of testing experiments on phase transformations of the upper-mantle minerals under high pressure were used for evaluation of a probable lower-mantle mineral assemblage (Ringwood 1975). It has been obtained that the lower-mantle matter can be composed of periclase MgO—29, stishovite SiO_2—22, $(MgSiO_3{\cdot}Al_2O_3)_{ss}$ of ilmenite structure—24, $(CaSiO_3{\cdot}FeSiO_3)_{ss}$ of perovskite structure—23, $NaAlSiO_4$—2 (wt%). In this case it was allowed that the chemical composition of the primitive upper-mantle garnet peridotite may be cited as a typical representative of the whole mantle deep-seated material.

The hypothesis for isochemical composition of the primitive mantle at all depths was used as a basis for the experimental testing subsolidus phase transformations of hypothetical garnet pyrolite and natural garnet lherzolites at pressures of

25–45 GPa (Takahashi 1986; Wood 2000; Hirose 2002). It was demonstrated that wadsleite Wd and ringwoodite Rw (both are Mg_2SiO_4 polymorphs) and majoritic garnet Maj $Mg_3(Fe,Al,Si)_2(SiO_4)_3$ represent the most probable ultrabasic rock-forming minerals of the transition-zone with their contents (wt%) $(Wd{\leftrightarrow}Rw)_{57}Maj_{43}$ at 450–550 km depths and, respectively, $Wds_{57}Maj_{37}Cpx_6$ at 410 km border with the upper mantle and $Rw_{57}Maj_{36}CaPrv_7$ at 670 km border with the lower mantle. Therewith ferropericlase FPer (Mg,Fe)O, bridgmanite Brd (Mg,Fe)SiO_3 and Ca-perovskite CaPrv $CaSiO_3$ may be the rock-forming minerals of lower-mantle ultrabasic rock $FPer_{17}FBrd_{70}CaPrv_{13}$ (Akaogi 2007). Bridgmanite as a high-pressure mineral of the composition (Mg,Fe)SiO_3 takes its name in 2014 from a detection in a shocked meteorite and structural determination (Tschauner et al. 2014). Earlier bridgmanite was named as "Mg-perovskite" for as mineral inclusions inside ultra-deep diamonds so experimentally justified phases of corresponding chemical composition. It turned out that stishovite Sti SiO_2 is absent among subsolidus phases in the testing experiments with the use of ultrabasic garnet lherzolite and pyrolite compositions. This may be considered as evidence that formation in situ of stishovite does not proceed in the lower-mantle ultrabasic material.

A pressure range of the experiments includes the major seismic boundaries "upper mantle–transition zone" (410 km) and "transition zone–lower mantle" (670 km) at pressures 13–14 and 23–24 GPa, respectively. In the experiments with pyrolites it has been found that the upper-mantle rock-forming mineral may be represented by olivine $(Mg,Fe)_2SiO_4$, orthopyroxene (Mg,Fe)SiO_3, clinopyroxene $Ca(Mg,Fe,Na)(Si,Al)_2O_6$ and pyropic garnet $(Mg,Fe,Ca)_3(Al,Cr)_2Si_3O_{12}$ with their proportions in the upper-mantle peridotite $Ol_{59}Opx_{19}Cpx_{10}Grt_{12}$ (Akaogi 2007). Olivine undergoes a polymorphic transition into the denser wadsleite that is responsible for formation of the 410 km seismic disruption. The 520 km seismic disruption is created by the polymorphic transition of wadsleite into ringwoodite inside the transition zone. At higher pressure, ringwoodite Rw $(Mg,Fe)_2SiO_4$ must be broken down into the assemblage of ferropericlase FPer (Mg,Fe)O and bridgmanite FBrd (Mg,Fe)SiO_3 that should determine the 670 km seismic disruption. Moreover, the conversion of ringwoodite may be responsible for more than 60 vol% petrological composition of the lower mantle.

Under the transition zone conditions, the crystal chemical reactions of the opthopyroxene and clinopyroxene components are activated during their dissolution in garnet with formation of the majoritic garnets solid solutions with the components as majoritic MgMaj $Mg_4Si_4O_{12}$ (Ringwood and Major 1971) as Na-majoritic NaMaj $Na_2MgSi_5O_{12}$ (Dymshits et al. 2010; Bobrov et al. 2011; Bobrov and Litvin 2011). Majoritic garnet together with wadsleite↔ringwoodite phases within the pressure 16–17 GPa interval becomes the determining phases of the transition zone ultrabasic rocks. Within 20–26 GPa the majoritic garnet solid solutions have been experienced in phase transformations with formation and liberation of the (Mg,Fe,Al)-bridgmanite and Ca-perovskite. Hence on testing experimental data grounds, mineralogy of the lower mantle upper horizons is mainly determined by ferropericlase, bridgmanite and Ca-perovskite.

The assumed mineralogy of the transition zone and lower mantle material of a subduction origin can be arrived from experimental studies of subsolidus phase relations of the mid-ocean ridge basalts (MORB) at pressures of 25–45 GPa (Irifune and Ringwood 1993; Hirose et al. 1999; Ono et al. 2001; Akaogi 2007). As a result it was established that stishovite, Ca-perovskite, bridgmanite and aluminous phases based on $Mg_2CaAl_6O_{12}$ component (in the absence of the periclase-wustite solid solution phases) are most probable as the rock-forming minerals of the hypothetic transition-zone basic rocks. The experimental data on subsolidus transformations of the MORB basalts have drawn to a substantiation of the version that stishovite represents a subducted mineral of the transition zone and lower mantle but not a mineral capable to be formed in situ from the native material of the lower mantle. Hence the subduction mantle mineralogy is taken as an adjunct to the native in situ mineralogy of the transition zone and lower mantle. Therewith it is allowed that stishovite formation could proceed in association with ultra-deep diamonds and other minerals originated from the oceanic crust while the crust blocks have been subducted to the transition zone and lower mantle depths (Ono et al. 2001; Stachel et al. 2005; Walter et al. 2008). At the same time, it is necessary to point out the essential indicatory importance of the presence of ferropericlase and bridgmanite for the ultrabasic whereas stishovite for the basic rocks of the Earth's lower mantle.

2.3 Primary Mineral Inclusions in Upper-Mantle Diamonds

Analytical mineralogy of heterogeneous inclusions in diamonds has been turned out as the result of intense microprobe investigations (Meyer and Boyd 1972; Sobolev 1977; Navon et al. 1988; Schrauder and Navon 1994; Zedgenizov et al. 2004; Titkov et al. 2006; Logvinova et al. 2008). The generality of the growth melts for diamonds and paragenetic phases-inclusions has substantiated. A paragenetic fixation of the starting positions of diamonds and associated phases is exhibited by the primary inclusions in diamonds, diamond-bearing peridotites and eclogites, and accrete specimens of upper-mantle minerals and diamonds.

High residual pressure inside the hermetic inclusions in diamonds also points to the generality of the parental melts of diamonds and their inclusions as well as to their genesis at PT-conditions of diamond stability. The residual pressure is remained in the hermetic cameras of mineral inclusions in diamonds after their cooling to normal temperature during transportation by kimberlitic magma from the mantle depths to the Earth's crust. Diamond-formation pressures of 5–7 GPa at 1000–1400 °C were calculated from the residual pressures of 1.5–2.5 GPa which have been determined for hardened carbonatite melt multiphase inclusions with solid and liquid phases of volatile compounds (Navon 1991). The pressure of coesite entrapment by growing diamonds is estimated as 5.5 ± 0.5 GPa at 1210 °C from the residual pressure of 3.62 ± 0.18 GPa in the inclusion (Sobolev et al.

2000; Fursenko et al. 2001). Residual pressures were reported for monocrystalline graphite (Glinnemann et al. 2003) and olivine (Nestola et al. 2014; Angel et al. 2015) included in diamonds. The residual pressures within primary inclusions are unambiguously evidenced that the inclusions were trapped from the growth melts for diamonds and associated phases. Nevertheless, a paragenetic or xenogenetic origin of mineral phases inside inclusions is only possible to ascertain with the use of physico-chemical experiments. The residual pressure in inclusions allows to calculate the conditions of their entrapment, which correspond to PT-parameters of thermodynamic stability of diamond.

Chemical compositions of mineral inclusions in the natural upper-mantle diamonds demonstrate that chemically varied minerals and melts with dissolved volatiles have been trapped by the growing diamonds as the primary (syngenetic) inclusions. Among syngenetic inclusions (synchronous caption) there are disclosed as paragenetic (grown with diamond in common parental melts) so xenogenetic (outside newcomers into parental melts) mineral phases belonging to peridotite-pyroxenite and eclogite parageneses. The facts testify that diamond crystal growth have been proceeded in parental melts of extremely changeable ultrabasic and basic compositions.

Mineral inclusions in the upper-mantle diamonds demonstrate that the diamond-parental media are compositionally highly variable, with respect to the major silicate-oxide components especially. Among the basic mineral inclusions, omphacite Omph and garnet Grt of eclogitic paragenesis are most abundant whereas corundum Crn, kyanite Ky, coesite Coe and orthopyroxene Opx are rare in occurrence. Olivine Ol, orthopyroxene Opx, clinopyroxene Cpx, garnet Grt, Cr-spinel CrSpl inclusions belong to peridotitic paragenesis. Accessory assemblages include magnetite Mag, ilmenite Ilm, rutile Rt, zircon Zrn, chromite Chr as well as pseudomorphs of quartz Qtz and phlogopite over coesite and olivine, respectively. Sulfide minerals pyrrhotite Po, pentlandite Pn, pyrite Py, chalcopyrite Cpy, Cu-Fe-Ni-monosulfide solid solutions Mss belong to the abundant inclusions in diamonds whereas djerfisherite Dj is rare. It can be seen that diamond-hosted minerals are analogous to the rock-forming and characteristic accessory mineral phases of the native peridotite-pyroxenite and eclogite rocks of the upper mantle. Carbonate minerals magnesite Mgs, dolomite Dol, siderite Sd, calcite Cal (as a polymorphic product of aragonite Arg) are not common (Schrauder and Navon 1994; Wang et al. 1996; Stachel et al. 1998; Titkov et al. 2006). Native metals iron Fe^0 and alloys of iron with Cr and Ni $FeNi^0$ as well as moissanite Mois SiC are rare in occurrence (Sobolev et al. 1981; Leung et al. 1990, 1996; Mathez et al. 1995).

The multicomponent heterogeneous inclusions in diamonds of silicate-carbonate substance with volatile compounds (Schrauder and Navon 1994; Izraeli et al. 1998, 2001; Logvinova et al. 2003; Navon et al. 2003; Klein-BenDavid et al. 2003, 2006, 2007a, b; Zedgenizov et al. 2004, 2009, 2011) adequately characterize the solidified products of the major components and phases for the diamond-producing parental melts. Investigations of a variety of phases included in diamonds makes it possible to establish that these inclusions represent oxide, silicate, carbonate, phosphate apatite Ap, sulfide, chloride, carbide, native metal micro-minerals and

rarely-occurred silicate-carbonate (carbonatitic) hardened melts. The inclusions occasionally contain the solitary phases of volatile components CO_2, CH_4, H_2O and K-Na-chloride-water brines. The silicate-carbonate substances of inclusions in Botswanian diamonds have approximated by two boundary carbonatic and silicisic compositions (Schrauder and Navon 1994). There also were calculated the average compositions of the alkaline-chloride-water brines included into diamonds of the Koffifontein pipe (Izraeli et al. 2001). Compositionally similar inclusions of the hardened melts are occasionally observed in association with the primary inclusions of peridotite and eclogite minerals (Izraeli et al. 1998; Logvinova et al. 2003). It is significant that the hardened melts were turned out to be similar to the inclusions in diamonds together with as the P-type (peridotitic) so the E-type (eclogitic) minerals. Studying the inclusions of the probable hardened silicate-carbonate melts led to a cautious suggestion that the melts were trapped by the growing diamonds and would constitute the carbon-bearing melt-solutions from which diamonds were able to crystallize (Navon 1999). Hardened Fe-Ni-sulfide melts have discovered as inclusions in diamonds together with the hardened carbonatite melts and peridotite minerals (Klein-BenDavid et al. 2003).

Paragenetic with diamond minerals of peridotites and eclogites that crystallized from the growth melts could be trapped together with the completely miscible silicate-carbonate-carbon parental melts (Litvin 2007, 2012). With this the growing diamonds have a chance of trapping xenogenetic sulfide and titaniferous ilmenite Ilm and rutile Rt melts which are completely immiscible with carbonatitic growth melts. The trapping of inclusions has been came to the end by their hermetization with growing layers and subsequent hardening the growth melts under cooling of the diamond-producing mantle reservoirs-chambers. Xenogenetic sulfide melts have also been hardened. Volatile components have been emitted from hardening carbonatite melts and could create the gas phases and alkaline-chloride-water brines. By this means a complete dissoluble state of the volatile components in diamond-parental melts-solutions but existence of own volatile phases inside the hardened parental melts materials in the diamond-hosted inclusions.

Thus, primary mineral inclusions in the upper-mantle diamonds belong to the peridotite–pyroxenite (olivine, orthopyroxene, clinopyroxene, garnet, spinel, Mg–Fe ilmenite, etc.) and eclogite–grospydite (omphacitic clinopyroxene Omph, garne Grtt, chromite Chr, ilmenite Ilm, sanidine Sa, corundum Crn, kyanite Ky, coesite/quartz Coe/Qtz, rutile Rt, etc.) assemblages. In fact, the mineralogical data characterize the bulk composition of the medium parental for diamond and syngenetic inclusions as the multicomponent system MgO–CaO–FeO (Fe, Fe_2O_3)–MnO–NiO (Ni)–Na_2O–K_2O–Al_2O_3–Cr_2O_3–(Cr)–TiO_2–ZrO_2–SiO_2–P_2O_5–CuS (Cu_2S)–FeS (FeS_2)–NiS–KCl–NaCl–SiC–Fe_3C–CO_2 (CO, CH_4)–H_2O–C. Wide variability of chemical and phase compositions of the parental media ranging from peridotite with modal olivine to eclogite with modal coesite, kyanite, and corundum is one of its main features. The carbonatite component of the parental media is also variable, primarily with respect to its alkalinity (Schrauder and Navon 1994). The components and phases of volatile compounds are also diverse (Izraeli et al. 2001). It has been established that the substances of primary inclusions in diamonds are

derivatives of separate mantle media, and this circumstance comes into conflict with the assumption that primary inclusions are products of the direct entrapment of fragments of the upper-mantle peridotites and eclogites by growing diamonds (Sobolev 1977; Taylor and Anand 2004; Spetsius and Taylor 2008). To all appearances, the mantle peridotite is the main source of silicate components of parental media at the initial stage of their formation with participation of alkaline C–O–H-bearing metasomatic agents (Litvin 1998).

Mineralogical methods cannot establish genetic relationships between diamond and mineral phases initially entrapped therein, and thus an unbiased and reliable chemical mode of diamond formation in the natural multicomponent heterogeneous medium cannot be proved. Diamond crystallization in silicate (Williams 1932), metallic (Wentorf and Bovenkerk 1961), carbonate (Von Eckermann 1967), sulfide (Marx 1972), or C–O–H volatile (Haggerty 1986) growth media were suggested, but none of these suggestions deduced from mineralogical evidence has gave rise to a reliable solution. Almost all of the substances pertaining to the heterogeneous multicomponent parental medium were assumed to be a possible diamond-bearing media. The diamond-forming capability of mantle melts and genetic relationships between mineral phases of natural diamond-producing systems can only be established by physico-chemical experiments at high pressure and temperature. The testing experiment is the most important at the initial stage of experimental research concerned with diamond origin.

2.4 Primary Mineral Inclusions in Transition-Zone and Lower-Mantle Diamonds

Diagnostics of mineral inclusions for the asthenosphere and transition zone derived diamonds is essentially complicated due to a reversible polymorphism of wadsleite Wd and ringwoodite Rw, both of $(Mg,Fe)_2SiO_4$ composition, with the formation of "retrograde" olivine. Also, low-Ca clinopyroxenes transform into orthopyroxenes due to temperature lowering during transportation of diamonds from their mantle reservoirs-chambers to the Earth's crust. All this is conditioned by the diminution of diamond and inclusion thermal expansion and corresponding pressure reduction within the hermetic cameras with inclusions. At high-pressure experiments with the pyrolytic compositions (Akaogi and Akimoto 1979) it has determined that the contents of Al_2O_3 higher than 0.3 wt% in wadsleite and the more in ringwoodite are the indications which allow to bring them in correlation with the transition zone mineralogy. The transition zone majoritic garnets are also disequilibrated and partially transformed into the assemblage of garnet and pyroxene under the upper mantle conditions. The exsolution of pyroxene from majoritic garnet have been evidenced in the inclusion in diamond and at the majorite-bearing rock (Bobrov and Litvin 2011). Nevertheless the inclusions of majorite garnets in diamonds may only be operable as acceptable indicators of the genesis of diamond and associated

phases under conditions of the transition zone (Stachel et al. 2000a, b; Stachel 2001). Their compositions are not sufficiently differ from the lithospheric eclogitic and astenospheric majoritic garnets, with the exception of elevated siliceousty, the tendency for increase at contents of Na and Ti components and decrease at concentration of Fe components.

Identification of the transition zone majoritic garnets from inclusions in the deep mantle derived diamonds has been made possible by the barometric effect which is caused by near-linear increasing of the excess-Si content in garnets within 7–15 GPa interval at 1200 °C. This effect is demonstrated when experimental results (Akaogi and Akimoto 1979; Irifune 1987; Gasparik 2002) and mineralogical data for inclusions in diamonds of the Monastery and Jagersfontein pipes (South Africa), the placers of the regions of Kankan (Guinea) and Juina (Brazil), and some others sources has been composed (Stachel et al. 2005).

Experimental studies at 6–20 GPa and 1800–2100 °C of the system pyrope—Na-majorite (Dymshits et al. 2010; Bobrov and Litvin 2011) made possible to synthesize Na-bearing majoritic garnets which composition is characterized with a regular increase of the Na-majoritic component $Na_2MgSi_5O_{12}$ from 5 mol% at 8 GPa up to 32–38 mol% at 20 GPa. These results are in agreement with the data of experimental investigation of the system forsterite–jadeite up to 22 GPa (Gasparik and Litvin 1997) which allow to reveal the effect of forsterite garnetization during the reaction of forsterite and jadeite components at pressures higher 4.5 GPa. Moreover, the high contents of Na-majorite component up to 40 mol% have determined in the resultant garnets at 22 GPa. The thermobarometric properties of the Na-majoritic garnet solid solutions have made an identification of the transition-zone majoritic garnets by Na_2O contents (Bobrov and Litvin 2011). The majoritic garnets of the transition zone ultrabasic rocks can be distinguishing by a high content of Cr_2O_3 (up to 14 wt%). The concentration of earths in majoritic garnets distinguishes markedly them from the mid-ocean basalts enriched with the light rare elements and C–O–H–N volatile components (Palot et al. 2014).

Determination of mineral inclusions inside the lower mantle ultra-deep diamonds is relatively more simply from the fact that their chemical and structural peculiarities would be basically conserved during transportation to the Earth's crust. Ultrabasic primary inclusions in the lower-mantle diamonds are presented by periclase-wustite solid solution phases FPer $(MgO{\cdot}FeO)_{ss}$, bridgmanite FBrd (Mg, Fe)SiO_3, and Ca-perovskite $CaSiO_3$ CaPrv (Harte and Harris 1994; Stachel et al. 2000a, b, 2005; Kaminsky et al. 2001; Zedgenizov et al. 2014). The phases included in super-deep diamonds are analogous to the anticipated major rock-forming minerals of the lower-mantle rocks which have justified by experimental transformation of the upper-mantle garnet lherzolites or hypothetic pyrolites (Akaogi 2007). Inclusions of ferropericlase as separate grains less than 1 mm or intergrowths with bridgmanite and Ca-perovskite are the most frequent. An important marker for belonging of other minerals to ultrabasic lower-mantle assemblage is their syngenesis with ferropericlase and (Mg,Fe)-bridgmanite in super-deep diamond-hosted inclusions. Among these minerals is tetragonal almandine-pyrope phase $(Mg,Fe)(Al,Cr,Mn)_2(Mg,Fe^{3+})_2Si_3O_{12}$ (TAPP) (Kaminsky

2012). Along with this, it was noticed (Stachel et al. 2005) that the TAPP phases are chemically different as compared with the common peridotitic garnets by the nearly complete absence of Ca-components at their composition (less than 0.1 wt% CaO). Besides, the TAPP density is less than that measured for garnet under the lower mantle conditions. All this permits to suggest that the TAPP mineral is a "retrograde" phase stabilized at influence of the high ratio Fe^{3+}/Fe^{2+} during diamonds transfer over the transition zone depths. In this case it may be demonstrative the TAPP samples within inclusions of diamonds from the Kankan alluvial deposits (Guinea). The unit grains of titaniferous Ca-perovskites associated with ilmenite, non-identified Si–Mg-phase and majoritic garnet have discovered as inclusions in diamonds from the Juina placers (Brazil) (Kaminsky et al. 2001). The main admixture in the majoritic garnet composition is presented by Na-component at a typical concentration of 0.27–1.12 wt% Na_2O (Kaminsky 2012). The majoritic garnets may appear among mineral association of most upper horizons of the lower mantle that is well consistent with experimental data on their stability (Irifune and Ringwood 1993). The inclusions with compositions of olivine, magnetite, titanite Ttn, picroilmenite PIlm and manganoilmenite, spinel and Cr-spinel, as well as sulfides bornite Bn, violarite Vio and heazlewoodite Hz, carbides chalipite Chal and cogenite Cog, native iron, nickel and alloy haxonite Hax are also referred to the ultrabasic lower-mantle association.

It is paradoxical that the basic mineral stishovite SiO_2 from inclusions in the lower-mantle diamonds from the kimberlite pipes and ancient placers of Juina (Brazil), Kankan (Guinea), Slave (Canada) and Koffifontein pipe (South Africa) is in an intimate association with the phases of periclase-wustite solid solutions $(MgO{\cdot}FeO)_{ss}$ (Hayman et al. 2005; Harte 2010; Kaminsky 2012). The assemblage of stishovite with ferropericlase and bridgmanite in common inclusion is not infrequent. The complex bimineral inclusions in the forms of intimate paragenetic intergrowths of stishovite and phases of peridotite-wustite solid solutions have been discovered. The paragenetic association of stishovite SiO_2 and ferropericlase (Mg, Fe)O, which is definitely the lower mantle in situ mineral, is obviously indicative that stishovite is also the lower-mantle in situ phase (as in the case of ultradeep diamonds with inclusions of these minerals).

The paragenetic coexistence of stishovite and mineral phases of periclase-wustite solid solutions $(MgO{\cdot}FeO)_{ss}$ in hermetical inclusions within the lower-mantle diamonds put down to the effect of "stishovite paradox" (Litvin 2014). The major consideration is in that an origination of the paradoxical paragenetic assemblage $SiO_2 + (MgO{\cdot}FeO)_{ss}$ is inherent of stishovite exclusively. In contradiction to stishovite, the other lower-pressure SiO_2 polymorphs quartz and coesite can react with the MgO and FeO oxides with the formation of stable intermediate compounds —enstatite $MgSiO_3$ and ferrosilite $FeSiO_3$ as well as their continuous solid solutions $(MgSiO_3{\cdot}FeSiO_3)_{ss}$ under PT-conditions of the Earth's crust, upper mantle and transition zone. For this reason, the association of quartz (coesite) and (Mg,Fe)-oxides is believed to be "under a ban" for the conditions of the Earth's crust and upper mantle.

A ferriferousity of the periclase-wustite solid solution phases inside inclusions in the lower mantle ultradeep diamonds is variable over a wide range (fe = 0.10–0.64). The ferriferousity values for the lower mantle plausible composition are bound to be within fe = 0.12–0.27 on experimental and rating assessments (Wood 2000; Lee et al. 2004). Inasmuch as it is reasoned that the native lower mantle minerals have been included into diamond, the obvious inconsistency of this sort was explained by the subsolidus reaction of bridgmanite decomposition to ferriferous phase of the periclase-wustite solid solutions $(MgO{\cdot}FeO)_{ss}$ and SiO_2 (Fei et al. 1996). Most probably, a large ferriferousity change for periclase-wustite mineral inclusions paragenetic to diamond-hosts can result from the fractional ultrabasic-basic evolution of grown melts which are parental for diamonds and associated phases. As this takes place under the lower mantle conditions, a paradoxical assemblage of Mg–Fe-oxides and stishovite SiO_2 is formed as the result of the physico-chemical mechanism of "stishovite paradox" (Litvin 2014). This is agreed with existence of the unlimited periclase-wustite solid solutions in the MgO–FeO system at the lower mantle pressures.

Stishovite together with (Mg,Fe,Al)-bridgmanite and Ca–Na-perovskite should be related to basic inclusions in the lower mantle diamonds taking into account the experimental subsolidus transformations of the mid-oceanic basalts (Akaogi 2007). Their belonging to the basic in situ association of mineral inclusions in the lower-mantle diamonds may be established with the use of the definite typomorphic indicators (apart from their paragenetic association with stishovite). For the basic bridgmanites it may be a relatively higher content of Al_2O_3 which is close to 10 wt % by comparison to the less than 3 wt% Al_2O_3 for the ultrabasic bridgmanites (Stachel et al. 2005), that is commensurable to the real values of 8.3–12.6 wt% Al_2O_3 for the bridgmanite inclusions in diamonds of the Sao-Luis alluvial placers (Brazil) (Harte et al. 1999). The (Mg,Fe,Al)-bridgmanites are characterized by elevated ferriferousity. This is also consistent with the data of experimental studies at 24–26.5 GPa on subsolidus garnet-to-bridgmanite reaction in the system $MgSiO_3$–$Mg_3Al_2Si_3O_{12}$ (Irifune et al. 1996). The reaction is resulted in formation of bridgmanite enriched in Al_2O_3 and applicable to simulation of the compositional relationship over the boundary between the transition zone and lower mantle. At the same time, the Al_2O_3 content in Ca-perovskites are notably low (0.01–0.66 wt% Al_2O_3) for both ultrabasic and basic Ca-perovskites from inclusions in the lower mantle diamonds. The positive Eu-anomaly which is supposedly related to the basic association (Kaminsky 2012) has been detected within the rare earths distribution patterns for some inclusions. The Ca-perovskites with relatively elevated contents of Na- and K-components, magnesiowustites (Fe,Mg)O and aluminous phase "Egg" of $AlSiO_3{\cdot}OH$ composition may be assigned to the basic paragenesis. Hence the primary inclusions in the lower-mantle diamonds testify that not only ultrabasic but also basic stishovite-bearing associations have been involved into the in situ diamond-producing processes. The primary inclusions make also it apparent that the ultrabasic-basic evolution of the lower-mantle "ultradeep" diamonds is the realistic natural process. This conclusion may be carried over the transition-zone growth melts for diamonds and associated phases.

The combined and mutually complementary data of analytic mineralogy of primary inclusions in diamonds and results of physico-chemical experimental studies on the diamond-producing systems give sufficient proof of the concept of physico-chemically similar mechanisms which are responsible for genesis of diamonds and associated phases at all mantle depths. The obtained conclusions are contradictory to alternate hypotheses on the subduction transfer of the basic oceanic crust, including the ultradeep diamond-producing components, into the ultrabasic lower mantle. The primary inclusions of variable carbonate minerals especially aragonite Arg $CaCO_3$, dolomite $Ca(Mg,Fe)(CO_3)_2$ Dol, nyererite Nyer $Na_2Ca(CO_3)_2$, nahkolite Nah $NaHCO_3$ in the transition zone and lower mantle ultradeep diamonds (Brenker et al. 2010; Stagno et al. 2011; Kaminsky 2012) are symptomatic as the crystallization products of the multicomponent oxide-silicate-carbonate-carbon parental melts for diamonds and heterogeneous primary inclusions. This circumstance makes it possible to attack the problem of ultradeep diamonds origin within the framework of the mantle-carbonatite concept of diamond genesis (Litvin 2007, 2009, 2013; Litvin et al. 2012, 2014).

2.5 Xenoliths of Diamond-Bearing Rocks in Kimberlites

Highly differentiated ultrabasic peridotite-pyroxenite and basic eclogite-grospydite rocks are presented as the upper-mantle xenoliths in kimberlitic pipes of South Africa, Yakutia, Australia, Northern America, the northern European region of Russia and other provinces. In the main, the xenolitic rocks are diamond-free but occasionally diamond-bearing peridotites, pyroxenites, eclogites, and grospydites have occurred among them. Diamond-bearing basic rocks in 1–2 order dominate over the ultrabasic ones. Thereto the peridotitic rocks dunites and harzburgites prevail over lherzolites, pyroxenitic garnet websterites over verhlites, and eclogitic bimineral variety over corundum, kyanite, coesite eclogites and grospydites. The weight for a majority of diamond-bearing xenoliths is about 50–70 g. The greatest samples are eclogites from kimberlite pipes Roberts Victor, South Africa (8.6 kg) (Jacob and Jagoutz 1994), Udachnaya, Yakutia (6.9 kg) (Shatsky et al. 2008) and 8.8 kg (Stepanov et al. 2007, 2008).

Serpentinized diamond-bearing peridotites have been found in kimberlitic pipe Aikhal, Yakutia (Sobolev et al. 1969). The rock-forming garnets demonstrate high Cr_2O_3, moderate CaO contents and low ferriferousity (14.3 wt%) that is completely identical to the garnets from inclusions in diamonds (Sobolev 1977). Later on, the xenolith of diamond-bearing peridotites with retaining olivine were disclosed including dunite (Ilupin et al. 1982), harzburgite (Logvinova et al. 2005), lherzolites (Griffin et al. 1993; Barashkov and Zudin 1997 Sobolev et al. 2008, 2009) and pyroxenite (Ponomarenko et al. 1980). It was also reported about investigations of the diamond-bearing peridotites xenoliths from the craton Slave, Canada (Creighton et al. 2008; Aulbach et al. 2011), pipes Finch, Roberts Victor and Premier, South Africa (Dawson and Smith 1975; Viljoen et al. 1992, 1994, 2004), Southern

Wyoming, USA (McCallum and Eggler 1976) and Udachnaya pipe, Yakutia (Logvinova et al. 2015).

Historically, the first finds of diamond-bearing rocks are represented by two xenoliths of eclogites with two and ten diamond crystals over its surfaces from the diamond-bearing pipe Newlands, Griqualand-West, South Africa (Bonney 1899, 1900). These samples are kept on deposit at the mineralogic museum of the Mining Academy in Freiburg (#№ 001508) and in the Natural History Museum in London (№ 84661), respectively. Later on, it was stated that diamond-bearing eclogites are found in the pipes Crawn, Djagerfontein, Roberts Victor, Premier, and repeatedly in Newlands, South Africa (Corstophine 1908; Wagner 1909, 1928; Holmes and Paneth 1936; Williams 1932). The sample of diamond-bearing eclogite rock is shown in the Fig. 2.3. Numerous diamond crystals and polycrystalline intergrowth of 80 diamond grains in a reasonably large-sized xenolith of diamond-bearing eclogite have been disclosed (Bartoshinsky 1960) as well as "eclogitic" composition of ferriferous garnet was first determined (Bobriyevich et al. 1959). Thereafter it has repeatedly reported of the new finds and investigations of diamond-bearing eclogites (Rickwood et al. 1969; Sobolev 1977; Spetsius and Taylor 2008; Sobolev et al. 2008; Taylor et al. 2000). Diamond-bearing corundum eclogites, coesite eclogites, grospydites have been found in kimberlites of South Africa and Yakutia (Sobolev and Kuznetsova 1965; Davidson 1967; Dawson 1968; Gurney et al. 1969; Switzer and Melson 1969; Rickwood and Mathias 1970; MacGregor and Carter 1970; Sobolev et al. 1974; Ponomarenko et al. 1976; Pokhilenko et al. 1982). Most of them was presented in the xenolith association of the Roberts Victor pipe that is a rare exception among kimberlitic pipes because of essential predominance of the diamond-free eclogitic xenoliths (more than 90 vol%) over the peridotitic ones.

Investigation of omphacite and garnes compositions from inclusions in diamond of diamond-bearing eclogite in a comparison with the compositions of rock-forming eclogitic minerals is extremely significant (Sobolev et al. 1972). The resulting data testifies that the minerals included in diamond, on the one hand, and the

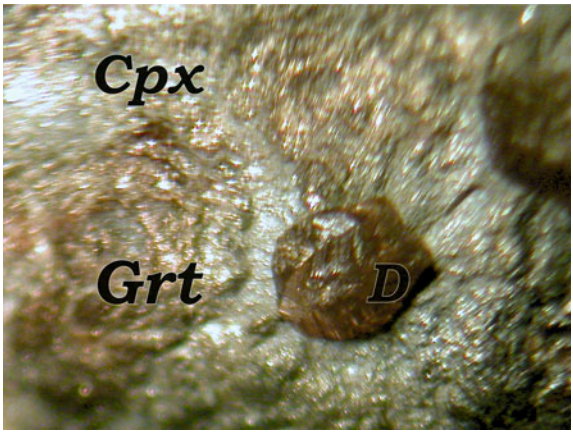

Fig. 2.3 Diamond-bearing eclogite

rock-forming minerals of the enclosing diamond-bearing eclogite, on the other hand, have closely analogous compositions and are typical for eclogite rocks. The FeO content in garnet from inclusion is somewhat higher than for the rock-forming eclogite but the K_2O content in omphacite from inclusion is considerably above than at the rock-forming omphacite. Most likely the original mineral compositions inside the hermetic inclusions is kept constant, whereas the eclogitic rock-forming minerals having most probably the same initial composition could partially change the FeO and K_2O contents in their open contacts to the transporting kimberlitic magmas with the volatile compounds. The K_2O content of omphacite in inclusion may be a marker of the K-component elevated concentration in the silicate-carbonate growth media of diamonds and associated mineral phases. This is in a good agreement with variable compositions of the hardened K-rich silicate-carbonatitic diamond-parental media of the fragmentary inclusions in Botswanian diamonds (Schrauder and Navon 1994) with the high diamond-forming efficiency which has been experimentally established (Litvin and Zharikov 1999, 2000). The role of the high-potassium growth melts for the upper-mantle origin of diamonds and associated phases has taken into account at the mantle-carbonatite concept of diamond genesis (Litvin 2012, 2013). The practical coincidence of garnets and omphacites chemical compositions in the case of the diamond-included and rock-forming eclogitic minerals is particularly remarkable fact. The coincidence is demonstrative in that the both rock-forming and diamond-hosted minerals are belonging to the overall mineral generation which phases have been originated in association with diamonds at their common silicate-carbonate parental melts with dissolved carbon.

A number of typomorphic indications of the diamond-bearing rocks and their rock-forming minerals allow to distinguish them from the native diamond-free rocks of the upper mantle. It was stated (Sobolev 1977) that garnets of the diamond-bearing peridotites have characterized with higher Cr_2O_3 and lessened CaO content in distinction to their diamond-free analogues. A similar behavior of Cr_2O_3 and CaO components is typical for garnet inclusions in diamonds as well as for the paragenetic accretions of peridotitic garnets with diamonds. Compared to the upper-mantle diamond-free eclogite rocks, garnets of the diamond-bearing eclogitic mineral assemblages are of higher Na_2O content (0.10–0.22 wt%) due to an admixed Na-majoritic component $Na_2MgSi_5O_{12}$ (Bobrov et al. 2011; Bobrov and Litvin 2011; Dymshits et al. 2013). A compositional resemblance of mineral inclusions in diamonds with rock-forming minerals of the diamond- bearing peridotites and eclogites is extremely significant. The typomorphic features are basically confirmed in the example of the rock-forming minerals and diamond-hosted mineral inclusions without the profound secondary alterations (Taylor and Anand 2004; Shatsky et al. 2008; Spetsius and Taylor 2008).

The diamond-bearing peridotites, pyroxenites, and eclogites have essential distinctions in compositions and origin by comparison with the native diamond-free differentiated ultrabasic-basic rocks of the garnet peridotite facies.

At all times mineralogical analyses of diamond-associated rocks, minerals and volatiles has been accompanied by the attempts to discern the natural chemical conditions of diamond formation. Disclosure in 1897 of first diamond-bearing

eclogites in south-African kimberlitic pipes gave rise to consider eclogitic magma as the diamond-parental medium (Bonney 1899). Speculations about potential diamond-producing silicate peridotitic and eclogitic magmas can be followed to till recently (Williams 1932; Meyer and Boyd 1972; Sobolev 1977; Marakushev and Bobrov 1998; Taylor and Anand 2004). The presumption of silicate diamond-parental chemistry was based on modal similarity of rock-forming minerals of upper-mantle peridotitic and eclogitic rocks with silicate phases of diamond-hosted inclusions. Much attention is given to kimberlitic version of diamond-parental magma (Sobolev 1960) due to the visible diamondiferousity of kimberlites that was actually happened as a consequence of diamonds capturing by kimberlitic magmas in transportation them from parental chambers to the crust pipes. The "brain attack" was also led to the versions of sulfide (Marx 1972), carbonatite (Von Eckermann 1967), C–O–H–fluid (Haggerty 1986), metallic (Wentorf and Bovenkerk 1961) diamond-forming natural media. But no one of the versions is beneath criticism because diamond-forming efficiency of these substances at melting cannot be detected by any one of analytical mineralogical methods. Moreover, diamond-forming efficiency of melts-solutions for all these and some other materials was disclosed in testing syntheses of diamonds. It was found that melts of some alkaline silicates, chlorides, and fluid phases of water and carbon dioxide are also effective. But all the tested materials associated with natural diamond do not match the requirements of the syngenesis criterium for diamonds and paragenetic phases.

References

Akaogi M (2007) Phase transitions of minerals in the transition zone and upper part of the lower mantle In: Ohtani E (ed) Advances in high-pressure mineralogy, Geological Society of America Special Paper 421, pp 1–13. doi:10.1130/2007.2421(01)

Akaogi M, Akimoto S (1979) High-pressure phase equilibria in a garnet lherzolite, with special reference to Mg^{2+}–Fe^{2+} partitioning among constituent minerals. Phys Earth Planet Inter 19:31–51

Angel RJ, Alvaro M, Nestola F, Mazzucchelli MI (2015) Diamond thermoelastic properties and implications for determining the pressure of formation of diamond-inclusion systems. Russ Geol Geophys 56(1–2):208–220

Aulbach S, Stachel T, Heaman LM, Carlson JA (2011) Microxenoliths from the Slave craton: archives of diamond formation along fluid conducts. Lithos 126:419–434

Barashkov YP, Zudin NG (1997) Composition of garnets with diamond inclusions from kimberlite pipe Krasnopresnenskaya (Yakutia). Geol Geofiz 38(2):353–357

Bartoshinsky ZV (1960) On diamonds from eclogites of the kimberlitic pipe Mir. Geol Geofiz 6:129–131

Bobriyevich AP, Bondarenko MN, Gnevushev MA et al (1959) Diamond deposits of Yakutia. Gosgeoltechizdat, Moscow

Bobrov AV, Litvin YA (2009) Peridotite-eclogite-carbonatite systems at 7.0–8.5 GPa: concentration barrier of diamond nucleation and syngenesis of its silicate and carbonate inclusions. Russ Geol Geophys 50(12):1221–1233

Bobrov AV, Litvin YA (2011) Mineral equilibria of diamond-forming carbonate-silicate systems. Geochem Int 49(13):1–97

Bobrov AV, Litvin YA, Dymshits AM (2011) Experimental studies of mantle carbonate–silicate systems and problem of the diamond formation. GEOS, Moscow, p 208

Bonney TG (1899) The parent rock of the diamond in South Africa. Geol Mag 6:309–321

Bonney TG (1900) Additional notes on boulders and other rock specimen from the Newlands Diamond Mines, Griqualand-West. Proc R Soc Lond 67:475–484

Brenker FE, Vollmer C, Vincze L et al (2010) Carbonates from the lower part of transition zone or even the lower mantle. Earth Planet Sci Lett 260:1–9. doi:10.1016/j.epsl.2007.02.038

Corstophine GS (1908) The occurrence in kimberlite of garnet-pyroxene nodules carrying diamonds. Trans Geol Soc S Afr 10

Creighton S, Stachel T, McLean H et al (2008) Diamondiferous peridotitic microxenolith from the Diavik Diamond Mine, NT. Contrib Miner Petrol 155:541–554

Davidson CF (1967) The so-called "cognate xenoliths" of kimberlite. In: Wyllie PJ (ed) The ultramafic and related rocks. New York, pp 269–278

Dawson JB (1968) Recent researches on kimberlite and diamond geology. Econ Geol 63(5): 504–511

Dawson JB (1980) Kimberlites and their xenoliths. Springer, Berlin

Dawson JB, Smith JV (1975) Occurrence of diamond in a mica-garnet lherzolite xenoliths from kimberlite. Nature 254:580–581

Dymshits AM, Bobrov AV, Litasov KD et al (2010) Experimental study of the pyroxene-garnet phase transition in the $Na_2MgSi_5O_{12}$ system at pressures of 13–20 GPa: first synthesis of sodium majorite. Dokl Earth Sci 434(1):1263–1266

Dymshits AM, Bobrov AV, Bindi L et al (2013) Na-bearing majoritic garnet in the $Na_2MgSi_5O_{12}$–$Mg_3Al_2Si_3O_{12}$ join at 11–20 GPa: phase relations, structural peculiarities and solid solutions. Geochim Cosmochim Acta 105(1):13. doi:10.1016/j.gsa.2012.11.032

Fei Y, Wang Y, Finger LW (1996) Maximum solubility of FeO in (Mg, Fe)SiO_2 perovskite as a function of temperature at 26 GPa: implication for FeO content in the lower mantle. J Geophys Res 101(B5):11525–11530

Forbes RB (1965) The comparative chemical composition of eclogite and basalts. J Geophys Res 70:1515–1521

Fursenko BA, Goryanov SB, Sobolev NV (2001) High pressures in coesite inclusions in diamond: combination scattering spectroscopy. Dokl Earth Sci 379:812–815

Gasparik T (2002) Stability of $Na_2Mg_2Si_2O_7$ and melting relations on the forsterite-jadeite join at pressures up to 22 GPa. Eur J Miner 9(2):311–326

Gasparik T, Litvin YuA (1997) Stability of $Na_2Mg_2Si_2O_7$ and melting relations in the forsterite-jadeite join at pressures up to 22 GPa. Eur J Mineral 9:311–326

Glinnemann J, Kusaka K, Harris JW (2003) Oriented graphite single-crystal inclusions in diamond. Z Kristallogr 218:733–739

Griffin WL, Sobolev NV, Ryan CG et al (1993) Trace elements in garnets and chromites: diamond formation in the Siberian lithosphere. Lithos 29:235–256

Gurney JJ, Siebert JC, Whitefield GG (1969) A diamondiferous eclogite from the Roberts Victor mine. In: Upper mantle project. Geological Society of South Africa Special Publication 2, pp 351–357

Haggerty SE (1986) Diamond genesis in a multiply-constrained model. Nature 520:34–38

Harte B (2010) Diamond formation in the deep mantle: the record of mineral inclusions and their distribution in relation to mantle dehydration zones. Mineral Mag 74(2):189–215

Harte B, Harris JW (1994) Lower mantle mineral association preserved in diamonds. Mineral Mag 58A:384–385

Harte B, Cox KG, Gurney JJ (1975) Petrography and geological history of upper mantle xenoliths from the Matsoku kimberlite pipe. Phys Chem Earth 9:477–506

Harte B, Harris JW, Hutchison MT et al (1999) Lower mantle mineral association in diamonds from Sao Luiz, Brazil. In: Fei Y, Bertka CM, Mysen BO (eds) Mantle petrology: field observations and high pressure experimentation: a tribute to Francis R. (Joe) Boyd. Geochemical Society Special Publication 6, pp 125–153

Hayman PC, Kopylova MG, Kaminsky FV (2005) Lower mantle diamonds from Rio Soriso (Juina area, Mato Grosso, Brazil). Contrib Mineral Petrol 149:430–445

Hirose K (2002) Phase transitions in pyrolytic mantle around 670-km depth: Implications for upwelling of plumes from the lower mantle. J Geophys Res 107. doi:10.1029/2001JB000597

Hirose K, Fei Y, Ono S et al (1999) The fate of subducted basaltic crust in the Earth's lower mantle. Nature 397:53–56. doi:10.1038/16225

Holmes A, Paneth FA (1936) Helium ratios of rocks minerals from the diamond pipes of South Africa. Proc Royal Soc Lond A154:385–413

Ilupin IP, Yefimova ES, Sobolev NV et al (1982) Inclusions in diamond from diamond-bearing dunite. Dokl Acad Nauk SSSR 264(2):454–456

Irifune T (1987) An experimental investigation of the pyroxene-garnet transformation in a pyrolite composition and its bearing on the constitution of the mantle. Phys Earth Planet Inter 45: 324–336

Irifune T, Ringwood AE (1993) Phase transformations in subducted oceanic crust and buoyancy relationships at depths of 600–800 km in the mantle. Earth Planet Sci Lett 117:101–110. doi:10.1016/0012-821X(93)90120-X

Irifune T, Koizume T, Ando J (1996) An experimental study on the garnet-perovskite transformation in the system MgSiO3–Mg3Al2Si3O12. Phys Earth Planet Inter 96:147–157. doi:10.1016/0031-9201(96)03147-0

Izraeli ES, Schrauder M, Navon O (1998) On the connection between fluid and mineral inclusions in diamonds. In: VII International Kimberlite Conference Extended Abstracts, Cape Town, p. 352–354

Izraeli ES, Harris JH, Navon O (2001) Brine inclusions in diamonds: A new upper mantle fluid. Earth Planet Sci Lett 187:323–332. doi:10.1016/S0012-821X(01)00291-6

Jacob D., Jagoutz E (1994) A diamond-graphite bearing xenolith from Roberrs Victor (South Africa): indications from petrogenesis from Pb-, Nb-, and Sr-isotopes. In: Meyer HOA, Leonardos OH (eds) Kimberlites, Related rocks and Mantle Xenoliths. Special Publication 1A-CPRM, p. 304–317

Kaminsky F (2012) Mineralogy of the lower mantle: a review of 'super-deep' mineral inclusions in diamond. Earth Sci Rev 110:127–147. doi:10.1016/.earscirev.2011.10.005

Kaminsky FV, Zakharchenko OD, Davies R et al (2001) Superdeep diamonds from the Juina area, Mato Grosso State, Brazil. Contrib Mineral Petrol 140:734–753

Klein-BenDavid O, Logvinova AM, Izraeli ES et al (2003) Sulfide melt inclusions in Yubileinayan (Yakutia) diamonds. In: 8th International kimberlite conference extended abstracts, p 111

Klein-BenDavid O, Wirth R, Navon O (2006) TEM imaging and analysis of microinclusions in diamonds: a close look at diamond-growing fluids. Am Mineral 91(2–3):353–365

Klein-BenDavid O, Izraeli FS, Hauri I, Navon O (2007a) Mantle fluid evolution—a tale of one diamond. Lithos 77:243–253

Klein-BenDavid O, Izraeli FS, Hauri I, Navon O (2007b) Fluid inclusions in diamonds from the Diavik mine, Canada and the evolution of diamond-forming fluids. Geochim Cosmochim Acta 71(3):723–744

Lee KKM, O'Neil B, Panero WR et al (2004) Equation of state of the high-pressure phases of a natural peridotite and implications for the Earth's lower mantle. Earth Planet Sci Lett 223(3–4):381–393

Leung IS, Guo W, Friedman I, Gleason J (1990) Natural occurrence of silicon carbide in diamondiferous kimberlite from Fuxian. Nature 346:352–354. doi:10.1038/346352a0

Leung IS, Taylor LA, Tsao CS, Han Z (1996) SiC in diamond and kimberlites: implications for nucleation and growth of diamond. Int Geol Rev 37:483–496

Litvin YA (1991) Physicochemical studies of melting in the earth's interior. Nauka, Moscow, p 312

Litvin YA (1998) Hot spots of the mantle and experiment to 10 GPa: alkaline reactions, lithosphere carbonatization, and new diamond-generating systems. Russ Geol Geophys 39(12):1761–1767

Litvin YA (2007) High-pressure mineralogy of diamond genesis. In: Ohtani E (ed) Advances in high-pressure mineralogy. Geological Society of America Special Paper 421, pp 83–103. doi:10.1130/2007.2421(06)

Litvin YuA (2009) The physicochemical conditions of diamond formation in the mantle matter: experimental studies. Russ Geol Geophys 50(12):1188–1200

Litvin YA (2012) Physico-chemical formation conditions of natural diamond deduced from experimental study of the eclogite-carbonatite-sulfide-diamond system. Geol Ore Deposits 54(6):443–457

Litvin YA (2013) Physico-chemical conditions of syngenesis of diamond and heterogeneous inclusions in the carbonate-silicate parental melts (experimental study). Mineral J 35(2):5–24

Litvin YuA (2014) Stishovite paradox in genesis of the super-deep diamonds. Dokl Earth Sci 455 (1):274–278. doi:10.1134/S1028334X14030064

Litvin YA, Zharikov VA (1999) Primary fluid-carbonatite inclusions in diamond: experimental modeling in the system K_2O–Na_2O–CaO–MgO–FeO–CO_2 as a diamond formation medium at 7–9 GPa. Dokl Earth Sci 367A:801–805

Litvin YA, Zharikov VA (2000) Experimental modeling of diamond genesis: diamond crystallization in multicomponent carbonate-silicate melts at 5–7 GPa and 1200–1570 °C. Dokl Earth Sci 373:867–870

Litvin YA, Litvin VY, Kadik AA (2008) Experimental characterization of diamond crystallization in melts of mantle silicate-carbonate-carbon systems at 7.0–8.5 GPa. Geochem Int 46(6):531–553

Litvin YA, Vasiliev PG, Bobrov AV et al (2012) Parental media of natural diamonds and primary mineral inclusions in them: evidence from physicochemical experiment. Geochem Int 50(9):726–759

Litvin YA, Spivak AV, Solopova NA, Dubrovinsky LS (2014) On origin of lower-mantle diamonds and their primary inclusions. Phys Earth Planet Int 228:176–185. doi:10.1016/j/pepi/2013.12.007

Litvin YA, Spivak AV, Kuzyura AV (2016) The bases of the mantle-carbonatite conception of diamond genesis. Geochem Int 10 (accepted)

Logvinova AM, Klein-BenDavid O, Izraeli ES et al (2003) Microinclusions in fibrous diamonds from Yubileinaya kimberlite pipe (Yakutia). In: VIII International kimberlite conference long abstract. Mineralogical Society of America, Victoria, Canada

Logvinova AM, Taylor LA, Floss C, Sobolev NV (2005) Geochemistry of multiple diamond inclusions of harzburgitic garnets as examined in-situ. Int Geol Rev 47:1223–1233

Logvinova AM, Wirth R, Fedorova EN, Sobolev NV (2008) Nanometre-sized mineral and fluid inclusions in cloudy Siberian diamonds: new insights on diamond formation. Eur J Mineral 20:317–331

Logvinova AM, Taylor LA, Fedorova EN et al (2015) A unique diamondiferous peridotite xenolith from the Udachnaya kimberlite pipe (Yakutia): role in subduction in diamond formation. Russ Geol Geophys 56(1–2):397–415

MacGregor ID, Carter JL (1970) The chemistry of clinopyroxenes and garnets of eclogite and peridotite xenoliths from the Roberts Victor Mine, South Africa. Phys Earth Planet Int 3:391–397

Marakushev AA (1984) Peridotite nogules in kimberlites as the indicators for depp structure of lithosphere. In: Doklady of soviet geologists to the 27th session of international geological congress. Petrology. Publishing House “Nauka”, Moscow, pp 153–160

Marakushev AA, Bobrov AV (1998) Specificity of crystallization of eclogitic magmas within the diamond deep-situated facies. Dokl Acad Sci 358(4):526–530

Marx PC (1972) Pyrrotine and the origin of terrestrial diamonds. Mineral Mag 38:636–638

Mathez EA, Fogel RA, Hutcheon ID, Marshintsev VK (1995) Carbon isotopic composition and origin of SiC from kimberlites of Yakutia, Russia. Geochim Cosmochim Acta 59:781–791. doi:10.1016/0016-7037(95)00002-H

Mathias M, Siebert JC, Rickwood PC (1970) Some aspects of the mineralogy and petrology of ultramafic xenoliths in kimberlite. Contrib Mineral Petrol 26:75–123
McCallum ME, Eggler DH (1976) Diamonds in upper mantle peridotite nodule from kimberlite in Southern Wyoming. Science 192:253–256
Meyer HOA, Boyd FR (1972) Composition and origin of crystalline inclusions in natural diamonds. Geochim Cosmochim Acta 36:1255–1273
Navon O (1991) High internal pressures in diamond fluid inclusions determined by infrared absorption. Nature 353:746–748. doi:10.1038/353746a0
Navon O (1999). Diamond formation in the Earth's mantle In: Gurney JJ, Gurney JL, Pascoe MD, Richardson SH (eds) Proceedings of the VII international kimberlite conference: red roof design, Cape Town, vol 2, pp 584–604
Navon O, Hutcheon ID, Rossman GR, Wasserburg GL (1988) Mantle-derived fluids in diamond micro-inclusions. Nature 335:784–789. doi:10.1038/335784a0
Navon O, Izraeli ES, KleinBen-David O (2003) Fluid inclusions in diamonds of the carbonatitic connection. In: VIII International kimberlite conference long abstract. Mineralogical Society of America, Victoria, Canada
Nestola F, Nimis P, Angel RJ et al (2014) Olivin with diamond-imposed morphology included in diamond. Syngenesis or protogenesis? Int Geol Rev 56:1658–1667
O'Hara MJ (1968) The bearing of phase equilibria on synthetic and natural systems on the origin and evolution of basic and ultrabasic rocks. Earth Sci Rev 4:69–133
O'Hara MJ, Yoder HS (1967) Formation and fractionation of basic magmas at high pressure. Scott J Geol 3:67–117
Ono S, Ito E, Katsura T (2001) Mineralogy of subducted basaltic crust (MORB) from 25 to 37 GPa, and chemical geterogeneity of the lower mantle. Earth Planet Sci Lett 190:57–63. doi:10.1016/S0012-821X(01)00375-2
Palot M, Pearson DG, Stern RA et al (2014) Isotopic constraints on the nature and circulation of deep mantle C–O–H–N fluids: carbon and nitrogen systematics within ultra-deep diamonds from Kankan (Guinea). Geochim Cosmochim Acta 139:24–46
Pokhilenko NP, Sobolev NV, Sobolev VS, Lavrent'ev YG (1976) Xenolith of diamond-bearing ilmenite-pyropic lherzolite from Udachnaya pipe (Yakutia). Dokl Acad Nauk SSSR 231(2):438–441
Pokhilenko NP, Sobolev NV, Yefimova ES (1982) Xenolith of kataklazed diamond-bearing disten eclogites from the Udachnaya pipe, Yakutia. Dokl Acad Nauk SSSR 266(1):212–216
Ponomarenko AI, Sobolev NV, Pokhilenko NP et al (1976) Diamond-bearing grospydite and diamond-bearing disten eclogites from the kimberlite pipe Udachnaya, Yakutia). Dokl Acad Nauk SSSR 226(4):927–930
Ponomarenko AI, Spetsius ZV, Sobolev NV (1980) New type of diamond-bearing rocks—garnet-bearing pyroxenites. Dokl Acad Nauk SSSR 251(2):438–441
Rickwood PC, Mathias M (1970) Diamondiferous eclogite xenoliths in kimberlite. Lithos 3:223–235
Rickwood PC, Gurney J, White-Cooper DB (1969) The nature and occurrences of eclogite xenoliths in the kimberlites of Southern Africa. Geol Soc S Afr Spec Pub 2:371–393
Ringwood AE (1975) Composition and petrology of the earth's mantle. McGraw-Hill, New York, p 618
Ringwood AE, Major A (1971) Synthesis of majorite and other high pressure garnets and perovskites. Earth Planet Sci Lett 12:411–418
Satsukawa T, Griffin WT, Piazolo S, O'Reilly SY (2015) Messengers from the deep: fossil wadsleite-chromite microstructures from the mantle transition zone. Sci Rep 5:16484. doi:10.1038/srep16484
Schrauder M, Navon O (1994) Hydrous and carbonatitic mantle fluids in fibrous diamonds from Jwaneng, Botswana. Geochim Cosmochim Acta 58:761–771. doi:10.1016/0016-7037(94)90504-5
Shatsky VS, Ragozin A, Zedgenizov D Mityukhin S (2008) Evidence for multistage evolution of diamond-bearing eclogite from the Udachnaya kimperlite pipe. Lithos 105:289–300

Snyder GA, Taylor LA, Crozaz G et al (1997) The origin of Yakutian eclogite xenoliths. J Petrol 38:83–113
Sobolev NV (1977) The deep-seated inclusions in kimberlites and the problem of the composition of the upper mantle. American Geophysical Union, Washington, D.C., 304 p
Sobolev NV, Kuznetsova IK (1965) New data on mineralogy of eclogites from kimberlitic pipes of Yakutia. Dokl Acad Nauk SSSR 163(2):471–474
Sobolev NV, Botkunov AI, Lavrent'ev YG (1974) Diamond-bearing corundum eclogite from kimberlite pipe Mir, Yakutia. Geol Geofiz 5
Sobolev NV, Efimova ES, Pospelova LN (1981) Native iron in diamond from Yakutia and its paragenesis. Geol Geofiz 22:25–29
Sobolev NV, Fursenko BA, Goryainov SV et al (2000) Fossilized high pressure from the Earth's deep interior: coesite-in-diamond barometer. Proc Nat Acad Sci U S A 97(22):11875–11879
Sobolev NV, Logvinova AM, Zedgenizov DA et al (2008) Petrogenetic significance of minor elements in olivines from diamonds and peridotite xenoliths from kimberlites of Yakutia. Lithos 112S:701–713
Sobolev NV, Logvinova AM, Yefimova ES (2009) Syngenetic inclusions of phlogopite of diamonds from kimberlites: evidence concerning the role of volatiles in diamond formation. Geol Geofiz 50(2):1588–1606
Sobolev VS (1960) Formation conditions of diamond deposits. Geol Geofiz 1:7–22
Sobolev VS, Naii BS, Sobolev NV et al (1969) Xenolith of diamond-bearing pyropic serpentinites from Aikhal pipe. Dokl Acad Nauk SSSR 188(5):1141–1143
Sobolev VS, Sobolev NV, Lavrent'ev YG (1972) Inclusions in diamonds from a diamond-bearing eclogite. Dokl Acad Nauk SSSR 207(1):164–167
Spetsius ZV, Taylor LA (2008) Diamonds of siberia: photographic evidence for their origin. Tranquility Base Press, Lenoir City, Tennessee, 278 p
Spetsius ZV, Bogush IN, Kovalchuk OE (2015) FTIR mapping of diamond plates of eclogitic and peridotitic xenoliths from the Nyurbimskaya pipe (Yakutia): genetic implications. Russ Geol Geophys 56(1–2):442–454
Stachel T (2001) Diamonds from the asthenosphere and the transition zone. Eur J Mineral 13(5):883–892
Stachel T, Harris JW, Brey GP (1998) Rare and unusual mineral inclusions in diamonds from Mwadui, Tanzania. Contrib Mineral Petrol 132:34–47. doi:10.1007/s004100050403
Stachel T, Brey G, Harris JW (2000a) Kankan diamonds (Guines) I: from the lithosphere dawn to the transition zone. Contrib Mineral Petrol 140:1–15
Stachel T, Brey GP, Harris W, Joswig W (2000b) Kankan diamonds (Guinea) II: lower mantle inclusion parageneses. Contrib Mineral Petrol 140:16–27
Stachel T, Brey G, Harris JW (2005) Inclusions in sublithospheric diamonds: glimpses of deep earth. Elements 1(2):73–78
Stagno V, Tange Y, Miayjima N et al (2011) The stability of magnesite in the transition zone and the lower mantle as function of oxygen fugacity. Geophys Res Lett 38:L19309. doi:10.1029/2911GL049560
Stepanov AS, Shatsky VS, Zedgenizov DA, Sobolev NV (2007) Causes of variations in morphology and impurities of diamonds from the Udachnaya Pipe eclogite. Russ Geol Geofiz 48:758–769
Stepanov AS, Shatsky VS, Zedgenizov DA, Sobolev NV (2008) Chemical heterogeneity in the diamondiferous eclogite xenolith from the Udachnaya kimberlite pipe. Dokl Earth Sci 419:308–311
Streckeisen A (1976) To each plutonic rock its proper name. Earth Sci Rev 12:1–33
Switzer G, Melson WG (1969) Partially melted kyanite eclogite from the Roberts Victor mine, South Africa. Contrib Earth Sci 1:1–9
Takahashi T (1986) Melting of dry peridotite KLB-1 up to 14 GPa: implication to on the origin of peridotitic upper mantle. J Geophys Res 91:899367–899382
Taylor LA, Anand M (2004) Diamonds: time capsules from the Siberian mantle. Chem Erde 64:1–74. doi:10.1016/j.chemer.2003.11.006

Taylor LA, Keller RA, Snyder GA et al (2000) Diamonds and their mineral inclusions, and what they tell us: a detailed «pull-apart» of a diamondiferous eclogites. Int Geol Rev 42:959–983
Titkov SV, Gorshkov AI, Solodova YP et al (2006) Mineral microinclusions in diamonds of cubic habitus from Yakutian deposits by data of analytic electronemicroscopy. Dokl Earth Sci 410 (2):255–258
Tschauner O, Ma C, Becket JR et al (2014) Discovery of bridgmanite, the most abundant mineral in Earth, in a shocked meteorite. Science 346(6213):1100–1102
Viljoen KS, Swash PM, Otter MI et al (1992) Diamondiferous garnet garzburgites from the Finsch kimberlite, Northern Cape, South Africa. Contrib Mineral Petrol 110:133–138
Viljoen KS, Robinson DN, Swash PM et al (1994) Diamond and graphite-bearing peridotite xenoliths from the Roberts Victor kimberlite, South Africa. In: Meyer HOA, Leonardos OH (eds) Proceedings of fifth international kimberlite conference, vol 1. Araxa, Brazil, pp 285–303
Viljoen KS, Dobbe R, Smit B et al (2004) Petrology and geochemistry of a diamondiferous lherzolites from the premier diamond mine, South Africa. Lithos 77:539–552
Von Eckermann HA (1967) Comparison of Swedish, African and Russian kimberlites. In: Wyllie PJ (ed) Ultramafic and related rocks. Wiley, New York, pp 302–312
Wagner PA (1909) Die diamantfuehrenden Gesteine Suedafrikas. Ihre Abbau und ihre Aufbereitung, Berlin
Wagner PA (1928) The evidence on the kimberlite pipes on the constitution of the outer part of the Earth. S Afr J Sci 25:125–148
Walter MJ, Bulanova GP, Armstrong LS et al (2008) Primary carbonate melt from deeply subducted oceanic crust. Nature 454:622–625
Wang A, Pasteris JD, Meyer HOA, Dele-Duboi ML (1996) Magnesite-bearing inclusion assemblage in natural diamond. Earth Planet Sci Lett 141:293–306. doi:10.1016/0012-821X(96)00053-2
Wentorf RH, Bovenkerk HP (1961) On the origin of natural diamonds. J Astrophys 134: 995–1005. doi:10.1086/147227
Williams AF (1932) The genesis of the diamond, vols 1 and 2. Ernest Benn Ltd. London, 636 p
Wood BJ (2000) Phase transformation nd partitioning relations in peridotite under lower mantle conditions. Earth Planet Sci Lett 174:341–354. doi:10.1016/80012-821X(99)00273-3
Yoder HS, Tilley CE (1962) Origin of basalt magmas: an experimental study of natural and synthetic rock systems. J Petrol 3:342–532
Zedgenizov DA, Kagi H, Shatsky VS, Sobolev NV (2004) Carbonatitic melts in cuboid diamonds from Udachnaya kimberlite pipe (Yakutia): evidence from vibrational spectroscopy. Mineral Mag 68:61–73
Zedgenizov DA, Ragozin AL, Shatsky VS et al (2009) Mg and Fe-rich carbonate-silicate high-density fluids in cuboid diamonds from the Internationalnaya kimberlite pipe (Yakutia). Lithos 112:638–647
Zedgenizov DA, Ragozin AL, Shatsky VS et al (2011) Carbonate and silicate media of crystallization of fibrous diamonds from placers of north-eastern Siberian platform. Russ Geol Geophys 52(11):1649–1664
Zedgenizov DA, Kagi H, Shatsky VS, Ragozin AL (2014) Local variations of carbon isotope composition in diamonds from São-Luis (Brazil): evidence for heterogenous carbon reservoir in sublithospheric mantle. Chem Geol 363:114–124

Chapter 3
Strongly Compressed Carbonate Systems in Diamond Genesis

The crucial role of carbonate constituents in diamond genesis has warranted by the results of physico-chemical experimental investigations of diamond-parental systems under pressures typical for depths of the upper mantle, transition zone and lower mantle. Currently available evidence to the effects of congruent melting of carbonate minerals and the peculiarities of melting of deep-seated multicomponent carbonate systems is of critical importance for the diamond-producing processes. The relationships between melting temperatures of multicomponent carbonate systems and geothermal temperatures make it possible to produce carbonatitic melts within the deep Earth's interior. Effects of a complete liquid miscibility of components of silicate-carbonate melts and the reasonably high values of solubility of diamond and metastable graphite in them are the governing factors in initiation of the principal physico-chemical mechanisms of genesis of diamonds and associated phases. Diamond-forming processes are also characterized by extraordinary kinetic effect of the joint crystallization of diamond and metastable graphite. Association of stable diamond and metastable graphite has detected among the primary inclusions in diamonds that is unusual from the thermodynamic point of view. The problem of carbon natural source in genetic mineralogy of diamonds and associated phases is still much-disputable. Testing experiments on diamond synthesis using melts of heterogeneous inclusions in diamonds indicate that the melts are effective solvents of elementary carbon. Nevertheless, importance of testing data in solution on the problem of diamond genesis is not decisive. The effective solutions of the major diamond-origin problems may be attained owing to the comprehensive physico-chemical experimental studies of multicomponent multiphase heterogeneous systems with their boundary compositions which are comparable with these of the natural diamond-producing media.

Y.A. Litvin, *Genesis of Diamonds and Associated Phases*,
Springer Mineralogy, DOI 10.1007/978-3-319-54543-1_3

3.1 Congruent Melting of Carbonate Minerals at High Pressure

At the upper-mantle conditions the growing diamonds have captured the carbonate minerals magnesite $(Mg,Fe)CO_3$ (Wang et al. 1996; Leost et al. 2003), siderite $FeCO_3$ (Stachel et al. 2000), aragonite $CaCO_3$ (or its "retrograde" polymorph calcite) (Titkov et al. 2006), dolomite $Ca(Mg,Fe)CO_3$ (Stachel et al. 1998; Logvinova et al. 2008) from their partially molten parental media. This offers a clearer view that carbonate components of the upper-mantle diamond-parental melts may be predominantly determined by the K_2CO_3–Na_2CO_3–$MgCO_3$–$FeCO_3$–$CaCO_3$ system. The hardened multicomponent alkaline silicate-carbonate parental melts from inclusions in Botswanian diamonds (Navon 1991; Schrauder and Navon 1994) are symptomatic for the natural diamond-parental chemistry. Their variable compositions were basically reproduced as the most plausible for the diamond-producing carbonate-silicate melts (with 16.7, 17.5 and 36.7 wt% SiO_2) taking CO_2 contents into consideration (Table 3.1) (Litvin 2007). The carbonates $MgCO_3$, $FeCO_3$, $CaCO_3$, Na_2CO_3 and K_2CO_3 were used for preparation of the starting materials. In the testing experiments under mantle PT-conditions (Litvin and Zharikov 1999, 2000) the Botswanian inclusions melts (of multicomponent silicate-carbonatite as well as of the boundary carbonatite compositions), which were oversaturated with dissolved elementary carbon, have demonstrated a high diamond-producing efficiency with short-term nucleation of the diamond phase (Fig. 3.1). The main morphological features at formation of natural diamonds (octahedral smooth-faced single-crystalline growth, spinel-law and polysynthetic twinning, polycrystalline crystallization) were experimentally reproduced. Hence the correlated mineralogical and experimental evidence testifies that the K–Na–Mg–Fe–Ca-carbonate constituents are of the key significance at the peridotite/eclogite—carbonatite-carbon parental melts of diamonds and associated phases of the upper-mantle diamond-producing reservoirs-chambers. In the subsequent mineralogical works, the alkaline-carbonate inclusions have been repeatedly shown (Tomlinson et al. 2006; Klein-BenDavid et al. 2009; Weiss et al. 2009; Zedgenizov et al. 2009; Logvinova et al. 2011).

Paragenetic carbonate minerals among the primary inclusions of the transition zone and lower mantle are represented by aragonite and "retrograde" calcite $CaCO_3$ (Bulanova et al. 2010; Zedgenizov et al. 2011), magnesite $MgCO_3$ (Wang et al. 1996; Stachel et al. 1998), dolomite $CaMg(CO_3)_2$ (Wirth et al. 2009), nyerereite $Na_2Ca(CO_3)_2$ and nahcolite $NaHCO_3$ (Kaminsky et al. 2009, 2013). Finally the mineralogical data substantiate the key role of the Na–Mg–Fe–Ca-carbonate ingredient (without a clearly defined involvement of K-carbonate component) at the composition of the ultrabasic/basic-carbonatite-carbon parental melts for diamonds and associated phases of the transition-zone and lower-mantle diamond-producing reservoirs-chambers.

For the problem of diamonds and associated phases genesis, physico-chemical features of melting of the simple carbonates K_2CO_3, Na_2CO_3, $MgCO_3$, $FeCO_3$,

Table 3.1 Chemical compositions of silicate-carbonatite inclusions in mantle diamonds (Schrauder and Navon 1994) and their model compositions used as starting materials in high pressure high temperature experiments (Litvin and Zharikov 2000)

Component	Natural samples			End members	
	JWN108	JWN90	JWN91	Carbonatitic	Silicic
1. Natural compositions of silicate-carbonatite inclusions in upper-mantle diamonds					
SiO_2	23.9	25.1	45.1	13.6	58.4
TiO_2	4.6	4.7	4.9	4.6	4.3
Al_2O_3	2.5	2.5	5.4	0.8	6.8
FeO	15.2	16.1	10.7	19.5	7.6
MgO	10.9	10.1	5.7	13.2	3.3
CaO	13.5	15.6	5.1	20.5	0.0
Na_2O	2.2	2.6	1.6	2.2	2.2
K_2O	22.2	18.3	16.4	20.7	12.3
P_2O_5	2.2	2.4	1.0	2.4	0.7
Cl	1.5	1.3	0.8	1.3	0.9
Total	98.8	98.7	96.7	98.8	96.5
CO_2/H_2O, m.r.				9/1	1/9
2. Experimental starting materials					
SiO_2	16.7	17.5	36.7	8.8	
TiO_2	3.2	3.3	4.0	3.0	
Al_2O_3	1.7	1.7	4.4	0.5	
FeO	10.6	11.2	8.8	12.7	
MgO	7.6	7.0	4.6	8.6	
CaO	9.4	10.9	4.1	13.3	
Na_2O	1.0	1.0	1.1	0.8	
K_2O	17.7	15.0	14.4	15.6	
P_2O_5	1.6	1.7	0.8	1.6	
Cl	0.5	0.9	0.6	0.9	
CO_2	30.0	29.8	20.5	34.2	

$CaCO_3$ and, most notably, of the multicomponent carbonate systems K_2CO_3–Na_2CO_3–$MgCO_3$–$FeCO_3$–$CaCO_3$ and Na_2CO_3–$MgCO_3$–$FeCO_3$–$CaCO_3$ belong to very important. The decisive importance of these systems at compositions of the silicate-(±oxide)-carbonate-carbon parental media of diamonds and associated phases over the upper mantle, transition zone and lower mantle depths is apparent from the mineralogical data for paragenetic carbonate growth inclusions in diamonds. The alkaline carbonates K_2CO_3 and Na_2CO_3 are melted congruently at 891 and 858 °C, correspondingly, under normal pressure. In the system K_2CO_3–Na_2CO_3 the continuous solid solutions $(K_2CO_3 \cdot Na_2CO_3)_{ss}$ have formed at temperatures higher than 610 °C. Melts of these solid solution alkaline phases are also completely miscible, and their phase diagram has an invariant minimum on the solidus line for the composition $(K_2CO_3)_{43}(Na_2CO_3)_{57}$ (mol%) at 710 °C (Reisman 1959).

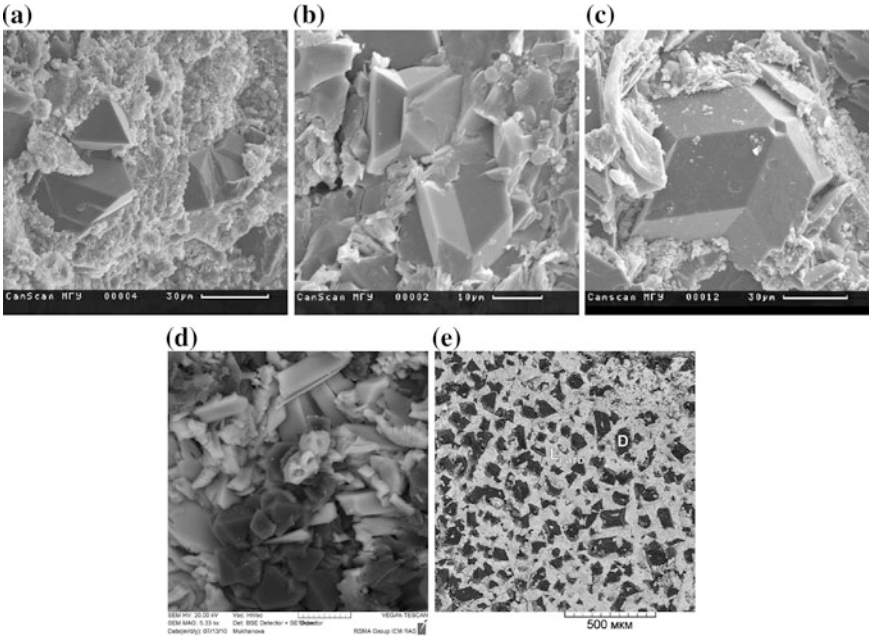

Fig. 3.1 Scanning electron micrograph (SEM) images of diamonds formed in testing experiments with the multicomponent carbonatite-carbon melts-solutions (similar to hardened melt-like inclusions in Botswanian diamonds): **a** individual octahedral crystals, **b** spinel-law twins, **c** polysynthetic twins, **d** polycrystalline intergrowth—diamondite, **e** view of example of highest density of nucleation and mass crystallization

Incongruent melting of the ferriferous and alkali-earthy carbonates has conjugated with decarbonation and decomposition into oxides and CO_2: $FeCO_3$ at 490 °C, $MgCO_3$ at 500–650 °C, $CaCO_3$ at 880–900 °C, $CaMg(CO_3)_2$ at 600 °C. The incongruent melting of the simple carbonates of Mg, Fe and Ca has evolved into the congruent melting at elevated pressure. This effect happens in the singular points in case of $MgCO_3$ at 2.7 GPa, 1600 °C (Huang and Wyllie 1976; Katsura and Ito 1990), $FeCO_3$ at 6.5 GPa, 1680 °C by estimation (Shatskiy et al. 2015) and $CaCO_3$ at 0.7 GPa, 1370 °C (Irving and Wyllie 1975; Suito et al. 2001). The congruent melting of K_2CO_3 and Na_2CO_3 can be followed to 6 ГПа, 1400 °C and 6 GPa, 1370 °C, correspondingly (Shatskiy et al. 2013a, b, 2015).

Dolomite $CaMg(CO_3)_2$ is stable as an intermediate compound at subsolidus conditions of the system $CaCO_3$–$MgCO_3$ on experimental evidence up to 1380 °C at 3 GPa (Irving and Wyllie 1975) and to 1350 °C at 6 GPa (Buob et al. 2006; Shatskiy et al. 2015). The boundary components $CaCO_3$ and $MgCO_3$ are congruently melted at 1610 and 1580 °C (3 GPa), 1700 and 1900 °C (6 GPa), correspondingly. Dolomite is incongruently melted at 1360 °C (6 GPa) with formation of the magnesite limited solid solution $(MgCO_3)_{82}(CaCO_3)_{18}$ (mol%) and melt composed as $(MgCO_3)_{58}(CaCO_3)_{42}$ (mol%). This is determining for the invariant

peritectic point Dol = Mgs + L on the liquidus curve. The invariant peritectic point is mated with the invariant minimum on the solidus curve at 1350 °C for the composition $(MgCO_3)_{52}(CaCO_3)_{48}$ (mol%). An information of subsolidus disproportionation of dolomite with formation of the association aragonite $CaCO_3$ + magnesite $MgCO_3$ at temperatures lower 1050 °C in the 3.5–6.0 GPa pressure interval at experiments using the multianvil press with in situ X-ray diffraction method (Martinez et al. 1996) has not be confirmed.

Siderite $FeCO_3$ (melting temperature T_m is 1670 °C) and magnesite $MgCO_3$ (T_m is 1900 °C) are completely miscible in the solid and liquid states at 6 ГПа (Shatskiy et al. 2015). The limited solid solutions are formed at 900–1280 °C in the reaction of siderite with calcite $CaCO_3$ and ankerite $CaFe(CO_3)_2$ within the system compositions up to 3.5 mol% $FeCO_3$. Completely miscible melt appears at 1280 °C and 56 wt% $CaCO_3$ in invariant minimum on the solidus curve. In the system $CaCO_3$–$MgCO_3$–$FeCO_3$, temperature of the invariant minimum (and of the peritectic point, correspondingly) is shifted to ~1280 °C at 6 ГПа under the influence of ferriferous component.

The intermediate binary compounds $K_6Ca_2(CO_3)_5$, $K_2Ca_3(CO_3)_4$, $K_2Mg(CO_3)_2$, $K_2Fe(CO_3)_2$, $Na_4Ca(CO_3)_3$, $Na_2Ca_3(CO_3)_4$, $Na_2Mg(CO_3)_2$ of the multicomponent alkali-carbonate system K_2CO_3–Na_2CO_3–$CaCO_3$–$MgCO_3$–$FeCO_3$ are stable and congruently melted at 6 GPa and 1220, 1330, 1260, 1190, 1210, 1320, 1230 °C, correspondingly (Shatskiy et al. 2015). Melting of the double carbonate $Na_2Fe(CO_3)_2$ only is incongruent at 1050 °C with formation of siderite and peritectic melt. It was also reported about formation of $K_2Ca(CO_3)_2$ and $Na_2Ca_4(CO_3)_5$ which are not stable at subsolidus conditions and broken down at 960 ad 1060 °C, respectively. All the binary systems with stable intermediate compounds are of eutectic melting in the temperature 1000–1200 °C range. The unlimited solid solutions $[K_2Mg(CO_3)_2 \cdot K_2Fe(CO_3)_2]$ss of intermediate compounds of the ternary system K_2CO_3–$MgCO_3$–$FeCO_3$ form completely miscible melts along the univariant cotectics over surface of the ternary liquidus. Melting processes of the ternary system Na_2CO_3–$MgCO_3$–$FeCO_3$ and the distinctive features of its liquidus surface are under control of the univariant cotectic curve for magnesium and peritectic curve for ferriferous compositions.

The experimental data on melting phase relations of the simple, binary and ternary carbonate systems discussed above reveal their physico-chemical properties which are claimed in the study of the problem of diamond genesis at the upper mantle conditions. However a determination of the multicomponent multiphase composition of the parental medium, which has the capability to make possible the joint formation of diamonds and associated phases, presents the principal interest as the key to effective solution of the major problem of genetic mineralogy of diamond. It is of principal interest the experimental evidence of congruent melting of simple carbonates K_2CO_3, Na_2CO_3, $MgCO_3$, $FeCO_3$, $CaCO_3$ and their intermediate compounds of decisive significance as well as of stability of the simple carbonate melts at the upper mantle depths. This is caused by the capability of carbonate melts to be effective solvents for the solid carbon phases—diamond and graphite. The formed carbonate melts-solutions of carbon provide physico-chemical capacity to

formation of diamonds and paragenetic carbonate minerals. Physico-chemical behavior at melting of simple carbonates of the system Na_2CO_3–$MgCO_3$–$FeCO_3$–$CaCO_3$ of determining importance for the ultra-deep diamonds genesis has been experimentally studied for the transition zone and lower mantle depths.

Phase PT-diagram of the one-component $CaCO_3$ system (Fig. 3.2) was studied at experiments up to 43 GPa and 3600 °C (Spivak et al. 2011, 2012; Litvin et al. 2014). In this case the high-pressure high-temperature cell with diamond anvils and infrared Nd:YLF laser (wave length 1064 nm) for high-temperature heating was used. Starting material was ^{13}C-based carbonate $Ca^{13}CO_3$ that allowed to judge unequivocally about the carbon source in the case of appearance carbon-bearing phases in the experimental products. The curve of aragonite congruent melting was found to be an extension of calcite melting curve from the singular point calcite + aragonite + melt (at 5.5 GPa, 1700 °C) up to 43 GPa, 2350 °C. For the first time, it was determined in static experiment that one-phase field of the $CaCO_3$ melt extents within the 4–43 GPa pressure interval to about 3100–3600 °C. In these conditions the field proved to be bounded (as viewed from higher temperatures) with the curve of the melt decomposition by the reaction $CaCO_3$-melt → CaO + C + O_2 resulting in diamond ^{13}C formation. The high-temperature boundary has been earlier investigated with the use of shock-wave experiments by the effect of the volume sudden change. The high-temperature boundary was interpreted as a result of the reaction: $CaCO_3$-melt → CaO + CO_2 with an emitting

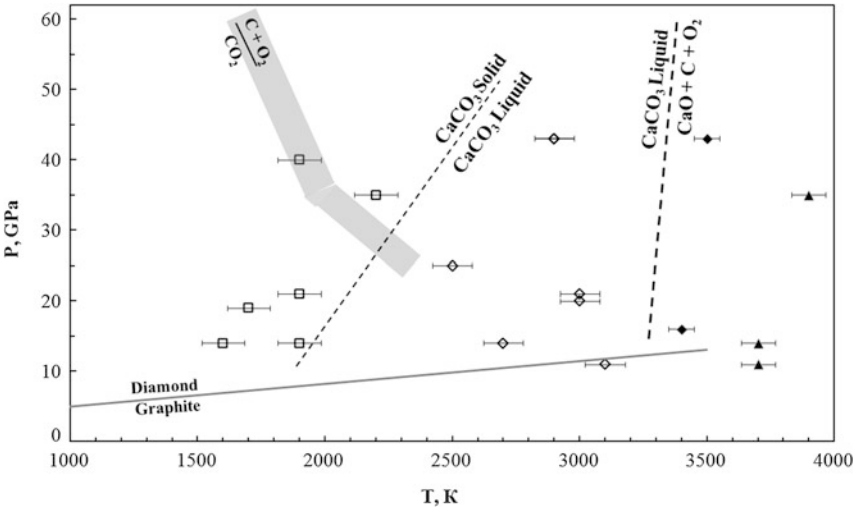

Fig. 3.2 Melting phase diagram of carbonate system $CaCO_3$. Symbols for experimental points: *open square*—solid carbonate, *open rhomb*—carbonate melt, *black rhomb*—diamond, *black triangle*—graphite. Congruent melting curve of solid $CaCO_3$ (*left*) and decomposition boundary of $CaCO_3$ melt (*right*) are presented by dashed lines. Diamond-graphite equilibrium line after (Bundy et al. 1996). The shaded region characterizes PT-conditions of diamond formation of CO_2 fluid phase in the DAC-LH experiments by Tschauner et al. (2001)

of the fluid phase CO_2 but without diamond formation (Bobrovsky et al. 1976). Experimental study of CO_2 behavior at high pressures and temperatures in the diamond anvil cell with laser heating (DAC-LH) has showed the CO_2 breakdown with liberation of carbon and formation of diamond (Tschauner et al. 2001). Because of this diamond formation in the static experiments is still unclear and may be result of reduced conditions connected with the redox state of diamond-anvil cell ("instrumental effect").

PT-conditions of primary melting of magnesite $MgCO_3$ and its melts phase field limits were investigated at 12–84 GPa and 1300–3000 °C with the use of the cell with diamond anvils and laser heating (Solopova et al. 2014; Litvin et al. 2014). Experimental results (Fig. 3.3) attest a congruent melting of magnesite within the range of 10 GPa, 1900 °C–84 GPa, 2300 °C. An expanded field of the $MgCO_3$ melts is found with the high-temperature boundary marked off by the reaction $MgCO_3 \rightarrow MgO + C + O_2$ within the interval of 2400 °C, 12 GPa–2600 °C, 84 GPa.

Siderite $FeCO_3$ together with Na_2CO_3 is important as a relatively low-melting component of the multicomponent diamond-parental medium having involved in the Na–Mg–Fe–Ca-carbonate constituent. Experimental study of $FeCO_3$ at room temperature up to pressure of 90 GPa (Lavina et al. 2009) and at high temperatures up to 1730 °C and pressures to 47 GPa (Santillan and Williams 2004) points to stability of $FeCO_3$ under these PT-conditions. The $FeCO_3$ component is also stable at compositions of the Mg–Fe-carbonate solid solutions under the upper mantle pressures (Boulard et al. 2012; Spivak et al. 2014).

The curve of congruent melting of $Na_2{}^{13}CO_3$ has been preliminary determined within the PT-interval of 10 GPa, 1150 °C–25 GPa, 1200 °C (Fig. 3.4) (Solopova

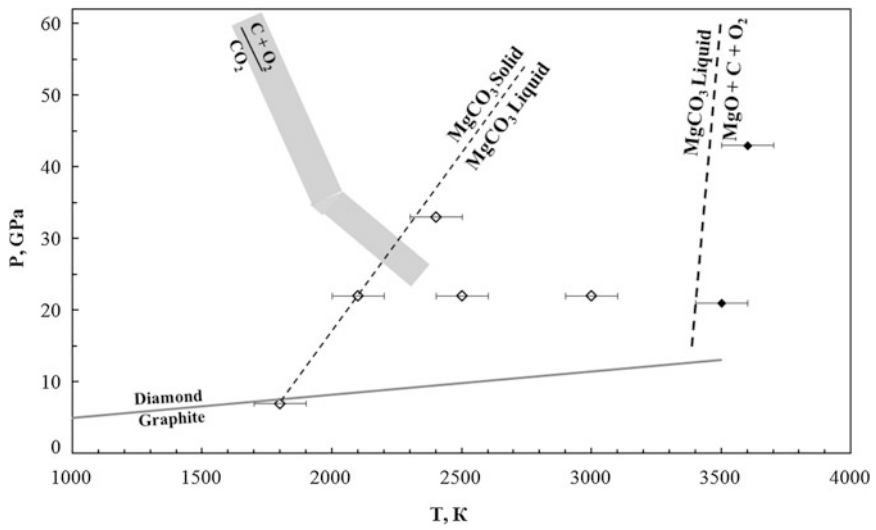

Fig. 3.3 Melting phase diagram of carbonate system $MgCO_3$. Symbols at captions to Fig. 3.2

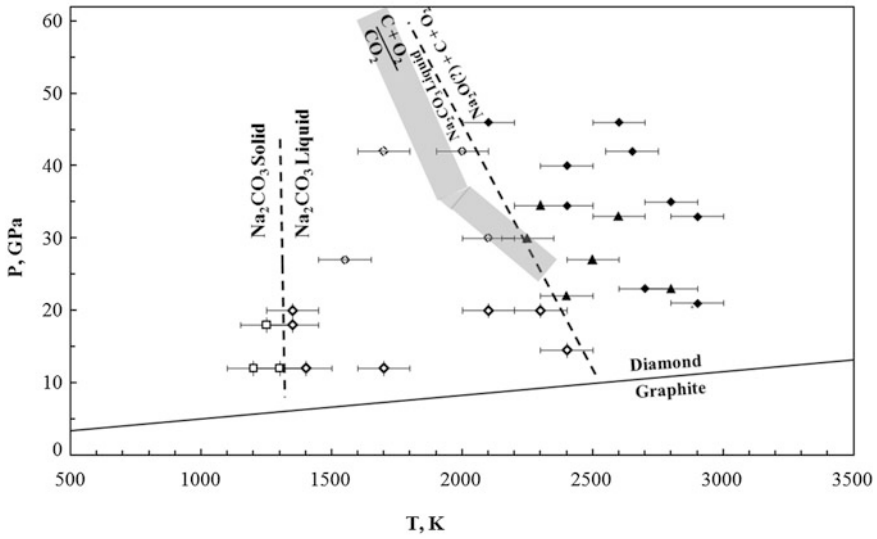

Fig. 3.4 Melting phase diagram of carbonate system Na_2CO_3. Symbols at captions to Fig. 3.2

et al. 2013; Litvin et al. 2014). The high-temperature boundary for the Na_2CO_3 stable melts field is characterized with a negative slope within the interval of 2300 °C, 12 GPa–1600 °C, 50 GPa. The boundary is marked by the reaction of the Na_2CO_3 melt decomposition $Na_2CO_3 \rightarrow Na_2O + C + O_2$. The experiments were carried out using the cell with diamond anvils and laser heating.

The relative positions of the $CaCO_3$, $MgCO_3$ and Na_2CO_3 solidus boundaries in respect to the geothermal lines at the upper mantle, transition zone and lower mantle depths bear witness to that melting can only result in case of the alkaline carbonate (Litvin et al. 2014).

A plausible role of carbonates has been estimated for the processes of carbonatized peridotite subduction (Litasov and Ohtani 2009) and carbon transferring between the deep-seated geochemical reservoirs (Dasgupta and Hirschman 2010).

3.2 Melting of Multicomponent Carbonate Systems as to Mantle Geothermal Regime

Optimal concord between mineralogical data for syngenetic inclusions in natural diamonds and results of physico-chemical experimental studies of diamond-producing systems makes it possible to substantiate the changeable silicate-(±oxide)-carbonatite-carbon partial melts as the parental media for diamonds and primary inclusions at all upper mantle, transition zone and lower mantle depths. Experimental investigations of one-component carbonate systems melting have

merely an auxiliary value for studying of the diamond genesis problem. The reason is that the real mantle mineral systems, responsible for genesis of diamonds and associated phases, are multicomponent and heterogeneous by their nature. First and foremost it has cropped up the problem of physico-chemical behavior of the multicomponent carbonate systems which have been involved into the processes of natural origin of diamonds.

The system Na_2CO_3–$MgCO_3$–$FeCO_3$–$CaCO_3$ represents the generalization to the major components of multicomponent carbonate constituent for growth melts of the transition-zone and lower-mantle ultra-deep diamonds. The pressure-temperature phase relations of the multicomponent system are experimentally studied at pressure 10–25 GPa and temperature 800–1800 °C ranges (Spivak et al. 2015a, b). As a result the PT-phase diagram on melting of the composition $(Na_2CO_3)_{25}(MgCO_3)_{25}(FeCO_3)_{25}(CaCO_3)_{25}$ (wt%) was constructed (Fig. 3.5). In this case, an averaged starting composition of the experimental carbonate system is preferable in so far as a relationship among components of the natural diamond-producing melts cannot be evaluated from mineralogical data for carbonate inclusions. This is conditioned by that the quantity of accidentally included minerals is not proportional to contents of the relevant components of diamond-producing melts. Moreover, the silicate-oxide-carbonate parental melts are variable over a broad range from ultrabasic to basic compositions.

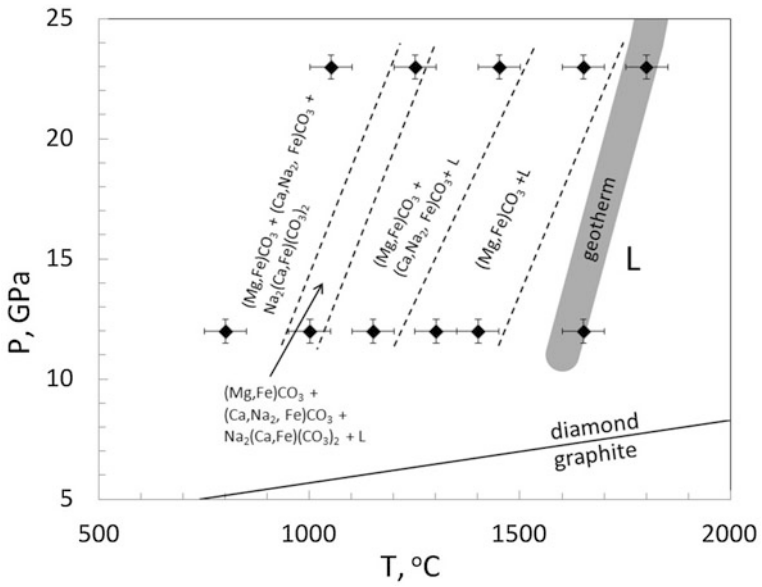

Fig. 3.5 Phase PT-diagram of $MgCO_3$–$FeCO_3$–$CaCO_3$–Na_2CO_3 system. *Black diamonds*—experimental points, *dashed lines*—boundaries of phase fields, *black line*—equilibrium diamond-graphite boundary (Bundy et al. 1996), *thick gray area*—the geothermal PT-conditions (Stacey 1992)

The experimental results unravel genetically essential physico-chemical properties of Na–Mg–Fe–Ca-carbonate constituents of the diamond-producing systems. To begin with, it has been ascertained that primary melting of the multicomponent carbonate system is eutectic. The PT-curve of eutectic solidus is monotonously increases between the experimental isobaric points at 11.8 GPa, 930 °C and 23 GPa, 1200 °C. Accordingly, in these pressures interval the geothermal temperatures vary from 1600–1650 to 1750–1800 °C (Liebermann and Schreiber 1969; Stacey 1992; Karato et al. 2000; Harte 2010) that is very closely with the liquidus curve for the complete melting of the Na–Mg–Fe–Ca-carbonate composition studied. A content of the carbonate components for the complete melt is changeable (mol%) within the limits for $MgCO_3$ 0.24–0.26, $FeCO_3$ 0.19–0.26, $CaCO_3$ 0.27, Na_2CO_3 0.24–0.29 (after quenching). The essential difference between the carbonate solidus and geothermal temperatures points to the fact that natural conditions for the primary melting are in existence as for particularly carbonate solvents of elementary carbon so for real diamond-parental silicate-oxide-carbonatite melts at the transition zone and lower mantle depths.

Experimental data show also that multicomponent carbonate melts are completely miscible and stable over the practically whole temperature interval at the region of partial melting of the multicomponent carbonate system. Under these conditions, magnesite $(Mg,Fe)CO_3$ with impurities of 0.1–0.4 мол. % Na–Ca-carbonates is a liquidus phase. At lower temperatures magnesite is crystallized together with solid-solution phases of Ca–Na–Fe-aragonite with impurity of about 0.5 mol% Mg-carbonate and nyererite $Na_2(Ca,Fe)(CO_3)_2$ with impurity of about 0.07 mol% Mg-carbonate. Finally magnesite, aragonite and nyererite form subsolidus assemblage of the experimental system that agrees closely with the mineralogical data for primary inclusions in super-deep diamonds. It is essential for diamond origin that carbonate melts are effective solvent of elementary carbon in contrast to oxide and silicate melts. The very possibility of diamond genesis is determined by the physico-chemical properties.

Similar physico-chemical behavior would be expected for the carbonate system K_2CO_3–Na_2CO_3–$MgCO_3$–$FeCO_3$–$CaCO_3$ at pressures of 6–13 GPa (as at the upper mantle depths of 150–419 km). The system is representative in respect of the major components at multicomponent carbonate constituent of the upper-mantle diamond-parental media. A high diamond-forming efficiency of similar multicomponent carbonate system (Litvin and Zharikov 1999) as well as of silicate-carbonate system with analogous carbonate constituent (Litvin and Zharikov 2000) has been first discovered in melts with compositions reproducing these at primary inclusions in natural diamonds (Schrauder and Navon 1994). The experimental composition of multicomponent carbonate growth melts-solvents of elementary carbon is corresponding to (wt%): K_2CO_3 27.21, Na_2CO_3 2.89, $MgCO_3$ 17.35, $FeCO_3$ 25.63, $CaCO_3$ 26.91. The examples of effective crystallization of diamond in the multicomponent carbonate-carbon melt-solutions are demonstrated in the Fig. 3.1. Experimentally-based data demonstrate that multicomponent alkaline carbonate and, the more so, silicate-carbonate systems can melt at temperatures much lesser than the geothermal values.

3.3 Complete Liquid Miscibility in Silicate-(±Oxide)-Carbonate Systems

Multicomponent carbonate systems are of critical importance in formation of diamond-parental silicate-(±oxide)-carbonate-carbon media at all depths of the Earth's mantle. Carbonate melts are represented as the effective solvents of rock-forming silicate, oxide, alumina-silicate mantle minerals as well as of C–O–H–N-volatile components and phases. Likewise, the accessory minerals which are paragenetic to diamonds have considerable solubility in the diamond-parental carbonatite melts. Not only silicate, oxide, alumina-silicate but also phosphate and chloride phases are identified among the accessory paragenetic minerals. Chemical compounds of volatile components of the C–O–H–N system are readily soluble in the mantle carbonatite melts. The solvents are capable to form a homogenized completely miscible melts with the volatiles when critical point is reached. Physico-chemical reactions of this sort were experimentally confirmed for the systems of oxide SiO_2–H_2O (Kennedy et al. 1962; Keppler and Audetat 2005), silicates leucite–H_2O and albite–H_2O (Shen and Keppler 1997; Bureau and Kepple 1999; Audetat and Keppler 2004; Keppler and Audetat 2005) as well as modelled for carbonates (Watson et al. 1990). Completely miscible multicomponent peridotite-carbonatite and eclogite-carbonatite melts are usually guenched into uniformly distributed fine grained dendritic mineral assemblies. More emphatically the complete liquid miscibility is demonstrated by the quenched SiO_2-rich melt of coesite-bearing eclogite composition (Fig. 7.4c for example) (Kuzyura et al. 2015). Formation of completely miscible silicate-carbonate melts is also exhibited by experimental data on melting of carbonated mantle peridotites (Brey et al. 2008; Keshav et al. 2011).

When all things are considered, it is unlikely that the C–O–H–N-volatile components are capable to form their own fluid phases coexisting with the silicate-oxide-carbonate completely miscible growth melts for diamonds and associated phases. The reason is that the natural volatiles are high soluble in the growth melts but being of low relative content at the same time. In all likelihood, the own volatile phases, as an example see (Schrauder and Navon 1993), may be formed in the remains of diamond-parental melts in the closing stages of their crystallization at near-solidus temperatures. In such a situation, a seldom if ever capture of the volatile phases by growing diamonds should occur. In all probability, a presence of the volatile phases within some hermetic mineral inclusions in diamonds is conditioned by their release from the liquid remains of the multiphase parental media during consolidation at lowering temperature and formation of subsolidus assemblages.

Carbonate minerals and melts are effectively dissolved in the mantle silicate and silicate-oxide melts. A mutual high solubility of the carbonate and silicate-oxide melts has culminated in the important physico-chemical effect of their complete liquid miscibility at the total melting. As a result, the homogeneous silicate-oxide-carbonate liquid phases are formed. The multicomponent silicate-oxide-carbonatite

liquids transmit hereditary properties of the carbonate melts as good solvents of solid carbon phases (primarily, diamond and graphite) and, correspondingly, as effective diamond-producing media. The complex of physico-chemical properties of the multicomponent silicate-(±oxide)-carbonate-carbon systems at the states of complete and partial melting provides the capability of the natural parental melts for the combined crystallization of diamonds and paragenetic minerals.

All these peculiarities are elucidated at the physico-chemical experiments in consequence of studies on melting phase relations of the multicomponent heterogeneous silicate-oxide-carbonate-carbon systems and diamond crystallization in their melts-solutions. This creates the comprehensive pattern in respect to the natural origin of diamonds and associated phases that is inwardly coordinated and does not contradict to rigid requirements of the criterion of syngenesis of diamonds and primary inclusions (Litvin 2007). The joint crystallization of diamonds and paragenetic minerals is provided for diamonds formation through elementary carbon dissolving in the completely miscible silicate-oxide-carbonatite melts whereas the associated silicate, oxide and carbonate minerals—at the expense of components of the silicate-oxide-carbonate solvent of carbon. These physico-chemical mechanisms are capable to provide formation of the minerals of ultrabasic and basic parageneses over the whole course of genesis of diamonds and associated phases.

The complete miscibility of carbonate and silicate melts with formation of their miscible phases at experimental study of melting phase relations and, especially, of diamond crystallization is emphasized by their complete immiscibility with sulfide melts (Shushkanova and Litvin 2008).

3.4 Diamond Solubility and Carbon-Oversaturated Carbonate-Bearing Melts-Solutions

Phase diagram of carbon belongs among the major physico-chemical groundworks for the theory of diamond origin. Determination of coordinates of the ternary point graphite + diamond + melt at about 11.5 GPa, 4600 °C made possible to generalize thermodynamic and experimental data in the form of PT-phase diagram of the one-component system carbon depicted in the Fig. 3.6 (Bundy et al. 1996). The PT-conditions of formation of diamond and graphite are thermodynamically controlled by the equilibrium graphite-diamond boundary. However the actual kinetic state of the solid carbon phases does not favored to complementary direct transformation of graphite into diamond at the deviation of the carbon system PT-conditions for the equilibrium boundary. That is extremely significant that both graphite and diamond phases representing the thermodynamically stable modifications of solid carbon are capable to retain as thermodynamically metastable but kinetically time-steady phases over a wide range of pressure and temperature. Diamond can occur as a thermodynamically metastable phase within the field of graphite stability, and metastable graphite is kinetically tolerant phase within the

field of diamond stability. It is no small importance that both the stable and metastable phases are capable to coexist steadily to one another. The corresponding kinetic boundaries of the metastable fields for the solid phases of carbon are pictured in Fig. 3.6.

The equilibrium and non-equilibrium states in the system graphite-diamond with stable and metastable phases of solid carbon may be expressed by relationships between the molar isobaric potentials for both graphite and diamond stable (G_{gs}, G_{ds}) and metastable (G_{gm}, G_{dm}) phases (where G—molar isobar potential, g—graphite, d—diamond, s—stable phase, m—metastable phase):

(i) $G_{gs} = G_{ds}$, or $G_{gs} - G_{ds} = \Delta G_{gs\text{-}ds} = 0$ (graphite-diamond equilibrium curve),
(ii) $G_{dm} > G_{gs}$, or $G_{dm} - G_{gs} = \Delta G_{dm\text{-}gs} > 0$ (graphite stability field),
(iii) $G_{gm} > G_{ds}$, or $G_{gm} - G_{ds} = \Delta G_{gm\text{-}ds} > 0$ (diamond stability field).

Thus, both graphite and diamond are stable at the equilibrium boundary whereas metastable diamond tends to transform into stable graphite, and metastable graphite

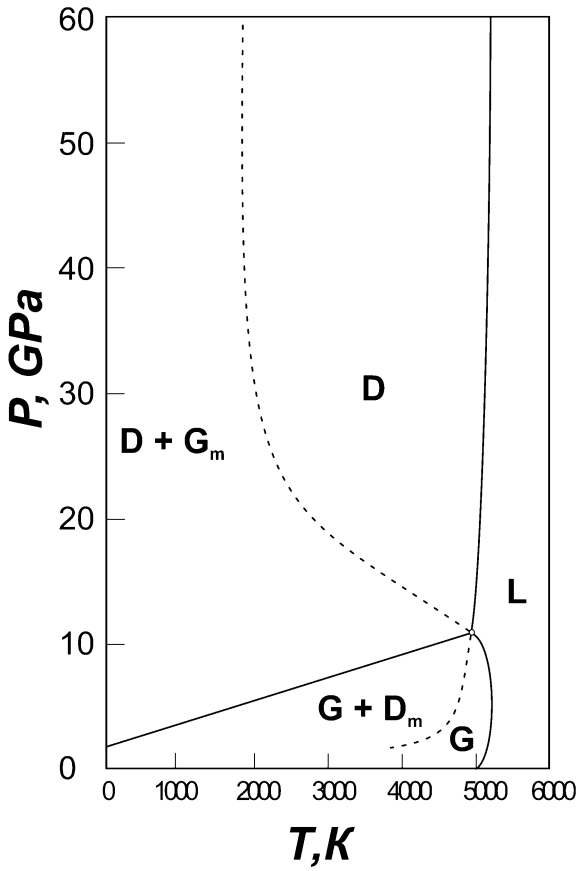

Fig. 3.6 Phase and transition PT-diagram for carbon (Bundy et al. 1996): *solid lines*—equilibrium phase boundaries for graphite (G), diamond (D) and their melts (L); *dashed lines*—kinetic thresholds for direct transformation of metastable diamond (Dm) to graphite and metastable graphite (Gm) to diamond

into stable diamond within the stability fields for corresponding solid carbon phases. For one-component carbon system, the thermodynamic tendency of metastable phases to transformation into the stable ones is effectively retarded kinetically due to too high energy barrier for these solid state polymorphic transitions. The removal of PT-state of the carbon system from the equilibrium graphite-diamond boundary is attended with increasing of the molar isobar potentials difference for the metastable and respective stable phases that is bound to enhance energetically the tenency of metastable carbon phases to transition into the stable ones.

The equilibrium phase diagram of carbon characterizes also the thermodynamically reversible phase relations of graphite and diamond with melts. Equilibrium melting of graphite proceeds at relatively low pressures along a univariant curve graphite + melt with maximum at about 5 GPa, 4900 °C. Melting curve of graphite can transfer via the invariant point graphite + diamond + melt to the univariant curve diamond + melt with a positive slope which is experimentally traced up to 50 ГПа, 4900 °C (Bundy et al. 1996).

Natural diamond-producing media belong to the systems of more complicated compositions for which carbon is one of the boundary components. On melting, systems of this sort can interact with solid carbon phases on their dissolving and crystallization. In these cases components of the diamond-producing systems are practically not soluble in the carbon solid phases. This retains the equilibrium PT-position of the graphite-diamond phase boundary under the conditions of diamond genesis. Thus, the equilibrium graphite-diamond boundary gives precise control over the PT-conditions of crystallization for the solid carbon phases at natural diamond-producing systems of any complexity.

The driving forces and physico-chemical mechanisms which controls the processes of nucleation and crystal growth of natural diamonds have unraveled in the "solid carbon-solvent" systems at PT-conditions of diamond thermodynamic stability. This mechanism is similar to these of the systems of metal-carbon (Litvin 1969), carbonate-carbon (Litvin and Spivak 2004; Spivak and Litvin 2004), silicate-carbonate-carbon with completely miscible silicate-carbonate melts-solvents for carbon (Litvin 2009), sulfide-carbon (Litvin et al. 2002), K-chloride-carbon (Litvin 2003) and carbon-oversaturated melts of carbonatite (Litvin et al. 2001) and silicate-carbonatite (Litvin et al. 2003) rocks of Chagatai (Uzbekistan) and Kokchetav (Kazakhstan) massifs, respectively. The same mechanism play a crucial role in a high-speedy crystallization of the microdiamond accretions—synthetic "diamondites" (Litvin and Spivak 2003; Litvin et al. 2005) the natural rock-similar mono-mineral samples of which are known and have described in details (Kurat and Dobosi 2000).

Equilibrium state of the system solid carbon—solvent is characterized by the relationship between the molar isobar potentials g of solid phases and chemical potentials μ of carbon dissolved in solutions which are saturated in respect to corresponding solid phases—diamond or graphite (as to stable so metastable phases —μ^c_{ds}, μ^c_{gs}, μ^c_{dm}, μ^c_{gm}). As this takes place, the equilibrium between diamond and carbon-in-melt, saturated in respect to diamond, has been in existence and corresponds to the equation $G_{ds} = \mu^c_{ds}$ (at the diamond stability conditions). Therewith it

formally is allowable the equilibrium state between metastable graphite and carbon-in-melt, saturated in respect to metastable graphite, that can be expressed as $G_{gm} = \mu^c_{gm}$. The equilibrium state of graphite and metastable diamond with saturated in respect to them carbon melts-solutions (at the graphite stability conditions) may be expressed in an analogous way.

To a thermodynamic proposition for the diamond stability conditions, it is essential that solubility of metastable graphite phase is bound to be higher than that of stable diamond phase. Correspondingly, the relation between chemical potentials and concentrations of carbon in the melts-solutions saturated in respect to metastable graphite and stable diamond can be described with the following equation: $\mu^c_{gm} - \mu^c_{ds} = \Delta\mu^c_{gm} - \mu^c_{ds}$ $(=\Delta G_{gm} - G_{ds}) = kT \ln N^c_{gm}/N^c_{ds}$, where k is Boltzmann constant, T is temperature (K), N^c_{gm} is concentration of carbon in melt-solution saturated in respect to metastable graphite ("equilibrium" solubility of metastable graphite), N^c_{ds} is concentration of carbon in melt-solution saturated in respect to diamond (equilibrium solubility of stable diamond), and the quantity N_{gm}/N_{ds} is oversaturation coefficient (β) for solution at any PT-point of metastable phase existence. It should be noted that expressions $\mu_i = \mu^o_i + kT \ln \alpha_i$ and $\alpha_i = \gamma N_i$ are used at the equation deriving, where α_i is activity and γ is activity coefficient.

If the $\Delta\mu^c_{gm} - \mu^c_{ds} = 0$, then $\beta = 1$. By this is meant that PT-position of the system is related to any point of the graphite-diamond equilibrium curve, and the solubility of diamond and graphite should be equal in the chemically same carbon melt-solution. If $\Delta\mu^c_{gm} - \mu^c_{ds} > 0$, then $\beta > 1$. In this case the system belongs to the PT-conditions of diamond stability with metastable graphite state. Solubility of metastable graphite should exceed the solubility value of stable diamond therewith an extent of the solubility excess is built up as PT-conditions of the system recede from the graphite-diamond equilibrium curve. If $\Delta\mu^c_{gm} - \mu^c_{ds} > 0$, then $\beta > 1$. Under these conditions the carbon system is in the stable graphite field, and solubility of metastable diamond exceeds the solubility of stable graphite.

The oversaturated state of dissolved carbon in respect to diamond phase in molten melts-solvents should determine the driving force of the processes of nucleation and crystallization of diamond in melts-solvents from chemically different materials. The carbon source plays a specific role in formation of oversaturated state of the melt-solution in respect to diamond. If diamond will serve as carbon source during diamond-producing process under isothermal conditions, then the melt-solutions can only attain an equilibrium state that has been determines as "diamond solubility". Diamond solubility as the maximum value for concentration of elementary carbon, which was incoming into the melt-solvent on diamond dissolving, defines the equilibrium state of the diamond-solvent system.

The relationships between the equilibrium solubility values for thermodynamically stable and metastable solid carbon phases are different for the dissimilar physico-chemical conditions.

Thus, both graphite and diamond are in equilibrium in the graphite-diamond curve, and their solubilities in any melt-solvent are equal. As a result, the melt-solvent is simultaneously saturated in respect to diamond and graphite phases, and initiation of carbon-oversaturated melt-solution in respect to any of the

equilibrium solid carbon phases is excluded. Cardinal changes are powered if the equilibrium system of graphite, diamond and carbon-saturated melt-solution becomes displaced in PT-position inside the field of thermodynamic stability of diamond. At these conditions the solubility of metastable graphite is higher than that of stable diamond. Under isothermal conditions the melt-solution becomes carbon-oversaturated in respect to stable diamond due to dissolution of metastable graphite. In the limiting case the value of carbon-oversaturation of the melt-solution in respect to diamond is bound to be determined with the difference of metastable graphite and stable diamond equilibrium solubility. The state of melt-solution oversaturated in respect to diamond is metastable in the thermodynamic sense, and the oversaturation state becomes as the powerful driving force for nucleation and crystallization of diamond. The driving force of diamond formation in the melts-solutions of carbon is kinetic by its nature; the transfer of dissolved elementary carbon from the dissolving metastable graphite to growing stable diamond may be diffusive and convective. If the equilibrium system of graphite, diamond and carbon-saturated melt-solution has displaced in PT-position inside the field of thermodynamic stability of graphite, then a similar scenario takes place in which diamond is a metastable phase and graphite is stable.

Diamond may be used as a carbon source under the condition of its own stability. In this case the effective carbon-oversaturated melts-solutions may be set up by a thermogradient field when the diamond solubility is greater at higher than at lower temperature due to the positive relationship of the solubility from temperature. This will cause of the physico-chemical mechanisms of diamond nucleation and crystal growth within the low-temperature zone. The mechanism is analogous to these discussed above.

The concentration of carbon-oversaturated melt-solution is responsible for the determining kinetic parameters of diamond crystallization as a density of nucleation and crystal growth rate. The available theoretical and experimental data permit to construct a generalized PTN_c-diagram of carbon-oversaturation for the system graphite-diamond-solvent (Fig. 3.7) including the stable and metastable phases of solid carbon (Litvin 1969; Litvin and Spivak 2004). The line of equal solubility of thermodynamically stable graphite and diamond (ab) is the support element for the oversaturation diagram. The support element has superposed the equilibrium graphite-diamond curve on the projection onto a coordinate PT-plane. The intersection in Fig. 3.7 of graphite (nprk) and diamond (slmt) solubility surfaces, which are common for the stable and metastable phases of solid carbon, takes place in the line of their equal solubility. The area of carbon-oversaturated melt-solutions in respect to diamond (abrplm) is arranged in the diamond stability field between the solubility surfaces for stable diamond and metastable graphite. The area of carbon-oversaturated melt-solutions in respect to graphite (abtsno) is located symmetricly in the graphite stability field. The areas of carbon-oversaturated melts-solutions are originated due to that metastable phases are of greater carbon solubility at the same melt-solvent than the stable ones. Thus, the

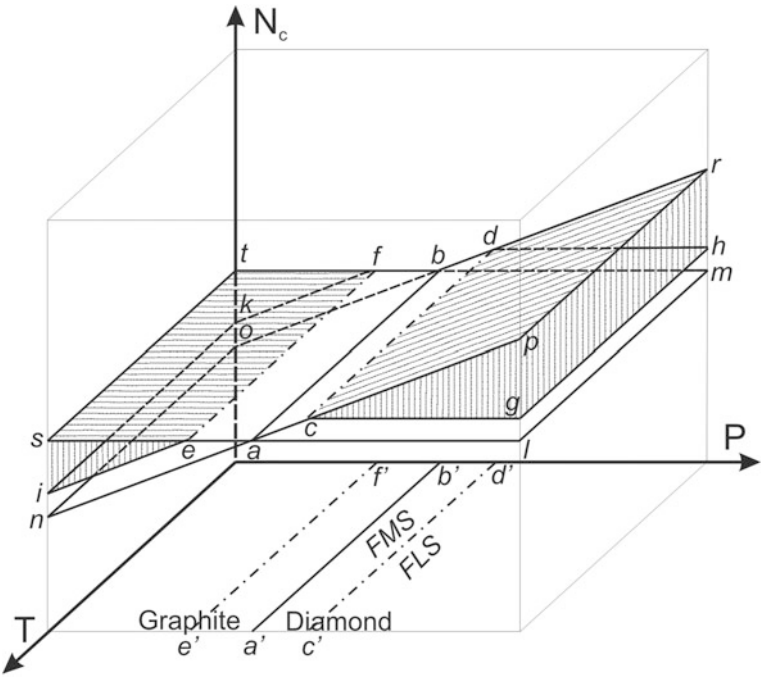

Fig. 3.7 *PTN$_c$*-diagram of carbon oversaturation in the melt-solvent: (*ab*)—projection of *PT*-curve of graphite-diamond equilibrium (*a′b′*); (*cdhg*)—boundary between the field of labile (*cdhgpr*) and metastable (*cdhglabm*) carbon-oversaturated melt-solution in respect to diamond; (*efkj*)—boundary between the field of labile (*efkjst*) and metastable (*efkjnoba*) carbon-oversaturated melt-solution in respect to graphite; the boundary lines (*cd*) and (*ef*) are projected as (*c′d′*) and (*e′f′*) onto the boundary *PT* plane on each side of the graphite-diamond equilibrium curve (*a′b′*); *FMS* and *FLS*—positions of the fields of metastably and labily saturated melts-solutions (view from above)

carbon-oversaturated melt-solutions in respect to stable phase are originated as the difference of the metastable and stable phases solubilities in these conditions. In other words, the PTN$_c$-diagram of state for the system graphite-diamond-solvent is simultaneously representative as diagram of carbon-oversaturation melt-solution in respect to the thermodynamically stable solid carbon phases.

It should be stressed that the key to the diamond-producing process with the use of the "melt-solution" physico-chemical mechanism lies with the formation of diamond-oversaturated melts-solutions independently of nature of carbon source for the dissolved elementary carbon. The carbon-oversaturated melt-solution in respect to diamond phase represents the driving force which has stimulated the nucleation and crystallization of diamond crystals. The diamond crystallization has no come to the end as long as the oversaturated in respect to diamond melt-solution is became saturated. Hence the disappearance of oversaturated state in the diamond-producing melt-solution controls the duration of diamond crystal growth between the states

of oversaturation at nucleation and equilibrium solubility. It is also of prime importance that the higher "labile" carbon-oversaturation is required for diamond phase nucleation (Fig. 3.1) whereas the relatively lower "metastable" carbon-oversaturation—for the following diamond crystal growth using the nuclei. The boundary between labile and metastable states of the carbon-oversaturated solutions in respect to diamond has taken into account and marked as a kinetic boundary (cdhg) in the PTN_c-diagram of oversaturation. The labile carbon-oversaturated Ni–Fe-metallic melts-solutions are practically used at the industrial processes of mass spontaneous crystallization of synthetic diamonds whereas the metastable ones for seeded growth of single-crystalline diamonds. The processes of seeded growth of diamond have also realized in single (Litvin et al. 1997, 1998, 1999) and multi-component carbonate-carbon (Litvin and Zharikov 1999) and silicate-carbonate (Litvin and Zharikov 2000; Litvin et al. 2008, 2012) melts-solutions (Fig. 3.8a–c).

The boundary (cd) between the fields of labile carbon-oversaturated solutions (FLS) and metastable carbon-oversaturated solutions (FMS) at their projection onto the coordinate PT-surface (Fig. 3.7) is presented by a subparallel line in respect to the graphite-diamond equilibrium curve. Therewith the field of labile oversaturation is placed between the diamond-graphite equilibrium curve and the FMS/FLS boundary. Experimental studies of diamond crystallization in the metal-carbon and carbonate-carbon systems demonstrate that seeded growth of single-crystalline diamonds under the FMS-conditions is accompanied with the kinetic effect of nucleation and mass crystallization of metastable graphite (Fig. 3.8e, f). By this means the formation of labile carbon-oversaturated in respect to diamond melts-solutions is among the most important physico-chemical conditions of natural diamonds origin.

The problem of mantle carbon source for diamond formation is a widely debate topic among mineralogists (Navon 1999). The version of primordial carbon may be justified as preferential. The version correlates well with formation model the early Earth by heterogeneous accretion with participation of carbonaceous chondrites (Urey 1956, 1962; Turekian and Clark 1969; Murthy and Hall 1972; Ringwood 1966, 1975). Elementary carbon was found as graphite, amorphous phase and diamond in the Earth's mantle xenoliths and inclusions in diamonds (Wagner 1916; Sobolev 1977; Dawson 1980; Pineau et al. 1987). Most likely the stable graphite phase had been initially formed at the early stages of Earth's history. With increase of planet mass, the internal pressure in central parts of the growing Earth becomes gradually increased primarily within the PT-values for the field of graphite thermodynamic stability. With further increase of the internal pressure, the PT-values for the field of diamond stability should be achieved but the graphite phase will continue to persist as thermodynamically metastable but kinetically tolerant phase in accordance with the PT-diagram of carbon by (Bundy et al. 1996). It is worthy of note that the metastable graphite tolerance is propagated to the Earth's lower mantle depths in excess of more than 1800 km. The version of primordial elementary carbon phase (graphite) is easily compatible with the criterion of syngenesis of diamonds and associated phases.

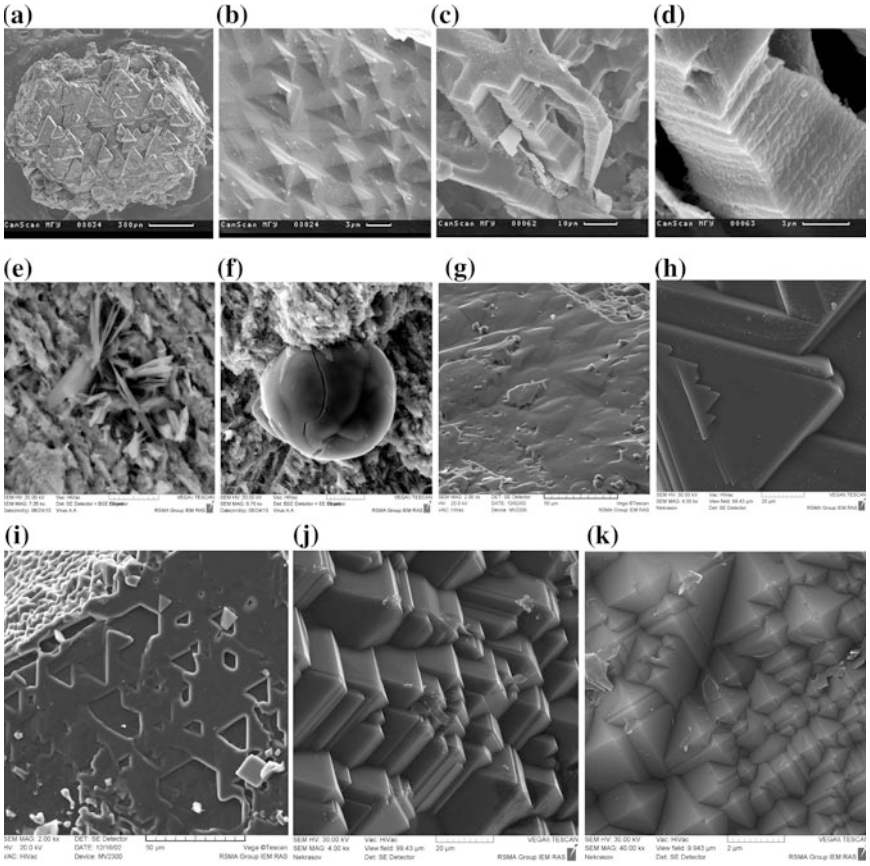

Fig. 3.8 Scanning electron micrograph (SEM) images of diamond overgrowths formed in silicate-carbonate-carbon melts-solutions on the seed crystals at the FMS field together with nucleation and mass crystallization of nonstable graphite: **a** the polycentric growth on the octahedral face; **b** micropyramids on the cubic face; **c**, **d** fibrous growth on the cubic face; **e**, **f** tabular and spherulitic forms of nonstable graphite crystallized together with diamond seeded growth; **g**, **h** diamond growth on octahedral faces of seeds; **i** diamond growth on both octahedral and cubic seed faces; **k**, **l** diamond polycentric growth of cubic seed face

References

Akaishi M (1996) Effect of Na_2O and H_2O addition to SiO_2 on the synthesis of diamond from graphite. In: Proceedings of the 3rd NIRIM (National Institute for Research in Inorganic Materials) international symposium on advanced materials (ISAM'96), Tsukuba, Ibaraki, Japan, pp 75–80

Akaishi M, Yamaoka S (2000) Crystallization of diamond from C–O–H fluids under high-pressure and high-temperature conditions. J Cryst Growth 209:999–1003. doi:10.1016/S0022-0248999000756-3

Arima M, Kozai Y, Akaishi M (2002) Diamond nucleation and growth by reduction carbonate melts under high-pressure and high-temperature conditions. Geology 30:691–694. doi:10.1130/0091-7613(2002)030<0691:DNAGBR>2.0.CO;2

Audetat A, Keppler H (2004) Viscosity of fluids in subduction zones. Science 303:513–516

Bobrov AV, Litvin YA (2011) Mineral equilibria of diamond-forming carbonate-silicate systems. Geochem Int 49(13):1267–1363

Bobrovsky SV, Godolev VM, Zamyshlyaev BV et al (1976) The study of thermal decompression influence on the spallation velocity for strong waves in solids. In: Physico-Tekhnicheskie Problemy Razrabotki Polezhykh Iskopaemykh, vol 3, pp 49–57 (and in: Soviet Mining Science)

Boulard E, Guyot F, Fiquet G (2012) The influence of Fe content on Raman spectra and unit cell parameters on magnesite-siderite solid solutions. Phys Chem Miner 39:239–246. doi:10.1007/s00269-011-0479-3

Brey GP, Bulatov VK, Girnis AV, Lahaye Y (2008) Experimental melting of carbonated peridotite at 6–10 GPa. J Petrol 49(4):797–821

Bulanova GP, Walter MJ, Smith CB et al (2010) Mineral inclusions in sublithospheric diamonds from Collier 4 kimberlite pipe, Juina, Brazil: subducted protholiths, carbonated melts and primary kimberlite magmatism. Contrib Mineral Petrol 160:489–510

Bundy FP, Basset WA, Weathers MS et al (1996) The pressure-temperature phase and transformation diagram for carbon; updated through 1994. Carbon 34:141–153

Buob A, Luth RW, Schmidt MW, Ulmer P (2006) Experiments on $CaCO_3$-$MgCO_3$ solid solutions at high pressure and temperature. Amer Miner 91:435–440

Bureau H, Keppler H (1999) Complete miscibility between silicate melts and hydrous fluids in the upper mantle: experimental evidence and geochemical applications. Earth Planet Sci Lett 165:187–196

Dasgupta R, Hirschmann MM (2010) The deep carbon cycle and melting in Earth's interior. Earth Planet Sci Lett 298:1–13. doi:10.1016/j.epsl.2010.06.039

Dawson JB (1980) Kimberlites and their xenoliths. Springer, Berlin

Harte B (2010) Diamond formation in the deep mantle the record of mineral inclusions and their distribution in relation to mantle dehydration zone. Mineral Mag 74(2):180–215

Hong SM, Akaishi M, Yamaoka S (1999) Nucleation of diamonds in the system of carbon and water under very high pressure and temperature. J Cryst Growth 200:326–328. doi:10.1016/S0022-0248(98)01288-3

Huang WL, Wyllie PJ (1976) Melting relationships inCaO-CO_2 and MgO-CO_2 to 36 kilobars with comments on CO_2 in the mantle. Earth Planet Sci Lett 40:129–132

Irving AJ, Wyllie PJ (1975) Subsolidus and melting relationships for calcite, magnesite and join $CaCO_3$-$MgCO_3$ to 36 kb. Geochim Cosmochim Acta 39:35–53

Kaminsky F, Wirth R, Matsyuk S et al (2009) Nyerereite and nahcolite inclusions in diamond: evidence for lower-mantle carbonatitic magmas. Mineral Mag 73(5):797–816

Kaminsky FV, Wirth R, Schreiber A (2013) Carbonatitic inclusions in deep mantle diamond from Juina, Brazil: new minerals in the carbonate-halide association. Canad Mineral 140(6):734–753

Karato S, Forte AM, Liebermann RC et al (2000) Earth's deep interiors: mineral physics and tomography from the atomic to the global scale. Geophysics monograph series 117, p 289

Katsura T, Ito E (1990) Melting and subslidus relations in the $MgSiO_3$-$MgCO_3$ system at high pressures: implications to evolution of the Earth's atmosphere. Earth Planet Sci Lett 99:110–117

Kennedy GC, Wasserburg GJ, Heard HC, Newton RC (1962) The upper three-phase region in the system SiO_2-H_2O. Am J Sci 260:501–521

Keppler H, Audetat A (2005) Fluid-mineral interaction at high pressure. In: Miletich R (ed) Mineral behaviour at extreme conditions. Eoetvoes University Press, Budapest, pp 225–251

Keshav S, Gudfinnsson GH, Presnall DC (2011) Melting phase relations of simplified carbonated peridotite at 12–26 GPa in the systems CaO–MgO–SiO_2–CO_2 and CaO–MgO–Al_2O_3–SiO_2–CO_2: highly calcic magmas in the transition zone of the Earth. J Petrol 32(11):2265–2291

Klein-BenDavid O, Logvinova AM, Schrauber M et al (2009) High-Mg carbonatitic microinclusions in some Yakutian diamonds—a new type of diamond-forming fluid. Lithos 112: 648–659

Kurat G, Dobosi G (2000) Garnet and diopside-bearing diamondites (framesites). Mineral Petrol 69:143–159. doi:10.1007/s007100070018

Kuzyura AV, Litvin YA, Jeffrises T (2015) Interface partition coefficients of trace elements in carbonate-silicate parental media for diamonds and paragenetic inclusions (experiments at 7.0-8.5 GPa). Russ Geol Geophys 56:221–231

Lavina B, Dega P, Downs RT et al (2009) Siderite at lower mantle conditions and the effects of the pressure-induced spin-pairing transition. Geophys Res Lett 36:L23306. doi:10.1029/2009GL039652

Leost I, Stachel T, Brey GP et al (2003) Diamond formation and source carbonation: Mineral associations in diamonds from Namibia. Contrib Mineral Petrol 145:15–24

Liebermann RC, Schreiber E (1969) Critical geothermal gradients in the mantle. Earth Planet Sci Lett 7:77–81

Litasov KD, Ohtani E (2009) Solidus of carbonated peridotite in the system CaO-Al_2O_3-MgO-SiO_2-Na_2O-CO_2 to the lower mantle depths. Phys Earth Planet Int 177:46–58

Litvin YA (1969) To the diamond origin problem. Zapiski Vsesoyuzn Mineralogich Obschestva 98(2):114–121

Litvin YA (2003) Alkali-chloride components in growth processes of diamond under conditions of the upper mantle and high-pressure experiments. Dokl Akad Nauk 389(3):382–386

Litvin YA (2007) High-pressure mineralogy of diamond genesis. In: Ohtani E (ed) Advances in high-pressure mineralogy. Geological Society of America Special paper 421, pp 83–103. doi:10.1130/2007.2421(06)

Litvin YA (2009) The physicochemical conditions of diamond formation in the mantle matter: experimental studies. Russ Geol Geophys 50(12):1188–1200

Litvin YA (2012) Experimental studies of physico-chemical conditions of natural diamond origin at the example of the system eclogite-carbonatite-sulfide-diamond. Geol Ore Depos 54(6): 443–457

Litvin YA (2013) Physico-chemical conditions of syngenesis of diamond and heterogeneous inclusions in the carbonate-silicate parental melts (experimental study). Mineral J 35(2):5–24

Litvin YA, Spivak AV (2003) Rapid growth of diamondite at the contact between graphite and carbonate melt: experiments at 7.5–8.5 GPa. Dokl Earth Sci 391A:888–891

Litvin YA, Spivak AV (2004) Crystal growth of diamond at 5.5–8.5 GPa in carbonate- carbon melt-solutions being chemical analogues of natural diamond forming melts. Mater Sci Trans 84(3):27–34

Litvin YA, Zharikov VA (1999) Primary fluid-carbonatite inclusions in diamond: experimental modeling in the system K_2O-Na_2O-CaO-MgO-FeO-CO_2 as a diamond formation medium at 7–9 GPa. Dokl Earth Sci 367A:801–805

Litvin YA, Zharikov VA (2000) Experimental modeling of diamond genesis: diamond crystallization in multicomponent carbonate-silicate melts at 5–7 GPa and 1200–1570 °C. Dokl Earth Sci 373:867–870

Litvin YA, Chudinovskikh LT, Zharikov VA (1997) Experimental crystallization of diamond and graphite from alkali-carbonate melts at 7–11 GPa. Trans (Doklady) Russ Acad Sci Earth Sci Sect 355A(6):908–911

Litvin YA, Chudinovskikh LT, Zharikov VA (1998) The seeded growth of diamond in the $Na_2Mg(CO_3)2$–$K_2Mg(CO_3)_2$-C system at 8–10 GPa. Dokl Earth Sci 359A(3):464–466

Litvin YA, Chudinovskikh LT, Saparin GV et al (1999) Diamonds of new alkaline carbonate-graphite HP syntheses: SEM morphology, CCL-SEM and CL spectroscopy studies. Diamond Relat Mater 8:267–272. doi:10.1016/S0925-9635(98)00318-5

Litvin YA, Jones AP, Beard AD et al (2001) Crystallization of diamond and syngenetic minerals in melts of diamondiferous carbonatites of the Chagatai Massif, Uzbekistan: experiment at 7.0 GPa. Dokl Earth Sci 381A:1066–1069

Litvin YA, Butvina VG, Bobrov AV, Zharikov VA (2002) First synthesis of diamond in sulfide-carbon systems: the role of sulfides in diamond genesis. Dokl Akad Nauk 321:106–109

Litvin YA, Spivak AV, Matveev YA (2003) Crystallization of diamond in the molten carbonate-silicate rocks of the Kokchetav metamorphic complex at 5.5–7.5 GPa. Geochem Int 11:1090–1098

Litvin YA, Kurat G, Dobosi G (2005) Experimental study of diamondite formation in carbonate-silicate melts: a model approach to natural processes. Russ Geol Geophys 46 (12):1285–1299

Litvin YA, Litvin VY, Kadik AA (2008) Experimental characterization of diamond crystallization in melts of mantle silicate-carbonate-carbon systems at 7.0–8.5 GPa. Geochem Int 46(6):531–553

Litvin YA, Vasiliev PG, Bobrov AV et al (2012) Parental media of natural diamonds and primary mineral inclusions in them: evidence from physicochemical experiment. Geochem Int 50(9):726–759

Litvin YA, Spivak AV, Solopova NA, Dubrovinsky LS (2014) On origin of lower-mantle diamonds and their primary inclusions. Phys Earth Planet Int 228:176–185. doi:10.1016/j/pepi/2013.12.007

Logvinova AM, Wirth R, Fedorova EN, Sobolev NV (2008) Nanometre-sized mineral and fluid inclusions in cloudy Siberian diamonds: new insights on diamond formation. Eur J Mineral 20:317–331

Logvinova AM, Wirth R, Tomilenko AA et al (2011) Peculiarities of phase composition of nano-sized crystal-fluid inclusions in аллювиальных diamonds of North-Eastern Siberian platform. Russ Geol Geoph 52(11):1634–1648

Martinez I, Zhang J, Reeder RJ (1996) In situ X-ray diffraction of aragonite and dolomite at high pressure and high temperature: evidence for dolomite break down to aragonite and magnesite. Amer Mineral 81:611–624

Murthy RV, Hall H (1972) The origin and composition of the Earth's core. Phys Earth Planet Int 6:125–130

Navon O (1991) High internal pressures in diamond fluid inclusions determined by infrared absorption. Nature 353:746–748. doi:10.1038/353746a0

Navon O (1999) Diamond formation in the Earth's mantle. In: Gurney JJ, Gurney JL, Pascoe MD, Richardson SH (eds) Proceedings of the VII international kimberlite conference: red roof design, Cape Town, vol 2, pp 584–604

Palyanov YN, Sokol AG, Sobolev NV (2005) Experimental modeling of the mantle diamond-forming processes. Russ Geol Geophys 46(12):1290–1303

Pineau F, Javoy M, Kornprobst J (1987) Primary igneous graphite in ultramafic xenoliths: II. Isotopic composition of the carbonaceous phases presented in xenoliths and host lava at Tissemt (Eggere, Algerian Sahara). J Petrol 28:313–332

Reisman A (1959) Heterogeneous equilibriain the system K_2CO_3–$MgCO_3$. J Am Chem Soc 81:807–811

Ringwood AE (1966) Chemical evolution of the terrestrial planets. Geocim Cosmochim Acta 30:41–104

Ringwood AE (1975) Composition and petrology of the Earth's Mantle. McGraw-Hill, New York, 618 p

Safonov OG, Perchuk LL, Litvin YA (2007) Melting relations in the chloride-carbonate-silicate systems at high-pressure and the model for formation of alkali diamond-forming liquids in the upper mantle. Earth Planet Sci Lett 253:112–128

Santillan J, Williams Q (2004) A high-pressure infrared and X-ray study of $FeCO_3$ and $MnCO_3$: comparison with $CaMg(CO_3)_2$-dolomite. Phys Earth Planet Sci Lett 143:291–304. doi:10.1016/j.pepi.2003.06.007

Schrauder M, Navon O (1993) Solid carbon dioxide in a natural diamond. Nature 365:42–44

Schrauder M, Navon O (1994) Hydrous and carbonatitic mantle fluids in fibrous diamonds from Jwaneng, Botswana. Geochim Cosmochim Acta 58:761–771. doi:10.1016/0016-7037(94)90504-5

Shatskiy AF, Sharygin IS, Gavryushkin PN et al (2013a) The system K_2CO_3-$MgCO_3$ at 6 GPa and 900–1450 °C. Am Miner 98:1593–1603

Shatskiy AF, Gavryushkin PN, Sharygin IS et al (2013b) Melting and subsolidus phase relations in the system Na_2CO_3–$MgCO_3$ ± H_2O at 6 GPa and the stability of $Na_2Mg(CO_3)_2$ in the upper mantle. Am Miner 98:2172–2182

Shatskiy AF, Litasov KD, Palyanov YN (2015) Phase relations in carbonate systems at pressures and temperatures of lithospheric mantle: review of experimental data. Russ Geol Geophys 56 (1–2):149–187

Shen AH, Keppler H (1997) Direct observation of complete miscibility in the albite—H_2O system. Nature 385:710–712

Shushkanova AV, Litvin YA (2008) Experimental evidence for liquid immiscibility in the model system $CaCO_3$-pyrope-pyrrhotite at 7.0 GPa: the role of carbonatite and sulfide melts in diamond genesis. Canad Mineral 46:991–1005

Sobolev NV (1977) The deep-seated inclusions in kimberlites and the problem of the composition of the upper mantle. American Geophysical Union, Washington, DC, 304 p

Sokol AG, Palyanov YN, Palyanova GA et al (2001) Diamond and graphite crystallization from C-O-H fluids under high pressure and high temperature conditions. Diam Relat Mater 10:2131–2136. doi:10.1016/S0935-9635(01)00491-5

Solopova NA, Litvin YA, Spivak AV et al (2013) Phase diagram of Na-carbonate, the alkaline component of growth media of the super-deep diamond. Dokl Earth Sci 453(1):1106–1109

Solopova NA, Dubrovinsky L, Spivak AV et al (2014) Melting and decomposition of $MgCO^3$ at pressures up to 84 GPa. Phys Chem Miner 08. doi:10.1007/s00269-014-0701-1

Spivak AV, Litvin YA (2004) Diamond syntheses in multi-component carbonate-carbon melts of natural chemistry: elementary processes and properties. Diamond Relat Mater 13:482–487. doi:10.1016/j.diamond.2003.11.104

Spivak AV, Dubrovinsky LS, Litvin YA (2011) Congruent melting of calcium carbonate in a static experiment at 3500 K and 10-22 GPa: its role in the genesis of ultra-deep diamonds. Dokl Earth Sci 439(2):1171–1174

Spivak AV, Litvin YA, Ovsyannikov SV et al (2012) Stability and breakdown of $Ca^{13}CO_3$ melt associated with formation of ^{13}C-diamond in high-pressure static experiments up to 43 GPa and 3900 K. J Solid State Chem 191:102–106

Spivak A, Solopova N, Cerantola V et al (2014) Raman study of $MgCO_3$-$FeCO_3$ carbonate solid solution at high pressures up to 55 GPa. Phys Chem Miner 41:633–638. doi:10.1007/s00269-014-0676-y

Spivak A, Solopova N, Dubrovinsky L, Litvin Y (2015a) Melting relations of multicomponent carbonate MgCO3–FeCO3–CaCO3–Na2CO3 system at 11–26 GPa: application to deeper mantle diamonds formation. Phys Chem Miner. doi:10.1007/s00269-015-0765-6

Spivak AV, Solopova NA, Dubrovinsky LS, Litvin YA (2015b) The $MgCO_3$–$FeCO_3$–$CaCO_3$–Na_2CO_3 system at 12–23 GPa: phase relations and significance for the genesis of super-deep diamonds. Dokl Earth Sci 464(1):946–950

Stacey FD (1992) Physics of the Earth, 3rd edn. Brookfield Press, Brisbane, p 514

Stachel T, Harris JW, Brey GP (1998) Rare and unusual mineral inclusions in diamonds from Mwadui, Tanzania. Contrib Mineral Petrol 132:34–47. doi:10.1007/s004100050403

Stachel T, Brey G, Harris JW (2000) Kankan diamonds (Guines) I: from the lithosphere dawn to the transition zone. Contrib Mineral Petrol 140:1–15

Suito K, Namba J, Horikawa T et al (2001) Phase relations of $CaCO_3$ at high pressure and high temperature. Am Miner 86:997–1002

Taniguchi T, Dobson D, Jones AP et al (1996) Synthesis of cubic diamond in the graphite-magnesium carbonate and graphite-$K_2Mg(CO_3)_2$ systems at high pressure of 9–11 GPa region. J Mater Res 11:2622–2632

Tomlinson EL, Jones AP, Harris JW (2006) Co-existing fluid and silicate inclusions in mantle diamond. Earth Planet Sci Lett 250:581–595

Titkov SV, Gorshkov AI, Solodova YP et al (2006) Mineral microinclusions in cubic diamonds from the Yakutian deposits based on analytical electron microscopy data. Dokl Earth Sci 410:1106–1108

Tschauner O, Mao H, Hemley RJ (2001) New transformation of CO_2 at high pressures and temperatures. Phys Rev Lett 87(7):075701–075704

Turekian K, Clark SP (1969) Inhomogeneous accumulation of the Earth from the primitive solar nebula. Earth Planet Sci Lett 6:346–348

Urey HC (1956) Diamonds, meteorites and the origin of the solar system. Asrtrophys J 124: 623–637

Urey NC (1962) Evidence regarding the origin of the Earth. Geochim Cosmochim Acta 26:1–13

Wagner PA (1916) Graphite-bearing xenoliths from the Jagersfontein diamond pipe. Trans Geol Soc S Afr 19:54–56

Wang A, Pasteris JD, Meyer HOA, Dele-Duboi ML (1996) Magnesite-bearing inclusion assemblage in natural diamond. Earth Planet Sci Lett 141:293–306. doi:10.1016/0012-821X(96)00053-2

Watson EB, Wood BJ, Carroll MR (1990) Distribution of fluids in the mantle. In: Menzies MA (ed) Continental mantle. Clarendon Press, Oxford, pp 111–125

Weiss Y, Kessel R, Griffin WL et al (2009) A new model for the evolution of diamond-forming fluid: evidence from microinclusion-bearing diamonds from Kankan, Guinea. Lithos 112: 660–674

Wirth R, Kaminsky FV, Matsyuk S, Schreiber A (2009) Unusual micro- and nano-inclusions in diamonds from Juina area, Brazil. Earth Planet Sci Lett 112:660–674

Yamaoka S, Shaji Cumar MD, Kanda H, Akaishi M (2002) Formation of diamond from $CaCO_3$ in a reduced C-O-H fluid at HP-HT. Diamond Relat Mater 11:1496–1504. doi:10.1016/S0925-9635(02)00053-5

Zedgenizov DA, Ragozin AL, Shatsky VS et al (2009) Mg and Fe-rich carbonate-silicate high-density fluids in cuboid diamonds from the Internationalnaya kimberlite pipe (Yakutia). Lithos 112:638–647

Zedgenizov DA, Ragozin AL, Shatsky VS et al (2011) Carbonate and silicate media of crystallization of fibrous diamonds from placers of north-easterh Siberian platform. Russ Geol Geophys 52(11):1649–1664

Chapter 4
Upper-Mantle Diamond-Parental Systems in Physico-Chemical Experiment

The criterion of syngenesis of diamonds and primary mineral inclusions presents an effective instrument in determination of chemical composition of the growth melts of diamonds and genetically associated phases. Its role is sufficiently helpful at planning the experimental investigations on melting phase relations of the diamond-produced systems. Physico-chemical experiments are currently directed towards the construction of syngenesis diagrams for diamonds and associated phases of peridotitic and eclogitic parageneses. The concentration barrier of diamond nucleation in diamond-producing silicate-carbonate-carbon melts establishes the boundary conditions for nucleation of diamond phase in the growth melts which are variable by the relative content of silicate and carbonate components. The silicate-carbonate-carbon compositions of the parental melts for diamonds and paragenetic minerals are justified by the combined evidence of physico-chemical experiments and analytic mineralogy of diamond-associated phases. As a consequence, the physico-chemical mechanisms of genesis of diamonds and associated phase are experimentally disclosed. Deduced from experiments the genetic solutions are applied to the problem of origin of the diamond-bearing rocks among upper-mantle xenoliths in kimberlites. The complex of experimental physico-chemical results and analytic mineralogy data for diamond-associated phases offers a clearer view of the principal genetic markers for the primary inclusions in the upper mantle derived diamonds. Physico-chemical experimental results for the multicomponent silicate-oxide-carbonate-carbon systems has enabled to substantiate the mantle-carbonatite concept of genesis of diamond and associated phases and develop the genetic classification of syngenetic inclusions in the upper mantle derived diamonds.

Y.A. Litvin, *Genesis of Diamonds and Associated Phases*,
Springer Mineralogy, DOI 10.1007/978-3-319-54543-1_4

4.1 Syngenesis Criterion for Parental Melts of Diamonds and Associated Minerals

The ability of various natural molten substances to formation of diamond can be checked by testing experiments on spontaneous nucleation and crystallization of diamonds, i.e. on diamond synthesis. Mass crystallization of diamond in metallic melts with dissolved carbon oversaturated in respect to diamond (Bundy et al. 1955) is the well-known example. In this case the Ni–Mn–Fe-metal-graphite mixture (for example) is melted at PT-conditions of diamond stability forming carbon-oversaturated melt-solution that causes nucleation and crystallization of diamond (Litvin 1968). Similar testing experiments with peridotitic and eclogitic melts as well as their rock-forming minerals have discovered their inefficiency for diamond nucleation. At the same time the nucleation and growth of diamond have been experimentally tested and primarily observed in the carbon-oversaturated in respect to diamond melts-solutions for a number of chemically variable carbonate systems. The most interesting systems for natural diamond origin are shortly reviewed in (Litvin 2007). The graphite-bearing carbonate system $K_2Mg(CO_3)_2$–$K_2Fe(CO_3)_2$–$K_2Ca(CO_3)_2$–$Na_2Mg(CO_3)_2$–$Na_2Fe(CO_3)_2$–$Na_2Ca(CO_3)_2$–C was experimentally tested at 7–11 GPa and 1400–1900 °C for diamond formation with the use of the joins $K_2Mg(CO_3)_2$–C (Taniguchi et al. 1996; Litvin et al. 1997, 1998), $K_2Mg(CO_3)_2$–$Na_2Ca(CO_3)_2$–[$\pm K_2Fe(CO)_3$]–C and $K_2Ca(CO_3)$–$Na_2Ca(CO_3)_2$ [$\pm K_2Fe(CO_3)_2$]–C (Litvin et al. 1998, 1999a, 1999b). Diamonds were also synthesized effectively at 7 GPa and 1700–1750 °C in the carbonate-carbon $CaMg(CO_3)_2$–C system (Sato et al. 1999; Sokol et al. 2001). Nucleation and growth of diamonds have also observed in the systems of (Fe–Ni–Cu–sulfide)–carbon (Fig. 4.1) (Litvin et al. 2002; Litvin and Butvina 2004), K-chloride KCl–C (Fig. 4.2a) (Litvin 2003), Na-alkaline silicate Na_2SiO_3–C (Akaishi 1996),Ca–silicate $CaSiO_3$–C (Litvin 2009) and KCl–K_2CO_3–C (Tomlinson et al. 2004). Growth of diamond on seeds (metal-synthetic diamonds) has been effected in the metastable carbon-oversaturated melts-solutions of K-alkaline silicate K_2SiO_3 (Fig. 4.2b) and Na-alkaline silicate mixture $(Na_2SiO_3)_{50}(NaAlSi_3O_8)$ (wt%) (Fig. 4.2c). Therewith the seeded growth of diamond at 8.5 GPa and 1500–1590 °C was accompanied with nucleation and crystallization of metastable graphite as single-crystalline plates and spherules (Fig. 4.2d) that is a usual effect at crystallization of the carbonate-carbon and silicate-carbonate-carbon melts-solutions at PT-conditions of the field of metastable oversaturation (FMS).

Diamond has been successfully synthesized with graphite carbon-source using volatile components such as hydro-oxides (Akaishi et al. 1990), strongly compressed water at 7.7 GPa and 1900 °C (Hong et al. 1999; Sokol et al. 2001) and H_2O–SiO_2 mixture (Akaishi 1996). Efficient nucleation of diamond has also been demonstrated by the oxalic acid dehydrate $(COOH)_2 \cdot H_2O$ at 7.7 GPa and 1400–2000 °C (Akaishi and Yamaoka 2000). Diamond nucleation was reported for

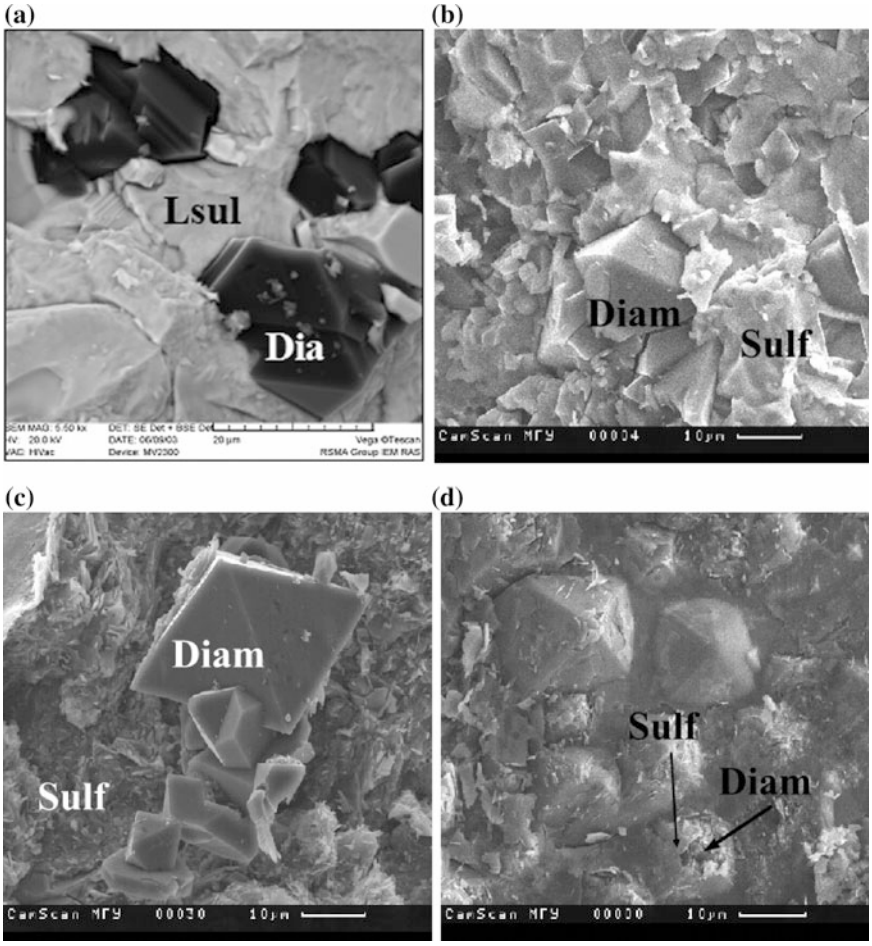

Fig. 4.1 Scanning electron micrograph (SEM) images of diamonds crystallized in the sulfide melts with dissolved elementary carbon: **a** octahedral and spinel-law crystals in quenched pyrrhotite melt, **b** octahedral crystals in the quenched $Cu_{17}Fe_{35}S_{48}$ melt, **c** intergrowth of octahedral and spinel-law crystals in quenched $Cu_{17}Fe_{35}S_{48}$ melt, **d** *thin* sulfide film covering cubic face of seed crystal with newly grown micropyramids (diffusion of dissolved elementary carbon from sulfide melt-solvent to growing diamond crystals was effected through the liquid films). *Symbols* Sul—solid sulfides, Lsul—quenched sulfide melt, Diam—diamond

carbon dioxide and H_2O–CO_2 mixture generated by oxalic acid dehydrate (Akaishi and Yamaoka 2000; Shaji Kumar et al. 2000, 2001; Akaishi et al. 2001; Yamaoka et al. 2000, 2002) and for mixtures of Na_2CO_3 and K_2CO_3 with oxalic acid dehydrate at 5.7 GPa and 1150–1420 °C (Palyanov et al. 1999, 2002). It was also shown that carbonates could be effective as a carbon source for diamond formation in strongly reduced conditions (Arima 1996; Yamaoka et al. 2002).

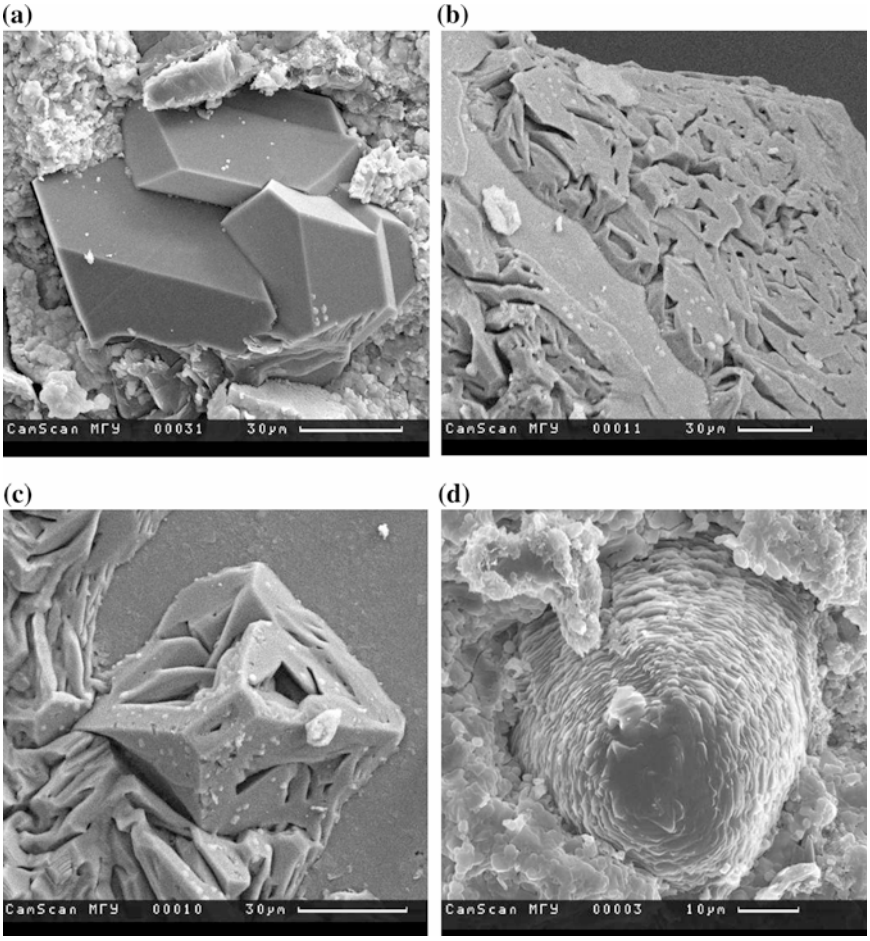

Fig. 4.2 Scanning electron micrograph (SEM) images of diamonds crystallized in the chloride melts with dissolved elementary carbon: **a** spinel-law crystals in quenched KCl melt, **b** growth patterns of octahedral face of seeded metal-synthetic crystal, **c** growth patterns of cubic face of seeded metal-synthetic crystal, **d** big graphite spherule within a basket-shaped shell of the solidified KCl melt and small-sized graphite spherules alongside

The carbonate–silicate melts with dissolved carbon are preferable because of their ability to form a rather wide set of paragenetic major and accessory minerals. Diamond formation in the silicate-carbonate systems with metastabile graphite as the carbon source was found at 7.0–7.7 GPa and 1800–2000 °C for the natural kimberlitic composition (Arima et al. 1993). These results are not directly applicable to the problem of chemical and physico-chemical properties of the parental media for the natural diamonds due to the fact that kimberlitic magmas are

exclusively the transportation facility for the transfer of natural diamonds from the mantle diamond-producing chambers to the Earth's surface. It was also found that silicate-carbonate melts with dissolved carbon of magmatic carbonatites of Chagatai, Uzbekistan (Fig. 4.3) and Kokchetav, Kazakhstan complexes (Fig. 4.4) (Litvin et al. 2001, 2003) are effective in joint formation of diamonds and paragenetic phases. Multicomponent carbonate-carbon and carbonate-silicate-carbon assemblages similar to the primary fluid-bearing inclusions in diamond (Schrauder and Navon 1994) show high efficiency for diamond nucleation and growth (Litvin and Zharikov 1999, 2000). Carbonate and silicate-carbonate systems have also shown highest efficiency characterized by the formation of polycrystalline fine-grained diamond intergrowths (Fig. 4.5) (Litvin and Spivak 2003; Litvin et al. 2005a, b, c) similar to those observed in natural diamondite rocks (Kurat and Dobosi 2000). It was also disclosed that multicomponent as carbonate so silicate-carbonate melts are completely miscible whereas both the melts show a complete liquid immiscibility with sulfide melts (Litvin and Butvina 2004). Titanoferous ilmenite and rutile minerals melts are also completely immiscible with carbonate and silicate-carbonate melts (Litvin et al. 2016).

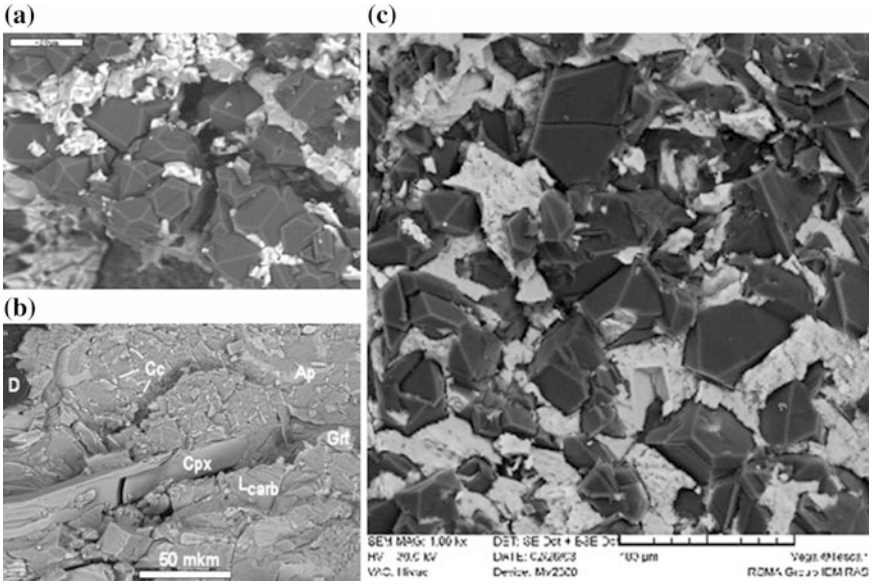

Fig. 4.3 Scanning electron micrograph (SEM) images of diamonds and associated phases formed in experiments with carbon-oversaturated melts-solution of Chagatai carbonatite rocks: **a** diamond (*black*) and quenched carbonate melt (*grey*) with coesite intergrowths (*white*), **b** diamond (Diam) and syngenetic garnet (Grt), clinopyroxene (Cpx), apatite (Ap), and host calcite (Cal) formed during cooling of completely miscible carbonatitic melt; calcite (*gray*) contains garnet intergrowths (*white*), **c** formation of diamond polycrystalline intergrowth—diamondite (DDT) in carbonatite melts (*white* substance after quenching)

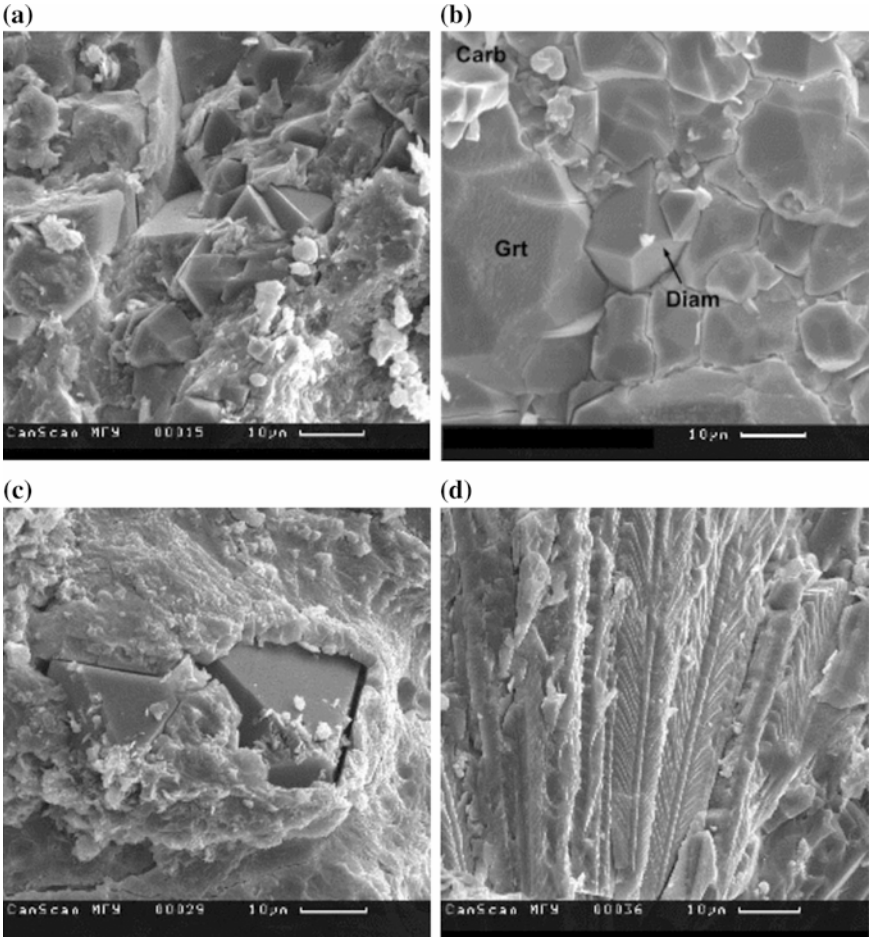

Fig. 4.4 Scanning electron micrograph (SEM) images of diamonds and other phases formed in experiments with Kokchetav silicate-carbonate rock: **a** extensive diamond crystallization; **b** syngenetic diamond and garnet formation from carbonate-silicate melt; Diam—diamond; Carb—carbonate; Grt—garnet; **c** octahedral diamond single crystals in carbonate-silicate melt (view after quenching); **d** fibrous dendritic crystallization of parental silicate-carbonate-melt during quenching

Thus, the testing experiments that use nucleation criterion made it possible to confirm a high diamond-forming capability of many chemically different natural media associated with diamond. At the same time, there is no reliable criterion which can determine which among the effective diamond-forming media is responsible for the formation of most natural diamonds. Attempts to coordinate the results of test experiments with analytical mineralogical data failed because of the lack of unbiased criteria for the unambiguous choice. So the experimental criterion of diamond nucleation is necessary but insufficient in determination of the realistic

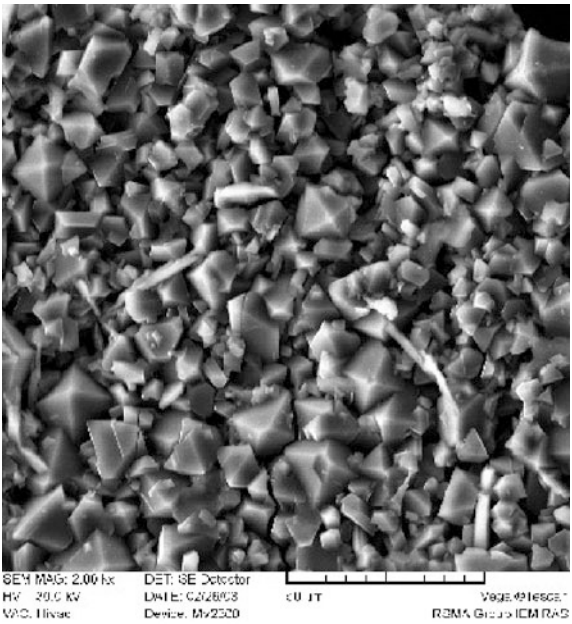

Fig. 4.5 Scanning electron micrograph (SEM) images after quenching of experimental crystallization of diamondite in carbon-oversaturated melts-solutions of Algeti $CaCO_3$ limestone: **a** densely intergrown diamondite of octahedral microcrystals; **b** fragment of diamondite after chemical treatment

composition of the growth medium for natural diamonds. Therefore the chemical mode of diamond formation in the natural multicomponent heterogeneous growth medium not be substantiated by the combined methods of analytical mineralogy and testing experiments. Meanwhile, the experimental testing may be sometime helpful at active searching for a reliable composition of natural diamond-producing systems.

Short-run experimental testing of some silicate-carbonate systems allowed to reveal a concentration barrier of diamond nucleation (CBDN) caused by inhibitory properties of silicate constituents of these melts (Litvin et al. 2008). It has been shown that both the peridotitic and eclogitic silicate-carbonate growth melts belong to the field of carbonatite compositions (Bobrov and Litvin 2009). Diamond nucleation was also reported (with a long run duration of 40 h) for the carbonate-rich melt compositions in the oxide-carbonate SiO_2–K_2CO_3–C up to 25 wt% SiO_2 and silicate-carbonate Mg_2SiO_4–K_2CO_3–C system up to 50 wt% Mg_2SiO_4 (Shatskii et al. 2002) at 6.3 GPa and 1650 °C. Therewith the seeded growth of diamond was observed in these systems up to 75 wt% SiO_2 and 90 wt% Mg_2SiO_4.

The experimental diamond nucleation criterion is a tool for a rapid searching the efficient diamond-forming media. Results of testing experiments indicate that diamond can be formed efficiently in a wide variety of chemically contrasting natural

media closely associated with diamond. It means that diamond synthesis experiments have evaluated a diamond-forming efficiency for several heterogeneous media. However, such experiments cannot provide an unambiguous conclusion on the chemical and phase compositions for the real parent media of natural diamond. To achieve this goal, one has to reformulate this objective as a problem of syngenesis of diamonds and their primary growth inclusions (Litvin 2007). The approach is needed to estimate the role of silicates, sulfides and other chemically different minerals in diamond genesis and to substantiate the chemical properties of the natural parent media for diamond genesis.

The criterion of syngenesis of diamonds and associated phases is more informative and can be used for unbiased assessment of chemical and phase composition of the natural diamond-parental medium on the united basis of mineralogical analytical data and results of physico-chemical experiments. The current concept is that diamond-hosted mineral inclusions, both paragenetic and xenogenetic in respect to diamond represent heterogeneous fragments of partially molten diamond-parental medium, This conclusion is based on rigid requirements of the syngenesis criterium (Litvin 2012; Litvin et al. 2012): a natural diamond-parental medium has to be physico-chemically capable for producing diamonds and formation of the whole complex of paragenetic and xenogenetic phase-inclusions. By this is meant, that the mantle inclusions were trapped by growing diamonds from heterogeneous parental medium. Therefore, the role of primary inclusions in determination of chemical and phase composition of heterogeneous parental medium of diamonds became decisive and initiates the purposeful physico-chemical experimental study. When planning an experiment based on the syngenesis criterium, it is necessary to choose the most appropriate multicomponent composition of the diamond-forming system, which is mainly possible by invoking valid mineralogical information.

The variable realistic compositions of parental melts for diamonds and associated phases are determined from the mineralogical data for chemical and phase compositions of primary inclusions in upper-mantle diamonds in a coherent unity with the physico-chemical experimental results of diamond-parental systems studies. The mantle-carbonatite concept of the silicate-carbonate-carbon parental partial growth melts for diamonds and paragenetic inclusions has received considerable support (Litvin et al. 2012; Litvin 2013). The distinguishing features of the upper-mantle diamond-parental melts: (1) the multicomponent K–Na–Mg–Fe–Ca-carbonate melt in the state of complete liquid miscibility with molten major and accessory silicate, aluminosilicate and oxide minerals of peridotite and eclogite parageneses from inclusions in diamonds; (2) the elementary carbon, dissolved possibly in atomic and/or clasteric forms, in the parental melts; (3) the paragenetic major and accessory minerals crystallized from the parental melts; (4) the xenogenetic accessory minerals and melts which are insoluble and immiscible with respect to the miscible silicate-oxide-carbonate parental melts; (5) the low-abundant accessory volatile components are completely dissolved in the parental melts and can form their own volatile phases inside the hermetic cameras of inclusions after solidification of the parental melts.

4.2 Concentration Barrier of Diamond Nucleation

The determination of chemical composition of the parent media is crucial for the problem of diamond genesis under the conditions of the Earth's mantle. The model of strongly compressed multicomponent carbonate–silicate melts with dissolved carbon is in adequate agreement with experimental and mineralogical data. The model satisfies also to the experimental criterion of syngenesis of diamond and growth inclusions according to which diamond-parent media must provide the formation of both diamonds and primary inclusions. Variable proportions of carbonate and silicate components have observed in the hardened fragments of parent carbonatite media from inclusions in natural diamonds (Schrauder and Navon 1994). Mineral inclusions also indicate that the parent media contain oxide–silicate components of the main mantle assemblages, from olivine-bearing peridotitic and pyroxenitic rocks to eclogitic and grospyditic assemblages with coesite or "retrograde" quartz (Sobolev 1977). Variable natural carbonate–silicate diamond-forming media may belong to either carbonatite (more than 50 wt% carbonate components) or ultrabasic–basic compositions enriched in silicate components. It is impossible to determine the chemical nature and compositions of media responsible for diamond formation on the basis of mineralogical data only. The chemical composition can be constrained by high-pressure physico-chemical experimental investigations, and the key criterion is the efficiency of the acceptable medium in diamond nucleation and growth jointly with the included paragenetic minerals (Litvin 2007).

The variable chemical and phase compositions of the diamond-parental medium belong to the multicomponent heterogeneous peridotite-eclogite-carbonatite-carbon system (Fig. 4.6). The basic composition triangle of the system (with the addition of carbon) characterizes the diamond-parental compositions by the major components for most upper mantle derived diamonds. Formally, the symbol of carbon in Fig. 4.6 is indicated outside the triangle of parental compositions for the sake of simplification. The boundary compositions are representatively definable with the use of diamond-hosted inclusions of peridotite and eclogite parageneses as well as carbonate minerals among them. The apexes of the main composition triangle touch three tetrahedrons of the auxiliary boundary compositions. Such a presentation of the compositional diagram is due to the fact that the natural parental media are strongly variable in major and minor components. This variability can be accounted for by movement of the apexes of the main triangles over the surfaces and inside the volumes of the auxiliary tetrahedrons.

A good agreement between the phases of peridotite and eclogite parageneses of the primary inclusions in diamonds and rock-forming minerals of the upper-mantle peridotites and eclogites is definitely symptomatic. The mineralogical agreement is evidenced for the existence of a direct genetic link between the ultrabasic and basic minerals of the upper mantle rocks, on one side, and similar minerals in diamond-hosted inclusions formed from the diamond-parental silicate-carbonate-carbon melts, on the other. The auxiliary tetrahedrons carry information on the boundary compositions for the multicomponent diamond-growth medium. The

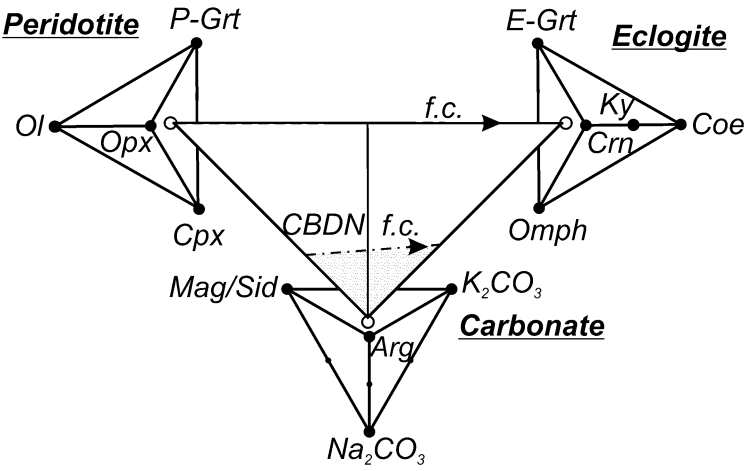

Fig. 4.6 Composition diagram of the upper-mantle diamond-parental system peridotite Prd—eclogite Ecl—carbonatite Carb—carbon C, including only major components. Line of concentration barrier of diamond nucleation (CBDN) presents kinetic boundary of the diamond-parental compositions field. See text for more details

apexes of the auxiliary tetrahedron for boundary mantle peridotite are olivine (Ol), orthopyroxene (Opx), clinopyroxene (Cpx), and garnet of the peridotite paragenesis (P–Grt). In the case of eclogite, these are omphacite (Jd–Cpx = Omph), garnet of the eclogite paragenesis (E–Grt), corundum (Crn), and silica (SiO_2). The apexes of the auxiliary tetrahedron for Mg–Fe–Ca–Na–K-carbonate components of mantle carbonatites are ($MgCO_3$ + $FeCO_3$), $CaCO_3$, Na_2CO_3 and K_2CO_3. Complete liquid miscibility of carbonate (congruently melting under the conditions of diamond formation) and silicate melts with the formation of a single liquid phase is an important physico-chemical feature of silicate–carbonate-carbon growth melts for diamond (Shushkanova and Litvin 2005, 2008). The composition of the system includes elementary carbon which is soluble in silicate-carbonate melts and is among the major components of natural diamond-producing silicate-carbonate-carbon melts-solutions.

The melts of the multicomponent K–Na–Ca–Mg–Fe-carbonate–silicate system which is a chemical analogue of carbonatite inclusions in Botswanian diamonds and described in (Schrauder and Navon 1994) provide efficient diamond nucleation immediately after melting at 5.5–7.0 GPa and 1200–1570 °C (Litvin and Zharikov 2000). During the first minutes, an extensive mass crystallization of single-crystalline diamonds of octahedral habit and avalanche-like formation of fine-grained (0.01–100 μm) polycrystalline intergrowths was observed during the first seconds after melting (Litvin and Spivak 2003). A high-efficiency crystallization of diamontides was also found in the silicate-carbonate-carbon systems of more complicated compositions (Litvin et al. 2005a, b, c).

Thus, high-pressure high-temperature experiments have showed that silicate-carbonate melts enriched in carbonate components are very efficient diamond-forming media. The silicate–carbonate melts are of particular interest for the problem of genesis of diamonds and associated phases. A characteristic property of the chemical and phase composition of parent melts is their variability that is distinctly reflected in compositions of the silicate mineral inclusions. Material of inclusions records the complicated history of evolution of parental carbonate–silicate magmas in the peridotite mantle. The experimental investigation of diamond formation conditions in variable carbonate–silicate melts allows determining the natural concentration boundaries for the multicomponent diamond-parental melts and revealing the physico-chemical nature of these boundaries.

The questions of the boundary conditions of diamond formation in various systems are fundamentally important for the interpretation of experimental and mineralogical data; therefore, it is expedient to define preliminarily some relevant concepts and terms. The pressure-temperature boundary conditions of diamond crystallization in the melt-solvent—carbon system is characterized by the PT-projection (Fig. 3.7b) of the PTNc-diagram of carbon oversaturation (Fig. 3.7a). The diagram-projection includes physico-chemical details which are essential for nucleation and crystallization of diamond: (1) the graphite–diamond equilibrium curve (Kennedy and Kennedy 1976; Bundy et al. 1996) which position is independent of the composition of the diamond-forming system, (2) the curve of the pressure dependence of the solidus temperature of the diamond-forming system which position is sensitive to its composition, and (3) the boundary curve between the fields of metastable oversaturation (FMS) and labile solutions (FLS) (Litvin 1969). The kinetic FMS/FLS boundary is controlled by the activation energy of spontaneous diamond nucleation, and the boundary position depends on the composition of the system.

The main physico-chemical difference between the kinetically controlled fields is that oversaturation with respect to diamond in carbonate–carbon melt–solutions under the conditions of the FMS is sufficient to provide diamond growth on the seed crystals but inadequate for diamond nucleation. The degrees of oversaturation attained under the FLS conditions are sufficient for the spontaneous formation of diamond nuclei. Physico-chemical reasons for the appearance of the LSF and MSF in diamond-forming systems were discussed in detail elsewhere (Litvin 1968, 1969; Litvin and Spivak 2004).

The concentration barriers of diamond nucleation (CBDN) have been determined in the carbon-oversaturated melts with variable proportions of silicate and carbonate components. In the system peridotite-K–Na–Ca–Mg–Fe-carbonate-carbon the CBDN corresponds to the concentration of 30 wt% peridotite at 8.5 GPa. The mineral content for the peridotite ingredient corresponds to 60 wt% olivine, 6 wt% orthopyroxene, 12 wt% clinopyroxene, and 12 wt% garnet. In the system eclogite-K–Na–Ca–Mg–Fe-carbonate-carbon the CBDN corresponds to the concentration of 35 wt% eclogite. The mineral content for eclogite corresponds to 50 wt% clinopyroxene and 50 wt% garnet. The data make possible to display the CBDN line at Fig. 4.6 as a kinetic boundary for the triangle field of diamond

nucleation and crystallization in the peridotite-eclogite-carbonatite system. An increase in the content of silicate components in the peridotite-K–Na–Ca–Mg–Fe-carbonate or eclogite-K–Na–Ca–Mg–Fe-melt inhibits diamond nucleation, gradually lowering its efficiency and eventually completely depressing it. The mechanism of such an influence is related to a decrease in oversaturation levels from labile ones to the concentration barrier of diamond nucleation and further to the metastable region beyond the barrier. Diamond growth on seeds from metastable oversaturation solutions was observed within a considerable part of the silicate-rich segment of compositions (up to 70 wt% silicate components). Thus, silicate components of the natural diamond-growth melts shows themselves as effective inhibitors which slow down the kinetic parameters of diamond formation —the nucleation density for diamond phase and rates of diamond mass crystallization.

It was also found that diamond crystal growth may be continued onto the seed crystals with increasing of the silicate content in the diamond-producing melts beyond the kinetic boundary CBDN where diamond phase nucleation is ceased. It was experimentally shown that the seeded growth of diamond is accompanied with the mass crystallization of metastable graphite in the forms of single-crystalline plates and spherules (Fig. 3.8). Similar forms of metastable graphite are identified among the primary inclusions in diamonds (Glinnemann et al. 2003) and diamond-bearing rocks (Sobolev 1977). The concentration barrier of diamond nucleation is physico-chemically corresponding to the kinetic FMS/FLS boundary on the oversaturation PTN_c-diagram (Figs. 3.7 and 4.6) therewith the FMS/FLS boundary position is sensitive to chemical composition of the diamond-producing melt-solution (Litvin et al. 2008).

This indicates that the inhibiting role of the silicate component is a powerful factor, and natural carbonatite melts may lose their high efficiency with respect to diamond formation in response to an increase in the content of silicate components. The investigation of systems of such a type, multicomponent and sufficiently representative for the probable growth media of natural diamonds, is very important to outline the compositions of variable natural parent diamond-forming media which, as becomes obvious, are bounded by the concentration barriers of diamond nucleation. Experimental investigations on the basis of the criteria of diamond nucleation and syngenesis of diamond and inclusions coupled with the determination of the concentration barriers of nucleation provide a fundamental basis for the determination of chemical boundaries of natural parental media.

The speciation of carbon in carbonate–silicate melts during the formation of diamond can be indirectly characterized by the presence of microscopic graphite and diamond crystals detected by micro-Raman spectroscopy (Spivak et al. 2008) in homogeneous areas of quenched melts free of solid carbon phases (according to the data of electron microscopy). Such microscopic phases are formed under the conditions of rapid quenching (300 °C/s) of carbonate–silicate-carbon melts nearly saturated in carbon, when the degree of oversaturation with respect to diamond increases sharply. This is in agreement with the concept of the atomic and cluster–atomic state of dissolved carbon. Quench microscopic phases of solid carbon were

also detected in experiments on the investigation of carbon isotope fractionation during diamond formation (Litvin et al. 2005a, b, c).

According to experimental data, the carbonate–carbon and carbonate–silicate–carbon systems are stable oxide buffer associations. At high pressures, multicomponent carbonates melt congruently, and carbonate components are stable during the whole experiment and show no signs of decomposition with liberation of carbon dioxide. The compositions of the carbonate–silicate–carbon systems include substances of very different redox activity, carbonates and solid carbon (graphite and diamond). The analysis of the material of quench melts showed that carbonate compounds and their melts occurring in a prolonged and continuous contact with elemental carbon (graphite or diamond or dissolved elemental carbon) are not reduced by it. Therewith carbon in the form of graphite, diamond, and carbon dissolved in the elemental form is not oxidized, i.e., there is no significant redox interaction between carbonates and carbon. The reason is that buffer associations, for instance, carbonate–silicate–solid carbon, are formed and maintain the redox potential of diamond-forming processes at the level of the Fe/FeO buffer (Litvin et al. 2008).

4.3 Physico-Chemical Mechanisms of Syngenesis of Diamonds and Associated Phases

Changeable chemical and phase compositions of the natural media, parental for diamonds and genetically associated phases, were derived from melting relations and compositions of solid and liquid phases of the Earth's mantle multicomponent heterogeneous mineral systems. It is reasonable that analytical data for ultrabasic and basic syngenetic inclusions in natural diamonds is necessary to use for evaluating the boundary compositions of the experimental diamond-producing systems. As a consequence, the chemical compositions and phase relations of the diamond-producing partially molten media can result from physico-chemical experimental study of multicomponent systems reproducing conceptually the natural diamond-parental chemistry by the major components. This provides a determination of equilibrium phase diagrams for a joint formation of diamonds and mineral inclusions of peridotite and eclogite parageneses as the "syngenesis diagrams". Experimental syngenesis phase diagrams (Litvin 2009, 2013; Litvin et al. 2012, 2016a, b) for diamonds and primary inclusions create the basis for analyzing physico-chemical scenarios of diamond nucleation and growth which is accompanied with capturing paragenetic and xenogenetic minerals by growing diamonds. The syngenesis diagrams make it possible to establish the physico-chemical mechanisms of nucleation and crystallization of diamonds as well as of an attendant formation of mineral phases of ultrabasic and basic parageneses. This opens up a way for unambiguous untangling the genetic links between diamonds and associated paragenetic minerals. The xenogenetic minerals, insoluble in diamond-parental

melts, or their melts, immiscible with diamond-parental melts, can be presented as inert phases which came to parental melts from the enclosing mantle material and were captured by diamonds together with the paragenetic phases.

The boundary peridotite–carbonatite-carbon and eclogite–carbonatite-carbon joins are determinant in the natural multicomponent diamond-producing system peridotite–eclogite–carbonatite-carbon containing also some secondary heterogeneous accessory components and phases. Volatile C–O–N–N-components are among those which are soluble in the diamond-parental silicate-carbonate-carbon melts-solutions. Judging by the limited participation of volatile compounds in natural diamond formation, their role in this process is subordinate. In the mantle processes of natural diamonds formation the volatile components should be completely dissolved in diamond-parental melts and are not capable to form their own phases in fluid state under high-pressure high-temperature conditions of diamond genesis. So their influence may to some extent qualitatively effect on the temperatures of diamond-forming melts and boundaries between stability fields of the minerals paragenetic with diamond as well as the solubility of elemental carbon in the growth carbonate–silicate melts and the kinetics of diamond crystallization. Compressed liquid and gas phase can be formed after complete hardening of parental melts-solutions within diamond-hosted inclusions and have revealed themselves at room temperature. The volatile phase among the solidified fragments of the diamond-parental melts have attracted considerable attention from mineralogists. The physico-chemically plausible behavior of the volatile components during diamond-producing natural processes is supported by mineralogical data on primary inclusions and agrees with the available experimental data on the effects of volatile components on melting of mantle rocks (Wyllie 1979).

The syngenesis diagram of the diamond-producing system peridotite-carbonatite-diamond is defined as a particular polythermal section $Prd_{30}Carb_{70}$–D (Fig. 4.7) of the generalized system diamond-parental peridotite-eclogite-carbonatire-carbon of the Earth's upper mantle. Peridotite is presented by garnet lherzolite of the composition (wt%) $Ol_{60}Opx_{16}Cpx_{12}Grt_{12}$. The compositions of its rock-forming minerals: olivine (Ol)–SiO_2 40.02, FeO 14.35, MgO 45.63; orthopyroxene (Opx)–SiO_2 57.80, Al_2O_3 0.49, FeO 7.26, MgO 33.34, CaO 0.81, Na_2O 0.30; clinopyroxene (Cpx)–SiO_2 55.90, Al_2O_3 4.28, FeO 4.68, MgO 16.88, CaO 15.66, Na_2O 2.60; garnet (Grt)–SiO_2 42.55, Al_2O_3 24.07, FeO 8.48, MgO 20.93, CaO 3.97; total composition–SiO_2 45.07, Al_2O_3 3.48, FeO 11.35, MgO 37.25, CaO 2.49, Na_2O 0.36. A model carbonatite $(K_2CO_3)_{25}(MgCO_3)_{50}(CaCO_3)_{25}$ has the total composition–MgO 21.4, CaO 14.0, K_2O 25.1, CO_2 38.7. Therewith the figurative points of the garnet lherzolite and model carbonatite have displaced into the peridotite volume and onto the K–Mg–Ca face of corresponding boundary tetrahedrons in the Fig. 4.6.

The peridotite-carbonatite boundary composition of the diamond-producing system corresponds to the point of the concentration barrier of diamond nucleation (CBDN). The experimental samples after quenching are indicative of liquidus crystallization of diamond in the completely miscible peridotite-carbonatite ultrabasic melts with dissolved carbon and paragenetic crystallization of diamond

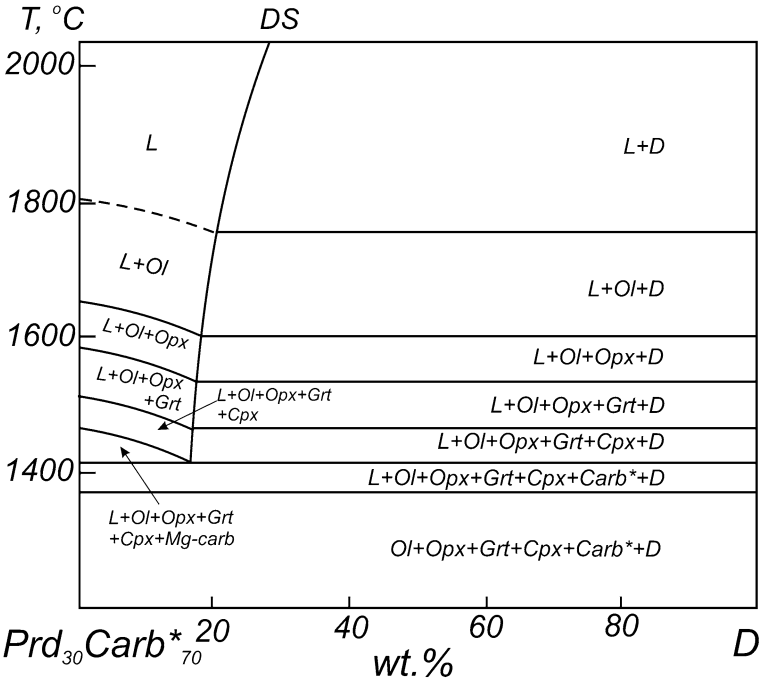

Fig. 4.7 Syngenesis diagram for diamond and associated phases at the ultrabasic system $Prd_{30}Carb_{70}$–D at 7 GPa. *Symbol* Prd—peridotite, Carb—carbonate composition $(K_2CO_3)_{25}(MgCO_3)_{50}(CaCO_3)_{25}$ (wt%). D—diamond, Carb*—carbonate minerals, DS—diamond solubility

together with olivine of the peridotite paragenesis. It has been earlier found (Litvin 1991) that the solidus phase relations of the upper-mantle garnet-lherzolite system Ol–Opx–Cpx–Grt are peritectic (the key reaction is Opx + L → Cpx), the subsolidus phase fields Ol + Opx + Grt, Ol + Opx + Cpx + Grt and Ol + Cpx + Grt have been formed. The composition of garnet lherzolite in the system $Prd_{30}Carb_{70}$–D discussed belongs to the subsolidus field Ol + Opx + Cpx + Grt, in this connection the assemblage Ol + Opx + Cpx + Grt + Carb* + D is stable at subsolidus conditions of the system (Fig. 4.7).

In fact, magnesite, Ca–Mg carbonate, and K carbonate are formed consecutively, and each carbonate adds a new phase to the relatively low temperature mineral assemblage and complicates the phase diagram. For the sake of simplicity, all carbonate phases are denoted as Carb*, and this does not distort the general physico-chemical trend in formation of diamond and inclusions.

The increase in carbon content in the system gradually lowers temperature of complete melting of its boundary $Per_{30}Carb_{70}$ composition therewith the carbon-free boundary silicate-carbonate melt is initially changing to a carbon-unsaturated melt-solution. The equilibrium curve of diamond solubility in completely miscible silicate-carbonate melts, the most important topological element of

the syngenesis diagram, is resulting when the concentration of dissolved carbon attains saturation in respect to the diamond phase. The diamond solubility curve controls the processes of diamond formation under experimental and natural conditions. The physico-chemical mechanism of such controlling is caused by a spontaneous generation of the oversaturated state in the silicate-carbonate melt-solution in respect to diamond at temperature depression.

The diamond solubility curve is coincident at about 1780 °C and 22 wt% with the liquidus curve for diamond and at higher temperatures outlines the field $L_{carb–sil}$ + D (which transforms into the field $L_{carb–sil}$ + G in the way) up to the melting point of carbon solid phase (graphite) at about 5000 K (Bundy et al. 1996). By the experimental evidence (Litvin et al. 2012), the diamond solubility has attained about 20–22 wt% carbon for the liquidus curve of the system at 7 GPa and 1700–1750 °C. The diamond solubility values were estimated using single crystalline diamonds as the indicators, which can turn partially dissolved in the carbon-unsaturated in respect to diamond melt, behave inertly in the saturated solutions, and become overgrown with epitaxial layers in the carbon-oversaturated melts-solutions. The temperature-composition solubility curve (at P = Const) is characterized by a positive slope.

Within 1400 (pseudo-eutectics)–1780 °C interval the diamond solubility curve intersects all the phase fields at the peridotite-carbonatite-carbon (diamond) system, causing the phase boundary between the field of carbon-unsaturated in respect to diamond silicate-carbonate-carbon melts (nucleation of diamond phase is impossible) and the field of carbon-saturated in respect to diamond silicate-carbonate-carbon melts (diamond formation field). Thus the diamond formation field is bordered with the diamond solubility curve on the lower carbon concentrations side and the solidus boundary on the lower temperatures side. Within the diamond formation field the silicate and carbonate minerals of peridotitic paragenesis can be formed together with diamonds at the same silicate-carbonate-carbon melts in an orderly sequence with temperature lowering. Only phases which are formed and coexisted with growing diamonds can be captured as the primary diamond-hosted inclusions. So diamonds can only captured a completely miscible silicate-carbonate melt in the field $L_{carb–sil}$ + D, the melt and olivine in the field $L_{carb–sil}$ + Ol + D and so on up to the solidus field $L_{carb–sil}$ + Ol + Opx + Cpx + Grt + Carb* + D. The liquidus crystallization of diamond and paragenetic formation of diamond and olivine in the peridotite-carbonatite-carbon growth melts is demonstrated in the Fig. 4.8. The capture of the growth melts at conditions of slow diamond crystallization can be difficult but become possible at an accelerated kinetic regime of diamond growth. Sulfide mineralization (pyrrhotite–pentlandite–chalcopyrite) occupies a substantial place in the assemblage of primary inclusions contained in natural diamonds.

A stabilization of the geothermal regimes at the diamond-producing upper-mantle chambers is practicable at 1650–1750 °C over the depths 150–250 km (Harte 2010). In the case of the potential diamond-producing peridotite-carbonatite melts are still not saturated in respect to diamond, their saturated state can be reached as the reservoir-chamber is cooled. Therewith a figurative point of

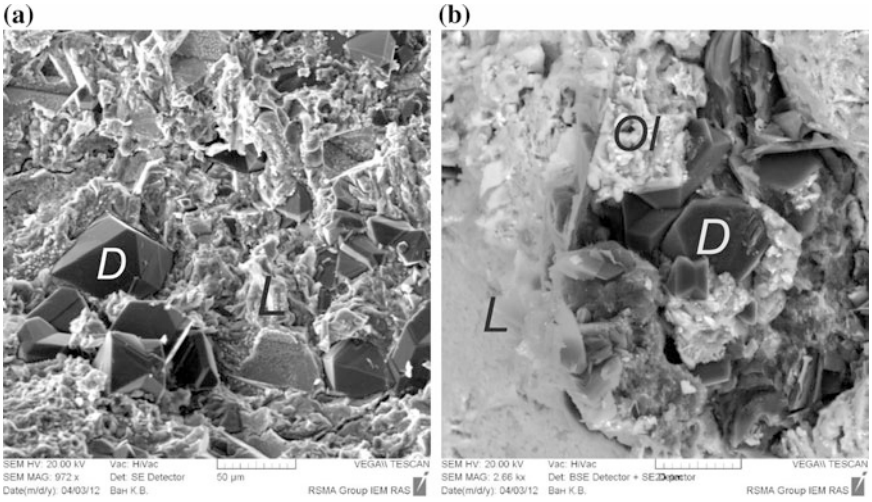

Fig. 4.8 Experimental samples of the system $Prd_{30}Carb_{70}$–D after quenching: **a** liquidus crystallization of diamond, **b** paragenetic crystallization of diamond and olivine

the carbon melt-solution has to transfer in the diamond solubility curve by that the initial temperature and parental melt composition of the diamond-producing process is determined. The realization of the diamond solubility curve under the upper mantle conditions provides the necessary but not sufficient condition for the diamond genesis because the nucleation and crystallization of diamond cannot be carried out under the equilibrium regime. On further cooling of the chamber, the initial composition point must escape the equilibrium diamond solubility curve and can transfer along the temperature axis to the field of carbon-saturated solutions where the initial melt-solution becomes metastable and can automatically turn into the carbon-oversaturated state in respect to diamond. This activates the kinetic physico-chemical mechanisms of diamond genesis. At temperature lowering, the metastable, lesser carbon-oversaturated in respect to diamond melts-solutions first originated but the carbon concentration therein is still deficient for a spontaneous diamond nucleation. Then the labile, more carbon-oversaturated in respect to diamond melts-solutions are coming into play and in so doing the energetic barrier for diamond phase nucleation has to be overcame. This initiates the mass crystallization of diamond that can take the carbon-oversaturated labile states into metastable. During the subsequent cooling of the diamond-producing chamber, the metastable carbon-oversaturation states in respect to diamond have to be maintained, and the mechanisms of new diamond layers overgrowths on the earlier spontaneous diamonds as at seeds may be realized. The crystal growth of diamonds in the peridotite-carbonatite-carbon melts-solutions must be accompanied by crystallization of the paragenetic minerals of peridotitic paragenesis and fragmentary including tiny samples or fragments of the minerals into the growing diamonds.

The syngenesis phase diagram of the diamond-producing system eclogite-carbonatite-diamond (Fig. 4.9) is defined as a particular polythermal section $Ecl_{40}Carb_{60}$ – D (Fig. 4.6) of the determining diamond-parental system peridotite-eclogite-carbonatire-carbon of the Earth upper mantle. Eclogite for the boundary composition is presented by a two-mineral variety of the composition (wt%) $Omph_{50}Grt_{50}$. The compositions of its rock-forming minerals: omphacitic clinopyroxene (Omph)–SiO_2 54.64, TiO_2 0.48, Al_2O_3 9.76, Cr_2O_3 0.05, MgO 8.93, MnO 0.07, FeO 6.37, CaO 13.07, Na_2O 6.63; garnet (Grt)–SiO_2 39.20, TiO_2 0.46, Al_2O_3 21.86, Cr_2O_3 0.04; MgO 8.83, MnO 0.52, FeO–20.75, CaO 8.17, Na_2O 0.17. The general composition of the eclogite rock: SiO_2 46.77, TiO_2 0.47, Al_2O_3 15.77, Cr_2O_3 0.05; MgO 8.85, MnO 0.30, FeO 13.53, CaO–10.87, Na_2O–3.39. The compositions of the model carbonatite of the experimental eclogite-carbonatite and peridotite-carbonatite systems are analogous. Therewith the figurative points of the bimineral eclogite and model carbonatite have displaced into the edge of the eclogite volume and onto the K-Mg–Ca face of corresponding boundary tetrahedrons in the Fig. 4.6. The eclogite-carbonatite boundary composition corresponds to the point of the concentration barrier of diamond nucleation (CBDN). The liquidus crystallization of diamond in the completely miscible eclogite-carbonatite

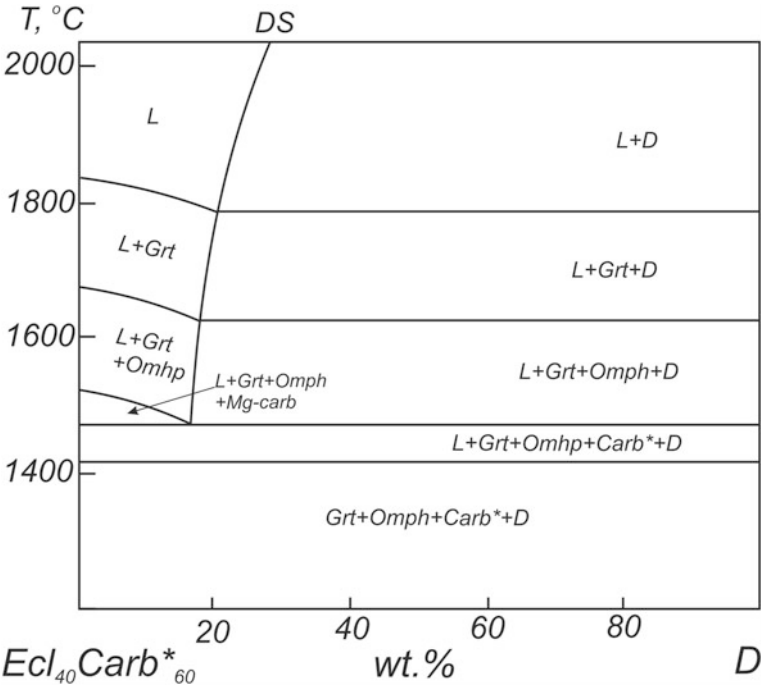

Fig. 4.9 Syngenesis diagram for diamond and associated phases at the basic system $Ecl_{40}Carb_{60}$–D at 7 GPa. *Symbol* Ecl—eclogite, Omph—omphacite. See legend of Fig. 4.6 for others

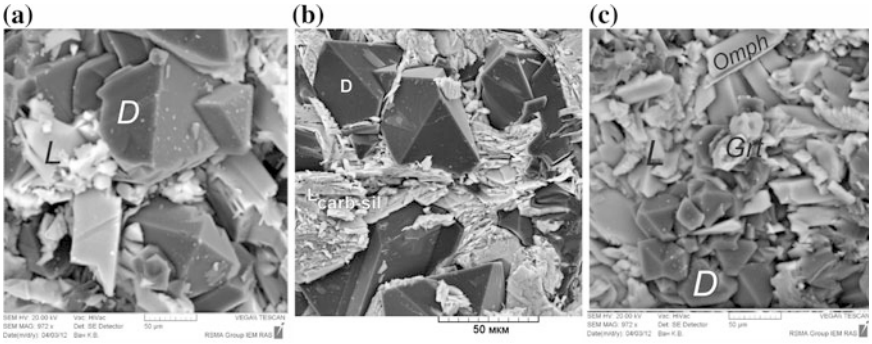

Fig. 4.10 Experimental samples of the system $Ecl_{40}Carb_{60}$–D after quenching: **a**, **b** liquidus crystallization of diamond, **c** paragenetic crystallization of diamond with omphacite and garnet

basic melts with dissolved carbon and paragenetic formation of diamond together with omphacite and garnet of the eclogite paragenesis are demonstrated at (Fig. 4.10).

The physico-chemical features of the equilibrium syngenesis diagram for the eclogite-carbonate-carbon system are basically of the same kind as in case of that for the peridotite-carbonate-carbon discussed above. A complete melting of the boundary $Ecl_{40}Carb_{60}$ composition is accompanied with formation of the completely miscible silicate-carbonate melt $L_{carb–sil}$. The increase in carbon content in the system leads to formation of the equilibrium diamond solubility curve that divides the syngenesis diagram onto the f carbon-unsaturated melts-solutions field and the carbon-saturated diamond formation field. Temperature lowering leads to a sequential formation of the next phase assemblies:(Grt + $L_{carb–sil}$), (Grt +Cpx + $L_{carb–sil}$) and (Grt + Cpx + Carb* + $L_{carb–sil}$). The syngenesis phase diagram exercises strict physico-chemical control over the processes of joint paragenetic formation of diamonds and associated phases.

It is worthy of note that regular development of the joint genesis of diamond with silicate and carbonate phases is controlled by the melting phase relations of diamond-producing systems and has been clarified due to the syngenesis phase diagrams. Only the phases that coexist with growing diamonds can be entrapped by this mineral as primary inclusions. The relatively low-melting minerals including carbonates have formed at the near-solidus temperatures that are responsible for their rare occurrence at the inclusions in the upper mantle derived diamonds. The majority of diamonds has been crystallized at higher temperatures therefore silicate minerals are most frequent than carbonates at the inclusions in diamonds. The unambiguous physico-chemical evidence to the paragenetic nature of the primary inclusions which have been formed jointly with diamonds at the same completely miscible silicate-carbonate melts with dissolved carbon is of considerable significance for the untangling the compositions of the Earth's mantle melts-solutions parental for diamonds and associated phases.

4.4 Xenogenetic Upper-Mantle Minerals in Diamond-Producing Processes

The identification of paragenetic and xenogenetic components and phases in the association of primary inclusions in natural diamonds is of special importance for the problem of diamond genesis. It is important to keep in mind that the genetic-like conclusions on the natural diamonds origin, if based solely on the analytic data for primary inclusions, are discrepant and invalid as a rule without the unequivocal physico-chemical ground.

The multicomponent multiphase diamond-parental medium in the state of partial melting consists of growth melts, diamonds, paragenetic and xenogenetic phases. The primary inclusions in diamonds would be expressed as syngenetic if were captured by growing diamond from the parental medium. Therewith, paragenetic minerals have formed synchronously and, what is genetically most important, at the common growth melts with the host diamonds. However, xenogenetic phases both solid and liquid, of no concern, have other genetic history than diamonds and paragenetic phases. The xenogenetic phases behave as inert newcomers from the enclosing rocks and are capable to penetrate into and freely move inside the diamond-parental completely miscible silicate-carbonate-carbon melts-solutions. In these conditions the xenogenetic phases can also be captured by the growing diamonds synchronously with paragenetic ones.

According to modern physico-chemical experimental data (Litvin and Butvina 2004; Shushkanova and Litvin 2005, 2008; Litvin et al. 2012; Litvin 2007, 2012, 2013), sulfide minerals and melts are among the group of xenogenetic phases. The upper-mantle diamond-hosted inclusions and diamond-bearing peridotites and eclogites contain abundant sulfides mainly pyrrhotite FeS, pentlandite $(Fe, Ni)_9S_8$, chalcopyrite $CuFeS_2$, pyrite FeS_2, monosulfide solid solutions, and djerfisherite $K_6(Cu, Fe, Ni)_{23}S_{26}Cl$ (Efimova et al. 1983; Bulanova et al. 1990,1998; Guo et al. 1999; Sharygin et al. 2003; Logvinova et al. 2008; Stachel and Harris 2008). It should be noted in passing that experimental testing at high pressures (6.0–8.5 GPa) has revealed that diamonds are also capable to crystallized efficiently from the melts of sulfide-graphite mixtures with different Fe–Ni–Cu–S compositions (Litvin et al. 2002). Spontaneous crystallization of diamond from the sulfide melts has produced octahedral diamond crystals with flat faces and occurred quickly within 1–2 min after reaching the eutectic melting of a sulfide-graphite mixture (Fig. 4.2). Newly grown diamond layers were also observed on the seeds of metal-synthetic diamond grown at Ni–Mn-melts oversaturated with carbon (Fig. 4.2d). When sulfides are in molten state, the sulfide-carbon melts-solutions serve as a transfer medium for dissolved carbon during diamond growth. No indications were observed of sulfide breakdown with formation of free metal phases which could form the metal-carbon melts-solutions effective for diamond crystallization. Additionally, only sulfide phases were identified as the quenched melts in intimate contact with newly formed diamonds. All of these observations

demonstrate high efficiency of sulfide melts for diamond nucleation and growth under the conditions of diamond stability if the melts are oversaturated with dissolved carbon.

An interaction of sulfides with silicate and carbonate phases from inclusions in diamonds, particularly on melting, has not clear and arouses considerable interest. Melting equilibrium of the eclogitic garnet-pyrrhotite mixture was studied at 7.0 GPa and 1400–1900 °C (Litvin et al. 2005a, b, c), which correspond to the conditions of diamond stability. A melting phase diagram of the system was constructed, and it is shown in Fig. 4.11. The subsolidus assemblage consists of garnet and pyrrhotite. Pyrrhotite is melted at a solidus temperature of 1530 °C, and a two-phase assemblage of solid garnet and pyrrhotite melt forms. Garnet, as a multicomponent solid solution, is molted partially between 1675 and 1735 °C, and a three phase assembly consisting of garnet, silicate partial melt, and sulfide melt (Fig. 4.12a) was formed. In this case, the silicate and sulfide melts are immiscible.

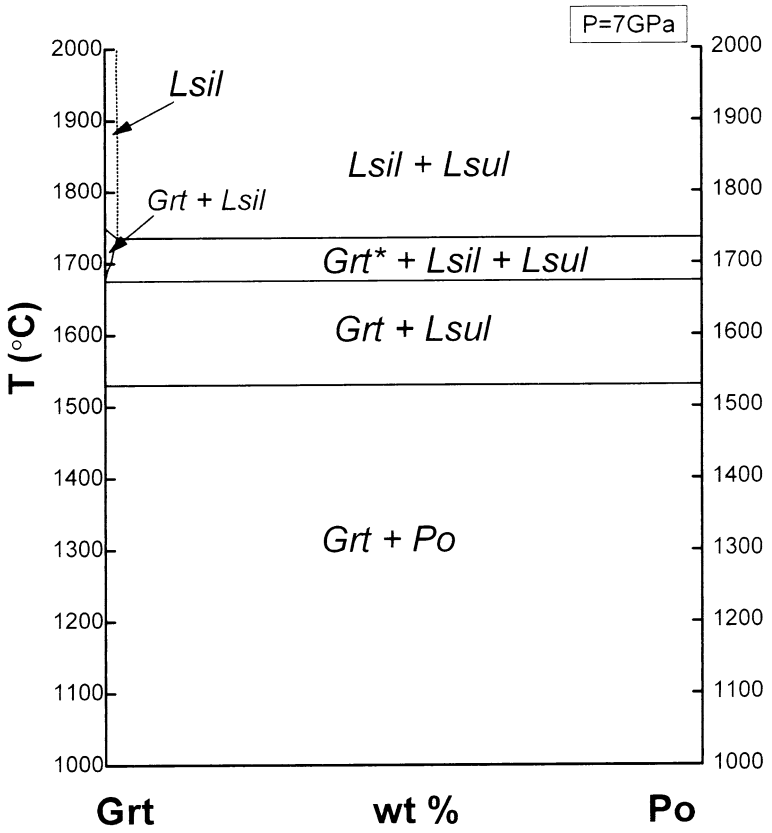

Fig. 4.11 Melting phase diagram of the eclogitic garnet—pyrrhotite (Po) join at a pressure of 7 GPa. *Symbols* Lsil—silicate liquid, Lsul—sulfide melt, Grt—garnet

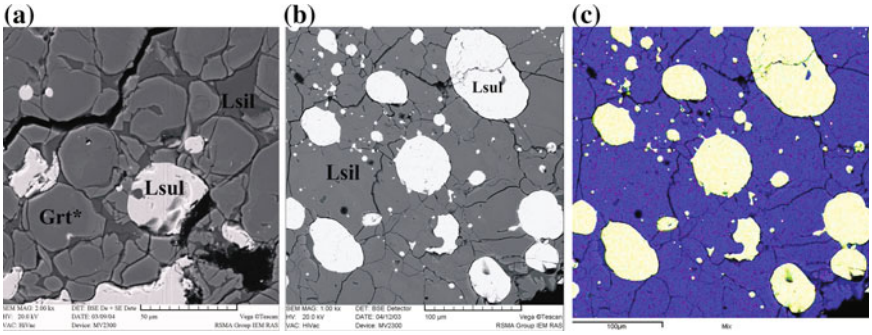

Fig. 4.12 Scanning electron micrograph (SEM) images of phase relations on the eclogitic garnet-pyrrhotite join: **a** three-phase assemblage garnet (Grt) + silicate melt Lsil + sulfide melt (Lsul) is formed by partial melting of garnet at 7 GPa, 1730 °C, 5 min, **b**, **c** two-phase assemblage of silicate melt + sulfide melt is formed at complete melting of garnet

Garnet has a higher Mg content by removal of iron into the silicate melt. Complete melting of garnet proceeds at temperatures above 1735 °C, and a two-phase field of immiscible silicate and sulfide melts forms (Fig. 4.12b). Although a low solubility 0.5–0.8 wt% FeS component in the silicate melts was recognized, the solubility of the garnet component in the sulfide melt was found to be negligible below the microprobe detection limits for all the "silicate" components. The "silicate" boundary for the two liquid immiscible fields is also shown in Fig. 4.11. The "sulfide" boundary is nearly coincident with the temperature ordinate. It is important to note that both solid and molten garnets are not dissolved in the sulfide melt. This implies that the silicate phase is not soluble in the sulfide melt, and, consequently, garnet cannot be crystallized from the melt. Therefore, a syngenetic formation of diamond and garnet inclusions from sulfide melts with dissolved carbon is not possible, although it was shown that the pyrrhotite melt with dissolved carbon is very efficient for diamond nucleation (Fig. 4.1). This seems to be applicable also to the other silicate mineral inclusions. The effect of liquid immiscibility of sulfide melt and carbonate or carbonate-silicate melt was also observed in the model silicate-carbonate-sulfide-carbon system (Litvin and Butvina 2004) (Fig. 4.13). It is evident that diamonds are formed only in the completely miscible silicate-carbonate melts oversaturated with dissolving carbon. It is interesting that, even at the contact of immiscible silicate-carbonate and sulfide melts, diamond is formed from the carbonatitic medium. Diamonds growing in the silicate-carbonate-carbon melt even penetrate into the sulfide melts being in tight contact with them, which is evident from imprints of diamond faces on some hardened sulfide melts.

High-pressure experimental study of the multicomponent system eclogite-carbonatite-sulfide-carbon gives physico-chemical insight into the heterogeneous interaction of minerals and melts that is combined with diamond-producing processes (Litvin et al. 2012; Litvin 2012, 2013). The experimental scenarios are in a

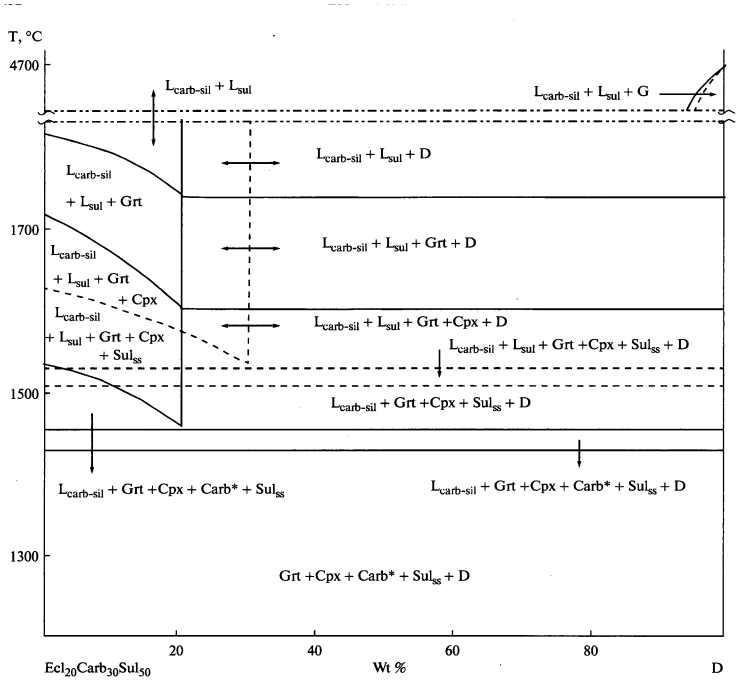

Fig. 4.13 Phase diagram of syngenesis of diamond and mineral phases of the eclogite paragenesis in the polythermic section $Ecl_{20}Carb_{30}Sul_{50}$—diamond of the heterogeneous system Ecl–Mg–(Mg–Ca–K–Carb)–(Fe–Ni–Cu–Sul)–C at 7 GPa; (Fe, Ni, Cu)S_{ss} is monosulfide solid solution

quite good approximation to the natural conditions of the upper-mantle genesis of diamond and associated phases. In this case, a biminerallic eclogite is chosen with the next mineral compositions (wt%): omphacite Omph–54.80 SiO_2, 0.48 TiO_2, 9.79 Al_2O_3, 0.05 Cr_2O_3, 8.97 MgO, 0.07 MnO, 6.40 FeO, 13.10 CaO, 6.70 Na_2O, and 0.30 K_2O; garnet Grt–40.00 SiO_2, 0.46 TiO_2, 22.00 Al_2O_3, 0.04 Cr_2O_3, 9.02 MgO, 0.52 MnO, 20.90 FeO, 8.18 CaO, and 0.17 Na_2O. A representative multicomponent sulfide pyrrhotite-pentlandite-chalcopyrite substance $Po_{40}Pn_{40}Ccp_{20}$ is used as the sulfide boundary composition in the eclogite–carbonatite-sulfide-carbon system.

The peculiarities of physico-chemical behavior of diamond-producing eclogite-carbonatite-carbon and sulfide-carbon melts within the frames of common system are illustrated by the syngenesis phase diagram for the polythermal section $(Ecl_{40}Carb_{60})_{50}Sul_{50}$–D of the heterogeneous system eclogite-carbonatite-sulfide-carbon (Fig. 4.14). The diagram of syngenesis consists of two relatively simpler subsystems: eclogite–carbonatite–diamond (solid lines) and sulfide–diamond (dashed lines). As mentioned, the carbonate–silicate melts are completely immiscible with sulfide melt, so that there is almost no chemical interaction

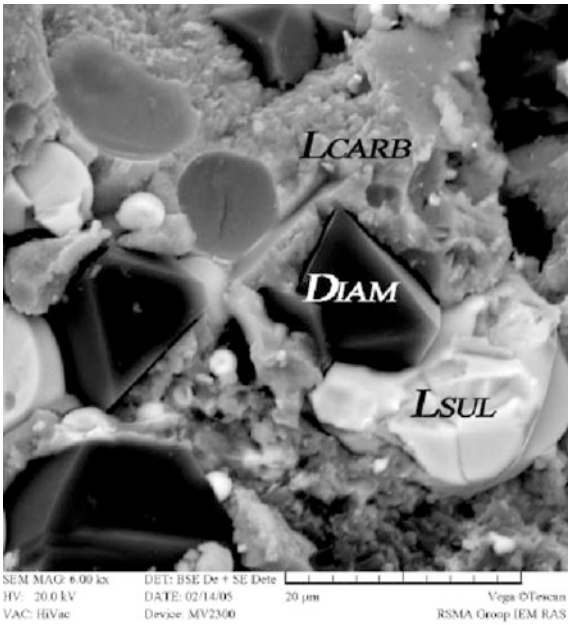

Fig. 4.14 Diamond-producing carbonatite melts (Lcarb) with completely immiscible sulphide melts (L_{sul}) after quenching at 7 GPa; Diam—diamond

between eclogite–carbonatite and sulfide components and phases. This suggests that eclogite–carbonatite components and phases, on the one hand, and sulfide components and phases, on the other hand, practically do not interact with each other. Therefore, these subsystems can be investigated separately with subsequent projection on the joint diagram of syngenesis. This makes possible the separate study of the respective boundary $Ecl_{40}Carb_{60}$–D and Sul–D with subsequent projection of the obtained phase diagrams onto each other to obtain the general diagram of syngenesis. A topology of the diagram of syngenesis of eclogite–carbonatite–diamond subsystem with phase field boundaries shown by solid lines is analogous to the similar system discussed above (Fig. 4.9).

Now, let us consider the diagram of syngenesis of the sulfide–diamond subsystem, the phase boundaries of which are depicted by dashed lines, missing all details pertaining to the eclogite–carbonatite subsystem. The sulfide melt (L_{sul}) is formed as a product of complete melting of the boundary sulfide composition (a part of parental medium) at 1630 °C. The solid sulfide solution (Fe, Ni, Cu)S_{ss} denoted as Sul_{ss} crystallizes from this melt with decrease in temperature, forming the next $Sul_{ss} + L_{sul}$ phase field. The increasing carbon content in the sulfide subsystem gradually reduces its temperature of complete melting. The sulfide melt is first transformed into an non-saturated carbon solution. When concentration of the dissolved carbon attains saturation with the diamond phase, the curve of diamond solubility in sulfide melt appears to be the most important topological

element of the sulfide–diamond diagram of syngenesis. This curve controls diamond formation under experimental and natural conditions. The physico-chemical mechanism of this control is related to oversaturation of sulfide melt solution of carbon with diamond, when temperature falls. Above 1530 °C (pseudo-eutectics) and about 32 wt% carbon, the solubility curve coincides with the liquidus curve for diamond and contours the L_{sul} + D field up to the melting point of solid carbon at 4200–4300 °C. The curve of diamond solubility is a phase boundary between the field of sulfide melt non-saturated with diamond, where its crystallization is impossible, and the field of sulfide melt oversaturated with diamond (field of diamond formation). This field is bounded by the curve of diamond solubility on the side of lower concentration of carbon and by the solidus curve on the side of lower temperature. In the L_{sul} + D field, diamond can entrap only sulfide melt as primary inclusions, whereas sulfide melt and solid solution are entrapped in the $L_{carb–sil}$ + Sul_{ss} + D field.

The phase relations in the sulfide–diamond subsystem provide direct physico-chemical evidence for the paragenetic nature of the primary sulfide inclusions with respect to the diamond that crystallizes from the same sulfide melt with dissolved carbon. At the same time, it is known that silicate and carbonate minerals are insoluble in sulfide melt (Shushkanova and Litvin 2008). Thus, they cannot be formed in sulfide melt and are xenogenetic in respect to the diamond that crystallizes from sulfide melt. Sulfide melt is also practically insoluble in carbonate–silicate melt, and thus sulfide inclusions are xenogenetic with respect to the diamond that crystallizes from carbonate–silicate melt.

To choose which of diamond-forming sulfide or carbonate–silicate melt is preferable as a growth medium for most natural diamonds, a diagram of syngenesis for the integral eclogite–carbonatite–sulfide–diamond system should be considered (Fig. 4.14). The phase boundaries of both subsystems are retained in the diagram of the integral system. The combination of overlapping phase fields creates a new system of carbonate–silicate, silicate, carbonate, and sulfide phases. The crystallization sequence of minerals in the integral system hardly needs special comment. It should only be noted that carbonate–silicate and sulfide melts are immiscible above the melting temperature of sulfide pseudo-eutectics (1510 °C). Below this temperature, the carbonate–silicate melt coexists with sulfide solid solution. Both curves of diamond solubility in eclogite–carbonatite and sulfide melts are shown in the integral diagram of syngenesis. Their combination in the heterogeneous diamond-forming system is an important feature providing insight into the origin of diamond.

The concentration of carbon dissolved in the carbonate–silicate melt (20–22 wt%) is lower than the concentration of carbon dissolved in the sulfide melt (30–32 wt%). This implies that if carbon is dissolved in two immiscible diamond-forming melts, saturation with diamond is first attained in the melt with lower equilibrium solubility. In the studied heterogeneous system, it is the carbonate–silicate melt, so that its saturation with dissolved carbon creates necessary physico-chemical preconditions for crystallization of diamond. The labile oversaturation of carbonate–silicate melt-solution with diamond is a sufficient condition for its nucleation and

crystallization, which can be created in experiments by a temperature gradient in the sample (labile oversaturation arises on the low temperature side) or by the use of metastable graphite, the solubility of which is higher than the solubility of thermodynamically stable diamond (Litvin 1968, 2007). In certain circumstances, these mechanisms may be realized in the natural source of the diamond-forming melts, however, a mere decrease in temperature is more typical of natural conditions. The carbon at silicate-carbonate melt saturated in respect to diamond becomes oversaturated at a lower temperature, and oversaturation is retained up to the complete solidification of magma source. When diamond crystallizes in the carbonate–silicate growth medium, the concentration of dissolved carbon is stabilized at the solubility curve of diamond and any excess carbon in the oversaturated melt is consumed for crystallization of diamond. The concentration of dissolved carbon in the coexisting sulfide melt cannot be higher than its solubility in the carbonate–silicate melt. As a result, a sulfide melt with a higher solubility of diamond remains non-saturated with diamond. This implies that formation of diamond in the carbonate–silicate melt prevents further dissolution of carbon in the sulfide melt, so the conditions necessary for crystallization of diamond are not created (Fig. 4.14). Thus, the formation of diamond in the heterogeneous eclogite–carbonatite–sulfide–diamond system is controlled by the solubility curve of diamond in miscible carbonate–silicate melts. When growing, diamonds entrap paragenetic silicate and carbonate minerals and drops of carbonate–silicate liquid. The inclusions of sulfide melt and solid solutions in diamonds crystallized from carbonate–silicate melt are xenogenetic and unrelated to the eclogite–carbonatite subsystem.

The above physico-chemical arguments also have implications for characterization of the growth medium of natural diamonds. They allow us to consider the heterogeneous parental medium of natural diamonds deduced from mineralogical data in a new light. As follows from physico-chemical evidence, this medium consists of paragenetic and xenogenetic parts unlike mineralogical estimates, which assume that all heterogeneous constituents of the parental medium are paragenetic. This difference is reflected in the definition of term syngenetic inclusions, which has been introduced as a result of mineralogical study. The physico-chemical data also show that syngenesis of diamond with silicate and carbonate minerals in a sulfide melt is impossible.

It is therefore concluded that xenogenetic minerals could penetrate mechanically into the diamond-producing silicate-carbonate-carbon melts-solutions during the processes of assimilation of the upper-mantle rock-forming and accessory minerals which are effectively soluble in carbonatite melts. It is reasonable that paragenetic minerals and diamonds including them have been formed at the common parental medium. The xenogenetic nature of the primary mineral phases cannot be determined by mineralogical evidence that is responsible for the definite uncertainty in interpretation of their genetic significance. A strong evidence for the xenogenesis of the primary mineral inclusions in diamonds would be given by that they are practically insoluble at carbonate and completely miscible silicate-carbonate melts and, correspondingly, immiscible with them. This is evident from experimental data not only for sulfide minerals and melts but for the melts of titanoferous minerals

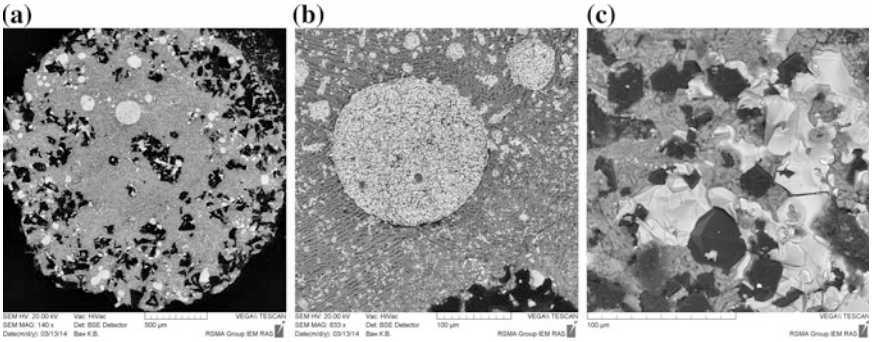

Fig. 4.15 Liquid immiscibility of carbonatite and ilmenite melts in the system (Mg–Fe–Ca–Na–K–carbonatite–ilmenite $FeTiO_3$–carbon at 8 GPa, 1600 °C, 25 min: **a**, **b** mass crystallization of diamond from carbonatite-carbon melt-solution immiscible with titaniferous ilmenite melt; **c** diamonds formed in carbonatite-carbon melt-solutions and ilmenite crystalized partially during quenching. Distinctive indications: *grey*–quenched carbonate melt, *white*—quenched ilmenite melts and crystals, *black*—diamond

ilmenite and rutile (Fig, 4.14) (Litvin et al. 2016) as well as for native metals and metallic alloys (Fig. 4.15).

4.5 Principles of Genetic Classification of Syngenetic Inclusions in Upper-Mantle Diamonds

The knowledge based on generalization of the mineralogical analytical and physico-chemical results has provided new clues of genetically important connecting links between mineral phases involved into the diamond-producing processes at the Earth's upper mantle. It should be remarked, that the term "syngenetic inclusion" is indefinite because it remains uncertain whether the inclusions are paragenetic or xenogenic in their origin. The term is still used as a synonym of the term "paragenetic inclusion" implying that entrapment of substance and formation of inclusion occurred synchronously with the growth of the host diamond. Whereas the physico-chemical conditions of some inclusion origin cannot be established from mineralogical data. Inasmuch as the origin of the inclusion remains ambiguous, the term primary inclusion is more suitable. Mineralogical data do not provide evidence for physico-chemical formation conditions of minerals and melts that occur in the parental medium and are entrapped by growing diamond, or for their genetic links to the host diamond. The possibility of all or some inclusions which are identified at room temperature to be formed simultaneously with diamond as products of the same physico-chemical process remains unsupported by mineralogical evidence. In this regard, a problem arises of which mineral substances of the syngenetic inclusions are paragenetic, i.e., formed from the same melt as diamonds, and which are xenogenetic, i.e., foreign to the growth melt of diamond. In addition, it remains

unclear which of heterogeneous substances syngenetically incorporated into diamond are responsible for nucleation and crystallization of host diamonds. In other words, there are no mineralogical or geochemical criteria of diamond-forming capability of any minerals, melts, and fluids associated with natural diamonds.

For most of natural diamonds, the concept of variable silicate-(±oxide)-carbonatite-carbon growth melts-solutions agrees with the mineralogical data on the chemical compositions of substances trapped by diamonds in situ from growth melts and with the results of experimental physico-chemical studies based on the diamond and inclusion syngenesis criterion. The phase diagrams of syngenesis are applicable to interpretation of diamond and syngenetic minerals formation in the common natural magma sources. They ascertain physico-chemical mechanism of natural diamond formation and conditions of entrapment of paragenetic and xenogenetic mineral phases by growing diamonds. The mantle-carbonatite concept permits the development of genetic classification of mineral, melt, and volatile inclusions in natural diamonds of upper-mantle genesis (Litvin 2009). The classification reveals a physico-chemical relationship of the included compounds with components of carbonatite growth melts. The proposed genetic classification of mineral, melt, and fluid components and phases entrapped as primary inclusions by growing diamonds is based on the mantle-carbonatite theory of the origin of natural diamonds (Litvin 2009). This classification provides insights into the origin of inclusions and reveals their physicochemical links to the major components of carbonate–silicate growth melts, as well as soluble and insoluble components and phases contained therein. The main items of this classification are as follows:

1. The main silicate, aluminosilicate and carbonate components of growth media are responsible for diamond-hosted inclusions of paragenetic silicate and aluminosilicate minerals of peridotite-pyroxenite and eclogite-grospydite assemblages, carbonate minerals, and carbonatite melts. They formed together with diamond in the completely miscible silicate–carbonate growth melt with dissolved elementary carbon and were trapped in situ under the PT-conditions of diamond formation. Evidence is provided that the main silicate and carbonate minerals are paragenetic.
2. The minor (accessory) soluble oxide, some silicate and aluminosilicate, phosphate and partly chloride impurity components of growth media occur as oxide and rare silicate and aluminosilicate minerals, apatite, and chlorides (at low concentrations of fluid components) in diamond. The inclusions were formed in the growth melt and entrapped in situ under the PT-conditions of diamond formation.
3. The minor admixtured soluble components of C–O–H fluid are responsible for inclusions filled with secondary paragenetic volatile phases (water H_2O, carbon dioxide CO_2, methane CH_4). The components were entrapped in situ at PT-conditions of diamond stability during diamond crystallization being dissolved in carbonate-silicate melts; but during the cooling and hardened of growth melts they released as separate individual phases of water, carbon

dioxide, and, sometimes, methane, making a "quenched" assemblage of associated carbonates, silicates, phosphates, oxides, sulfides, chloride, etc. at much lower P and T values lower than the parameters of diamond crystallization.

4. The xenogenetic sulfide, titanite and metallic minerals and melts insoluble in diamond-producing carbonatite melts and completely immiscible with them occur as inclusions in diamond. Thus these inclusions were not formed in the growth melt but are the-products trapped (as alone as in association with minerals produced in the growth melt) under the PT-conditions of diamond formation. The sulfide and other insoluble phases are xenogenetic with respect to diamond and must be assigned to the secondary insoluble and immiscible inclusions.
5. The carbon dissolved in carbonatite growth melt (and being in the state of metastable oversaturation with respect to diamond) is responsible for the paragenetic inclusions of thermodynamically metastable single-crystalline graphite, which are also entrapped in situ. This thermodynamically unstable phase formed in growth melt and was trapped in situ under the PT-conditions of diamond formation.

In conclusion it may be aid that at PT-conditions of thermodynamic stability of diamond, the completely miscible silicate-(±oxide)-carbonate melts are characterized by the capacity to effective dissolving rock-forming and accessory mantle minerals, solid carbon phases, and C–O–H–N-volatile compounds. Multicomponent multiphase melts-solitions of this kind are capable to providing formation of diamonds and associated paragenetic phases and, at the same time, are not threw obstacles to penetration inward of xenogenetic minerals and melts. The silicate-(±oxide)-carbonate-carbon melts-solutions, parental for diamonds and associated phases, are in excellent agreement with the syngenesis criterion for diamonds and associated phases.

It is pertitent to note that the genetic classification of syngenetic inclusions in upper mantle derived diamonds takes proper account of the new interpretation of origin of some diamond-hosted inclusions, such as paragenetic volatile and xenogenetic sulfide phases. The origin of sulfide inclusions has acquired importance because of their use as syngenetic for Re–Os dating (Pearson and Shirey 1999; Shirey et al. 2004). However a dissemination of the age measured for xenogenetic sulfide inclusion in diamond on the age of diamond hosting the inclusion is evidently of dubious value.

References

Akaishi M (1996) Effect of Na_2O and H_2O addition to SiO_2 on the synthesis of diamond from graphite. Proceedings of the 3rd NIRIM (national institute for research in inorganic materials) international symposium on advanced materials (ISAM'96). Tsukuba, Ibaraki, Japan, pp 75–80

Akaishi M, Yamaoka S (2000) Crystallization of diamond from C–O–H fluids under high-pressure and high-temperature conditions. J Cryst Growth 209:999–1003. doi:10.1016/S0022-0248(99)00756-3

Akaishi M, Kanda H, Yamaoka S (1990) High pressure synthesis of diamond in the systems of graphite-sulfate and graphite-hydroxide. Jpn J Appl Phys 29:L1172–L1174. doi:10.1143/JJAP.29.L1172

Akaishi M, Shaji Kumar MD, Kanda H, Yamaoka S (2001) Reactions between carbon and a reduced C–O–H fluid under diamond-stable HPHT conditions. Diamond Relat Mater 10:2125–2130. doi:10.1016/S0925-9635(01)00490-3

Arima M (1996) Experimental study of growth and resorption of diamond in kimberlitic melts at high pressures and temperatures. Proceedings of the 3rd NIRIM (national institute for research in inorganic materials) international symposium on advanced materials (ISAM'96). Tsukuba, Ibaraki, Japan, pp 223–228

Arima M, Nakayama K, Akaishi M et al (1993) Crystallization of diamond from silicate melt of kimberlite composition in high-pressure high-temperature experiments. Geology 21:670–968. doi:10.1130/0091-7613(1993)o21<0968:CODFAS>2.3.CO;2

Bobrov AV, Litvin YA (2009) Peridotite-eclogite-carbonatite systems at 7.0–8.5 GPa: concentration barrier of diamond nucleation and syngenesis of its silicate and carbonate inclusions. Rus Geol Geoph 50(12):1221–1233

Bulanova GP, Spetsius ZV, Leskova NV (1990) Sulfides in diamonds and xenoliths from kimberlite pipes of Yakutia. Nauka, Novosibirsk, p 117

Bulanova GP, Griffin WI, Ryan CO (1998) Nucleation environment of diamonds from Yakutian kimberlites. Min Magaz 62:409–419. doi:10.1180/002646198547675

Bundy FP, Hall HT, Strong HM, Wentorf RH (1955) Man-made diamonds. Nature 176:51–54. doi:10.1038/176051a0

Bundy FP, Basset WA, Weathers MS et al (1996) The pressure-temperature phase and transformation diagram for carbon; updated through 1994. Carbon 34:141–153

Efimova ES, Sobolev NV, Pospelova LN (1983) Inclusions of sulphides in diamonds and peculiarity of their paragenesis. Zapiski Vsesoyuzn Mineralogich Obschestva 92:300–309

Glinnemann J, Kusaka K, Harris JW (2003) Oriented graphite single-crystal inclusions in diamond. Z Kristallogr 218(11):733–739

GuO JF, Griffin WL, O'Reilly SV (1999) Geochemistry and origin of sulfide minerals in mantle xenoliths; Qilin, south-estern China. J Petro 40:1125–1149

Harte B (2010) Diamond formation in the deep mantle the record of mineral inclusions and their distribution in relation to mantle dehydration zone. Min Mag 74(2):180–215

Hong SM, Akaishi M, Yamaoka S (1999) Nucleation of diamond in the system of carbon and water under very high pressure and temperature. J Cryst Growth 200:326–332

Kennedy GS, Kennedy GC (1976) The equilibrium boundary between graphite and diamond. J Geophys Res 1(14):2467–2470

Kurat G, Dobosi G (2000) Garnet and diopside-bearing diamondites (framesites). Min Petrol 69:143–159. doi:10.1007/s007100070018

Litvin YA (1968) On the mechanism of diamond formation in metal-carbon systems. Izvestia Akad Nauk SSSR. Inorganic Mater 4:175–181

Litvin YA (1969) To the diamond origin problem. Zapiski Vsesoyuzn Mineralogich Obschestva 98(2):114–121

Litvin YA (1991) Physicochemical studies of melting in the earth's interior. Nauka, Moscow, p 312

Litvin YA (2003) Alkaline-chloride components in processes of diamond growth in the mantle and high-pressure experimental conditions. Dokl Earth Sci 389A(3):388–391

Litvin YA (2007) High-pressure mineralogy of diamond genesis. In: Ohtani E (ed) Advances in high-pressure mineralogy (edited by Eiji). Geological Society of America Special Paper, vol 421, pp 83–103. doi:10.1130/2007.2421(06)

Litvin YA (2009) The physicochemical conditions of diamond formation in the mantle matter: experimental studies. Russ Geol Geoph 50(12):1188–1200

Litvin YA (2012) Physico-chemical formation conditions of natural diamond deduced from experimental study of the eclogite-carbonatite-sulfide-diamond system. Geol Ore Depos 54(6):443–457

Litvin YA (2013) Physico-chemical conditions of syngenesis of diamond and heterogeneous inclusions in the carbonate-silicate parental melts (experimental study). Min J 35(2):5–24
Litvin YA, Butvina VG (2004) Diamond-forming media in the system eclogite-carbonatite-sulfide-carbon: experiments at 6.0–8.5 GPa. Petrology 12(4):377–382
Litvin YA, Spivak AV (2003) Rapid growth of diamondite at the contact between graphite and carbonate melt: experiments at 7.5–8.5 GPa. Dokl Earth Sci 391A:888–891
Litvin YA, Spivak AV (2004) Crystal growth of diamond at 5.5–8.5 GPa in carbonate-carbon melt-solutions being chemical analogues of natural diamond forming melts. Mater Sci Trans 84 (3):27–34
Litvin YA, Zharikov VA (1999) Primary fluid-carbonatite inclusions in diamond: experimental modeling in the system K_2O–Na_2O–CaO–MgO–FeO–CO_2 as a diamond formation medium at 7–9 GPa. Dokl Earth Sci 367A:801–805
Litvin YA, Zharikov VA (2000) Experimental modeling of diamond genesis: diamond crystallization in multicomponent carbonate-silicate melts at 5–7 GPa and 1200–1570 °C. Dokl Earth Sci 373:867–870
Litvin YA, Chudinovskikh LT, Zharikov VA (1997). Experimental crystallization of diamond and graphite from alkali-carbonate melts at 7–11 GPa. Trans (Dokl) Russ Acad Sci/Earth Sci Sect 355A(6):908–911
Litvin YA, Chudinovskikh LT, Zharikov VA (1998) Crystallization of diamond in the $Na_2Mg(CO_3)_2$–$K_2Mg(CO_3)_2$–C system at 8–10 GPa. Dokl Earth Sci 359A:464–466
Litvin YA, Aldushin KA, Zharikov VA (1999a) Diamond synthesis at 8.5–9.5 GPa in the $K_2Ca(CO_3)_2$–$Na_2Ca(CO_3)_2$ system modeling compositions of fluid-carbonatite inclusions in kimberlitic diamonds. Dokl Earth Sci 367:529–532
Litvin YA, Chudinovskikh LT, Saparin GV et al (1999b) Diamonds of new alkaline carbonate-graphite HP syntheses: SEM morphology, CCL-SEM and CL spectroscopy studies. Diamond and Relat Mater 8:267–272. doi:10.1016/S0925-9635(98)00318-5
Litvin YA, Jones AP, Beard AD et al (2001) Crystallization of diamond and syngenetic minerals in melts of diamondiferous carbonatites of the Chagatai Massif, Uzbekistan: experiment at 7.0 GPa. Dokl Earth Sci 381A:1066–1069
Litvin YA, Butvina VG, Bobrov AV, Zharikov VA (2002) The first synthesis of diamond in sulfide-carbon systems: the role of sulfides in diamond genesis. Dokl Earth Sci 382(1):40–43
Litvin YA, Spivak AV, Matveev YA (2003) Crystallization of diamond in the molten carbonate-silicate rocks of the Kokchetav metamorphic complex at 5.5–7.5 GPa. Geochem Int 11:1090–1098
Litvin YA, Kurat G, Dobosi G (2005a) Experimental study of diamondite formation in carbonate-silicate melts: a model approach to natural processes. Russ Geol Geoph 46(12):1285–1299
Litvin YA, Pineau F, Javoy M (2005b) Carbon isotope fractionation on diamond synthesis in carbonatite-carbon melts of natural chemistry (experiments at 6.5–7.5 GPa). In: Proceedings of 6th international symposium on applied isotope geochemistry. Prague, Czechia, p 143
Litvin YA, Shushkanova AV, Zharikov VA (2005c) Immiscibility of sulfide-silicate melts in the mantle: role in the syngenesis of diamond and inclusions (based on experiments at 7.0 GPa). Dokl Earth Sci 403:719–722
Litvin YA, Litvin VY, Kadik AA (2008) Experimental characterization of diamond crystallization in melts of mantle silicate-carbonate-carbon systems at 7.0–8.5 GPa. Geochem Int 46(6):531–553
Litvin YA, Vasiliev PG, Bobrov AV et al (2012) Parental media of natural diamonds and primary mineral inclusions in them: evidence from physicochemical experiment. Geochem Int 50(9):726–759
Litvin YA, Bovkun AV, Garanin VK (2016a) Titanium minerals ant their melts in the mantle chambers of diamond-forming systems (experiments at 7–8 GPa). Geochem Intern (accepted)
Litvin YA, Spivak AV, Kuzyura AV (2016b) Fundamentals of the mantle carbonatite concept of diamond genesis. Geochem Int 54(10):839–857. doi:10.1134/S0016702916100086
Logvinova AM, Wirth R, Fedorova EN, Sobolev NV (2008) Nanometre-sized mineral and fluid inclusions in cloudy Siberian diamonds: new insight on diamond formation. Eur J Miner 0:317–331

Palyanov Y, Sokol AG, Borzdov YM et al (1999) Diamond formation from mantle carbonatite fluid. Nature 400:417–418. doi:10.1038/22678

Palyanov YN, Sokol AG, Borzdov YM, Khokhryakov AF (2002) Fluid-bearing alkaline carbonate melts as the medium for the formation of diamonds in the Earth's mantle: an experimental study. Lithos 60:145–159. doi:10.1016/S0024-4937(01)00079-2

Pearson DG, Shirey SB (1999) Isotopic dating of diamonds. In: Lambert D, Ruiz J (eds) Economic geologists special publication, SEg reviewes, vol 12, pp 143–171

Sato H, Akaishi M, Yamaoka S (1999) Spontaneous nucleation of diamond in the system $MgCO_3$–$CaCO_3$–C at 7.7 GPa. Diamond Relat Mate 8:1900–1905. doi:10.1016/S0925-9635(99)00157-0

Schrauder M, Navon O (1994) Hydrous and carbonatitic mantle fluids in fibrous diamonds from Jwaneng, Botswana. Geochim Cosmochim Acta 58:761–771. doi:10.1016/0016-7037(94)90504-5

Shaji Kumar MD, Akaishi M, Yamaoka S (2000) Formation of diamond from supercritical H_2O–CO_2 fluid at high pressure and high temperature. J Cryst Growth 213:203–206. doi:10.1016/S0022-0248(00)00352-3

Shaji Kumar MD, Akaishi M, Yamaoka S (2001) Effect of fluid concentration on the formation of diamond in the CO_2–H_2O-graphite system under HP-HT conditions. J Cryst Growth 222:3–9. doi:10.1016/S0022-0248(00)00921-0

Sharygin VV, Golovin AV, Pokhilenko NP, Sobolev NV (2003) Djerfisherite in unaltered kimberlite of Udachnaya East pipe, Yakutia. Dokl Earth Sci 390:554–557

Shatskii AF, Bordzov YV, Sokol AG, Palyanov YN (2002) Features of phase formation and crystallization in ultrapotasc carbonate-silicate systems with carbon. Geol Geofiz 43(10): 940–950

Shirey SB, Richardson SH, Harris JW (2004) Integrated model of diamond formation and craton evolution. Lithos 77:923–944

Shushkanova AV, Litvin Y (2005) Phase relations in diamond-forming carbonate–silicate–sulfide-systems on melting. Russ Geol Geoph 46(12):1317–1326

Shushkanova AV, Litvin YA (2008) Experimental evidence for liquid immiscibility in the model system CaCO3–pyrope–pyrrhotite at 7.0 GPa: the role of carbonatite and sulfide melts in diamond genesis. Canad Min 46:991–1005

Sobolev NV (1977) The deep-seated inclusions in Kimberlites and the problem of the composition of the upper mantle. American Geophysical Union, Washington, p 304

Sokol AG, Palyanov YN, Palyanova GA et al (2001) Diamond and graphite crystallization from C–O–H fluids under high pressure and high temperature conditions. Diamond Rela Mater 10:2131–2136

Spivak AV, Litvin YA, Shushkanova AV et al (2008) Diamond formation in carbonate-silicate-sulfide-carbon melts: Raman- and IR-microspectroscopy. Eur J Min 20:341–347

Stachel T, Harris JW (2008) The origin of cratonic diamonds–constrains from mineral inclusions. Ore Geol Res 34:5–32

Taniguchi T, Dobson D, Jones AP et al (1996) Synthesis of cubic diamond in the graphite-magnesium carbonate and graphite-K2 Mg(CO3)2 system at high pressure of 9–10 GPa region. J Mater Res 11:2622–2632

Tomlinson E, Jones AP, Milledge JH (2004) High-pressure experimental growth of diamond using C–K_2CO_3–KCl as an analogue of Cl-bearing carbonate fluid. Lithos 77:287–294. doi:10.1016/j.lithos.2004.04.029

Wyllie PJ (1979) Magma and volatile components. AmMin 64(5–6):469–500

Yamaoka S, Shaji Kumar MD, Akaishi M, Kanda H (2000) Reactions between carbon and water under diamond-stable high pressure and high temperature conditions. Diamond Relat Mater 9:1480–1486. doi:10.1016/S0925-9635(00)00274-0

Yamaoka S, Shaji Kumar MD, Kanda H, Akaishi M (2002) Crystallization of diamond from CO_2 fluid at high pressure and high temperature. J Cryst Growth 234:5–8. doi:10.1016/S0022-0248(01)01678-5

Chapter 5
Physico-Chemical Features of Lower-Mantle Diamond-Parental Systems

Experimental investigations on the origin of paradoxical assemblages of Mg and Fe oxides with stishovite (Si oxide) among inclusions in the lower-mantle diamonds made it possible to reveal the physico-chemical mechanism of the effect of "stishovite paradox". The effect is of decisive importance for the ultrabasic-basic evolution of native lower-mantle magmas and diamond-parental melts. The mineralogy of primary inclusions in the lower-mantle derived diamonds in conjunction with results of physico-chemical experimental studies of the diamond-producing lower-mantle systems gave insight into the chemical and phase composition of the diamond-parental melts and physico-chemical mechanisms of genesis of the lower-mantle diamonds and their paragenetic minerals. Also the compositions of the diamond-parental melts for the transition zone are preliminary estimated. As a result, the genetic classifications of syngenetic inclusions in the transition-zone- and lower-mantle diamonds have been developed. A correlation between the scenarios of the natural diamonds origin for the conditions of the upper mantle, transition zone and lower mantle leads to the conclusion that a physico-chemically uniform "melt-solution" mechanism of diamond formation is operative within the Earth's mantle depths of at least 150–800 km.

5.1 Paradoxical Assemblage of Stishovite and Oxide Inclusions in Lower-Mantle Diamonds

There is no compelling indication on transference of natural substance of the silicate-oxide lower mantle to the Earth's surface (Stachel et al. 2005) similarly to the upper mantle xenoliths of ultrabasic peridotite and basic eclogite rocks. Early estimates of the Earth's lower-mantle mineralogy were based on assumptions that chemical composition of the upper-mantle peridotite (or pyrolite) is representative for whole of the Earth's mantle. A credible mineralogy of the upper-mantle

Y.A. Litvin, *Genesis of Diamonds and Associated Phases*,
Springer Mineralogy, DOI 10.1007/978-3-319-54543-1_5

ultrabasic garnet-peridotitic/pyrolitic primitive rock was reported as corresponding to olivine—64, orthopyroxene—27, clinopyroxene-3, garnet—4 (wt%) by the previous estimate (Mathias et al. 1970). At the same time, a probable lower-mantle mineral assemblage was specified based on circumstantial experimental evidence (Ringwood 1975) as periclase MgO 29, stishovite SiO_2 22, $(MgSiO_3 \cdot Al_2O_3)_{Ilm\text{-}ss}$ 24, $[(Ca, Fe)SiO_3]_{Per\text{-}ss}$ 23, $NaAlSiO_4$ 2 (wt%) where "Ilm" and "Per" are structural symbols.

Subsequent high-pressure high-temperature experiments (Akaogi 2007) on direct subsolidus conversion of the bulk pyrolite composition under the lower-mantle pressures of 25–45 GPa indicate a dominant role of the ultrabasic lower-mantle assemblage ferropericlase $(MgO \cdot FeO)_{ss}$ + bridgmanite (Mg, Fe) SiO_3 + Ca-perovskite $CaSiO_3$ with no in situ place for stishovite. It is reasonable that in experiments with basic mid-ocean-ridge basalt (MORB) at 30–45 GPa the assemblage of stishovite, Ca-perovskite, (Mg, Fe, Al)-bridgmanite and $Mg_2CaAl_6O_{12}$-based aluminous phase was produced. These experimental results led to conclusion that stishovite is not in situ lower-mantle mineral but subducted one. In this case stishovite is bound to be formed together with diamonds and other MORB-derived phases in the subducting transfer of the mid-ocean-ridge basalts over the upper-mantle and transition zone to the lower mantle depths (Stachel et al. 2000a, b; Harte 2010).

As similar to the experimentally originated minerals the primary inclusions in the lower-mantle diamonds are known (Harte and Harris 1994; Kaminsky 2012). But, these inclusions were trapped by the lower-mantle diamonds as fragments of heterogeneous silicate-oxide-carbonate-carbon parental medium (Litvin et al. 2014). Accumulation of diamond-parental melts creates their reservoirs-chambers inside the enclosing lower-mantle rocks. Hence, the ways of origin of the rock-forming and diamond-hosted minerals is different in spite of their similarity. The lower-mantle rocks are the in situ products of earlier global magmatic events. But the diamond-parental melts in local reservoirs-chambers were produced by dissolution of rock-forming ferropericlase, bridgmanite and Ca-perovskite minerals in primary carbonate melts (most probably, of metasomatic origin). Inclusions of these minerals together with carbonate minerals aragonite $CaCO_3$, dolomite $CaMg(CO_3)_2$, nyerereite $Na_2Ca(CO_3)_2$, nahcolite $NaHCO_3$ (Kaminsky 2012) are symptomatic for compositions of the multicomponent completely miscible silicate-oxide-carbonate-carbon diamond-parental melts. Inclusions in the lower-mantle diamonds are the crystallization products from the lower-mantle diamond-parental melts. In essence, the inclusions are products of the local re-crystallization of the lower-mantle rock-forming minerals in the diamond-parental melts.

The main discrepancy between the estimations in testing experiments of lower-mantle ultrabasic mineralogy, on one hand, and minerals included in diamonds, on the other, lies in the fact that stishovite SiO_2 is quite representative among the primary inclusions in super-deep diamonds. Moreover, by a paradoxical mineralogy of primary inclusions in lower-mantle diamonds (Stachel et al. 2000b; Hayman et al. 2005; Kaminsky 2012), the diamond-hosted stishovite SiO_2 is intimately associated with periclase-wustite solid solution phases $(MgO \cdot FeO)_{ss}$, even

forming closely related paragenetic intergrowths. The association of stishovite with a definitely in situ lower-mantle mineral ferropericlase (Mg, Fe)O demonstrates clearly that stishovite is also the in situ lower-mantle phase. The paragenetic coexistence of stishovite SiO_2 and ferropericlase-magnesiowustite phases $(MgO{\bullet}FeO)_{ss}$ in germetically closed inclusions of lower-mantle diamonds is defined as a "stishovite paradox" (Litvin 2014). The association is paradoxical due to conflicting with the natural and experimental evidence that parageneses of MgO, FeO or $(MgO{\bullet}FeO)_{ss}$ and SiO_2 (quartz or coesite) are impracticable (i.e., physico-chemically "forbidden") for the crustal and upper mantle conditions.

Thus, not only ultrabasic but stishovite-bearing basic material is drawn into the in situ lower-mantle diamond-forming process. It should be remarked that the associated stishovite and $(MgO{\bullet}FeO)_{ss}$ phases are natural substances of primary inclusions in lower-mantle diamonds and could be formed in paragenesis with the hosting diamonds in a common lower-mantle silicate-(±oxide)-carbonatite-carbon parental melts (Litvin 2014; Litvin et al. 2014).

The "stishovite paradox" gives evidence that diamond-parental silicate-oxide-carbonatite-carbon media has been experienced ultrabasic-basic magmatic differentiation inside their lower-mantle reservoirs-chambers. It may be suggested that the initial ultrabasic magma which was generated in the enclosing lower-mantle ferropericlase + Mg–Fe-bridgmanite + Ca-perovskite material would also be subjected to the ultrabasic-basic differentiation. For the upper mantle conditions, it was demonstrated that magmatic differentiation of such type provides physico-chemical links between the ultrabasic peridotitic and all the varieties of basic eclogitic rocks (Litvin 2012; Litvin et al. 2016a). Therefore, a significance of stishovite and "stishovite paradox" for composition and evolution of the lower mantle material is of special interest for mineralogy, petrology and mantle dynamics of the Earth's deep interiors. Because of this, the physico-chemical mechanism of "stishovite paradox" in the primitive silicate-oxide rock-forming material of the Earth's lower-mantle as well as in diamond-producing silicate-oxide-carbonatite-carbon melts-solutions is a subject of much current interest. Experimental syngenesis criterum demands a common parental medium for the lower-mantle diamonds and each of the included phases. The version of completely miscible silicate-oxide-carbonatite melts with dissolved carbon is a non-contradictory and demonstrable solution (Litvin 2014; Litvin et al. 2014, 2016a).

5.2 Physico-Chemical Mechanism of Stishovite Paradox by Experimental Evidence

The four-component MgO–FeO–SiO_2–$CaSiO_3$ system is most demonstrable for physico-chemical experimental study of "stishovite paradox" in the uppermost lower mantle silicate-oxide primitive material (Litvin 2014; Litvin et al. 2014). The system is representative for characterization of the major components of the

lower-mantle rocks which have been partially involved into formation of the diamond-producing silicate-oxide-carbonatite-carbon melts-solutions. Along with this, the lower-mantle rocks provide enclosing medium for the reservoirs-chambers of diamond-producing melts.

Physico-chemical mechanism of "stishovite paradox" in the silicate-oxide rock-forming material of the Earth's lower-mantle has been disclosed in experimental study and physico-chemical analysis of the representative MgO–FeO–CaO–SiO_2 system which is responsible for origin of the dominant lower-mantle mineral phases (Litvin et al. 2014, 2016b, c). The periclase-wustite solid solutions $(MgO•FeO)_{ss}$, (Mg, Fe)-bridgmanite (Mg, Fe)SiO_3, Ca-perovskite $CaSiO_3$ and stishovite SiO_2 hold the greatest interest. Moreover, it is appeared pertinent to estimate a feasibility of the mechanism in the case of the lower-mantle diamond-forming silicate-oxide-carbonatite-carbon melts. Hence, another task deals with experimental testing of diamond formation in the MgO–FeO–SiO_2–(Mg–Fe–Ca–Na-carbonatite)—carbon system that representatively characterizes in this case the natural diamond-parental magmas of the lower-mantle diamond-forming reservoirs-chambers.

The major substances involved into "stishovite paradox" are characterized by subsolidus assemblages of the ternary MgO–FeO–SiO_2 boundary join (Fig. 5.1) at pressures higher than 24 GPa. The assemblages demonstrate that periclase MgO and wustite FeO form unlimited solid solutions, whereas ferrobridgmanite solid solutions (Mg, Fe)SiO_3 are limited. Under the lower-mantle PT-conditions $FeSiO_3$ is not stable as intermediate component in the binary FeO–SiO_2 boundary join and has to decompose with formation of the oxides FeO and SiO_2 (Irifune and Tsuchiya 2007). For the lower mantle PT-conditions, it is symptomatic that experimental data show the phase field sequence of Brd +FPer, Brd + FPer/MWus + Sti, Sti + MWus in increasing of FeO content in the system composition. Earlier experimental data on the binary MgO–SiO_2 join with intermediate Brd as $MgSiO_3$ (Liebske and Frost 2012) have disclosed invariant eutectic points e_1: MgO + $MgSiO_3$ + L_1 (ultrabasic liquid) and, as very probable, e_2: $MgSiO_3$ + SiO_2 + L_2 (basic liquid) at lower-mantle pressures of 26–34 GPa. The melting phase diagram signals about existence of the maximal $MgSiO_3$ incongruent melting temperature that is an insuperable thermal barrier for evolution of the L_1 ultrabasic primary melts from the e_1 to e_2 to reach the conditions of stishovite SiO_2 formation in the e_2 eutectics. In this situation the thermal barrier makes formation of the "stishovite paradox" association MgO + SiO_2 ($\pm MgSiO_3$) over the MgO–SiO_2 join impracticable.

The oxides MgO, FeO and SiO_2 were used for preparation of starting boundary compositions in case of investigation of melting phase relations of the lower-mantle MgO–FeO–SiO_2 system for its polythermal section $(MgO)_{70}(FeO)_{30}$–$(SiO_2)_{70}(FeO)_{30}$ that is shown by arrows on the Fig. 5.1. Phase relations over the polythermal section $(MgO)_{70}(FeO)_{30}$–$(SiO_2)_{70}(FeO)_{30}$ at 24 GPa (Figs. 5.2 and 5.3) reveal a presence of ferropericlase Per as (Mg, Fe)O, magnesiowustite MWus as (Fe, Mg)O continuous solid solutions Per•Wus, i.e. $(MgO•FeO)_{ss}$, stishovite Sti (SiO_2) and limited solid solutions (Mg, Fe)-bridgmanite as $(MgSiO_3•FeSiO_3)_{ss}$ where $FeSiO_3$ is likely to be involved as a stabilized solid-solution component.

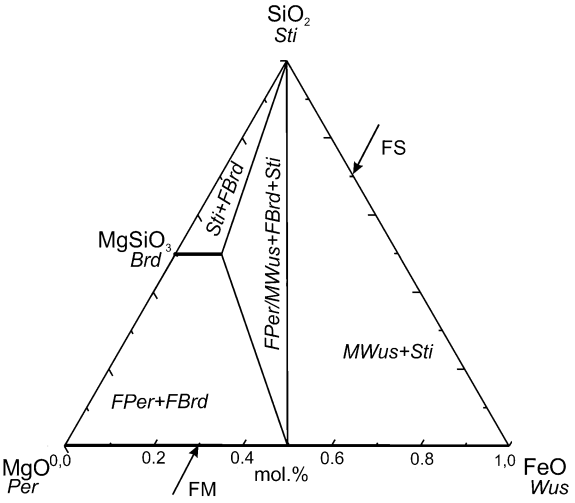

Fig. 5.1 Subsolidus associations of the system MgO–FeO–SiO_2 at 24 GPa (on basis of relevant experimental data). Symbols: *Per* periclase MgO, *FPer* ferropericlase (Mg, Fe)O, *Sti* stishovite SiO_2, *Brd* bridgmanite $MgSiO_3$, *FBrd* ferrobridgmanite (Mg, Fe) SiO_3, *Wus* wustite FeO, *MWus* magnesiowustite (Fe, Mg)Wus. FM–FS–position of the binary polythermal section $(MgO)_{70}(FeO)_{30}$–$(SiO_2)_{70}(FeO)_{30}$

Subsolidus phase relations testify that the most important assemblages are revealed by the section under study. The FPer + FBrd phase field is a representative model of the primary lower-mantle material. With increase in FeO content, the paradoxical oxide assemblage is initially displayed in the association FBrd + FPer/MWus + Sti (with participation of Mg–Fe-bridgmanite) and then by the Mws + Sti association (without bridgmanite). The sequence of subsolidus phase fields is comparable with the experimental results on the joins Mg_2SiO_4–Fe_2SiO_4 (Akaogi 2007) and $MgSiO_3$–$FeSiO_3$ (Irifune and Tsuchiya 2007) for the lower mantle conditions. However, the subsolidus phase relations are beyond the capabilities to determine a physico-chemical mechanism of formation of the paradoxial assemblage of stishovite and magnesiowustite at the partially molten lower-mantle material.

The melting phase diagram on the polythermal section $(MgO)_{70}(FeO)_{30}$–$(SiO_2)_{70}$ $(FeO)_{30}$ (Fig. 5.2) is pseudo-binary and demonstrates that liquidus phases are presented by ferropericlase FPer, bridgmanite (Mg, Fe)SiO_3, MWus and stishovite SiO_2. At temperature lowering, the crystallization of liquidus phases may take place over the divariant liquidus fields at the ternary system MgO–FeO–SiO_2, respectively, L + FPer, L + FBrd and L + Sti. It is well known that a shifting way of any figurative point of melt composition over the ternary-system liquidus surface is attended with composition change at temperature lowering. It should be realized here, that the figurative point way is projected onto the plane of the polythermal section as a displacement downwards along the temperature ordinate. In this case it may be only known the liquid composition for any of the liquidus figurative points whereas the compositions of other phases are not determinable from the polythermal section because their figurative composition points lie exterior to its plane. The problem may be only solved with the use of the instrumental analysis. Nevertheless, the method of polythermal sections over the Earth's mineral systems is indispensable in experimental evaluating and determinations of the physico-chemical mechanisms of natural multicomponent multiphase reactions.

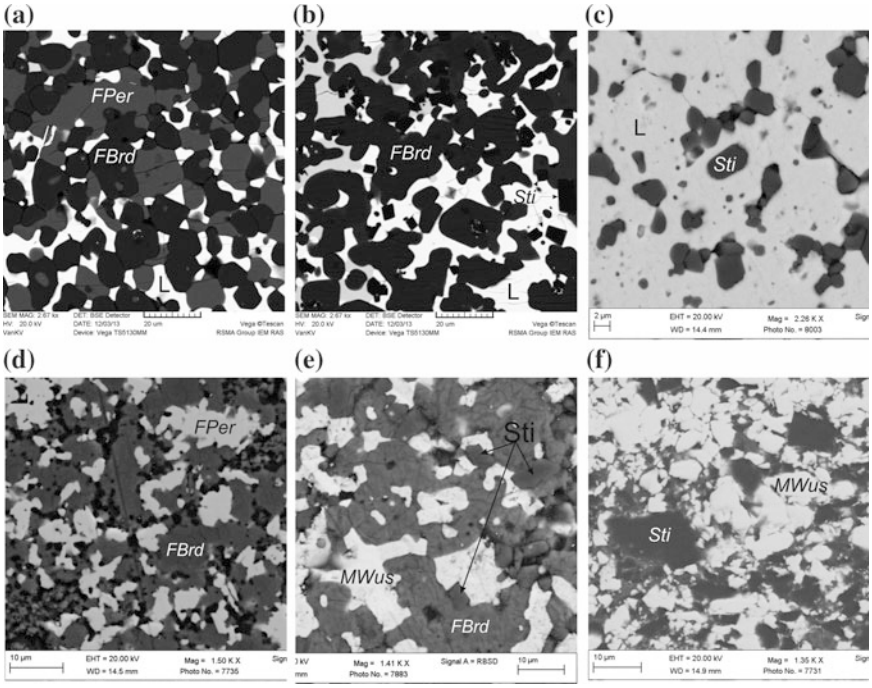

Fig. 5.2 Scanning electron micrographs (SEM) images of the quenched samples resulted from experimental study of melting phase relations on the polythermal section $(MgO)_{70}(FeO)_{30}$–$(SiO_2)_{70}(FeO)_{30}$ at 24 GPa: the samples S5858a (**a**), S5858b (**b**), H3834a (**c**), H3845c (**d**), H3845b (**e**), H3940-1b (**f**)

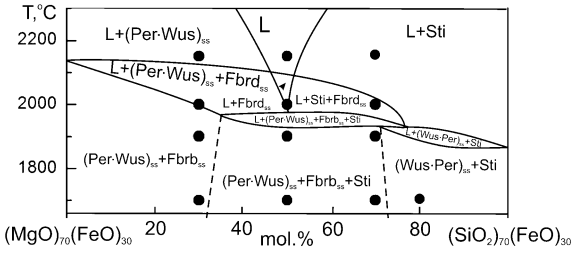

Fig. 5.3 Melting phase diagram for the polythermal section $(MgO)_{70}(FeO)_{30}$–$(SiO_2)_{70}(FeO)_{30}$ of the system MgO–FeO–SiO_2 at 24 GPa

Because of this, it is evident from the melting phase diagram of the polythermal pseudo-binary section $(MgO)_{70}(FeO)_{30}$–$(SiO_2)_{70}$ $(FeO)_{30}$ that figurative point of liquidus melts, shifting down along the L + FPer, L + FBrd and L + Sti divariant fields, may reach, respectively, the univarianf curves L + FPer + FBrd and L + Sti + Brd and then the quasi-invariant point L + FPer/MWus + FBrd + Sti (which is also directly achieved from the contact point with the divariant field L + Fbrd). It should be also realized that the quasi-invariant peritectic equilibrium L + FPer/MWus + FBrd + Sti, although pictured as a two-measured field, in essence is univariant because it is formed in the studied polytermal section by a

projection of short segment of the proper univariant curve in the composition volume for the multicomponent system. This is in agreement with the Rhines phase rule (Rhines 1956; Palatnik and Landau 1964). The term "quasi-invariant point" offers mentally to convert the two-measured field of interest into a line that is more habitual image for solidus phase relations in binary diagrams.

The peritectic reaction of bridgmanite FBrd and melt L with formation of paradoxical association of periclase-wustite solid solutions FPer/MWus and stishovite is responsible for the quasi-invariant point and final disappearance of bridgmanite and change to existence of the univariant association L + MWus + Sti. Now it becomes evident that the bridgmanite peritectic reaction with melt causes the "stishovite paradox" association of the lower-mantle Mg, Fe and Si oxides.

Thus, by experimental study of ternary MgO–FeO–SiO_2 join at 24 GPa it was found (Litvin et al. 2016) that melting relations are characterized by quasi-invariant peritectic point (Mg, Fe)SiO_3 + L (melt) = (Mg, Fe)O + SiO_2. In these conditions (Mg, Fe)-bridgmanite reacts with melt and disappears realizing the effect of stishovite paradox (Mg, Fe)O + SiO_2. It appears that the peritectic mechanism of origin of "stishovite paradox" retains its validity for the MgO–FeO–SiO_2–$CaSiO_3$ system which is representative for all the principal lower-mantle minerals including Ca-perovskite CaPrv as $CaSiO_3$. Melting relations of the system are based on available experimental data and schematically displayed by phase diagram (Fig. 5.4). On comparison with the Fig. 5.3 it is seen that ternary MgO–SiO_2–FeO system determines the mineralogy of subsolidus phase volumes of the MgO–FeO–SiO_2–$CaSiO_3$ composition diagram (with added CaPrv to each assemblage). Melting relations are marked by boundary eutectic points e_1 (L + Per + Brd + CaPrv), e_2 (L + Sti + Brd + CaPrv), e_3 (L + Sti + CaPrv + Wus) and boundary peritectic point p (Brd + L=Mws + Sti) as well as the chief peritectics P (Brd + CaPrv + L=Mws + Sti + CaPrv). The basic peritectic reaction of decisive importance in origin of stishovite paradox has retained.

The chief composition Per-Sti-Wus-CaPrv tetrahedron (Fig. 5.4) is divided to the inner tetrahedrons according to triangulation of the boundary Per-Sti-Wus composition triangle (Fig. 5.1). The inner tetrahedrons of important values for ultrabasic-basic magmatic evolution of the lower-mantle matter are marked as 1 for Per-Brd-(Per•Wus)ss-CaPrv), 2 for (Per•Wus)ss-Brd-Sti-CaPrv, and 3 for (Per•Wus)ss-Sti-Wus-CaPrv. One can envision that primary melting of the primitive lower-mantle material Per-Brd-(Per•Wus)ss-CaPrv begins in the eutectics e_1. With temperature lowering a figurative point of melt composition moves along the cotectic line L + (Per•Wus)ss + Brd + CaPrv and reaches the chief peritectics P Brd + CaPrv + L = Mws + Sti + CaPrv where "stishovite paradox" is realized and (Mg, Fe)–bridgmanite phase disappeared. Then the way is open over the cotectic line L + Sti + (Per•Wus)ss + CaPrv to the boundary e_3 eutectics.

So the bridgmanite-melt peritectic reaction acts also in the system MgO–FeO–SiO_2–$CaSiO_3$ (Fig. 5.4) providing the physico-chemical means for ultrabasic-basic magmatic evolution over the ultrabasic cotectic curve L + FPer + FBrd + CaPrv, peritectic point L + FPer/MWus + FBrd + Sti + CaPrv + L and basic cotectic curve L + MWus + Sti + CaPrv + L. The participation of melt in the peritectic

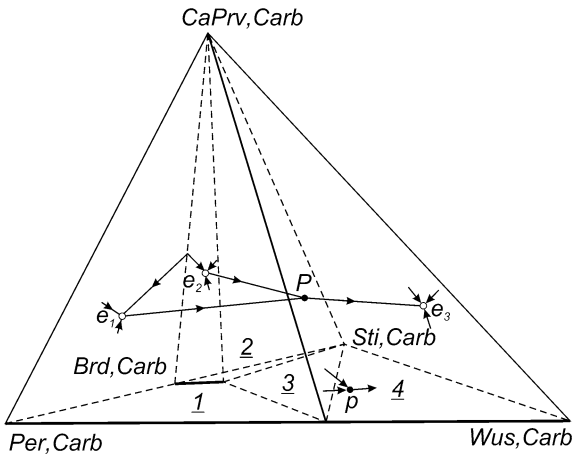

Fig. 5.4 Melting phase diagram of the lower-mantle system MgO–FeO–SiO_2–$CaSiO_3$ in a model approximation (constructed with the use of relevant experimental and physico-chemical data). In the boundary ternary system Per–Sti–Wus the fields of subsolidus associations FPer + FBrd, Sti + FBrd, FPer/MWus + FBrd + Sti and MWus + Sti are reproduced from the Fig. 5.1 as well as the position of peritectic point *p* [FBrd + L = FPer/MWus + Sti] is shown by symbol. The boundary ternary diagram of Per–Sti–Wus join provides a basis for triangulation subdividing of the composition tetrahedron MgO–FeO–SiO_2–$CaSiO_3$ into simplexes: (*1*) FPer + FBrd + CaPrv, (*2*) Sti + FBrd + CaPrv, (*3*) FPer/MWus + FBrd + Sti + CaPrv and (*4*) MWus + Sti + CaPrv. Major liquidus elements of the system MgO–FeO–SiO_2–$CaSiO_3$ are presented by *lines* with *arrows*. Invariant ultrabasic e_1 [L + Per + Brd + CaPrv] and basic e_2 [L + Sti + Brd + CaPrv] eutectic points belong to the ternary boundary system Per–Sti–CaPrv; the eutectic points e_1 and e_2 are separated by the thermal barrier which is conditioned by the temperature of bridgmanite congruent melting In the tetrahedron volume the univariant cotectic curves L + FPer + FBrd + CaPrv (**a**) and L + Sti + FBrd + CaPrv (**b**) are directed consequently from eutectic points e_1 and e_2 which connected in the invariant peritectic point *P* [FBrd +L + (CaPrv) = FPer/MWus + Sti + (CaPrv)]. Bridgmanite FBrd is lost in the peritectic reaction, and the closing phase composition evolution is under control of the univarint cotectic curve L + MWus + Sti + CaPrv (**c**) terminating in the eutectic point e_3 of the boundary ternary join Sti–Wus–CaPrv

reaction makes possible the in situ ultrabasic-basic magmatic evolution of the primary lower-mantle ultrabasic ferropericlase-bridgmanite-bearing rocks into the basic ferropericlase/magnesiowustite-stishovite-bearing assemblages. It may be concluded that the peritectic reaction of bridgmanite is responsible for the ultrabasic-basic magmatic evolution of the lower-mantle primitive rocks.

5.3 Parental Melts and Genetic Mechanisms for Lower-Mantle Diamonds and Inclusions

As is evident from the results of high-pressure experiments, the bridgmanite-melt peritectic reaction of "stishovite paradox" presents an inherent physico-chemical characterization of the native lower-mantle oxide-silicate magmatism. Experimental

physico-chemical data revealed the effect responsible for origin of the "forbidden" assemblage SiO_2 + $(MgO{\bullet}FeO)_{ss}$ with stishovite polymorph due to peritectic reaction of bridgmanite and lower-mantle ultrabasic magma.

The testing experiments at pressure of 26 GPa on crystallization of diamonds in the melts of lower-mantle diamond-parental oxide-silicate-carbonatite-carbon systems suggests that the bridgmanite-melt reaction is reproduced at the processes of common formation of diamonds and associated phases (Litvin et al. 2016b). In agreement with data on carbonate inclusions in lower-mantle diamonds, the chemicals of Mg, Fe, Ca, Na carbonates were stirred together to the multicomponent carbonate mixture of $MgCO_3$—26, $FeCO_3$—26, $CaCO_3$—25, Na_2CO_3—23 (wt%) to model changeable compositions similar to the lower-mantle diamond parental media. The mixtures $[(MgO)_x(FeO)_y(SiO_2)_z]_{30}[(Mg–Fe–Ca–Na–carbonate)]_{70}]_{60}graphite_{40}$ were used for diamond crystallization (where x-y-z were 49-30-21 for data of Fig. 5.5a, 35-35-30 of Fig. 5.5b and 21-30-49 of Fig. 5.5c. The paragenetical formation of super-deep diamonds jointly with ultrabasic mineral association of ferropericlase (Mg, Fe)O + bridgmanite (Mg, Fe)SiO_3 (Fig. 5.5a) as well as with basic mineral associations of stishovite SiO_2 + periclase/wustite $(MgO{\bullet}FeO)_{ss}$ + bridgmanite (Mg, Fe)SiO_3 (Fig. 5.5b) and stishovite SiO_2 + magnesiowustite (Fe, Mg)O (Fig. 5.5c). The testing experiments demonstrate that bridgmanite-melt peritectic reaction is also important for joint in situ genesis of the lower-mantle diamonds and primary ultrabasic and basic inclusions. By this it is shown that the physico-chemical mechanism of stishovite paradox is also run in the lower-mantle diamond-producing systems. This gives an insight into a formation of the paradoxical association of the Mg, Fe and Si oxides which exists among the primary inclusions in the lower-mantle diamonds. This shows that super-deep diamonds, similarly to periclase-wustite phases and stishovite, are also the in situ lower-mantle minerals. The results are compatible with the mantle-carbonatite concept of diamond genesis (Litvin et al. 2014, 2016) and reveal the

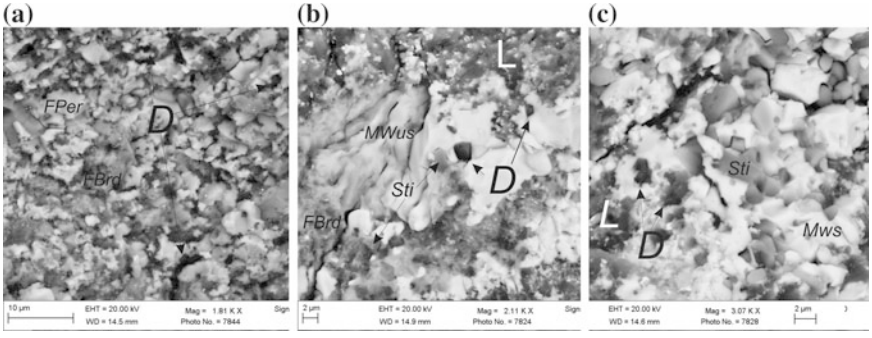

Fig. 5.5 Scanning electron micrographs (SEM) images of the quenched samples resulted from experimental study of paragenetic crystallization of ultra-deep diamonds and associated ultrabasic and basic minerals in melts-solutions of the system $[(MgO)_x(FeO)_y(SiO_2)_z]_{18}Carb_{42}graphite_{40}$ with a variation of the indexes x, y, z as **a** $[(MgO)_{49}(FeO)_{30}(SiO_2)_{21}$, **b** $[(MgO)_{35}(FeO)_{35}(SiO_2)_{30}$, **c** $[(MgO)_{21}(FeO)_{30}(SiO_2)_{49}$. Symbols: *L* carbon-oversaturated melt-solution, *D* diamond, *FPer* ferropericlase, *FBrd* (Mg, Fe)-bridgmanite, *MWus* magnesiowustite, *Sti* stishovite

physicochemical mechanism for ultrabasic-basic fractional evolution of lower-mantle magmas and diamond–parental melts.

In conclusion it may be said that new evidence from high-pressure experiments combined with mineralogy of primary inclusions in super-deep diamonds are in good agreement. They testify the in situ lower-mantle origin of "super-deep" diamonds and stishovite that is contradictory to the subduction version.

5.4 Some Remarks on Genetic Classification of Syngenetic Inclusions in Lower-Mantle Diamonds

The main features of genetic classifications of syngenetic inclusions in the transition-zone- and lower-mantle diamonds can be developed on the basis of the mantle-carbonatite concept for ultra-deep diamonds genesis (Litvin et al. 2016b, c). A correlation between the scenarios of the natural diamonds origin for the conditions of the upper mantle, transition zone and lower mantle leads to the conclusion that a physico-chemically uniform "melt-solution" mechanism of diamond formation is operative within the Earth's mantle depths of at least 150–800 km. Therefore all the mineral phases included in the mantle diamonds can be placed into the categories of (1) paragenetic major phases of genetic links with components of a determining contribution into the compositions of diamond-parental silicate-oxide-carbonatite-carbon melts and, consequently, to formation of paragenetic typomorphic minerals; (2) paragenetic minor or secondary phases, soluble in the diamond-parental melts, of genetic links with components responsible for formation of accessory solid and C–O–H-volatile phases; the metastable graphite phase can be placed here due to its genetic links with elementary carbon dissolved in the parental melts; (3) xenogenetic minor phases, solid and liquid, insoluble in the diamond-parental melts and completely immiscible with them, without physico-chemical genetic links with component of diamond-parental melts because are not formed in the growth melt.

The genetic classification of minerals, melts, and volatile phases and components entrapped as primary inclusions by growing diamonds is based on the mantle-carbonatite theory of the origin of natural diamonds (Litvin 2009). This classification provides insights into the origin of inclusions and reveals their physicochemical links to the major components of silicate-oxide-carbonatite-carbon growth melts, as well as soluble and insoluble components and phases contained therein.

References

Akaogi M (2007) Phase transitions of minerals in the transition zone and upper part of the lower mantle. In: Ohtani E (ed) Advances in high-pressure mineralogy. Geological Society of America Special Paper 421, pp 1–13. doi:10.1130/2007.2421(01)

Harte B (2010) Diamond formation in the deep mantle: the record of mineral inclusions and their distribution in relation to mantle dehydration zones. Miner Mag 74(2):180–215
Harte B, Harris JW (1994) Lower mantle mineral associations preserved in diamonds. Miner Mag 58A:384–385
Hayman PC, Kopylova MG, Kaminsky FV (2005) Lower mantle diamonds from Rio Soriso (Juina, Brazil). Contrib Miner Petrol 149(4):430–447
Irifune T, Tsuchiya T (2007) Mineralogy of the Earth—phase transitions and mineralogy of the Lower Mantle. In: Tretise on geophysics. Elsevier B.V., Chap. 2.03, pp 33–62
Kaminsky F (2012) Mineralogy of lower mantle: a review of "super-deep" mineral inclusions in diamond. Earth Sci Rev 110:127–147
Libske C, Frost DJ (2012) Melting phase relations in the MgO–$MgSiO_3$ system between 16 and 26 GPa: implication for melting in Earth's deep interior. Earth Planet Sci Lett 345:159–170
Litvin YA (2009) The physicochemical conditions of diamond formation in the mantle matter: experimental studies. Russ Geol Geoph 50(12):1188–1200
Litvin YA (2012) Ultrabasic-basic evolution of upper mantle magmas: petrogenetic links between diamond-bearing peridotites and eclogites (on evidence of physico-chemical experiment). Geoph Res Abstr 14, European Geosciences Union General Assembly (EGU2012-3610-1), Vienna, Austria
Litvin YA (2014) The stishovite paradox in genesis of ultradeep diamonds. Dokl Earth Sci 455(1):274–278. doi:10.1134/S1028334X14030064
Litvin YA, Spivak A, Solopova N, Dubrovinsky L (2014) On origin of lower-mantle diamonds and their primary inclusions. Phys Earth Planet Inter 228:176–185. doi:10.1016/j/pepi/2013.12.007
Litvin YA, Spivak AV, Kuzyura AV (2016a) Fundamentals of the mantle-carbonatite concept of diamond genesis. Geochem Internat 54(10):839–857. doi:10.1134/S0016702716100086
Litvin YA, Spivak AV, Dubrovinsky LS (2016b) Magmatic evolution of the Material of the Earth's lower mantle: stishovite paradox and origin of superdeep diamonds (experiments at 24–26 GPa). Geochem Internat 54(11):936–947. doi:10.1134/S0016702916090032
Litvin YA, Spivak AV, Simonova DA, Dubrovinsky LS (2016c) On origin and evolution of diamond-forming lower-mantle systems: physicochemical studies in experiments at 24 and 26 GPa. In: J Phys: Conference Series (JPCS)—IOP Conference Series (accepted)
Mathias M, Siebert JC, Rickwood PC (1970) Some aspects of the mineralogy and petrology of ultramafic xenoliths in kimberlite. Contrib Miner Petrol 26:75–123
Palatnik LS, Landau AI (1964) Phase equilibria jn multicomponent systems. Holt, Rinehart and Winston Inc., New York, p 454
Rhines FN (1956) Phase diagrams in metallurgy: their development and application. McGraw-Hill Book Company, Inc., New York/Toronto/London, 348 p
Ringwood AE (1975) Composition and petrology of the Earth's mantle. McGraw-Hill, New York, 618 p
Stachel T, Brey GP, Harris JW (2000a) Kankan diamonds (Guinea) I: from the lithosphere down to the transition zone. Contrib Miner Petrol 140:1–15
Stachel T, Brey GP, Harris JW, Joswig W (2000b) Kankan diamonds (Guinea) II: lower mantle inclusion parageneses. Contrib Miner Petrol 140:16–27
Stachel T, Brey G, Harris JW (2005) Inclusions in sublithospheric diamonds: glimpses of deep Earth. Elements 1(2):73–78

Chapter 6
Ultrabasic-Basic Fractionating of Mantle Magmas and Diamond-Parental Melts

Physico-chemical conditions for ultrabasic-basic evolution of the mantle magmas and diamond-producing melts of the upper mantle are created due to two sequential peritectic interaction: (1) the clinopyroxene-formed reaction of orthopyroxene and ultrabasic melt (orthopyroxene loss) and (2) the garnet-formed reaction of olivine with jadeite component of fractionating ultrabasic melt (olivine loss). Therewith the formation of diamonds and associated minerals as ultrabasic so basic parageneses becomes physico-chemically possible under regime of fractional crystallization of the diamond-producing melts. Origin of diamond-bearing peridotites and eclogites among xenoliths in kimberlites is also performed by the scenario. The physico-chemical possibility of ultrabasic-basic evolution of the lower-mantle magmas and diamond-producing melts is provided by virtue of the peritectic bridgmatite-melt reaction (effect of stishovite paradox). As a consequence the physico-chemical conditions for syngenesis of lower-mantle diamonds and associated phases as ultrabasic so basic parageneses are created. Fractionary evolution of diamond-producing melts and syngenesis of diamonds and associated ultrabasic and basic phases at the transition zone depths has still not been examined in physico-chemical experiments.

6.1 Peritectic Reactions of Orthopyroxene and Olivine in Upper-Mantle Magma Evolution

Physico-chemical potentials for petrogenesis of eclogites as the derivative rocks of primitive upper-mantle garnet lherzolite can be unraveled in the answer a question formulated earlier (Yoder 1976): what is wanted in order for the crystallization of partial melts of garnet lherzolite may be accompanied by disappearance of the two major phases—olivine and orthopyroxene with succeeding formation of garnet and clinopyroxene (i.e. eclogite)?

Y.A. Litvin, *Genesis of Diamonds and Associated Phases*,
Springer Mineralogy, DOI 10.1007/978-3-319-54543-1_6

Physico-chemical experimental study of the upper-mantle peridotite-pyroxenite system olivine (Ol)—orthopyroxene (Opx)—clinopyroxene (Cpx)—garnet (Grt) has been carried out at 4 GPa (Litvin 1991). The compositions of the boundary phases were used as following (wt%): olivine—SiO_2 40.02, FeO 14.35, MgO 45.63; orthopyroxene—SiO_2 57.80, Al_2O_3 0.49, FeO 7.26, MgO 33.34, CaO 0.81, Na_2O 0.30; clinopyroxene SiO_2 55.92, Al_2O_3 4.28, FeO 4.68, MgO 16.88, CaO 15.66, Na_2O 2.60; garnet SiO_2 42.55, Al_2O_3 24.07, FeO 8.48, MgO 20.93, CaO 3.97. By their major components the experimental compositions correspond to these of the natural minerals of the upper-mantle non-depleted rocks from xenoliths in kimberlites (Boyd and Danchin 1980).

Melting phase relations for the upper-mantle system Ol–Opx–Cpx–Grt were investigated over the representative polythermal sections (wt%): $Ol_9Opx_{51}Grt_{40}$–$Ol_9Cpx_{51}Grt_{40}$; $Ol_{15}Cpx_{45}Grt_{40}$–$Opx_{45}Cpx_{15}Grt_{40}$; $Ol_{43.5}Opx_{16.5}Grt_{40}$–$Opx_{43.5}Cpx_{16.5}Grt_{40}$; $Ol_{43.5}$Opx16.5Grt40–Cpx43.5Opx16.5Grt40 and Ol54Opx6Grt40–Cpx54Opx6Grt40. It was established that Opx disappears at the peritectic Opx-L reaction with formation of Cpx, the peritectic melt composition was determined as $Ol_{15.6}Opx_{10.7}Cpx_{47.7}Grt_{26}$ (wt%) that corresponds to the ultrabasic komatiitic composition SiO_2 50.2, Al_2O_3 8.3, FeO 7.5, MgO 24.1, CaO 8.6, Na_2O 1.3. The composition from the quasi-invariant point L + Ol + Opx + Cpx + Grt is transferred onto the univariant curve L + Ol + Cpx + Grt. The peritectic reaction characterizes primary melting of mineral assembly on the pseudo-binary join diopside (Di)–pyrope (Py) of the Opx–Di–Py system at 3 GPa (O'Hara 1963) and 4 GPa (Davis 1964; Davis and Shairer 1964) and retains its validity as the key element of melting relations for the upper-mantle system Ol–Opx–Cpx–Grt studied in (Litvin 1991). The liquidus peritectic surface of the system Ol–Opx–Cpx–Grt is projected onto its inner ternary section $Ol_{60}Grt_{40}$–$Opx_{60}Grt_{40}$–$Cpx_{60}Grt_{40}$ (Fig. 6.1) that gives a visual observation of the divariant liquidus fields L + Ol, Opx + L, Grt + L (the L + Cpx field is not fetched up into the projection). There also are presented the univariant cotectic curves L + Ol + Opx + Grt and L + Opx + Cpx + Grt which together with the non-fethed L + Ol + Opx + Cpx curve are directed with temperature lowering towards the quasi-invariant peritectic point *P* (L + Ol + Opx + Cpx + Grt) whereas the L + Ol + Cpx + Grt curve is originated in the point *P*.

In the subsequent experimental research it has revealed that olivine can react with jadeite to form pyrope, orthopyroxene and alkaline low-melting component $Na_2Mg_2Si_2O_7$ (Gasparik and Litvin 1997). By experimental study of the model system Fo–Jd–Di at 7 GPa it has been established (Butvina and Litvin 2009) that forsterite disappears at its liquidus surface in the 4-phase peritectics *P* (L + Fo + (Na, Ca)Cpx + Prp) when jadeite content in the system is about 4–6 wt%. As the result, the invariant peritectic assemblage has transformed into the univariant cotectics L + (Na, Ca)Cpx/Omph + Grt. Melting phase relations on the boundary ternary joins of the developed quadruple system Fo–Jd–Di–Prp at 7 GPa (Fig. 6.2) on the Fo–Jd–Di join show the quasi-invariant 4-phase peritectic point P (L + Fo + (Na, Ca)Cpx + Prp) together with two univariant 3-phase curves two of which (L + Fo + (Na, Ca)Cpx and (L + Fo + Prp) are directing to the peritectic

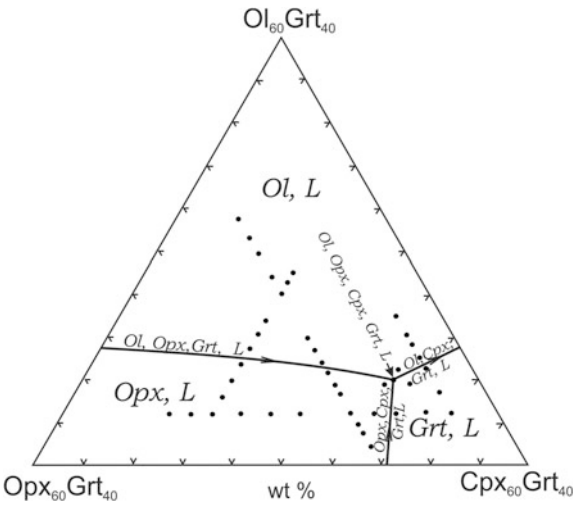

Fig. 6.1 Projection of liquidus elements of the upper mantle Ol–Opx–Cpx–Grt peridotite-pyroxenite system onto the plane of the inner ternary section $Ol_{60}Grt_{40}$–$Opx_{60}Grt_{40}$–$Cpx_{60}Grt_{40}$. The quasi-invariant 5-phase peritectic point *P* (L + Ol + Opx + Cpx + Grt) is evident together with three univariant 4-phase curves two of which (L + Ol + Opx + Grt) and (L + Opx + Cpx + Grt) are directing to the peritectic point *P* and one (L + Ol + Cpx + Grt) is emerging from the peritectics *P* with temperature lowering. Fourth univariant curve (L + Ol + Cpx + Cpx) is directing to the peritectics *P* but lies back of it and escapes crossing with the ternary section plane. Conventional designations: *thick lines* with *arrows*—univariant curves over the liquidus surface intersecting by the ternary section; *black dots*—highest-temperature experimental points

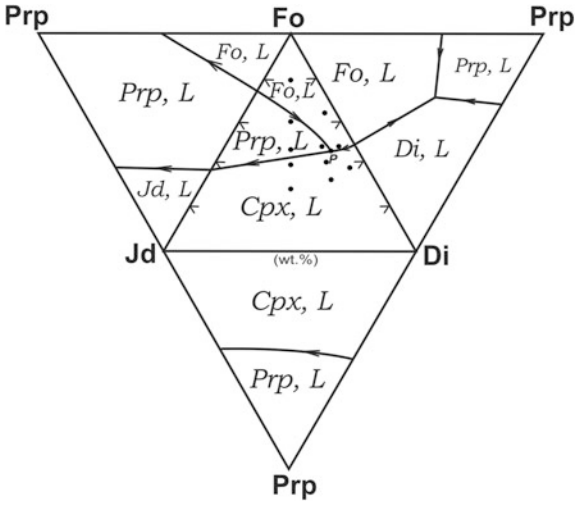

Fig. 6.2 Melting phase relations on the boundary ternary joins of the developed quadruple system Fo–Jd–Di–Prp at 7 GPa. Symbols: *P*—quasi-invariant 4-phase peritectic point L + Fo + (Na, Ca)Cpx + Prp, *lines* with *arrows*—liquidus invariant curves, *Fo* forsterite, *Di* diopside, *Cpx* clinopyroxene (Na, Ca)-Cpx/Omph, *Jd* jadeite, *Prp* pyrope, *black dots*—highest-temperature experimental points

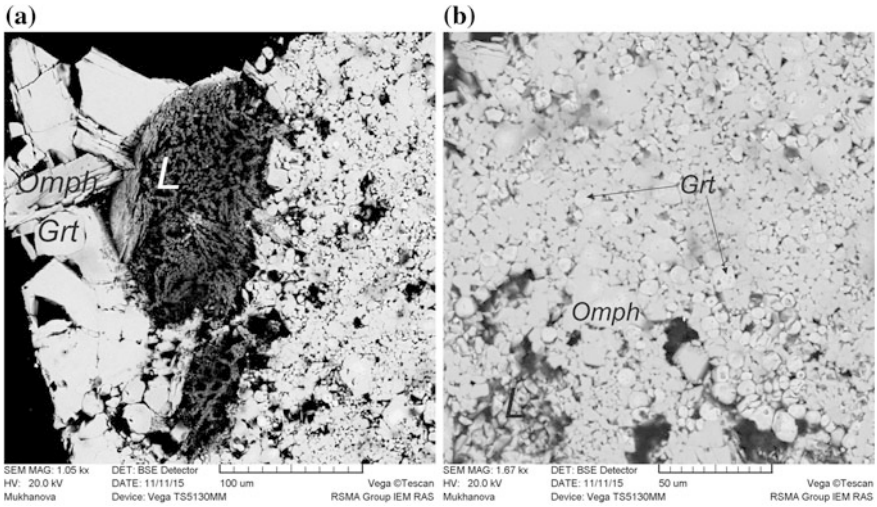

Fig. 6.3 Experimental garnetization of olivine in tiny-grained samples (**a**) and (**b**) of the system Ol–Cpx–Jd with formation of eclogitic mineral association

point *P*, The cotectic curve (L + (Na, Ca)Cpx/Omph + Prp) is emerging from the peritectics *P* with temperature lowering. The effect of olivine garnetizations has also revealed in the system Ol–Cpx–Jd with realistic boundary compositions (Fig. 6.3).

Thus, it would be expected for the upper-mantle garnet-peridotite system Ol–Opx–Cpx–Grt that the peritectic reactions of orthopyroxene and olivine with melts may be performed with a resulting transformation of the 4-phase association of garnet lherzolite Ol + Opx + Cpx + Grt into the two-phase eclogitic assemblage Omph + Grt under the regime of fractional crystallization.

6.2 Olivine Garnetization and Evolution of Upper-Mantle Diamond-Parental Melts

As a whole the regularities of ultrabasic-basic evolution of the upper-mantle magmas and formation of the peridotite-pyroxenite-eclogite rocks series are controlled by the melting phase relations of the multicomponent multiphase system olivine–clinopyroxene–corundum–coesite (Ol–Cpx–Crn–Coe) with a combined coordinate framework (“composition diagram-complex”) (Fig. 2.2) (Litvin 1991). The diagram-complex of the peridotite-pyroxenite-eclogite system consists of the primary diagrams-simplexes with each simplex containing the sole quasi-invariant 5-phase point of the deciding value. The composition coordinate axis of the inner binary join Cpx—Grt occupies the central position of the diagram-complex and presents oneself as the common element for all the simplexes.

The liquidus diagram for the multicomponent multiphase system Ol–Cpx–Crn–Coe in its projection onto the ternary section (Ol + Cpx)–(Crn + Cpx)–(Coe + Cpx) is presented in the Fig. 6.3 (the univariant cotectic curves are numbered) (Litvin et al. 2016a, b). Among the liquidus elements listed below those of them on the side of the foot system Ol–Crn–Coe have not projected into the liquidus diagram. This is noteworthy that the quasi-invariant 5-phase peritectic point P_1 Ol + Opx + Cpx + Grt + L of the peridotite-pyroxenite simplex Ol–Opx–Cpx–Grt becomes also the principal physico-chemical characteristics of the peridotite-pyroxenite complex Ol–Cpx–Crn–Coe system. It is also becomes evident that the quasi-invariant peritectics P_1 is directly tied with the quasi-invariant 5-phase eutectic point E_1 Ol + Cpx + Grt + Crn + L of the olivine-eclogite simplex due to the univariant cotectic curve Ol + Cpx + Grt + L.

The unitary liquidus of the peridotite-pyroxenite-eclogite system Ol–Cpx–Crn–Coe allows much room for the analyzing the magmatic genesis of minerals and rocks of the upper-mantle garnet-peridotite facies. Liquidus surface of the ultrabasic peridotite system (the simplex A in Fig. 2.2) consists of 5-phase quasi-invariant peritectics L + Ol + Opx + Cpx + Grt (P_1), invariant cotectics L + Ol + Opx + Cpx (1); L + Ol + Opx + Grt; L + Opx + Cpx + Grt (2); L + Ol + Cpx + Grt (3); divariant fields L + Ol + Opx; L + Ol + Cpx; L + Ol + Grt; L + Opx + Cpx; L + Opx + Grt; L + Cpx + Grt; and 3-variant volumes Ol + L; Opx + L; Cpx + L; Grt + L. Within the liquidus of the second ultrabasic Ol-Crn-eclogitic system (the simplex B) has combined 5-phase eutectics L + Ol + Cpx + Grt + Crn (E_1), univariant cotectics L + Ol + Cpx + Grt (4); L + Ol + Cpx + Crn (5); L + Ol + Grt + Crn; L + Crn + Cpx + Grt (6); divariant fields L + Ol + Cpx; L + Ol + Grt; L + Ol + Crn; L + Crn + Cpx; L + Crn + Grt; L + Cpx + Grt; and 3-variant volumes Ol + L; Crn + L; Cpx + L; Grt + L.

Among the basic eclogite systems are (*I*) Crn–Ky-eclogitic Crn–Omph–Grt–Ky (the simplex C) with 5-phase eutectics L + Crn + Omph + Grt + Ky (E_2); univariant cotectics L + Crn + Omph + Grt (7); L + Crn + Omph + Ky (8); L + Crn + Grt + Ky; L + Ky + Omph + Grt (9); divariant fields L + Crn + Omph; L + Crn + Grt; L + Ky + Omph; L + Ky + Grt; L + Crn + Ky; L + Omph + Grt; and 3-variant volumes L + Crn; L + Ky; L + Omph; L + Gr; (*II*) Ky–Coe-eclogitic Ky–Omph–Grt–Coe (the simplex D) with 5-phase eutectics L + Ky + Omph + Grt + Coe (E_3); univariant cotectics L + Ky + Omph + Grt (10); L + Ky + Omph + Coe (11); L + Ky + Grt + Coe; L + Coe + Omph + Grt + L (12); divariant fields L + Ky + Omph; L + Ky + Grt; L + Ky + Coe; L + Coe + Omph; L + Coe + Grt; L + Omph + Grt; and 3-variant volumes L + Ky; L + Coe; L + Omph; L + Grt; (*III*) Coe-Opx-eclogitic Coe–Omph–Grt–Opx (the symplex E) with 5-phase peritectics L + Coe + Omph + Grt + Opx (P_2) (where Opx is disappeared in the reaction Opx + L = Omph), univariant cotectics L + Coe + Omph + Grt, (13); L + Coe + Omph + Opx (14); L + Coe + Grt + Opx; L + Opx + Omph + Grt (15); divariant fields L + Coe + Omph; L + Coe + Grt; L + Coe + Opx; L + Opx + Omph; L + Opx + Grt; L + Omph + Grt; and 3-variant volumes L + Coe; L + Opx; L + Omph; L + Grt.

The physico-chemical mechanisms which could give insight into the petrogenesis of basitic eclogites during the processes of ultrabasic-basic magmatic evolution have been of the main interest here. This can be seen in Fig. 6.1 that the ultrabasic peritectics L + Ol + Opx + Cpx + Grt (P_1) is directly bound with the basitic peritectics L + Coe + Omph + Grt + Opx (P_2) by means of the univariant cotectics L + Opx + Cpx/Omph + Grt that has a temperature maximum positioned in the boundary plane Opx–Cpx–Grt. This maximum is defined as "eclogitic thermal barrier" (O'Hara 1968) and actually represents an insuperable obstacle for the ultrabasic-basic magmatic evolution under conditions of as equilibrium so fractional crystallization. However the reaction of "olivine garnetization" at the liquidus peritectic reactions between olivine and jadeite components has been the new physico-chemical mechanism which makes it possible to provide a formation of SiO_2-saturated eclogitic rocks as the products of ultrabasic-basic evolution of the magmas generated on melting the primitive Ol-saturated upper-mantle peridotites (Fig. 6.4).

Schematic diagram in Fig. 6.5 serves to illustrate that a topological connection between the ultrabasic compositions and liquidus elements of the peridotitic simplex (Ol + Opx)–(Ol + Cpx)–(Ol + Grt), on the one hand, and three basic SiO_2-saturated simplexes (Omph + Grt)–(Omph + Crn)–(Omph + Ky); (Omph + Grt)–(Omph + Ky)–(Omph + Coe), and (Omph + Grt)–(Omph + Coe)–(Omph + Crn) is realized through the common apex (Cpx + Grt) and immediately adjacent divariant fields (L + Omph + Grt). The schematic diagram of the Ol–Cpx–Jd system responsible for peritectics P_3 is inserted in the Fig. 6.5. The initial ultrabasic melts are disposed at the field (L + Ol + Opx) of peridotitic system. The reason is that compositions of primitive garnet lherzolites (pyrolites) have been estimated (wt %) as $Ol_{57}Opx_{17}Cpx_{12}Grt_{14}$ (Ringwood 1962) and $Ol_{60.3}Opx_{20.2}Cpx_{10.2}Grt_{3.3}$ (Carter 1970) where olivine and orthopyroxene prevail in respect to clinopyroxene

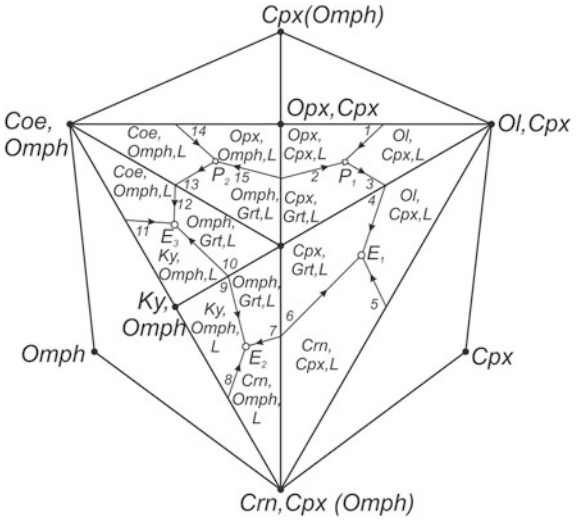

Fig. 6.4 Complex liquidus phase relations for the upper-mantle peridotite-pyroxenite-eclogite system Ol–Cpx–Coe–Crn as a projection onto the inner ternary section (Ol + Cpx)–(Crn + Cpx)–(Coe + Cpx), Symbols: P_1 and P_2—peritectic points, E_1, E_2, E_3 and E_4—eutectic points. See text for more details

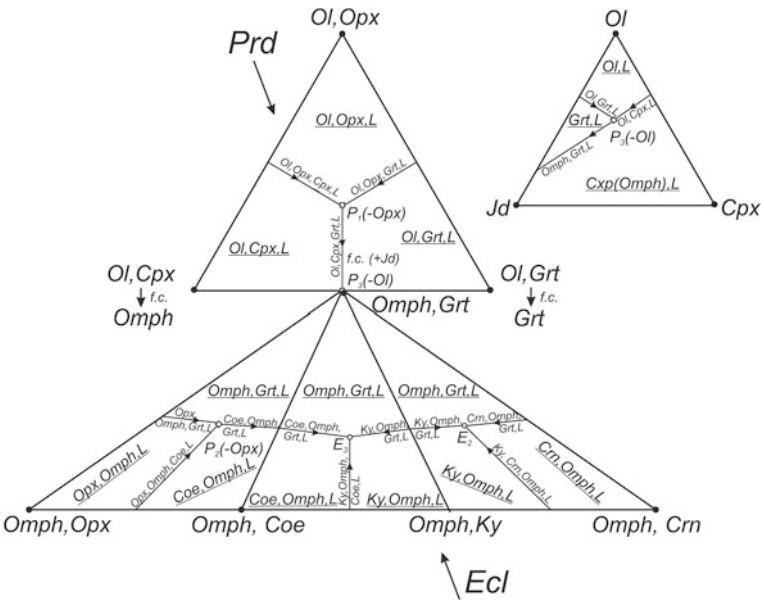

Fig. 6.5 Topological interrelation of ultrabasic and basic systems with peridotitic Ol-saturated compositions in the section (Ol + Opx)–(Ol + Cpx)–(Ol + Grt) and eclogitic SiO_2-saturated compositions in the section (Omph + Grt)–(Omph + Crn)–(Omph + Opx). The peridotite—eclogite conversion is symbolized by the boundary compositions Ol + Cpx → Omph and Ol + Grt → Grt due to Ol loss in the peritectic point P_3. The *arrows* indicate position of the section Prd (Ol + Opx + Cpx)–Ecl (Ky + Coe + Omph) that is used at the Fig. 6.6

and garnet by their contents. With temperature lowering the fractional crystallization is directing the figurative points of the melts compositions toward the univariant cotectic curvess L + Ol + Opx + Cpx or L + Ol + Opx + Grt. Therewith a choosing between them is determined by the initial chemical composition of peridotite as well as the relative position of figurative point of the composition in respect to the boundary systems (Ol + Opx)–(Ol + Cpx) or (Ol + Opx)–(Ol + Grt) because of the variability of Al_2O_3/SiO_2 ratio. The melt composition point can now transfer along one of the cotectic curves to the invariant peritectics P_1 where a loss of Opx takes place, and thereafter the figurative point moves over the cotectic curve L + Ol + Cpx + Grt.

It should be remarked that jadeite component incomes to the ultrabasic melts from peridotitic Cpx phase. According to experimental observation at 4 GPa (Litvin 1991), the equilibrium composition of the quasi-invariant peritectic point P_1 L + Ol + Opx + Cpx + Grt of primary melting of the primitive garnet lherzolite is essentially enriched by Cpx and has the mineral contents as $Ol_{15.5}Opx_{10}Cpx_{47.7}Grt_{26}$ (wt%) that corresponds to ultrabasic komatiite composition of the complete melt: SiO_2 50.2, Al_2O_3 8.3, FeO 7.5, MgO 24.1, CaO 8.6, Na_2O 1.3 (wt%). After moving over the cotectic curve L + Ol + Cpx + Grt, the melt figurative point

has attained the ternary boundary join Ol–Cpx–Grt at its eutectic point L + Ol + Cpx + Grt (that is a piercing point into the adjacent Ol-eclogite simplex) where the eutectic melt has komatiitic composition $Ol_{16.5}Cpx_{61}Grt_{22.5}$ corresponding to SiO_2 50.24, Al_2O_3 8.0, FeO 7.1, MgO 22.6, CaO 10.4, Na_2O 1.6.

The condition for the regime of fractional crystallization is imperative considering that this provides a way for jadeite component to accumulate in the restite melts owing to intense fractionation of the solid Ol, Cpx and Grt phases to accomplish a complete garnetization of olivine. Under these conditions the contents of jadeite component increase also in clinopyroxenes which can take on compositions of the eclogitic omphacites (Omph) as fractional crystallization is developed. It must not be ruled out that figurative point of the fractionated melt can transfer along the cotectic curve L + Ol + Cpx + Grt into the symplex of ultrabasic Ol–Crn-eclogites and even reach the quasi-invariant eutectics E_1 L + Ol + Cpx/Omph + Grt + Crn. This may be realized if jadeitic component contents in peridotitic Cpx are scarce. At the same time, however, the formation of olivine eclogites in the natural diamond-producing processes is problematic.

Melting phase diagram of the Ol–Cpx–Jd system is similar to that of the simplified system Fo–Jd–Di (Fig. 6.2) that is evident in comparison with the diagram of liquidus surface of the system Ol–Cpx–Jd (Fig. 6.5). The diagrams reveals the physico-chemical mechanism for disappearing of olivine at 4-phase peritectic point P_3 L + Ol + Cpx + Grt. In this case the reaction of olivine with jadeitic component bearing melt may result in formation of garnet. The diagram on Fig. 6.5 demonstrates the "olivine garnetization" at the Ol–Cpx–Jd system that is responsible for disappearing of olivine and arising of the univariant cotectics L + Omph + Grt which provides the formation of bimineral eclogites. This has made possible a movement of the melt figurative points towards the silica-saturated eclogitic melts and mineral parageneses of the complex system Omph, Grt–Crn, Omph–Opx, Omph consisting of three eclogitic simplexes—corundum-kyanitic, kyanite-coesitic and coesite-orthopyroxenic. So, when the peritectic reaction in P_3 is completed with disappearance of olivine, the figurative point of melt is brought into the field L + Omph + Grt of one of three eclogitic systems. A choice among the systems has been "vaguely" determined by the initial chemical and modal composition of the primitive peridotite and, probably, by a variability of Al_2O_3/SiO_2 ratio of its composition. If the melt composition point is later on transferring into the limits of the system Coe–Omph–Grt–Opx over the field L + Omph + Grt, it can arrive into the univariant cotectics L + Opx + Omph + Grt, where orthopyroxene eclogites are formed, or into the quasi-invariant peritectic point L + Coe + Omph + Grt + Opx (P_2), where coesite-orthopyroxene eclogites are originated, or into the invariant cotectics L + Coe + Omph + Grt, responsible for formation of coesite eclogites. The invariant cotectic curve L + Coe + Omph + Grt is continued into the adjacent system Ky–Omph–Grt–Coe where fractional crystallization has to be completed with formation of kyanite-coesite eclogites in the quasi-invariant eutectics L + Ky + Omph + Grt + Coe (E_3). For the basic system Crn–Omph–Grt–Ky the figurative point of melt is primarily transferred over the field L + Omph + Grt into

the cotectic curve L + Ky + Omph + Grt, providing formation of kyanite eclogites, or into the cotectic curve L + Crn + Omph + Grt, where corundum eclogites are formed, or into the quasi-invariant point L + Crn + Omph + Grt + Ky, responsible for origin of corundum-kyanite eclogites.

6.3 Fractionary Syngenesis Diagram for Upper-Mantle Diamonds and Associated Phases

Fractionary experimentally-based syngenesis diagrams make it possible to unravel the physico-chemical mechanisms responsible for the common origin of diamonds and paragenetic ultrabasic and basic phases. It also become appreciated the reasons why the chemical compositions of melts-solutions parental for diamonds and associated phases are so variable. It turns out that peritectic reactions of minerals and melts give effective control over the ultrabasic-basic paragenetic conversions and sequential genesis of corresponding diamond-hosted mineral associations. Figure 6.5 demonstrates that the liquidus surface of the ultrabasic peridotite-pyroxenite system Ol–Opx–Cpx–Grt with the quasi-invariant peritectics P_1 may be presented in projection onto the ternary section (Ol + Opx)–(Ol + Opx)–(Ol + Grt). The peridotitic liquidus diagram can be combined with the projection of common liquidus surface of the three basic eclogitic systems united in the (Omph + Grt)–(Omph + Opx)–(Omph + Crn) ternary section. The ancillary Grt-peridotitic and Ky–Coe-eclogitic melting phase diagrams (Fig. 6.6) belong to the common polythermal section peridotite (Prd)–eclogite (Ecl) (that is shown by arrows) and passing through the point Omph + Grt, coincident with the invariant peritectic point P_3, in which the phase diagrams come in contact. The phase diagrams in Fig. 6.6 characterize the equilibrium melting phase relations of Grt-peridotite and Ky–Coe-eclogite systems. Under equilibrium regime of crystallization the peridotite-to-eclogite paragenetic transfer would be impracticable, since the initial peridotite composition is bound to be unchanged from start to finish of melting and crystallization processes. Both the peritectic physico-chemical mechanisms can operate under regime of fractional crystallization, causing a figurative point of the initial ultrabasic melt inside the L + Ol + Opx field to travel the following way: L + Ol + Opx field → L + Ol + Opx + Cpx cotectic curve → L + Ol + Opx + Cpx + Grt peritectic point (with loss of Opx) → L + Jd–Cpx + Grt cotectic curve → L + Ol + (Cpx/Omph) + Grt peritectics (with loss of Ol) → L + Omph + Grt field → L + Ky + Omph + Grt cotectic curve → L + Ky + Coe + Omph + Grt eutectics → Ky + Coe + Omph + Grt subsolitus assemblage.

It must be taken into account that the physico-chemical mechanisms of fractional ultrabasic-basic magmatic evolution are responsible for the fundamental regularities in the upper-mantle origin of garnet peridotite and eclogite rocks. Similar physico-chemical mechanisms have been operable during ultrabasic-basic evolution

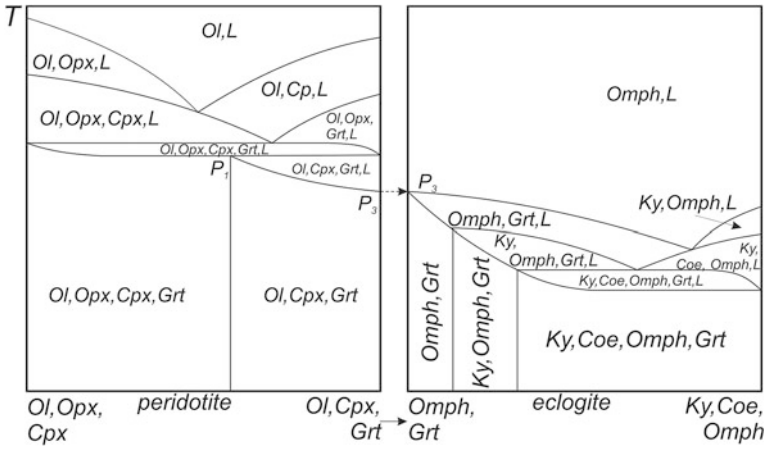

Fig. 6.6 Mating equilibrium diagrams of peridotitic and eclogitic systems for the polythermal section Prd (Ol + Opx + Cpx)–Ecl (Ky + Coe + Omph) in the Fig. 6.4. The *arrows* $P_3 \rightarrow P_3$ and Ol + Cpx + Grt → Omph + Grt symbolize a fractional conversion between the systems

of the diamond-producing upper-mantle melts-solutions. Products of the upper-mantle diamond-producing processes are represented by diamond-bearing peridotites and eclogites as well as primary mineral inclusions in diamonds of the discrete peridotite and eclogite parageneses. Physico-chemical mechanisms of the ultrabasic-basic evolution of the silicate-carbonatite-carbon diamond-producing melts are made clearer in the syngenesis diagrams for diamonds and associated phases under conditions of fractional crystallization. Methods for the construction of the fractionary phase diagrams have been previously discussed (Maaloe 1985; Litvin 1991). Something of specific features of equilibrium phase diagrams must be taken into account. It has been known that equilibrium peridotite system is characterized with the following subsolidus associations: Ol + Opx; Ol + Cpx; Ol + Opx + Cpx; Ol + Opx + Grt; Ol + Cpx + Grt and Ol + Opx + Cpx + Grt (Bobrov and Litvin 2011). The experimental equilibrium phase diagram on the diamond-producing join $Prd_{30}Carb^*_{70}$–D (Fig. 4.7) characterizes the physico-chemical formation conditions of diamonds and associated phases of peridotite paragenesis. The boundary composition $Prd_{30}Carb_{70}$ is located within the subsolidus field of the Opx-bearing association Ol + Opx + Cpx + Grt + Carb* + D while the melt and minerals at solidus assemblage are presented by the assemblage L + Ol + Opx + Cpx + Grt + Carb* + D + L. If the initial composition of the system corresponds to this subsolidus association, a loss of Opx and formation of the subsolidus assemblage Ol + Cpx + Grt + Carb* + D is not be happened under the conditions of equilibrium crystallization.

The syngenesis phase diagram for diamonds and paragenetic inclusions formed in the peridotite-carbonate system Prd + Carb[→ (Ky–Coe–Ecl) + Carb]–D at the regime of fractional crystallization (Fig. 6.7) has been constructed with the use of experimental physico-chemical results for the upper-mantle silicate and

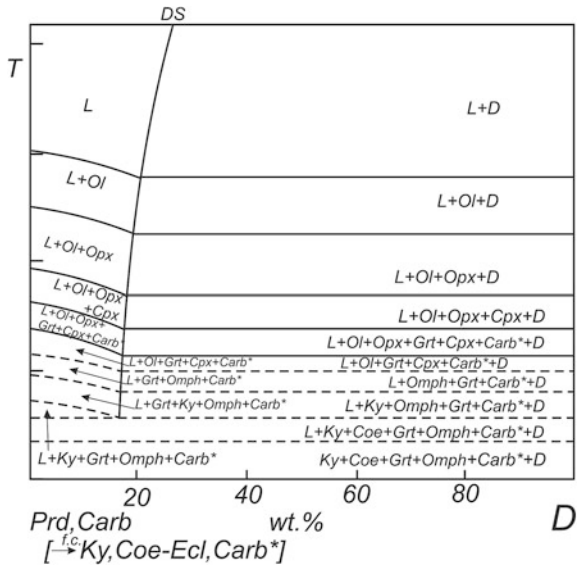

Fig. 6.7 Syngenesis phase diagram for diamond and minerals of ultrabasic and basic parageneses under conditions of fractional crystallization of the upper-mantle diamond-producing system (Prd + Carb)–D. In symbolism of the boundary composition (Prd, Carb [→ Ky–Coe–Ecl, Carb*], the starting composition (Prd + Carb) experienced a fractional crystallization (this is shown by *arrow*) and the forecasted result—the subsolidus mineral assemblage of Ky–Coe-eclogite

silicate-carbonate systems. A consideration must be given to the special designation for the system composition and diagram. In the designation the initial ultrabasic composition Prd + Carb* is displayed through the arrow together with final basic composition (Ky–Coe–Ecl) + Carb (in square brackets). The arrow symbolizes the regime of fractional crystallization (f.c.).

Physico-chemical role of the diamond solubility curve in genesis of diamonds and paragenetic peridotite and eclogite minerals at fractional crystallization is the same as for equilibrium conditions that has been detailed in Sect. 4.3. Fractional crystallization of minerals is evolved uniformly as in carbon-unsaturated so in carbon-saturated fields. The peritectic physico-chemical mechanisms Opx + L → Cpx and Ol + L → Grt are operated in the peridotite-carbonatite diamond-parental melts at their fractional crystallization. In consequence of this, the figurative point of initial ultrabasic melt composition in the L + D field traverses the following way: L + Ol + D field—L + Ol + Opx + D cotectic curve—L + Ol + Opx + Cpx + D cotectic curve—L + Ol + Opx + Cpx + Grt + Carb* + D peritectic point (the loss of Opx)—L + Ol + (Cpx + Jd) + Grt + Carb* + D cotectic curve—L + Ol + (Cpx → Omph) + Grt + Carb* + D peritectic point (the loss of Ol)—L + Omph + Grt + Carb* + D divariant field—L + Ky + Omph + Grt + Carb* + D cotectic curve—L + Ky + Coe + Omph + Grt + Carb* + D eutectic point—Ky + Coe + Omph + Grt + Carb* + D subsolidus assemblage.

Finely the physico-chemical mechanisms of fractional ultrabasic-basic evolution of diamond-parental melts were revealed. The mechanisms are the governing factors of the fundamental regularities in origin of diamonds and associated minerals of peridotitic and eclogitic parageneses. The physico-chemical experimental and theoretical results can be applied to the analysis of origin of diamond-bearing

peridotites and eclogites, formation of diamonds and primary inclusions in the upper-mantle reservoirs-chambers of diamond-parental silicate-carbonatite-carbon melts-solutions at their progressive cooling.

It becomes apparent the physico-chemical mechanism that is responsible for the continuous ultrabasic-basic transfer of diamond-forming silicate-carbonate growth melts-solutions with a consecutive formation of minerals of the peridotitic and eclogitic parageneses. Therewith it is elucidated why primary inclusions of two dissimilar parageneses are practically not coexisted inside the same diamond crystal. It may be deduced that a superposition of physico-chemical conditions for formation of the minerals of peridotite and eclogite parageneses is excluded and, consequently, the simultaneous capture of paragenetically different minerals by the growing diamonds is impossible. It seems that a seldom information about mineral inclusions of different parageneses in separate diamonds (Prinz et al. 1976; Wang 1998) is attributable to the fractional crystallization of exclusively ultrabasic peridotite—Ol-eclogite melts that was under control of the L + Cpx + Grt cotectic curve.

The fractional ultrabasic-basic evolution of magmatic and diamond-bearing systems of the transition zone must not be ruled out but physico-chemical mechanisms, which control the transformations, can be revealed exclusively with the use of physico-chemical experimental study.

6.4 Fractionary Evolution of Lower-Mantle Magmas and Diamond-Parental Melts

The lower-mantle system MgO–FeO–SiO_2–CaO is reasonably representative for the lower-mantle ultrabasic and basic mineral assemblages with dominating phases of periclase-wustite solid solutions $(MgO{\cdot}FeO)_{ss}$, bridgmanite (Mg, Fe)SiO_3, Ca-perovskite $CaSiO_3$ and stishovite SiO_2 (Akaogi 2007). The lower-mantle minerals have been partially dissolved in primary carbonatite melts early in the formation of diamond-parental silicate-oxide-carbonate-carbon melts-solutions. At the stage of diamond genesis the dissolved mineral components were crystallized from the melts-solutions into phases similar to the primary lower-mantle minerals. Melting phase relations on the lower-mantle oxide-silicate system MgO–FeO–SiO_2–$CaSiO_3$ were studied in physico-chemical experiments (Litvin et al. 2014, 2016a, b). Moreover crystallization of diamonds and associated ultrabasic and basic phases was performed in the parental oxide-silicate-carbonatite-carbon melts. The results have demonstrated an unequivocal correspondence of the experimental subsolidus phases to both the associations of lower-mantle minerals and diamond-hosted paragenetic mineral inclusions.

Of particular value is the experimental discovery of the bridgmanite and melt peritectic reaction with formation of periclase-wustite solid solutions and stishovite ("stishovite paradox") as the effective physico-chemical mechanism for

ultrabasic-basic evolution of the lower-mantle oxide-silicate magmas and oxide-silicate-carbonate-carbon diamond-parental melts. Judging from the available mineralogical and experimental data, the lower-mantle mineral assemblage that produces the primary magma for ultrabasic-basic evolution belongs to the subsolidus assemblage FPer + FBrd + CaPrv (Fig. 5.4). During the equilibrium melting and subsequent crystallization the starting composition of the system is rigidly fixed from start to finish. By this is meant that the ultrabasic-basic magmatic evolution is impossible under regime of equilibrium crystallization because the mechanism of "stishovite paradox" is unusable. To the contrary, during the fractional crystallization the newly formed minerals are permanently taken out of the melt that progressively changes the melt and the system compositions. So, due to the change of the system composition, the figurative point of the melt can travel between the boundary eutectic points e_1 and e_3 over the univariant cotectic curves L + (Per•Wus)ss + MgPrv + CaPrv and L + Sti + (Per•Wus)ss + CaPrv as well as over the invariant peritectics P between these curves. Notice that similar trip is impossible in case of eutectic instead of peritectic melting relations.

The peritectic reaction of bridgmanite (FBrd + L = MWus + Sti) occurs also in the diamond-producing system (Per + Carb)–(Wus + Carb)–(Sti + Carb)–(CaPrv + Carb) creating the physico-chemical mechanism for ultrabasic-basic evolution with the sequential control by the ultrabasic univariant cotectic curve L + FPer + FBrd + CaPrv + Carb*, quasi-invariant peritectic point L + (FPer → MWus) + FBrd + Sti + CaPrv + Carb* and basic univariant curve L + Sti + MWus + CaPrv + Carb*.

By the results of physico-chemical experimental investigation of the lower-mantle oxide-silicate and oxide-silicate-carbonate systems, the fractional syngenesis phase diagram for diamonds and paragenetic inclusions of the ultrabase-carbonatitic system FPer + FBrd + CaPrv + Carb[→MWus + Sti + CaPrv + Carb]–D is constructed (Fig. 6.8). In this case, the peritectic physico-chemical mechanism FBrd + L = (FPer → MWus) + Sti at the diamond-producing ultrabasic-basic-carbonatite melts has been used. In consequence of this, the figurative point of initial ultrabasic melt composition in the L + D field traverses the following way: L + FPer + D field—L + FPer + FBrd + D cotectic curve—L + FPer + FBrd + CaPrv + D cotectic curve—L + Fper + FBrd + CaPrv + Carb* + D cotectic curve—L + (FPer → MWus) + FBrd + Sti + CaPrv + Carb* + D peritectic point (the loss of FBrd)—L + MWus + Sti + CaPrv + Carb* + D cotectic curve—MWus + Sti + CaPrv + Carb* + D subsolidus assemblage. In this case the physico-chemical control is performed for the regular ultrabasic-basic transfer from bridgmanite-ferropericlase rocks to stishovite-magnesiowustite ones under the lower-mantle conditions. The examples of paragenetic crystallization of lower-mantle diamonds and minerals of both ultrabasic and basic parageneses in experiments at 26 GPa are given in the Fig. 5.5. The ultrabasic and basic mineral parageneses at the natural diamond-producing systems have been also originated sequentially in the processes

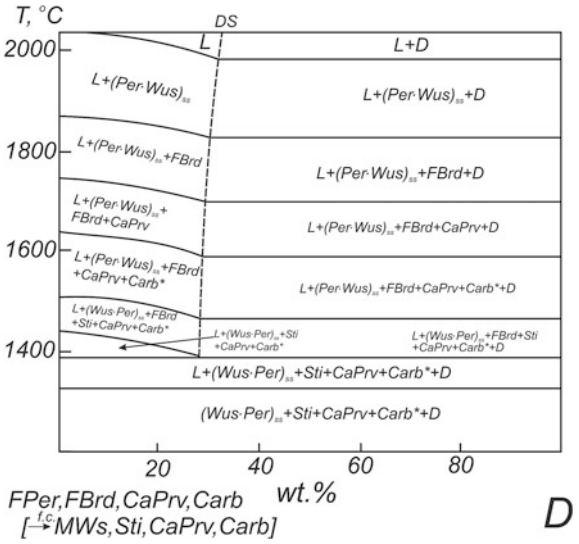

Fig. 6.8 Syngenesis phase diagram for diamond and minerals of ultrabasic and basic parageneses under conditions of fractional crystallization of the lower-mantle diamond-producing system FPer + FBrd + CaPrv + Carb–D. In symbolism of the boundary composition (FPer, FBrd, CaPrv, Carb [→ MWus, Sti, CaPrv, Carb*], the starting composition (FPer + FBrd + CaPrv + Carb) experienced a fractional crystallization (this is shown by *arrow*) and the forecasted result—the subsolidus mineral assemblage of the basic association

of fractional crystallization at the progressive cooling of the lower-mantle chambers of the growth melts-solutions for diamonds and associated phases.

The reality of this scenario receives support directly from results of physico-chemical experiments on multicomponent lower-mantle mineral systems and indirectly from data of analytical mineralogy of lower-mantle mineral inclusions in the "super-deep" diamonds. However, results of testing experiments on formation of "super-deep" diamonds and paragenetic inclusions in the multicomponent carbonatite-silicate-oxide system (Fig. 5.5) are in excellent agreement with the conclusion that the peritectic mechanism of "stishovite paradox" operates in partially molten ultra-deep diamond-parental melts too.

References

Akaogi M (2007) Phase transitions of minerals in the transition zone and upper part of the lower mantle In: Ohtani E (ed) Advances in high-pressure mineralogy. Geological Society of America Special paper 421, pp 1–13. doi:10.1130/2007.2421(01)

Bobrov AV, Litvin YA (2011) Mineral equilibria of diamond-forming carbonate-silicate systems. Geochem Internat 49(13):1267–1363

Boyd FR, Danchin RV (1980) Lherzolites, eclogites and megacrysts from some kimberlites of Angola. Amer J Sc 280(2):528–549

Butvina VG, Litvin YA (2009) Phase relations in the forsterite-diopside-jadeite system. In: Geophys Res Abstr, vol 11, EGU2009-3238

Carter JL (1970) Mineralogy and chemistry of the Earth upper mantle based on the partial fusion—partial crystallization model. Bull Geol Soc Amer 81:2021–2034

Davis BTC (1964) The system diopside-forsterite-pyrope at 30 kilobas pressure. Carn Inst Wash Yb 63:165–171

Davis BTC, Shairer JF (1964) Melting relations in the join Di-Fo-Py at 40 kbar and 1 atm. Carn Inst Wash Yb 64:183–187

Gasparik T, Litvin YuA (1997) Stability of $Na_2Mg_2Si_2O_7$ and melting relations in the forsterite-jadeite join at pressures up to 22 GPa. Eur J Mineral 9:311–326

Litvin YA (1991) Physico-chemical study of melting relations of the deep-seated Earth's substance. Nauka, Moscow, p 312

Litvin YA, Spivak AV, Solopova NA, Dubrovinsky LS (2014) On origin of lower-mantle diamonds and their primary inclusions. Phys Earth Planet Int 228:176–185. doi:10.1016/j/pepi/2013.12.007

Litvin YA, Spivak AV, Kuzyura AV (2016a) Fundamentals of the mantle-carbonatite concept of diamond genesis. Geochem Internat 54(10):839–857. doi:10.1134/S0016702716100086

Litvin YA, Spivak AV, Dubrovinsky LS (2016b) Magmatic evolution of the material of the Earth's lower mantle: stishovite paradox and origin of superdeep diamonds (experiments at 24–26 GPa). Geochem Internat 54(11):936–947. doi:10.1134/S0016702916090032

Maaloe S (1985) Principles of igneous petrology. Springer, Berlin, p 74

O'Hara MJ (1963) The join diopside-pyrope at 30 kilobars. Carn Inst Wash Yb 62:116–118

O'Hara MJ (1968) The bearing of phase equilibria in synthetic and natural systems on the origin and evolution of basic and ultrabasic rocks. Earth Sci Rev 4:69–133

Prinz M, Manson DV, Hlava PF, Keil K (1976) Inclusions in diamonds: garnet lherzolite and eclogite assemblages. In: Physics and chemistry of the Earth, vol 9. Pergamon Press, Oxford, NewYork, pp 197–815

Ringwood (1962) A model for the upper mantle. J Geophys Res 67:857–866

Wang W (1998) Formation of diamond with mineral inclusions of "mixed" eclogite and peridotite parageneses. Earth Planet Sci Lett 160:831–843

Yoder HS (1976) Generation of basaltic magma. National Academy of Sciences, Washington

Chapter 7
Mantle-Carbonatite Conception of Diamond and Associated Phases Genesis

The mantle-carbonatite conception of diamond genesis has been worked out as the result of consistent concordance of mineralogical and experimental evidence. This makes possible to have arrived to the construction of the generalized diagrams for compositions of diamond-producing melts under the upper mantle, transition zone and lower mantle conditions. The diagrams reveal the genetic links of diamond-parental melts with the whole mantle substance having regard to the genetic features of diamond-hosted inclusions for the main mantle layers of different mineralogy. The generalized diamond-parental composition diagram represents a peculiar kind of physico-chemically and mineralogically justified matrix for genetic classification of diamond-associated mineral components and phases. Based on the mantle-carbonatite conception, it has been made possible an experimental determination of the mineral-melt partition coefficients for the trace elements and their application to the natural diamond-producing systems. Also, it is serves as the basis for a development of physico-chemical model for origin and evolution of the mantle reservoirs-chambers of silicate-(±oxide)-carbonate-carbon melts serving as parental for diamonds and associated phases.

7.1 Generalized Composition Diagram of Upper-Mantle Diamond-Parental Medium

Variable chemical compositions of melts-solutions parental for the upper-mantle diamonds and associated phases have been revealed on the basis of intercomplementary evidence from analytic mineralogy of diamond-hosted primary inclusions and physico-chemical experiments on diamond-parental peridotite-carbonatite and eclogite-carbonatite systems. It has been eventually deduced that the diamond-parental media were formed with participation of components of peridotite and eclogite minerals as well as carbonatitic constituent which is occasionaly detected

Y.A. Litvin, *Genesis of Diamonds and Associated Phases*,
Springer Mineralogy, DOI 10.1007/978-3-319-54543-1_7

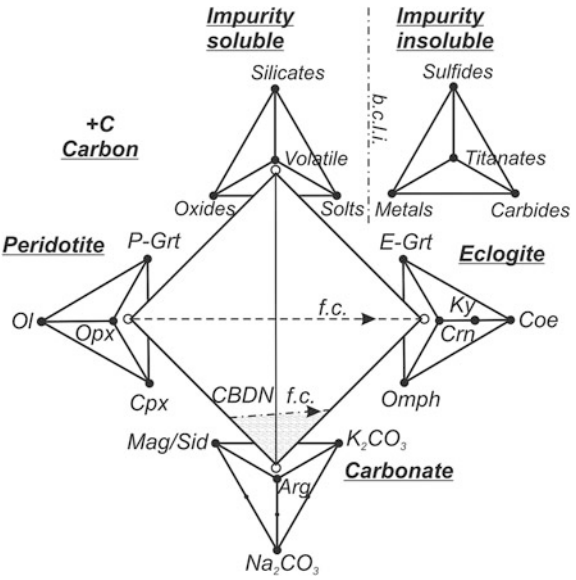

Fig. 7.1 Generalized composition diagram of diamond-producing partial melts-solutions of the *upper mantle*. Symbols *Ol* olivine, *Opx* ortuopyroxene, *Cpx* clinopyroxene, *P-Grt* garnet of peridotite paragenesis; *Omph* omphacite, *E-Grt* garnet of eclogite paragenesis, *Crn* corundum, *Ky* kyanite, *Coe* coesite: *Mag* magnesite, *Arg* aragonite, *Sid* siderite, *CBDN* concentration barrier of diamond nucleation, *c. l. i. b.* boundary of complete liquid immisctbility, *f.c.* fractional crystallization

among primary inclusions in diamonds. All this implies that the pseudo-ternary peridotite-eclogite-carbonate system makes it possible to characterize most representatively the chemical compositions of the upper-mantle diamond-parental media.

The basis for the generalized composition diagram of the upper-mantle diamond-producing melts-solutions (Fig. 7.1) is the major composition tetrahedron of the system peridotite—eclogite—carbonatite—soluble admixtured compounds (Litvin et al. 2012). The apexes of major tetrahedron have rested upon lesser boundary composition tetrahedrons in which the relevant phases and components are combined in accordance with the data of analytical mineralogy. The peridotite composition tetrahedron is represented by the ultrabasic Ol–Opx–(P-Cpx)–(P-Grt) system, the eclogite composition tetrahedron—by the basic (E-Cpx)–(E-Grt)–Crn–Coe system, and the carbonatitic tetrahedron—by the multicomponent K_2CO_3–Na_2CO_3–$MgCO_3$–$FeCO_3$–$CaCO_3$ system.

Thus, the boundary tetrahedrons of paragenetic peridotitic, eclogitic and carbonatic phases, which are soluble in the diamond-parental silicate-carbonate melts, belong to the major ones. The figurative points of the boundary compositions can be transferred over the surfaces and inside the boundary tetrahedrons that is consistent with variability of the natural diamond-parental melts. It may be qualified as secondary the boundary tetrahedron of paragenetic admixture components and phases which are also soluble in the parental melts. Therewith the tetrahedron of xenogenetic phases, which are insoluble in the parental melts, should be placed separately that is arbitrarily symbolized with the special boundary of a complete liquid immiscibility (b.c.l.i.). At the present, it has been experimentally determined that sulfides (Shushkanova and Litvin 2008), titanites (Litvin et al. 2016), native metals and metallic alloys are among the xenogenetic phases. Carbon is a common

component for all the boundary compositions and because of this its symbol may be disposed beyond the composition diagram for simplicity.

It is pertinent to note that mineral phase relations of naturally-composed mantle systems, including the diamond-producing ones, have been determined at physico-chemical experiments in an equilibrium approximation, and the correctness of experimental phase diagrams is under control of the Rhines phase rule for multicomponent multiphase systems (Rhines 1956; Palatnik and Landau 1964). Meanwhile the petrochemical data (Sobolev 1977; Marakushev 1984) are evidenced of the smooth compositional change for similar minerals of the upper-mantle peridotites and eclogites and, accordingly, of the absence of a drastic demarcation between the ultrabasic and basic compositions in spite that the typical ultrabasic lherzolites are distinctly detached from basic eclogite rocks. The petrochemical evidence is compatible with the mechanism of fractional differentiation of the natural magmas in response to the gravity. It is apparent that any physio-chemical contacts of the crystallizing phases with the parental system are bound to exhaust after their fractionation. In response to the fractional crystallization the compositions of residual melts and, correspondingly, the general composition of the fractionating system undergo some regular trends.

It can be seen that the field of parental melts for diamonds and paragenetic phases in the generalized composition diagram (Fig. 7.1) resides at the boundary pseudo-ternary peridotite-eclogite-carbonatite system in immediate contact with the carbonatite boundary tetrahedron. The compositions of diamond-hosted inclusions (Schrauder and Navon 1994a) point to the K–Na–Mg-Fe–Ca carbonate ingredient of the natural parental melts at the upper-mantle diamond-producing reservoirs-chambers. The multicomponent carbonate systems melt congruently at the PT-conditions of diamond genesis (Spivak et al. 2015). The major and many accessory minerals of peridotites and eclogites, their volatile compounds are effectively soluble in carbonate melts. The silicate-carbonate melts are completely miscible, and solubility of diamond and metastable graphite in the melts is limited and corresponds to 15–20 wt% by experimental estimation. It is discovered that an elevated content of silicate components in the silicate-carbonate-carbon growth melts may have a pronounced inhibitory effect on diamond crystallization, that lies in a lowering the density of diamond phase nucleation up to a complete termination at the critical composition at the concentration barrier of diamond nucleation (CBDN) (Litvin et al. 2008).

The critical boundary line for the field of diamond-producing compositions in the Fig. 7.1 is marked by the straight line CBDN. The boundary disposition corresponds to the region of silicate-carbonatitic compositions according to the experimental determination the CBDN concentration value for the boundary peridotite-carbonate (30 wt% peridotite) and eclogite-carbonate (35 wt% eclogite) systems (Bobrov and Litvin 2009; Litvin et al. 2012). In that case, the rock-forming minerals content (wt%) of starting garnet lherzolite $Ol_{60}Opx_{16}Cpx_{12}Grt_{12}$ (Prd) is similar to that of (Ringwood 1975; Boyd and Danchin 1980) with the general composition: SiO_2 45,07, Al_2O_3 3.48, FeO 11.35, MgO 37.25, CaO 2.49, Na_2O 0.36; of starting bimineral eclogite $Omph_{50}Grt_{50}$ (Ecl) similarly to (Sobolev et al.

1972) with the general composition SiO_2 47.62, Al_2O_3 15.56, FeO 12.89, MgO 9.00, CaO 12.28, Na_2O 2.65. The starting carbonatite composition corresponds to K_2O 18.55, Na_2O 1.69, MgO 8.30, CaO 15.05, FeO 15.89, CO_2 40.49 in accordance with (Schrauder and Navon 1994b; Litvin and Zharikov 2000). The critical KBDN compositions correspond for the completely molten diamond-parental peridotite-carbonatite-carbon melts-solutions to SiO_2 13.52, Al_2O_3 1.04, FeO 14.53, MgO 16.99, CaO 11.31, Na_2O 1.29, K_2O 12.99, CO_2 28.33 and for eclogite-carbonatite-carbon melts-solutions to SiO_2 16.67, Al_2O_3 5.45, FeO 14.84, MgO 8.55, CaO 14.10, Na_2O 2.03, K_2O12.99, CO_2 26.31. The diamond-forming efficiency of the growth melts increases with decrease of silicate components content in the direction to the carbonatite boundary composition.

As estimated (Ringwood 1975) peridotite rocks are dominated over eclogites in the heterogeneous upper-mantle material in the proportion 95: 5 (vol. %). It must be taken into account that the equilibrium change of ultrabasic composition of the mantle magmas and diamond-producing melts into the basic one over the growth melts compositions field in the Fig. 7.1 is physico-chemically impossible because of the exacting requirement for the starting composition of any equilibrium system to be kept constant at any phase transformations. The ultrabasic-basic paragenetic transition can be physico-chemically realizable at the regime of fractional crystallization that is symbolized by arrows marked as “f.c.” in the Fig. 7.1. Physico-chemical mechanism of this sort transition for the upper-mantle magmatic and diamond-parental systems will be discussed below.

7.2 Generalized Composition Diagrams of Lower-Mantle and Transition-Zone Diamond-Parental Media

Experimental study of subsolidus transformations of garnet lherzolites (or pyrolites) and middle oceanic ridge basalts (MORB) at PT-conditions of the transition zone and lower mantle provides a way to conceive a possible mantle mineralogy at these depths (Akaogi 2007). It is appeared that experimental phases are similar to the diamond-hosted minerals which have been crystallized in situ from the transition-zone and lower-mantle diamond-parental melts but not represent the native mantle minerals at the corresponding mantle depths. The lower-mantle mineral inclusions reviewed in (Kaminsky 2012) provide a possibility to determine oxide and silicate components of the growth melts-solutions for the lower mantle diamonds and associate paragenetic phases. Moreover, the carbonate inclusions of aragonite $CaCO_3$, dolomite $CaMg(CO_3)_2$, nyererite $Na_2Ca(CO_3)_2$ and nahkolite $NaHCO_3$ point to the Mg–Fe–Ca–Na-carbonate constituent of the lower-mantle diamond-parental melts. In accordance with mineralogical and experimental evidence, the parental media for the lower-mantle diamonds and associated phases can be represented by ultrabasic ferropericlase–bridgmanite–Ca-perovskite–carbonatite and basic stishovite–Ca-perovskite–magnesiowustite–carbonatite systems whose melts are capable to dissolve elementary carbon.

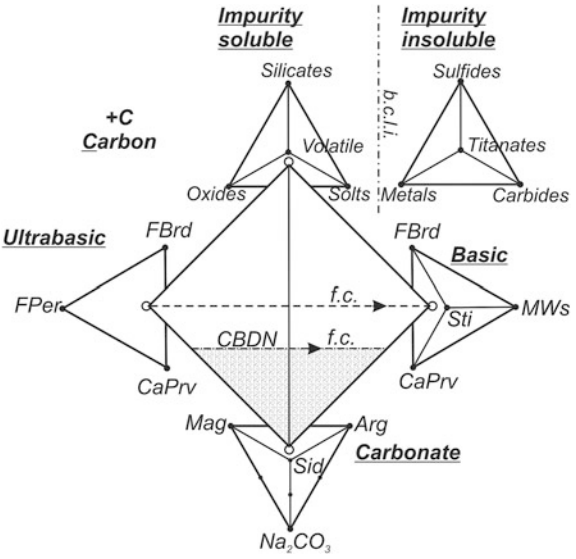

Fig. 7.2 Generalized composition diagram of diamond-producing partial melts-solutions of the *lower mantle*. Symbols *FPer* ferropericlase, *FBrd* bridgmanite, *CaPrv* Ca-perovskite, *MWus* magnesiowustite, *Sti* stishovite. See also designations to Fig. 7.1

Genetic classification of the constituents of diamond-parental medium and, correspondingly, primary major and secondary inclusions in the lower-mantle diamonds provides a possibility for development of a generalized composition diagram for the lower-mantle parental medium. At the generalized composition diagram (Fig. 7.2) (Litvin et al. 2014, 2016) the parental media belong to the ternary ultrabasic matter—basic matter—carbonatite system. The concentration barrier of diamond nucleation (CBDN) at the generalized diagram corresponds to 65 wt% according to preliminary experimental evidence. Therewith the CBDN line is shifted to the region of diamond-parental melts compositions richer in oxide-silicate components.

The compositions at the CBDN critical points and, correspondingly, of diamond-parental melts for ultrabasic-carbonatite and basic-carbonatite systems may be tentatively calculated considering the relative contents for mineral phases and compositions of the lower-mantle rocks predicted on the basis of the isochemical pyrolite model (Ringwood 1962; Akaogi 2007). The ultrabasic bridgmanite-ferropericlase-Ca-perovskite rock Brd + FPer + CaPrv + (Al-phase) can be of the pyrolite composition (wt%): SiO_2 45.3, Al_2O_3 4.9, FeO 7.9, MgO 38.6, CaO 3.1, Na_2O 0.6. Composition of the forecasting basic rock Sti + MWus + CaPrv + Brd + (NaAl-фаза) may be as follows: SiO_2 48.2, Al_2O_3 18.6, FeO 7.9, MgO 10.9, CaO 12.1, Na_2O 2.3. A multicomponent carbonatitic constituent may be simulated by the composition: $(MgCO_3)_{20}(CaCO_3)_{20}(FeCO_3)_{20}(Na_2CO_3)_{20}$ corresponding to: MgO 12.0, CaO 14.0, FeO 16.0, Na_2O 13.0, CO_2 45.0. The critical compositions at the CBDN points for the completely molten ultrabasic-basic-carbonatate diamond-parental melts correspond to: SiO_2 28.6, Al_2O3 3.2, FeO 10.8, MgO 29.6, CaO 6.9, Na_2O 5.0, CO_2 15.9 and for the

basic-carbonatite—to: SiO_2 31.3, Al_2O_3 12.1, FeO 10.7, MgO 11.3, CaO 12.8, Na_2O 6.1, CO_2 15.7. The diamond-forming efficiency of the parental melts is growing with decrease of ultrabasic and basic silicate-oxide components content in the direction of the carbonatitic boundary composition.

It must be remembered that the ultrabasic lower-mantle rocks are bound to dominate over the basic ones as 95:5 (vol. %) if the lower-mantle composition is in agreement with the isochemical pyrolytic model for whole mantle material (Ringwood 1975). The problem of basic rocks formation from the primitive ultrabasic lower-mantle material has been of obvious interest.

The most probable compositions of the transition-zone diamond-parental melts-solutions are belonging to the boundary ultrabasic-basic-carbonatite system that is demonstrated by the generalized composition diagram for diamonds and associated phases of the transition zone (Fig. 7.3). Majoritic garnets and other primary inclusions in diamonds (McKenna et al. 2004; Shatsky et al. 2010) together with experimental phases of the subsolidus transformations of pyrolites and MORB-basalts (Akaogi 2007) characterize the transition-zone ultrabasic and basic rocks which contribution into the growth melts of diamonds and paragenetic minerals is evidenced by the components of silicate inclusions. Carbonate inclusions in the transition-zone diamonds (Kaminsky 2012) have been formed at the cost of Mg–Fe–Ca–Na-carbonate components of the growth melts-solutions.

In the generalized transition-zone diamond-parental composition diagram (Fig. 7.3) the growth melts for diamonds and paragenetic minerals belongs to ultrabasic (wadsleite ↔ ringwoodite)—(majoritic garnet)—carbonatite and basic (majoritic garnet)—stishovite–carbonatite melts-solutions with dissolved elementary carbon. Clinopyroxene components participate in the diamond-parental melts compositions by the boundary of transition zone with the upper mantle, and silica

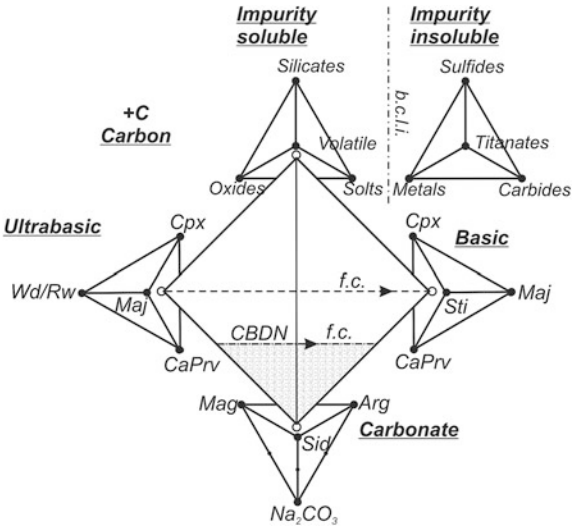

Fig. 7.3 Generalized composition diagram of diamond-producing partial melts-solutions of the transition zone. Symbols *Wd* wadsleite, *Rw* ringwoodite, *Maj* majorite, *CaPrv* Ca-perovskite, *MWus* magnesiowustite, *Cpx* clinopyroxene, *Sti* stishovite. See also designations to Fig. 7.1

component of stishovite at all depths of the transition zone. The field of diamond-parental compositions is bordered by the tentative CBDN line which position for ultrabasic and basic compositions remains to be experimentally determined. Because of this, the critical compositions for ultrabasic-carbonatite and basic-carbonatite systems related to the CBDN line are impossible to be calculated.

7.3 Basics of the Mantle-Carbonatite Theory of Diamond Genesis

The results of high-pressure physico-chemical experiments which are coordinated with the data of analytic mineralogy of primary inclusions in natural diamonds support the view that silicate—(±oxide)—carbonatite melts with dissolved carbon are responsible for formation of the mantle derived diamonds. As a consequence, the mantle-carbonatite theory of diamond origin under the mantle conditions has been developed (Litvin 2007, 2009, 2012, 2013; Litvin et al. 2014, 2016). Compositions of primary inclusions in diamonds from the upper mantle, transition zone and lower mantle diamond-producing reservoirs-chambers are not contradictory to the fact that a physico-chemically uniform mechanism of diamond formation is operative for any depths.

It is commonly supposed that heterogeneous primary inclusions in mantle derived diamonds are identical with original minerals of the mantle. By a typical concept, the inclusions represent ultrabasic minerals prevail in the mantle (to say, of in situ material source) and basic minerals of eclogite-like assemblages originated from subducting lithosphere (not of in situ material source). By alternative view, the mantle mineral inclusions, both paragenetic and xenogenetic in respect to diamonds, represent heterogeneous fragments of partially molten diamond-parental medium. This conclusion is based on rigid requirements of experimentally supported criterion of diamond and inclusions syngenesis (Litvin 2007; Litvin et al. 2012): a natural diamond-parental medium has to be physico-chemically capable for producing diamonds and a whole complex of paragenetic phases; along with this, the parental medium must be prepared to put at the disposal of growing diamonds the xenogenetic phases for capturing them as inclusions. By the criterion, the experimental growth melts are bound to realize the syngenesis of diamonds and associated phases similarly to the natural mode. By this is meant, that the primary inclusions were trapped by growing diamonds from heterogeneous parental medium. Therefore, the role of primary inclusions in determination of chemical and phase composition of heterogeneous parental media of diamonds becomes decisive and initiate the purposeful physico-chemcal experimental study.

Hence, it is beyond reason to identify mineral inclusions in diamonds with phases of the surrounding mantle. In all probability, the mantle mineral components were initially involved in diamond-parental melts at their formation. The mantle-similar minerals were formed together with the host-diamonds, and their fragments were trapped by growing diamonds as paragenetic inclusions from parental melts.

Principal problems of diamond genetic mineralogy may be formulated as follows:

(1) determination of chemical nature and compositions of the growth melts for diamonds and paragenetic phases over all the mantle depths; (2) elucidation of the physico-chemical mechanisms of diamonds and primary inclusions syngenesis; (3) substantiation of phase reactions that have formed the discrete ultrabasic and basic parageneses of mineral inclusions in natural diamonds. Experimental and theoretical studies of the principal problems have led to the improved results and conclusions that will give new insight into the problem of genesis of diamonds and associated phases.

The next solutions are of primary concern:

(1) construction of generalized diagrams for the diamond-parental media, which reveal changeable compositions of the growth melts of diamonds and associated phases, their genetic relations to the mantle substance, and classification connections of the primary inclusions in natural diamonds; the compositions of diamond-producing mantle melts are peridotite/eclogite–carbonatite–carbon for the upper mantle, (wadsleite↔ringwoodite)–majorite–stishovite–carbonatite–carbon for the transition zone, and (periclase•wustite)ss–bridgmanite–Ca-perovskite–stishovite–carbonatite-carbon for the lower mantle;
(2) experimental syngenesis diagrams for diamond-producing media reveal the changeable compositions of the growth melts for diamonds and paragenetic phases, their genetic links with the mantle materials and represent the basis for genetic classification of primary inclusions;
(3) experimental determination of equilibrium melting phase diagrams of syngenesis of diamonds and primary inclusions at the peridotite-carbonatite-carbon and eclogite-carbonatite-carbon systems; the diagrams characterize physico-chemical conditions and mechanisms of nucleation of diamond phase and crystal growth of diamonds and associated paragenetic minerals with capturing paragenetic (as well as xenogenetic) minerals by the growing diamonds;
(4) determination of syngenesis phase diagrams for diamonds and primary inclusions under the conditions of fractional crystallization; the diagrams discover the regularities of ultrabasic-basic evolution and paragenetic transitions in the mantle diamond-forming systems for the upper mantle (from peridotites to eclogites) and for the lower mantle (from the bridgmanite-ferropericlase rock to the stishovite-magnesiowustite one);
(5) evidence of the physico-chemically united mode of diamond genesis at the mantle depths with different mineralogy.

Some distinguishing features of the mantle-carbonatite theory of the origin of natural diamonds and associated phases may be briefly outlined as follows:

– the variable multicomponent heterogeneous growth melts-solutions and parental media for the overwhelming majority of natural diamonds comprise carbonate and silicate (aluminosilicate) components of the minerals of peridotite and

eclogite assemblages in the state of complete liquid miscibility, as well as elemental carbon dissolved in these melts-solutions;
- the growth melts-solutions contain major and minor components and phases; some of them are soluble in the completely miscible carbonate–silicate melts (oxides, accessory silicates and aluminosilicates, phosphates, chlorides, C–O–H volatile compounds: carbon dioxide, water, and methane);
- the minor sulfide and titanite components and phases are insoluble in diamond-parental silicate-(±oxide)-carbonate-carbon melts-solutions, and their insoluble melts are completely immiscible with the parental melts-solutions; in this case the low-viscosous silicate-carbonate melts-solutions do not preclude to the permeability and occasional transfers of xenogenetic phases inside them, that offers possibilities for xenogenetic phases to contact with and be trapped by the growing diamonds together with paragenetic phases;
- the majority of natural diamonds are formed at the expense of elemental carbon derived from external sources and dissolved in the carbonate–silicate melts rather than of the carbon contained in carbonates;

The kinetic physico-chemical mechanism of diamond nucleation and growth is related to the labile oversaturation of completely miscible carbonate–silicate growth melts-solutions with dissolved carbon.

7.4 Experimental TE Partition Coefficients for Diamond-Parental Systems

Trace elements in paragenetic phases included in natural diamonds make up the general geochemical background of diamond-forming processes in the Earth's mantle. Diamond-hosted paragenetic inclusions are fragments of multiphase diamond-forming media, which testify to their variable multicomponent chemical composition. The mantle-carbonatite theory of diamond genesis describes the patterns of variation in the chemical composition and phase state of parental media and resulting formation of diamonds and paragenetic inclusions.

Trace elements were determined in both the peridotitic (Stachel and Harris 1997) and eclogitic (Stachel et al. 2004) minerals of inclusions and in isolated carbonatite phases (Schrauder et al. 1996; Weiss et al. 2013). It seems the most likely that multicomponent carbonatite phases in diamond-hosted leak-tight inclusions are solidified fragments of completely miscible silicate-carbonate (carbonatitic) parental melts. The diamond-producing capability of such melts cannot be determined from mineralogical data alone. However testing experiments with melts whose compositions reproduced the compositions of carbonatite inclusions in diamonds of Botswana (Schrauder and Navon 1994b) clearly showed their high diamond-producing capability (Litvin and Zharikov 2000). Note that the SiO_2 content of the carbonatitic melts varied from 13.6 to 45.1 wt%. The fact that such parental melts

meet the criterion of syngenesis of diamonds and primary inclusions was confirmed by physico-chemical experiments (Litvin et al. 2012).

The trace-element contents of phases included in diamonds are sometimes used to find out the possible chemical nature of diamond-forming media. For example, the trace-element contents of isolated primary garnet and clinopyroxene inclusions in polycrystalline diamondites suggest the participation of carbonatitic melts in diamond genesis (Kurat and Dobosi 2000). This agreed with the results of test experiments on diamond crystallization in the carbonate–carbon systems (Litvin 1998; Sokol et al. 1998; Palyanov et al. 1999). Microinclusions of solidified high-density parental melts with a carbonatitic component were repeatedly detected in diamonds (Navon et al. 1988; Schrauder and Navon 1994a). Physicochemical experimental studies showed that such inclusions give an important insight into the fundamental physico-chemical features of the parental media of diamonds and their syngenetic inclusions (Litvin et al. 2012).

Abundant analytical data have been obtained on the trace-element contents of isolated inclusions with solidified melt and volatile components in fibrous and coated diamonds (Zedgenizov et al. 2007; Klein-BenDavid et al. 2010, 2014; Weiss et al. 2013). Particularly interesting are some analyses of the trace-element contents of silicate minerals and fragments of carbonatitic parental melts coexisting in one inclusion (Tomlinson et al. 2009). Note the low accuracy of the analysis of the included phases for major and trace elements because of their small size and, maybe, the inevitable contribution of the neighboring phases. Nevertheless, an attempt was made at estimating the partition coefficients of trace elements (Sr, Y, Lu, Tm, Er, Ho, Tb, Dy, Eu, Sm, Nd, Pr, Ce, La, Ti, and Nb) in inclusions in diamonds of the Panda kimberlite pipe, Canada, which contain peridotitic (Cr-clinopyroxene) and eclogitic (omphacite and garnet) mineral phases coexisting with a multiphase "fluid". In reality, the "fluid" is mainly a mixture of hardened multicomponent carbonate melt and potassium chloride with some amount of the volatile compound H_2O. Strictly speaking, the obtained trace-element partition coefficients cannot be extended to the pairs mineral–carbonatitic melt of parental media free of chloride inclusions, which is more typical of the association of primary inclusions in natural diamonds. The more so as carbonate and chloride melts can show liquid immiscibility under diamond-forming conditions, according to experimental data (Safonov et al. 2007). It is possible that the trace-element partition between these melts influences their relative contents in the pair mineral–carbonatitic melt. Therefore note that for the eclogitic pairs clinopyroxene –"fluid" and garnet–"fluid", the partition coefficients for almost all the trace elements considered in (Tomlinson et al. 2009) are more than an order of magnitude higher than the coefficients for the same trace elements experimentally determined for the pairs of eclogitic clinopyroxene and garnet with completely miscible silicate-carbonate melt (Kuzyura et al. 2010).

A direct approach to the study of the interface partition of trace elements between peridotitic and eclogitic paragenetic minerals and carbonatitic melts, which are parental for both diamonds and paragenetic minerals, is based on the mantle-carbonatite theory of diamond genesis. It has become possible to determine

the geochemical background of diamond-forming processes by experiment with a reliable modeling of the compositions of the mantle parental media of diamonds and paragenetic inclusions (Kuzyura et al. 2010, 2015). The study is aimed at direct experimental determination of the interface partition coefficients of Rb, Cs, Pb, Ba, Th, U, Nb, Ta, La, Ce, Sr, Pr, Nd, Zr, Hf, Sm, Eu, Gd, Tb, Dy, Y, Ho, Er, Tm, Yb, Lu, and Sc in the multicomponent diamond-forming peridotite–carbonatite and eclogite–carbonatite systems under PT-conditions of the thermodynamic stability of diamond.

The major- and trace-element contents of the experimental phases are given in (Kuzyura et al. 2015). The products of the experiments include pyrope–almandine–grossular garnets of the compositions (wt%): (Prp 0.76–0.83,Gros 0.12–0.16, Alm 0.02–0.12) and (Prp 0.13–0.71, Gros 0.25–0.77, Alm 0.03–0.60} for the eclogite–carbonatite and peridotite–carbonatite systems, respectively, as well as hedenbergite–diopside clinopyroxene with an aegirine component (0.40–4.72 wt% Na_2O), olivine with Fo 0.85-0.98, a mixture of carbonates, and the carbonate–silicate quenching melt (Fig. 7.4). The sample 2306 can be assigned to ultrabasic olivine eclogites, which rarely occur in kimberlite-hosted mantle xenoliths (Dawson 1980). Completely miscible silicate-carbonate melts were formed in the experiments. These melts transformed into fine-grained solid substances with a dendritic texture during the quenching. Areas of quenching silicate-carbonate glass are also observed similarly to melting experiments with the Chagatai (Uzbekistan) natural melanocratic carbonatites (Kuzyura et al. 2010). It is known from (Lee et al. 1994; Thibault et al. 1992; Brey et al. 2008) that the equilibrium conditions in molten systems with a carbonate component are reached at high rates.

The coefficients of trace-element partition between the minerals (garnet, clinopyroxene, and olivine) and carbonate–silicate melt (Table 7.1) were calculated based on the relationships of contents in the mineral and melt, in accordance with the terminology in (Beattie et al. 1993). Also, the mineral–mineral partition coefficients for the Grt–Cpx and Grt–Ol pairs were calculated. Spidergrams (Fig. 7.5) show the interface partition of trace elements.Analysis of the spidergram shows that the main participants of the trace-element partition are garnet and melt. The main feature of the obtained partition is different behavior of light trace elements (La, Ce, Pr, Rb, and Ba), on the one hand, and medium and heavy trace elements (Zr, Hf, Sm, Eu, Gd, Tb, Dy, Y, Ho, Er, Tm, Yb, and Lu), on the other. The light elements mainly remain in the melt, whereas the heavy ones are distributed into garnet. The crystallization of minerals from the melt causes a redistribution of heavy elements into garnet as it appears on the liquidus and the depletion of the residual melt in these elements. Scandium also accumulates mainly in garnet ($K_D^{ScGrt} = 58.08$ for the peridotite–carbonatite and 8.45 for the eclogite–carbonatite systems); the structure of olivine and clinopyroxene includes less Sc ($K_D^{ScOl} = 1.54$ and 1.43, and $K_D^{ScCpx} = 3.26$ and 1.22 for the peridotite–carbonatite the peridotite-carbonatite and eclogite–carbonatite systems, respectively). Note that all the K_D^{TE} in clinopyroxene and olivine are less than unity, except K_D^{Sc}. This shows that the minerals (except Sc) do not take part in the trace-element partition; i.e., they are of limited importance in the trace-element geochemistry.

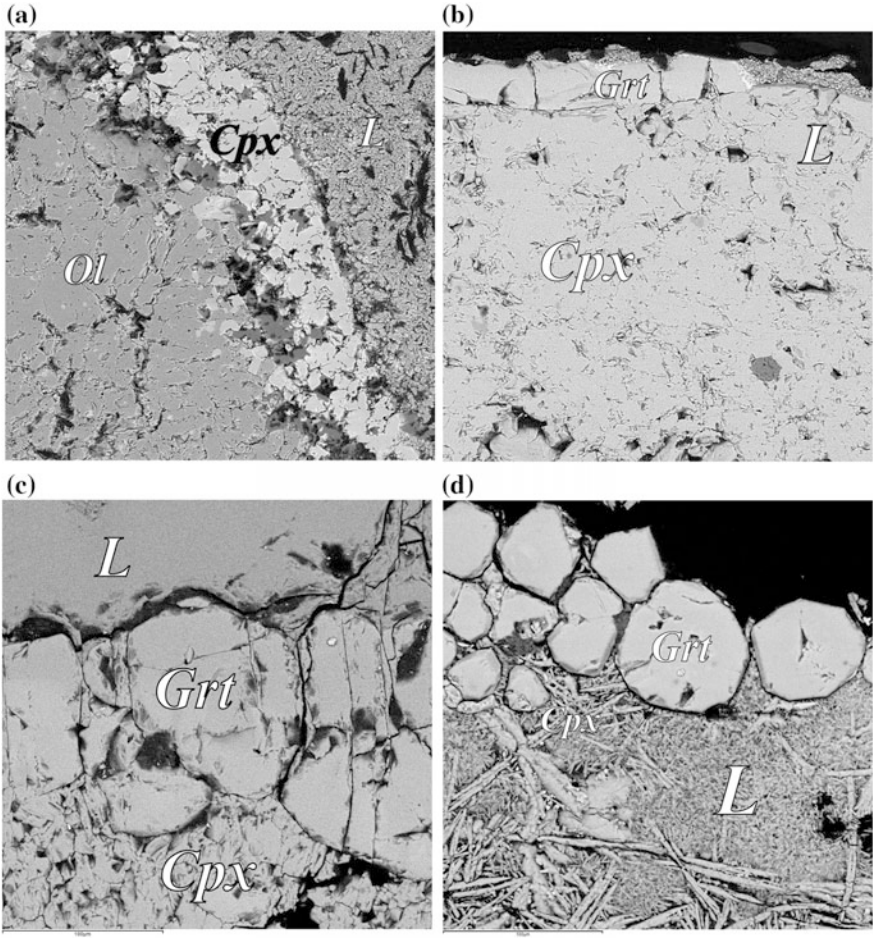

Fig. 7.4 Equilibrium mineral phases and completely miscible silicate-carbonate melts obtained in experiments with peridotite-carbonatite (**a**, **b**) and eclogite-carbonatite (**c**, **d**) systems. Symbols *L* quenched silicate-carbonate melts, *Ol* olivine, *Cpx* clinopyroxene, *Grt* garnet

There are no reliable data on the trace-element partition between peridotitic and eclogitic minerals, on the one hand, and the carbonate–silicate natural diamond-parental melts, on the other. Direct experimental determination of trace elements in coexisting phases (paragenetic minerals and solidified carbonate–silicate parental melts) and, therefore, calculations of the trace-element partition coefficients for the representative phases of the diamond-forming carbonate–silicate systems became possible owing to physico-chemical experiment. Such data can ensure a reliable interpretation of the trace-element contents of peridotitic and eclogitic mineral inclusions in natural diamonds and a more detailed interpretation of real diamond formation based on their geochemical background. Spidergrams

Table 7.1 Partition coefficients of trace elements between minerals and silicate-carbonate melt calculated from experimental data at PT-conditions of diamond stability (7.0–8.5 GPa and 1460–1600 °C)

Component	K_D(Grt-L)			K_D(Cpx-L)			K_D(Ol-L)		K_D(Grt Cpx)		K_D(Grt-Ol)	
	PC	EC	1638*	PC	EC	1638*	PC	EC	PC	EC	PC	EC
Rb	0.01	0.01	0.12	0.01	0.15	0.01	0.11	0.06	0.43	0.03	0.02	0.05
Cs	0.01	0.01	0.10	0.10	0.24	0.02	0.21	0.10	0.05	0.02	0.01	0.05
Ba	0.01	0.00	0.11	0.05	0.19	0.01	0.12	0.12	0.11	0.00	0.01	0.01
Th	0.00	0.00	0.16	0.00	0.00	0.02	0.20	0.13	1.50	0.38	0.50	0.18
U	0.00	0.00	0.25	0.00	0.00	0.02	0.43	0.44	2.00	0.65	1.00	1.00
Nb	0.05	0.01	0.17	0.03	0.14	0.01	0.16	0.06	1.14	0.08	0.10	0.10
Ta	0.18	0.03	0.16	0.03	0.16	0.02	0.14	0.06	4.34	0.14	0.29	0.24
La	0.00	0.00	0.12	0.06	0.21	0.01	0.20	0.07	0.03	0.01	0.00	0.02
Ce	0.01	0.01	0.15	0.10	0.31	0.02	0.28	0.08	0.07	0.02	0.01	0.05
Sr	0.01	0.01	0.06	0.39	0.46	0.05	0.29	0.07	0.01	0.01	0.01	0.02
Pr	0.04	0.03	0.22	0.14	0.35	0.02	0.32	0.07	0.17	0.04	0.05	0.10
Nd	0.10	0.08	0.32	0.18	0.25	0.02	0.37	0.07	0.36	0.10	0.15	0.20
Zr	6.68	1.97	0.85	0.07	0.32	0.09	0.24	0.14	67.97	5.10	5.04	6.11
Hf	5.51	1.61	0.95	0.15	0.36	0.20	0.28	0.14	25.17	4.43	4.16	5.88
Sm	0.67	0.31	0.71	0.25	0.52	0.04	0.46	0.07	1.75	0.31	0.94	0.60
Eu	1.44	0.62	0.85	0.33	0.61	0.04	0.53	0.08	2.94	0.54	1.85	1.14
Gd	2.57	0.94	1.25	0.31	0.63	0.04	0.50	0.10	5.45	0.80	2.68	1.68
Tb	5.19	1.59	1.58	0.35	0.66	0.05	0.52	0.13	9.92	1.09	4.14	2.58
Dy	9.43	2.45	1.92	0.39	0.69	0.06	0.58	0.18	16.14	1.86	5.31	3.35
Y	14.78	3.29	2.48	0.34	0.67	0.06	0.53	0.22	29.40	2.35	6.79	4.23
Ho	15.44	3.34	2.25	0.39	0.68	0.06	0.57	0.24	26.26	2.46	6.54	4.19
Er	21.22	4.49	2.54	0.36	0.73	0.07	0.63	0.29	39.55	2.96	7.42	4.82
Tm	30.77	5.48	2.66	0.37	0.71	0.08	0.64	0.38	56.66	3.46	8.28	5.12
Yb	42.44	6.78	2.81	0.36	0.72	0.08	0.68	0.48	78.30	4.18	9.36	5.80
Lu	52.03	7.97	2.90	0.34	0.69	0.09	0.67	0.59	101.36	4.79	9.24	5.84
Sc	58.08	8.45	3.01	3.26	1.22	1.47	1.54	1.43	11.98	3.98	4.34	6.25

Note PC peridotite-carbonatite system; *EC* eclogite-carbonatite system (generalized)
*Sample number from (Kuzyura et al. 2010)

(Fig. 7.5) show experimentally determined interface partition coefficients of trace elements K_D^{TE} in the diamond-forming peridotite–carbonatite and eclogite–carbonatite systems with the participation of completely miscible carbonate–silicate (carbonatitic) melts. For comparison, the K_D^{TE} values for the pairs silicate mineral–silicate melt and silicate mineral–carbonate melt are given, according to literature data (Blundy and Dalton 2000; Brenan and Watson 1991; Dasgupta et al. 2009; Girnis et al. 2013; Hammouda et al. 2009; Kuzyura et al. 2010; McDade et al. 2003; Pertermann et al. 2004; Sweeney et al. 1992, 1995; Tomlinson et al. 2009; van Westrenen et al. 1999; Walter et al. 2008; Bobrov et al. 2014). According to the experimental data, the peridotite–carbonatite and eclogite–carbonatite mantle

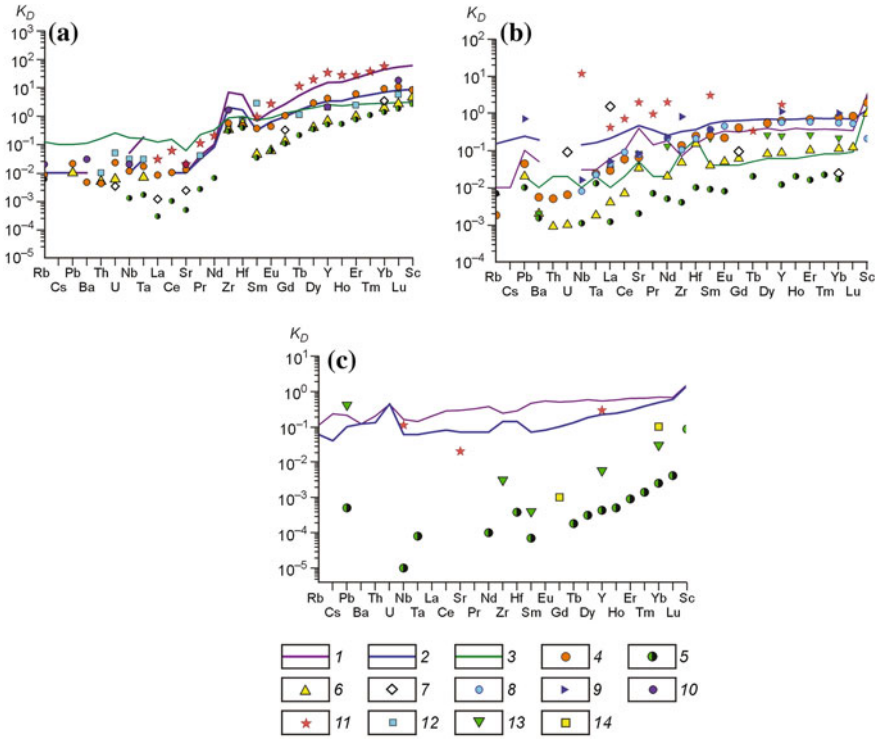

Fig. 7.5 Spidergrams for trace-element partition between silicate-carbonate melts and garnet (**a**), clinopyroxene (**b**) and olivine (**c**). Conventional designations: from (Kuzyura et al. 2015)—*1* for peridotite-carbonatite system and *2* for eclogite-carbonatite system; also from (Kuzyura et al. 2010)—*3*, (Pertermann et al. 2004)—*4*, Girnis et al. 2013)—*5*, Dasgupta et al. 2009)—*6*, (Hammouda et al. 2009)—*7*, (McDade et al. 2003)—*8*, (Blundy and Dalton 2000)—*9*, (Sweeny et al. 1995)—*10*, (Tomlinson et al. 2009)—*11*, (Van Westrenen et al. 1999)—*12*, (Sobolev 1977)—*13*, (Brenan and Watson 1991)

systems, including diamond- forming systems, show such trends in the mineral–melt partition coefficients K_D^{TE} at 7.0–8.5 GPa with the maximum redistribution into garnet. The garnet–melt pairs show similar partitions between garnet and carbonate–silicate melt in Fig. 7.5, that was also pointed out in (Kuzyura et al. 2010), as well as between garnet and silicate melt (Pertermann et al. 2004; van Westrenen et al. 1999), and garnet and carbonate melt (Sweeney et al. 1995; Tomlinson et al. 2009). Note that heavy trace elements are concentrated in garnet with the maximum Lu or Sc contents, and the rest are redistributed into the melts.

It should be stressed that the trace-element partition in (Tomlinson et al. 2009) is based on real data on mineral and multiphase fluid inclusions coexisting in a single inclusion in diamond. The partition coefficients K_D^{TE} were calculated for a limited number of elements. The partition coefficients for the Grt–L pair in the case of heavy elements are one to three orders of magnitude higher than all the rest, which

agrees with the direct experimental measurements in the Table 7.1. The K_D^{TE} between garnet and silicate carbonate melt in (Dasgupta et al. 2009; Girnis et al. 2013; Hammouda et al. 2009) are considerably lower (by one to two orders of magnitude) on the y-axis than the coefficients obtained in the Table 7.2. Also, a difference of one to four orders of magnitude is observed for K_D^{TE} between clinopyroxene and different melts as well as olivine and the melts, though the general distribution pattern preserved in the Fig. 7.5. The maximum difference is between the coefficients presented in Table 7.1 and in data of (Girnis et al. 2013) where the elevated (12.5–30.3 wt%) water contents of "silica–carbonate" melts associated with solid phases.

Despite significant differences in the physical parameters and chemical compositions of coexisting melt phases, the trace-element partitions for silicate-carbonate, carbonate, and silicate melts coincide; i.e., the mineral–melt partition in the silicate-carbonate systems does not depend on temperature, pressure, or composition of "the partner melt". This means that the above mentioned similarity between the trace-element partitions in mineral–melt pairs containing melts with absolutely different chemical compositions does not permit an unambiguous determination of the chemical nature of "the partner melt" from the trace-element content of the coexisting mineral, e.g., garnet (main phase concentrating trace elements in the cases under consideration). The experimentally obtained carbonate–silicate melts are diamond-producing provided that the systems are saturated with dissolved carbon. With regard to the concentration barrier of diamond nucleation (Litvin et al. 2008), these melts will be capable of spontaneous nucleation and crystal growth of the diamond phase. Thus, the products of the experiments model diamond-forming media with silicate minerals which formed in these media.

7.5 Formation and Evolution of the Mantle Reservoirs of Silicate-Oxide-Carbonate-Carbon Melts Parental for Diamonds and Associated Phases

Origin of the mantle silicate-(±oxide)-carbonatite-carbon melts-solutions parental for diamonds and associated mineral phases belongs physico-chemically, temporally and spatially to the repetitive episodes of magmatic evolution of the deep Earth's matter (Litvin 2012; Litvin et al. 2014, 2016). This is in reasonably good agreement with the idea that the diamond-parental melts-solutions have been capable to make up their own reservoirs-chambers within the enclosing mantle rocks. By mineralogical, petrological and geochemical evidence it may be safely suggested that the reservoirs-chambers of diamond-producing multicomponent silicate-(±oxide)-carbonatite-carbon melts-solutions were generated and consolidated within the peridotite and eclogite rocks of the upper-mantle garnet-peridotite facies. In a similar way the reservoirs-chambers of the diamond-producing ultrabasic and

basic silicate-(±oxide)-carbonatite-carbon melts-solutions can be formed and consolidated within the substances of the transition-zone and lower mantle.

The evolution of the Earth's mantle petrological and geochemical processes might have proceeded by the following scenario. At the first "metasomatic–magmatic stage", the mantle alkaline C–O–H-bearing metasomatic agents cause the partial carbonatization of the mantle ultrabasic rocks and generation of carbonate melts reservoirs (the size of the reservoirs is determined by the metasomatizing capacity of the agent). The real agents are likely to be multicomponent and variable in composition, with elevated alkalinity, acidity, and alumina contents and high content of carbon dioxide and limited of water. This is also evident from the compositions of residual melts that the agents may be formed during the fractional crystallization of ultrabasic-basic magmas in the mantle. Credible sources of such metasomatic agents could be the mantle plumes and sizable magmatic reservoirs within the deep mantle. At the next "dissolution–magmatic stage", both the rock-forming and accessory soluble minerals of the host ultrabasic rocks, volatiles, and carbon have to dissolve in the carbonate melts, which are also penetrated by insoluble phases (sulfides, titanites, etc.). This is responsible for formation of the (ultrabasic matter)–carbonatite–carbon parental melts-solutions for diamonds and associated phases. Note that these magmas contain both paragenetic soluble silicate and oxide minerals and xenogenic insoluble sulfide and titanite minerals or their immiscible melts. At the last "fractional-crystallization stage", natural cooling of the diamond-parental magmas in the reservoirs-chambers automatically causes syngenetic crystallization of diamond and mineral inclusions (which are in fact the recrystallized in carbonatitic melts minerals of the upper-mantle, transition-zone or lower-mantle rocks). Meanwhile, the parental magmas experience ultrabasic–basic evolution in the regime of fractional crystallization (Litvin 2013; Litvin et al. 2016), which is responsible for a transition from ultrabasic to basic parageneses in the assemblage of silicate and oxide minerals. This agrees with the general petrochemical trends for ultramafic and mafic mantle rocks and the diamond-bearing assemblages of the peridotitic and eclogitic parageneses (Sobolev 1977; Marakushev 1984). Volatiles are of limited importance in diamond genesis, because they are not capable of forming own stable phases under mantle conditions due to low concentrations, high chemical activity in respect to surrounding mantle rocks, highest solubility in magmatic melts and, respectively, effective miscibility with them.

The physico-chemical history of the melts-solutions parental for diamonds and associated paragenetic phases can be revealed with the use of the fractional syngenesis phase diagrams constructed above for the diamond-producing systems of the upper mantle (Fig. 6.6) and lower mantle (Fig. 6.7). The behavior of xenogenetic phases has to be of the same kind in all cases and is vividly demonstrated by the syngenesis phase diagram of the eclogite-sulfide-carbonatite-diamond system (Fig. 4.14) (Litvin et al. 2012; Litvin 2012). Let us assume that the initial temperature in the stable initially chamber corresponds to the field of diamond liquidus crystallization (Lcarb-sil + D). In the xenogenetic sulfide melt presence, the corresponding liquidus phase relations correspond to the (Lcarb-sil + Lsul + D) field. Primarily the figurative point of the equilibrium potentially diamond-forming melt-solution must lie in the solubility

curve of diamond. With decrease in temperature during natural cooling of the chamber, solubility of diamond in the melt lowers according to the solubility curve. As a result, the melt becomes oversaturated in respect to diamond. When concentration of silicate-(± oxide)-carbonate–carbon melt-solution arises and reaches the kinetic level of labile oversaturation in respect to diamond; nucleation and mass crystallization of diamond develop in this melt-solution. The subsequent cooling maintains oversaturation in respect to diamond and its growth. It is suggested that the time of diamond growth in the natural reservoirs-chambers of carbonate–silicate-(±oxide)-carbonate–carbon melts-solutions should be comparable with the chambers lifetime; crystallization of diamond ceases as soon as the growth melt completely solidifies at the solidus temperature. Thus, fractional syngenesis phase diagrams for the diamond-parental mantle systems (Figs. 6.7 and 6.8) show in what sequences paragenetic rock-forming silicate, oxide and carbonate minerals are recrystallized in the growth melts-solutions and what conditions ensure their entrapment. The xenogenetic sulfide and titaniferous melts or minerals that constantly occur in the diamond-producing systems are captured, as physico-chemically foreign phases, throughout the entire period of function of the natural localized diamond-forming reservoirs-chambers.

The hypothesis of metasomatic agent was put forward by many researchers who studied mantle matter. The formation of carbonate–silicate melts under upper-mantle conditions is considered in (Dalton and Presnall 1998). The agent is described as carbonatitic melts in (Wallace and Green 1988; Yaxley et al. 1998). The formation of such melts might be related to finds of microinclusions of carbonate–silicate melts in diamonds (Klein-BenDavid et al. 2007, 2009; Logvinova et al. 2008; Navon et al. 1988; Schrauder and Navon 1994a; Shiryaev et al. 2005; Skuzovatov et al. 2011; Zedgenizov et al. 2007, 2009) and the formation of reservoirs of diamond-producing carbonate–silicate melts owing to the primary reprocessing of garnet–lherzolite mantle by metasomatic agents (Litvin 2011, 2013).

It is believed that the chemical compositions of diamond-producing silicate-(±oxide)- carbonatitic magmas in terms of major and trace elements were probably determined by two main sources: mantle ultrabasic rocks and metasomatic agents. The resulting trace-element geochemical background is closely related to, accompanies, and adapts to the physico-chemical evolution and differentiation of parental media with the formation of diamonds and all syngenetic minerals, not excluding inclusion minerals, owing to mechanisms of interface trace-element partition.

Experimental determination of the interface partition coefficients of trace elements in the upper-mantle diamond-parental carbonate–silicate media for diamonds and paragenetic inclusions (Kuzyura et al. 2015) permits determining trace elements which were initially related to both mantle peridotite sources and metasomatic agents and then involved in the formation of diamonds and parental magma chambers. The trace-element contents of the chambers of diamond-producing carbonatitic melts were calculated based on (1) mineralogical data on the trace-element contents of peridotitic and eclogitic minerals included in diamonds and in diamond-bearing xenoliths of some kimberlite pipes (Harte and Kirkley 1997; Ionov 2004; Stachel and Harris 1997) and (2) the mineral–parental melt

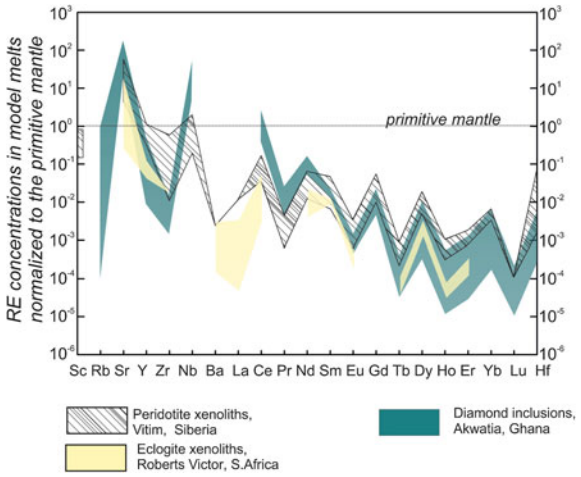

Fig. 7.6 Spidergram with the fields of experimental and natural melts. The trace-element contents are normalized to the primitive mantle (Lyubetskaya and Korenaga 2007). Conventional designations: *1*—peridotite xenoliths, Vitim pipe, Siberia (Ionov 2004), *2*—eclogite xenoliths, Roberts Victor pipe, South Africa (Harte and Kirkley 1997), *3*—inclusions in diamonds, Akwatia pipe, Ghana (Stachel and Harris 1997)

partition coefficients K_D^{TE} experimentally determined in (Kuzyura et al. 2015). The results are shown on a spidergram (Fig. 7.6) as fields of model melts. The elements on the x-axis are placed in the order of increasing charge.

The trace-element contents of experimental mineral phases and primary inclusions of silicate minerals in diamonds of the Akwatia kimberlite pipe, Ghana, were compared with those of minerals in diamond-bearing xenoliths of the Roberts Victor and Vitim pipes. The parental melts of the diamonds and inclusion phases are considerably depleted in medium (Ba, La, Ce, Pr, Nd, Sm, Eu, and Gd) and heavy (Tb, Dy, Ho, Er, Yb, Lu, and Hf) trace elements compared to the primitive peridotite. On the other hand, they are enriched in light (Rb and Sr) trace elements, heavy Zr and Nb, rare-earth Y, and transition Sc, but the contents of these elements in the melts are one to four orders of magnitude lower than those in the primitive-mantle peridotite (Lyubetskaya and Korenaga 2007). The trace elements are mainly the rare-earth components of peridotite mantle. Note the elevated contents of Sr, Nb, and Ce in the calculated parental melts, probably owing to the participation of a metasomatic agent. The field of melts from real diamond inclusions of Akwatia kimberlite pipe, Ghana (Stachel and Harris 1997) is shown on a spidergram. These melts are highly enriched in Sr, Nb, and Ce, which were, most likely, supplied by a metasomatic agent. Their low position on the spidergram suggests the zero tendency of the contents of di- to pentavalent elements (HREE and HFSE). This means that such a melt might have been at equilibrium with a representative garnet phase (in an eclogitic assemblage), which most of these elements were redistributed into. Conversely, less garnet was at equilibrium with the parental melt of the diamond-bearing peridotite xenolith from the Vitim pipe which testifies to the formation of a peridotitic assemblage.

The results are applied to the assessment of the metasomatic–magmatic model for the origin of the parental media of diamonds and syngenetic inclusions and the relative contribution of the mantle source, on the one hand, and its metasomatizing

agent, on the other. The geochemical background of diamond-forming processes is interesting for the identification and assessment of the contribution of different mantle sources of trace elements to the formation of carbonatite parental media for diamonds and their paragenetic inclusions. Direct compatibility of mineralogy of diamond-hosted inclusions and physico-chemical experimental results for diamond-forming systems are indicative for changeable mantle ultrabasic-basic-carbonatite-carbon melts-solutions and their chambers responsible for the joint diamonds and associated phases genesis A physico-chemical experiment and mineralogical analysis of diamond-hosted phases show that leak-tight primary inclusions (with signs of residual pressure) are fragments of heterogeneous diamond-forming media rather than the native mantle minerals.

It can be presumed that the decisive role in the formation of diamond-parental silicate-(±oxide)-carbonatite melts was played by physico-chemical interaction between the mantle ultrabasic substance and a metasomatic agent. This idea becomes the subject of permanent speculations on the analytical mineralogical basis (Pokhilenko et al. 2015). In physico-chemical experiments at pressures of lower 10 GPa it was found that the reaction of molten chemically active K-alkaline carbonate-silicate agent (K_2CO_3 + K_2SiO_3) with forsterite and enstatite, the major mineral components of the lithosphere, results in carbonates Mg_2CO_3 and $K_2Mg(CO_3)_2$ formation (Litvin 1998). At pressures above 4 GPa, the peritectic reactions of alkaline jadeitic $NaAlSi_2O_6$ and nephelinic $NaAlSiO_4$ aluminosilicates with forsterite and enstatite give rise to low-melting silicate $Na_2Mg_2Si_2O_7$ and pyropic garnet $Mg_2Al_2Si_3O_{12}$ (Gasparik and Litvin 1997; Litvin et al. 2000). It was also found that high-pressure reactions of alkaline carbonates with forsterite results in a series of carbonates with mixed Na, K, and Mg cations. The compositions of various transition-zone and lower-mantle phases and coexisting carbonatitic melts were determined by exploratory melting experiments in chemically complex CO_2-bearing systems at 20–24.5 GPa and 1600–2000 °C. The melts are highly ultramafic, enriched in K, Na, Ca, Fe, and Mg, and depleted in Al and Si (Gasparik and Litvin 2002). Carbonate-melt metasomatism is recognized as a process that could have a major effect on the composition and structure of the Earth's mantle, and thus play an important role in its evolution and formation of the diamond-parental melts-solutions and their local reservoirs-chambers.

References

Akaogi M (2007) Phase transitions of minerals in the transition zone and upper part of the lower mantle. In: Ohtani E (ed) Advances in high-pressure mineralogy, geological society of America special paper 421, p 1–13. doi:10.1130/2007.2421(01)

Beattie P, Drake M, Jones J et al (1993) Terminology for trace-element partitioning. Geochim Cosmochim Acta 57(7):1605–1606

Blundy J, Dalton J (2000) Experimental comparison of trace element partitioning between clinopyroxene and melt in carbonate and silicate systems, and implications for mantle metasomatism. Contrib Mineral Petrol 139(3):356–371

Bobrov AV, Litvin YuA (2009) Peridotite-eclogite-carbonatite systems at 7.0–8.5 GPa: concentration barrier of diamond nucleation and syngenesis of its silicate and carbonate inclusions. Russ Geol Geoph 50:1221–1233

Bobrov AV, Litvin YuA, Kuzyura AV et al (2014) Partitioning of trace elements between Na-bearing majoritic garnet and melt at 8.5 GPa and 1500–1900 C. Lithos 189:159–166

Boyd FR, Danchin RV (1980) Lherzolites, eclogites, and megacrysts from some kimberlites of Angola. Amer J Sci 280(2):528–549

Brenan JM, Watson EB (1991) Partitioning of trace elements between carbonate melt and clinopyroxene and olivine at mantle P-T conditions. Geochim Cosmochim Acta 55(8): 2203–2214

Brey GP, Bulatov VK, Girnis AV, Lahaye Y (2008) Experimental melting of carbonated peridotite at 6–10 GPa. J Petrol 49(4):797–821

Dalton JA, Presnall DC (1998) Carbonatitic melts along the solidus of model lherzolite in the system CaO–MgO–Al_2O_3–SiO_2–CO_2 from 3 to 7 GPa. Contrib Mineral Petrol 131(2–3): 123–135

Dasgupta R, Hirschmann MM, McDonough WF et al (2009) Trace element partitioning between garnet lherzolite and carbonatite at 6.6 and 8.6 GPa with applications to the geochemistry of the mantle and of mantle-derived melts. Chem Geol 262(1–2):57–77

Dawson JB (1980) Kimberlites and Their Xenoliths. Springer, New York, p 252

Gasparik T, Litvin YA (1997) Stability of $Na_2Mg_2Si_2O_7$ and melting relations on the forsterite-jadeite join at pressures up to 22 GPa. Eur J Miner 9(2):311–326

Gasparik T, Litvin YA (2002) Experimental investigation of the effect of metasomatism by carbonatic melt on the composition and structure of the deep mantle. Lithos 60(3–4):129–143

Girnis AV, Bulatov VK, Brey GP et al (2013) Trace element partitioning between mantle minerals and silico-carbonate melts at 6–12 GPa and applications to mantle metasomatism and kimberlite genesis. Lithos 160:183–200

Hammouda T, Moine B, Devidal J, Vincent C (2009) Trace element partitioning during partial melting of carbonated eclogites. Phys Earth Planet Inter 174(1–4):60–69

Harte B, Kirkley MB (1997) Partitioning of trace elements between clinopyroxene and garnet: data from mantle eclogites. Chem Geol 136(1–2):1–24

Ionov D (2004) Chemical variations in peridotite xenoliths from Vitim, Siberia: inferences for REE and Hf behaviour in the garnet-facies upper mantle. J Petrol 45(2):343–367

Kaminsky F (2012) Mineralogy of the lower mantle: a review of 'super-deep' mineral inclusions in diamond. Earth Sci Rev 110:127–147. doi:10.1016/.earscirev.2011.10.005

Klein-BenDavid O, Izraeli ES, Hauri E, Navon O (2007) Fluid diamonds from the Diavik mine, Canada and the evolution of diamond-forming fluids. Geochim Cosmochim Acta 71(3): 723–744

Klein-BenDavid O, Logvinova AM, Schrauder M et al (2009) High-Mg carbonatitic microinclusions in some Yakutian diamonds—a new type of diamond-forming fluid. Lithos 112 (Suppl. 2):648–659

Klein-BenDavid O, Pearson DG, Nowell GM et al (2010) Mixed fluid sources involved in diamond growth constrained by Sr–Nd–Pb–C–N isotopes and trace elements. Earth Planet Sci Lett 289(1–2):123–133

Klein-BenDavid O, Graham PD, Nowell GM et al (2014) The sources and time-integrated evolution of diamond-forming fluids—Trace elements and isotopic evidence. Geochim Cosmochim Acta 125:146–169

Kurat G, Dobosi G (2000) Garnet and diopside-bearing diamondites (framesites). Mineral Petrol 69(3–4):143–159

Kuzyura AV, Wall F, Jeffries T, Litvin YA (2010) Partitioning of trace elements between garnet, clinopyroxene, and diamond-forming carbonate-silicate melt at 7 GPa. Mineral Mag 74(2):227–239

Kuzyura AV, Litvin YA, Jeffrises T (2015) Interface partition coefficients of trace elements in carbonate-silicate parental media for diamonds and paragenetic inclusions (experiments at 7.0-8.5 GPa). Russ Geol Geoph 56:221–231

Lee WJ, Wyllie PJ, Rossman GR (1994) CO_2-rich glass, round calcite crystals, and no liquid immiscibility in the system CaO–SiO2–CO2 at 25 GPa. Amer Mineral 79(11–12):1135–1144

Litvin VY, Gasparik T, Litvin YA (2000) The System Enstatite-Nepheline in Experiments at 6.5-13.5 GPa: an Importance of $Na_2Mg_2Si_2O_7$ for the Melting of Nepheline-normative Mantle. Geochem Int 38(1):S100

Litvin YA (1998) Mantle's hot spots and experiment to 10 GPa: alkaline reactions, lithosphere carbonatization, and new diamond-generating systems. Russ Geol Geoph 39(12):1761–1767

Litvin YA (2007) High-pressure mineralogy of diamond genesis. In: Ohtani E (ed) Advances in high-pressure mineralogy, geological society of America special paper 421, p 83–103. doi:10.1130/2007.2421(06)

Litvin YA (2009) The physicochemical conditions of diamond formation in the mantle matter: experimental studies. Russ Geol Geoph 50(12):1188–1200

Litvin YA (2011) Mantle origin of diamond-parent carbonatite magma: experimental approaches. Geophys Res. Abstr, vol 13, EGU2011-3627, EGU General Assembly

Litvin YA (2012) Physicochemical formation conditions of natural diamond deduced from experimental study of the eclogite-carbonatite-sulfide-diamond system. Geol Ore Depos 54(6):443–457

Litvin YA (2013) Physico-chemical conditions of syngenesis of diamond and heterogeneous inclusions in carbonate-silicate parental melts (experimental study). Mineral J 35:24–25

Litvin YA, Zharikov VA (2000) Experimental modeling of diamond genesis: Diamond crystallization in multicomponent carbonate-silicate melts at 5–7 GPa and 1200–1570 °C. Dokl Earth Sci 373:867–870

Litvin YA, Litvin VY, Kadik AA (2008) Experimental characterization of diamond crystallization in melts of mantle silicate-carbonate-carbon systems at 7.0–8.5 GPa. Geochemistry International 46(6):531–553. doi:10.1134/S0016702908060013

Litvin YA, Spivak AV, Kuzyura AV (2016) Fundamentals of mantle carbonatite concept of diamond genesis. Geochem Internat 54(10):839–857. doi:10.1134/S0016702916100086

Litvin YA, Bovkun AV, Garanin VK (2017) Titanium minerals ant their melts in the mantle chambers of diamond-forming systems (experiments at 7–8 GPa). Geochem Internat (accepted)

Litvin Yu, Spivak A, Solopova N, Dubrovinsky L (2014) On origin of lower-mantle diamonds and their primary inclusions. Phys Earth Planet Inter 228:176–185. doi:10.1016/j/pepi/2013.12.007

Litvin YA, Vasiliev PG, Bobrov AV et al (2012) Parental media of natural diamonds and primary mineral inclusions in them: evidence from physicochemical experiment. Geochem Internat 50(9):726–759

Logvinova AM, Wirth R, Fedorova EN, Sobolev NV (2008) Nanometre-sized mineral and fluid inclusions in cloudy Siberian diamonds: newinsights on diamond formation. Eur J Miner 20(3):317–331. doi:10.1127/0935-1221/2008/0020-1815

Lyubetskaya T, Korenaga J (2007) Chemical composition of Earth's primitive mantle and its variance: Implications for global geodynamics. J Geoph Res 112(B3):B03212

McKenna NM, Gurney JJ, Klump J, Davidson JM (2004) Aspects of diamond mineralization and distribution at the Helam Mine, South Africa. Lithos 77:193–208

Marakushev AA (1984) Peridotite nogules in kimberlites as the indicators for depp structure of lithosphere. In: Doklady of Soviet Geologists to the 27th Session of International Geological Congress. Petrology. Nauka, Moscow, pp 153–160

Mathias M, Siebert JC, Rickwood PC (1970) Some aspects of the mineralogy and petrology of ultramafic xenoliths in kimberlite. Contrib Mineral Petrol 26(2):75–123

McDade P, Blundy JD, Wood BJ (2003) Trace element partitioning between mantle wedge peridotite and hydrous MgO-rich melt. Ame Mineral 88(11–12):1825–1831

Navon O, Hutcheon ID, Rossman GR, Wasserburg GJ (1988) Mantle derived fluids in diamond micro-inclusions. Nature 355(6193):784–789

Palatnik LS, Landau AI (1964) Phase Equilibria in Multicomponent Systems. New York, Holt, Rinehart and Winston, Inc., p 454

Palyanov YN, Sokol AG, Borzdov YuM et al (1999) Diamond formation from mantle carbonate fluids. Nature 400(6743):417–418

Pertermann M, Hirschmann MM, Hametner K et al (2004) Experimental determination of trace element partitioning between garnet and silica-rich liquid during anhydrous partial melting of MORB-like eclogite. Geochem Geophys Geosyst 5(5):0001. doi:10.1029/2003GC000638

Pokhilenko NP, Agashev AM, Litasov KD, Pokhilenko LN (2015) Carbonatite metasomatism of peridotite lithospheric mantle implications for diamond formation and carbonatite-kimberlite magmatism. Russ Geol Geoph 56(1–2):361–383

Rhines FN (1956) Phase Diagrams in Metallurgy: Their Development and Application. London, McGraw-Hill Book Company, Inc., p 348

Ringwood AE (1962) A model for the upper mantle. J Geophys Res 67:857–866

Ringwood AE (1975) Composition and Petrology of the Earth's Mantle. McGraw-Hill, New York et al.618 p

Schrauder M, Navon O (1994a) Hydrous and carbonatitic mantle fluids in fibrous diamonds from Jwaneng, Botswana. Geochim Cosmochim Acta 58:761–771. doi:10.1016/0016-7037(94)90504-5

Shatsky VS, Zedgenizov DA, Ragozin AL (2010) Majoritic garnets in diamonds from placers of the north-eastern region of Siberian platform. Dokl Akad Nauk 432(6):811–814

Shiryaev AA, Izraeli ES, Hauri EH et al (2005) Chemical, optical and isotopic investigation of fibrous diamonds from Brazil. Russ Geol Geoph 46(12):1185–1201

Shushkanova AV, Litvin YuA (2008) Experimental evidence for liquid immiscibility in the model system $CaCO_3$-pyrope-pyrrhotite at 7.0 GPa: the role of carbonatite and sulfide melts in diamond genesis. Canad Mineral 46:991–1005

Safonov OG, Perchuk LL, Litvin YuA (2007) Melting relations in the chloride-carbonate-silicate systems at high-pressure and the model for formation of alkalic diamond–forming liquids in the upper mantle. Earth Planet Sci Lett 253(1–2):112–128

Schrauder M, Navon O (1994b) Hydrous and carbonatitic mantle fluids in fibrous diamonds from Jwaneng. Botswana Geochim Cosmochim Acta 58(2):761–771

Schrauder M, Koeberl C, Navon O (1996) Trace element analyses of fluid-bearing diamonds from Jwaneng. Botswana Geochim Cosmochim Acta 60(23):4711–4724

Skuzovatov SYu, Zedgenizov DA, Shatsky VS et al (2011) Composition of cloudy microinclusions in octahedral diamonds from the Internatsional'naya kimberlite pipe (Yakutia). Russ Geol Geoph 52(1):85–96

Sobolev NV (1977) The Deep-Seated Inclusions in Kimberlites and the Problem of the Composition of the Upper Mantle. Washington, DC., American Geophysical Union, p 304

Sobolev VS, Sobolev NV, Lavrentiev VG (1972) Inclusions in diamond from diamond-bearing eclogite. Dok Akad Nauk SSSR 207(1):172–178

Sokol AG, Palyanov YuN, Borzdov YuM et al (1998) Diamond crystallization in a Na_2CO_3 melt. Dokl Akad Nauk 361(3):388–391

Spivak A, Solopova N, Dubrovinsky L, Litvin Yu (2015) Melting relations of multicomponent $MgCO_3$–$FeCO_3$–$CaCO_3$–Na_2O_3 system at 11–26 GPa: application to deeper mantle diamond formation. Phys Chem Miner 42:817–824. doi:10.1007/s00269-015-0765-6

Stachel T, Harris JW (1997) Diamond precipitation and mantle metasomatism: evidence from the trace element chemistry of silicate inclusions in diamonds from Akwatia. Ghana Contrib Mineral Petrol 129(2–3):143–154. doi:10.1007/s004100050328

Stachel T, Aulbach S, Brey GP et al (2004) The trace element composition of silicate inclusions in diamonds. A Rev Lithos 77(1–4):1–19. doi:10.1016/j.lithos.03.027

Sweeney RJ, Green DH, Sie SH (1992) Trace and minor element partitioning between garnet and amphibole and carbonatitic melt. Earth Planet Sci Lett 113(1–2):1–14

Sweeney RJ, Prozesky V, Przybylowicz W (1995) Selected trace and minor element partitioning between peridotite minerals and carbonatite melts at 18–46 kb pressure. Geochim Cosmochim Acta 59(18):3671–3683

Thibault Y, Edgar AD, Lloyd FE (1992) Experimental investigation of melts from a carbonated phlogopite lherzolite: implications for metasomatism in the continental lithospheric mantle. Amer Mineral 77(7–8):784–794

Tomlinson EL, Müller W (2009) A snapshot of mantle metasomatism: Trace element analysis of coexisting fluid (LA-ICP-MS) and silicate (SIMS) inclusions in fibrous diamonds. Earth Planet Sci Lett 279(3–4):362–372

Van Westrenen W, Blundy J, Wood B (1999) Crystal-chemical controls on trace element partitioning between garnet and anhydrous silicate melt. Amer Mineral 84(5–6):838–847

Wallace ME, Green DH (1988) An experimental determination of primary carbonatite magma composition. Nature 335(6188):343–346

Walter MJ, Bulanova GP, Armstrong LS et al (2008) Primary carbonatite melt from deeply subducted oceanic crust. Nature 454(7204):622–625

Weiss Y, Griffin WL, Navon O (2013) Diamond-forming fluids in fibrous diamonds: The trace-element perspective. Earth Planet Sci Lett 376:110–125

Yaxley GM, Green DH, Kamenetsky V (1998) Carbonatite metasomatism in the Southeastern Australian lithosphere. J Petrol 39(11–12):1917–1931

Zedgenizov DA, Rege S, Griffin WL et al (2007) Composition of trapped fluids in cuboid fibrous diamonds from the Udachnaya kimberlite: LAM-ICPMS analysis. Chem Geol 240(1–2): 151–162. doi:10.1016/j.chemgeo.2007.02.003

Zedgenizov DA, Ragozin AL, Shatsky VS et al (2009) Mg and Fe-rich carbonate–silicate high-density fluids in cuboid diamonds from the Internationalnaya kimberlite pipe (Yakutia). Lithos 112(Suppl. 2):638–647